TARGETING OF HISTONE ACETYLATION TO TRANSCRIBED CHROMATIN

by

BENJAMIN JOHN ELWOOD MARTIN

B.Sc., University of British Columbia, 2010

A THESIS SUBMITTED IN PARTIAL FULFILLMENT OF

THE REQUIREMENTS FOR THE DEGREE OF

DOCTOR OF PHILOSOPHY

in

THE FACULTY OF GRADUATE AND POSTDOCTORAL STUDIES

(Biochemistry and Molecular Biology)

THE UNIVERSITY OF BRITISH COLUMBIA

(Vancouver)

May 2018

ABSTRACT

The enrichment of histone acetylation within transcribed chromatin was first observed in the 1960s, and how specific histones are acetylated has been a central question of chromatin biology ever since. One mechanism for specificity is through the targeted recruitment of histone acetyltransferases (HATs) to transcribed chromatin, and we first focused on recruitment of the NuA3 HAT complex in *S. cerevisiae*. NuA3 is known to bind to cotranscriptional histone methylation through two domains: the PHD finger in Yng1 and the PWWP domain in Pdp3, which *in vitro* bind to H3K4 and H3K36 methylation, respectively. While the *in vitro* binding has been well characterized, the relative *in vivo* contributions of these histone methylation marks in targeting NuA3 is unknown. Here, through genome-wide colocalization and mutational interrogation, we demonstrate that the PHD finger of Yng1 and the PWWP domain of Pdp3 independently target NuA3 to H3K4 and H3K36 methylated chromatin, respectively. Interestingly however, the simple presence of NuA3 is insufficient to ensure the acetylation of associated nucleosomes, suggesting a secondary level of regulation that does not involve control of HAT-nucleosome interactions.

Next we studied targeting of histone acetylation itself, focusing on the causality of the relationship between histone acetylation and RNAPII transcription. Through genome-wide analysis of mammalian cell culture and budding yeast, we reveal that the preponderance of histone acetylation is tightly linked with RNAPII occupancy, and, in *S. cerevisiae,* chemically or genetically altering RNAPII localization results in a corresponding change in histone acetylation. These findings show that histone acetylation

is primarily targeted through RNAPII as a consequence of transcription. Importantly, several lines of evidence suggest that RNAPII does not promote acetylation by simple HAT targeting. First, we show that HAT occupancy is a poor predictor of histone acetylation. Second, NuA4 recruitment to upstream activation sequences of either Taf1 (TFIID) enriched or depleted promoters does not result in acetylation in the absence of transcription. Collectively, these data suggest that the activity of HATs is regulated post-recruitment by a mechanism that is dependent on RNAPII.

LAY SUMMARY

To the lay reader, I congratulate you on finding this thesis, which I imagine is more often read by the specialist. In this work, I study how the physical packaging of the genome is chemically modified when genes are expressed. Genetic material is tightly packaged, restricting its access, but a chemical modification called acetylation increases its accessibility. How this modification is directed to specific regions of the genome is the question I set out to answer, and I found that the process of gene expression itself specified where this modification occurred. As this thesis is something of a long read, I have endeavored to shorten to 34 syllables in the form of two haiku.

Chapter 2:

NuA3 binding

To histone methylation

Active not always

Chapter 3:

Histone acetyl

Is largely consequential

Of Pol2 presence

PREFACE

Chapter 2: This chapter is based on a first author manuscript published in the journal *Genetics* (Martin, B. J. E., McBurney, K. L., Maltby, V. E., Jensen, K. N., Brind'Amour, J., & Howe, L. J. (2017). Histone H3K4 and H3K36 Methylation Independently Recruit the NuA3 Histone Acetyltransferase in Saccharomyces cerevisiae. *Genetics*, *205*(3), 1113–1123). Experiments were designed by Dr. LeAnn Howe, Benjamin Martin, and Dr. Kristina McBurney. Dr. Kristina McBurney conducted the Sas3 ChIP-seq experiment, for which Dr. Julie Brind'Amour constructed the sequencing libraries (Figure 2.1). The subsequent analysis and all other experiments were conducted by Benjamin Maritn. Benjamin Martin, with input from Dr. LeAnn Howe, wrote the paper.

Chapter 3: This chapter is based on a first author manuscript currently in preparation. All experiments were designed by Dr. LeAnn Howe and Benjamin Martin. Dr. Julie Brind'Amour constructed ten of a total of 70 sequencing libraries for the ChIP-seq experiments and Kristopher Jensen conducted the *yng2* mutant immunoblot experiments (Figure 3.15). All other experiments and data analysis were performed by Benjamin Martin. Benjamin Martin wrote the paper, with input from Dr. LeAnn Howe, Dr. Matthew Lorincz, and Dr. Julie Brind'Amour.

See the first pages of these chapters to see footnotes with similar information.

TABLE OF CONTENTS

LIST OF TABLES

LIST OF FIGURES

LIST OF ABBREVIATIONS

°C	Degree Celsius
1,10-pt	1,10-Phenanthroline Monohydrate
1-NaPP1	1-Naphthyl-PP1
4tU-seq	4-Thiouracil Sequencing
µg	Microgram
µM	Micromolar
A	Alanine
ACF	ATP-Dependent Chromatin-Assembly Factor
ADA	Transcriptional Adaptor
ADD	ATRX–DNMT3A–DNMT3L
Asf1	Anti-Silencing Function 1
ATP	Adenosine Triphosphate
AWK	Aho–Weinberger–Kernighan
Bar1	Barrier to the Alpha Factor Response 1
BAH	Bromo Adjacent Homology
BAM	Binary Alignment Map
Bdf1	Bromofomain Factor 1
BED	Browser Extensible Data
bp	Basepair
Brd2	Bromodomain Containing 2
Brd3	Bromodomain Containing 3
Brd4	Bromodomain Containing 4

BRPF1	Bromodomain and PHD Finger Containing 1
BWA	Burrows-Wheeler Aligner
$CaCl_2$	Calcium Chloride
CBP	CREB Binding Protein
Cdk12	Cyclin Dependent Kinase 12
Cdk9	Cyclin Dependent Kinase 9
CEAS	Cis-regulatory Element Annotation System
Chd1	Chromatin Organization Modifier, Helicase, and DNA-Binding Domains
ChIP	Chromatin Immunoprecipitation
ChIP-chip	Chromatin Imunnoprecipiration Chip
ChIP-exo	Chromatin Immunoprecipitation Exonuclease
ChIP-seq	Chromatin Immunoprecipitation Sequencing
COMPASS	Complex Proteins Associated with Set1
CRAC-seq	UV Cross-Linking and Analysis of cDNA Sequencing
CTD	Carboxy-Terminal Domain
Ctk1	Carboxy-Terminal Domain Kinase 1
D	Aspartic Acid
Def1	RNAPII Degradation Factor 1
DMEM	Dulbecco Modified Eagle's Medium
DNA	Deoxyribonucleic Acid
DSIF	DRB-Sensitivity-Inducing Factor
E	Glutamic Acid
Esa1	Essential SAS2-related Acetyltransferase 1

Eaf3	Esa1p-Associated Factor 3
Eaf6	Esa1p-Associated Factor 6
EDTA	Ethylenediaminetetraacetic Acid
Epl1	Enhancer of Polycomb Like 1
eRNA	Enhancer RNA
FDR	False Discovery Rate
Gcn5	General Control Nonderepressible 5
GEO	Gene Expression Omnibus
GNAT	GCN5-related N-AcetylTransferase
GRO-seq	Global Run-On Sequencing
GTF	General Transcription Factor
HA	Hemagglutinin
HAT	Histone Acetyltransferase
Hat1	Histone AcetylTransferase 1
HAT-A2	Histone Acetyltransferase A2
HBO1	Histone Acetyltransferase Bound to ORC 1
HDAC	Histone Deacetylase Complex
HEPES	4-(2-hydroxyethyl)-1-Piperazineethanesulfonic Acid
H1-hESC	H1 Human Embryonic Stem Cell
H3K4ac	Acetylation of Lysine 4 on Histone H3
H3K4me1	Monomethylation of Lysine 4 on Histone H3
H3K4me2	Dimethylation of Lysine 4 on Histone H3
H3K4me3	Trimethylation of Lysine 4 on Histone H3

H3K9ac	Acetylation of Lysine 9 on Histone H3
H3K9cr	Crotonylation of Lysine 9 on Histone H3
H3K14ac	Acetylation of Lysine 14 on Histone H3
H3K18ac	Acetylation of Lysine 18 on Histone H3
H3K23ac	Acetylation of Lysine 23 on Histone H3
H3K27ac	Acetylation of Lysine 27 on Histone H3
H3K36ac	Acetylation of Lysine 36 on Histone H3
H3K36me2	Dimethylation of Lysine 36 on Histone H3
H3K36me3	Trimethylation of Lysine 36 on Histone H3
H3K56ac	Acetylation of Lysine 56 on Histone H3
H4ac	Acetylation of Histone H4
H4K5ac	Acetylation of Lysine 5 on Histone H4
H4K8ac	Acetylation of Lysine 8 on Histone H4
H4K12ac	Acetylation of Lysine 12 on Histone H4
H4K16ac	Acetylation of Lysine 16 on Histone H4
H4K91ac	Acetylation of Lysine 91 on Histone H4
IHEC	International Human Epigenome Consortium
ING	Inhibitor of Growth
K	Lysine
kb	Kilo basepair
Kin28	Protein Kinase 28
LiCl	Lithium Chloride
LOS1	Loss of Suppression 1

MBT	Malignant Brain Tumor
mESC	Mouse Embryonic Stem Cell
MEF	Mouse Embryonic Fibroblast
MgCl2	Magnesium Chloride
mL	Millilitre
mM	Millimolar
MNase	Micrococcal nuclease
MOZ	Monocytic leukemic Zinc-finger protein
MORF	MOZ-Related Factor
Mst2	MYST family histone acetyltransferase 2
MYST	MOZ-YBF2(SAS3)-SAS2-TIP60
NaCl	Sodium Chloride
NCP	Nucleosome Core Particle
NDR	Nucleosome Depleted Region
NELF	Negative Elongation Factor
NET-seq	Nascent Elongating Transcript Sequencing
NP-40	4-Nonylphenyl poly(ethylene glycol)
Nto1	NuA Three Orf 1
NuA3	Nucleosomal Acetyltransferase of H3
NuA4	Nucleosomal Acetyltransferase of H4
NUP145	Nuclear Pore 145
P	Proline
P300	Protein p300 (E1A associated 300-kDa cellular product)

PAF400	400 kDa PCAF-associated factor
PAR-clip	Photoactivatable Ribonucleoside-Enhanced Crosslinking
PAS	Polyadentylation Site
PBS	Phosphate-Buffered Saline
PCAF	P300/CBP-associated factor
Pdp3	PWWP Domain-containing Protein 3
PHD	Plant homeodomain
PIC	Preinitiation Complex
PMSF	Phenylmethylsulfonyl Fluoride
PRO-seq	Precision Run-On Sequencing
P-TEFb	Positive Transcription Elongation Factor b
PTM	Post-Translational Modification
PUT4	Proline Utilization 4
PWWP	Proline–Tryptophan–Tryptophan–Proline
qPCR	Quantitative Polymerase Chain Reaction
R	Arginine
rDNA	Ribosomal DNA
RI	Replication-Independent
RNA	Ribonucleic Acid
RNA-seq	Ribonucleic Acid Sequencing
RNAPII	RNA polymerase II
Rpb1	RNA Polymerase II Largest Subunit
Rpb2	RNA Polymerase II Second Largest Subunit

Rpb3	RNA Polymerase II Third Largest Subunit
Rpd3	Reduced Potassium Dependency 3
Rpd3S	Rpd3 Small Complex
RPS28A	Ribosomal Protein of the Small subunit 28A
RSC	Remodel the Structure of Chromatin
Rtt109	Regulator of Ty1 Transposition 109
S	Serine
SAGA	Spt-Ada-Gcn5-Acetyltransferase
Set1	SET domain-containing 1
Set1	SET domain-containing 2
Sas2	Something About Silencing 2
Sas3	Something About Silencing 3
SEC15	Secretory 15
Sgf29	SAGA Associated Factor
Spt5	Suppressor of Ty's 5
SRA	Sequence Read Archive
STAGA	SPT3-TAF(II)31-GCN5L Acetylase
SV40	Simian Virus 40
SWI/SNF	Switch/Sucrose Non-Fermentable
T	Threonine
Taf1	TATA Binding Protein-Associated Factor 1
Taf14	TATA Binding Protein-Associated Factor 14
Tip60	Tat Interactive Protein 60kDa

Tra1	Similar to Human TRRAP
tRNA	Transfer RNA
TSS	Transcription Start Site
SWI/SNF	(SWItch/Sucrose Non-Fermentable)
TATA	TATA(A/T)A(A/T)(A/G)
TRRAP	Transformation/Transcription Domain Associated Protein
TFIIA	Transcription Factor II A
TFIIB	Transcription Factor II B
TFIID	Transcription Factor II D
TFIIE	Transcription Factor II E
TFIIF	Transcription Factor II F
TFIIH	Transcription Factor II H
TFIIS	Transcription Factor II S
$TFIIS_{MUT}$	TFIIS Mutant (*D290A/E291A*)
TFTC	TATA-Binding Protein-Free TAF-Containing Complex
TSA	Trichostatin A
UAS	Upstream Activating Sequence
UCSC	University of California, Santa Cruz
W	Tryptophan
WD40	Trp-Asp (*W-D*) Dipeptide Repeats
Y	Tyrosine
YEATS	Ynl107, ENL, AF9, TFIIF and Sas5
Yng1	Yeast Ing1 Homolog 1

Yng2	Yeast Ing1 Homolog 2
YPD	Yeast Extract Peptone Dextrose

ACKNOWLEDGEMENTS

This work was made possible through the financial support of several funding agencies. The Natural Sciences and Engineering Research Council of Canada (NSERC) through The Alexander Graham Bell Scholarships and The University of British Columbia through the Four Year Doctoral Fellowship (4YF) program provided financial support for my stipend, while Sport Canada through the Athlete Assistance Program (AAP) supported my tuition. NSERC and The Canadian Institutes of Health Research (CIHR) funded the research and experiments conducted during my studies.

My decision to enter graduate school, and my initial love for research, can largely be attributed to my undergraduate laboratory instructors, Dr. Jason Read and, especially, Dr. Scott Covey. I am grateful for their teaching and mentorship, which first drew me to research and led me to seriously consider graduate school.

I would like to thank my committee members, Dr. Ivan Sadowski and Dr. Matthew Lorincz, for their guidance and support throughout my degree. With insightful questions and comments, they helped steer my projects and provided invaluable comments and edits to my dissertation.

I am grateful to everyone in the Molecular Epigenetics Group for their assistance and support. In particular, I am thankful to Dr. Jacob Hodgson, whose advice and stories over coffee were hugely influential to my development as a scientist, and Matthew Dahabieh for many scientific discussions. I would like to thank the many Lorincz Lab members,

including Dr. Julie Brind'Amour, Dr. Carol Chen, Preeti Goyal, and Julien Richard Albert, who assisted me in preparing sequencing libraries, tissue culture technique, and bioinformatic analysis.

Throughout my PhD, the Howe Lab has been a friendly and supportive environment to work in, which is a credit to all of the lab members, past and present. In particular, I want to thank Dr. Jennifer Choi, Dr. Kristina McBurney, Nick Irwin, and Mackenzie Lawrence for their support and friendship. I am grateful to Nicolas Coutin for the many long conversations and ideas for future experiments and for Dr. Vicki Maltby for helping to train me and putting up with what I imagine were far too many questions. I especially want to thank Dr. Adam Chruscicki for his mentorship, encouragement, and training.

I would like to extend my heartfelt gratitude to my supervisor, Dr. LeAnn Howe, who has supported me in both my scientific and athletic endeavors. Scientifically, she provided direction and guidance, while also giving space for me to explore and develop as an independent scientist. Athletically, she actively encouraged me to pursue my field hockey career, even as my training schedule led to irregular hours in the lab and my travel requests mounted. When I was playing tournaments in far-flung countries, LeAnn sent messages of support after watching Internet streams of the matches. I would not have been able to balance my studies with the demands of an international field hockey career without her selfless support and encouragement.

I would like to thank my field hockey teammates for their curiosity and engagement with my research, and for their (often late night) conversations about gene expression, chromatin, and “trimethylamine.” I am also grateful for my coaches, especially Anthony Farry, who supported my balancing of field hockey and scientific careers.

I am sincerely grateful for my friends and family and their support throughout my degree, most of which I spent stretched between field hockey and studies. They handled my frequent absences from family and social settings with grace, while still encouraging me in my endeavours. My parents and siblings were especially fantastic, taking an interest in my work and helping me to see my research in new and creative ways.

Finally, and most importantly, I am eternally grateful to my wife Kathryn for her companionship and support in our life together. I would be lost without her. Her patience, love, and encouragement sustain me and made my PhD such a joy to complete.

DEDICATION

To my parents, for all of your love and support.

CHAPTER 1 – INTRODUCTION

1.1 EUKARYOTIC GENE EXPRESSION

Genetic information contained in deoxyribonucleic acid (DNA) encodes proteins in distinct units called genes. To make a functional protein, a gene is first transcribed to produce a ribonucleic acid (RNA) transcript. Once processed this transcript is translated into the encoded protein, which may be subject to post-translational processing and modifications. Human cells typically produce 10,000 distinct proteins (Beck et al., 2011; Geiger et al., 2012), from a little over 20,000 protein-coding genes (ENCODE Project Consortium, 2004; Pertea and Salzberg, 2010; Pruitt et al., 2009), and protein copy number varies over a dynamic range of seven orders of magnitude (Beck et al., 2011; Geiger et al., 2012). This process dramatically increases the potential phenotypic complexity of a given genome, contributing to species and cellular diversity (Levine and Tjian, 2003). Underlining its significant role in phenotype, aberrant gene expression results in developmental defects and disease, and cells employ a variety of mechanisms to ensure proper expression of genetic material (reviewed in (T. I. Lee and Young, 2013)).

Transcription is the first step in gene expression, in which genetic information encoded in DNA is transcribed to produce a complementary RNA transcript. In eukaryotic cells, protein-coding transcripts are produced by RNA Polymerase II (RNAPII), a large 0.5 megadalton 12-subunit protein complex (Armache et al., 2003; Bushnell and Kornberg, 2003; Cramer et al., 2001). Transcription by RNAPII is highly regulated and proceeds

through three main steps: initiation, elongation, and termination (for review see (Fuda et al., 2009)).

To initiate transcription, RNAPII requires additional protein factors and specific DNA sequences. These include the general transcription factors (GTFs), a conserved class of proteins required for initiation (Aso et al., 1994; Cormack and Struhl, 1992; Matsui et al., 1980; Svejstrup et al., 1994). The GTFs, including TFIIA, -B, -D, -E, -F and –H, associate with RNAPII to form the preinitiation complex (PIC) (Murakami et al., 2013). PIC formation occurs at specific DNA sequences, called core promoters, which contain DNA elements positioning the GTFs (such as TATA elements) and specifying the transcription start site (TSS) (Burke and Kadonaga, 1996; Hahn et al., 1989; J. L. Kim et al., 1993; Smale and Baltimore, 1989; Weil et al., 1979). The GTFs permit basal levels of RNAPII transcription *in vitro*, but an additional class of proteins, called activators, is required for high levels of transcription (Brent and Ptashne, 1985; Parker and Topol, 1984; Topol et al., 1985). Activators are characterized by a bipartite organization (Brent and Ptashne, 1985), consisting of a sequence-specific DNA-binding domain and an activation domain. Activator DNA-binding sites are typically found in upstream activation sequences (UASs), which are located close to and upstream of the core promoter (Bram and Kornberg, 1985; Olesen et al., 1987), and in enhancer regions, which can be many kilobases away (Banerji et al., 1981; de Villiers and Schaffner, 1981; Hamada, 1986). Activators promote transcription through their activation domain, which contacts and recruits multi-protein complexes, termed co-activators (Ma and Ptashne, 1987; Ruden et al., 1991). The mediator complex, a crucial co-activator, is required for

activated transcription (Flanagan et al., 1991; Kelleher et al., 1990; Y. J. Kim et al., 1994; McDonagh et al., 1991). Mediator contacts both activators and RNAPII as part of the PIC, forming a dynamic bridge between them, and this is important for PIC formation and transcription initiation *in vitro* and *in vivo* (Y. J. Kim et al., 1994; Y. C. Lee et al., 1997; Myers et al., 1999; Robinson et al., 2016; Schilbach et al., 2017; C. M. Thompson et al., 1993). The assembled GTFs, RNAPII, and mediator comprises 52 proteins in a 2.5 megadalton structure (Robinson et al., 2016), enabling transcription initiation and subsequently RNAPII elongation.

Coincident with progression into elongation, RNAPII is phosphorylated on its repetitive carboxy-terminal domain (CTD) (Chesnut et al., 1992; Payne et al., 1989). The CTD consists of 26 (yeast) to 52 (human) repeats of the consensus sequence YSPTSPS (Allison et al., 1988; Nonet et al., 1987) and is dynamically phosphorylated on the tyrosine, threonine, and all three serine residues (Baskaran et al., 1993; Schüller et al., 2016; Suh et al., 2016; J. Zhang and Corden, 1991). First characterized for serines 5 and 2, phosphorylation of different residues occurs at specific stages of transcription (Buratowski, 2003; Komarnitsky et al., 2000). Serine 5 phosphorylation occurs during transcription initiation, catalyzed by a kinase in TFIIH (Cdk7/Kin28 in yeast) (Feaver et al., 1991; 1994), and aids promoter escape as well as proper processing of the nascent transcript (E. J. Cho et al., 1997; Jeronimo and Robert, 2014; Lu et al., 1991; Rodriguez et al., 2000; Wong et al., 2014). Following promoter escape, RNAPII enters into early elongation, where it is bound by the conserved RNAP processivity factor DSIF (Wada et al., 1998a). In metazoans, RNAPII can then enter a paused state called promoter-

proximal pausing, which occurs approximately 40 bp downstream of the TSS (Core et al., 2008; Gilmour and Lis, 1986; Kwak et al., 2013). Pausing is caused by the negative elongation factor NELF binding to DSIF (Yamaguchi et al., 1999) and often occurs at signal-responsive genes (Core et al., 2008; Min et al., 2011; Rahl et al., 2010). Pause release is mediated by the kinase and elongation factor P-TEFb, which facilitates NELF dissociation by phosphorylating DSIF (Y. Liu et al., 2009; Marshall and Price, 1992; Wada et al., 1998b), thus allowing resumption of elongation. P-TEFb also catalyzes some phosphorylation of the CTD at serine 2 (Murray et al., 2001; H. Qiu et al., 2009). However, the bulk of serine 2 phosphorylation is catalyzed by the Cdk12 kinase (Bartkowiak et al., 2010; Keogh et al., 2003; J. M. Lee and Greenleaf, 1991; 1989), and it functions in the recruitment of elongation and RNA processing factors (Ahn et al., 2004; Phatnani et al., 2004). Serine 2 phosphorylation increases along the transcribed gene, reaching saturation 600 – 1000 bp downstream of the TSS, and marks the CTD until termination (Kobor et al., 1999; Mayer et al., 2012; 2010).

Termination occurs at specific DNA sequences, termed “terminators”, and is coupled with 3’ end processing of the mRNA transcript (Connelly and Manley, 1988; Dedrick et al., 1987; Logan et al., 1987; Reines et al., 1987). This process requires the RNAPII CTD (Licatalosi et al., 2002; McCracken et al., 1997) and serine 2 phosphorylation (Ahn et al., 2004), which mediates recruitment of factors necessary for termination and RNA processing (Ahn et al., 2004). Termination and the associated dephosphorylation of RNAPII facilitate subsequent reinitiation as RNAPII is recycled to the start of the transcription process (H. Cho et al., 1999; Ganem et al., 2003; Kobor et al., 1999;

Mapendano et al., 2010), and this can involve coordinated juxtaposition of promoter and termination sequences in a gene looping mechanism (Ansari and Hampsey, 2005; O'Sullivan et al., 2004). Collectively, these steps of initiation, elongation, and termination are the underlying mechanism for eukaryotic transcription from DNA templates.

1.2 CHROMATIN STRUCTURE AND NUCLEOSOME POSITIONING

In almost all eukaryotes (Wargo and Rizzo, 2001), DNA is packaged into a nucleoprotein complex termed chromatin, consisting of DNA, histones, and non-histone proteins. The central repeating unit of chromatin is the nucleosome, which was first described in 1974 (D'Anna and Isenberg, 1974a; 1974b; Kornberg, 1974; Kornberg and Thomas, 1974; Noll, 1974; A. L. Olins and D. E. Olins, 1974; Sahasrabuddhe and van Holde, 1974; van Bruggen et al., 1974; van Holde et al., 1974). The nucleosome core particle (NCP) constitutes 147 bp of DNA wrapped 1.65 turns around the histone octamer, containing two copies of each of the four core histones: H2A, H2B, H3, and H4 (Davey et al., 2002; Luger et al., 1997). The DNA strands cross to make 2 turns with approximately 160 bp of DNA, and this can be bound by histone H1 to form the chromatosome (Muyldermans et al., 1981; Puigdomènech et al., 1983; Simpson, 1978). Nucleosomes repeat every 162 bp to over 200 bp depending on the species and cell type (I. R. Brown and Sutcliffe, 1987; Lohr et al., 1977; Pearson et al., 1984; Savić et al., 1981; Thomas and Furber, 1976; Thomas and R. J. Thompson, 1977; Whatley et al., 1981; Zalenskaya et al., 1981), and the intervening DNA is called linker DNA. Nucleosomes encapsulate over 80% of the genome (Chereji and Morozov, 2014; Noll, 1974) and sit at the nexus for a myriad of

mechanisms regulating gene expression (for in-depth reviews see (Lai and Pugh, 2017; Rando and Winston, 2012; Venkatesh and Workman, 2015)).

One functional consequence of chromatin structure is that it restricts access to underlying DNA elements (Archer et al., 1991; Hewish and Burgoyne, 1973; Kladde and Simpson, 1994), and nucleosomes prevent association of many transcription factors to enclosed DNA-binding sites (Cote et al., 1994; Imbalzano et al., 1994; Zhu et al., 2017). This occlusion largely restricts transcription factor binding to non-nucleosomal stretches of DNA, which are known as nucleosome depleted regions (NDRs). NDRs occur at key regulatory regions, including gene promoters and enhancers, and their formation regulates transcription by specifying which stretches of DNA are accessible to regulatory proteins such as sequence-specific activators and GTFs (Ozsolak et al., 2007; Schones et al., 2008; G.-C. Yuan et al., 2005). NDRs form due to the underlying DNA sequences being refractory to nucleosome formation, and via active regulation by chromatin modifying enzymes (N. Kaplan et al., 2009; Krietenstein et al., 2016; Lorch et al., 2014; Segal et al., 2006; Z. Zhang et al., 2011). Aberrant NDRs appear when chromatin structure is disrupted, resulting in spurious transcription events as the transcription machinery gains access to DNA elements normally occluded by chromatin (Cheung et al., 2008; C. D. Kaplan et al., 2003), thus illustrating how limiting access to DNA is a major mechanism by which chromatin structure regulates gene expression.

Chromatin structure is also regulated at the level of nucleosome positioning, and this is best characterized in *S. cerevisiae.* At a typical expressed gene, a promoter NDR is

flanked by strongly positioned nucleosomes termed the -1 and +1 nucleosomes (C. Jiang and Pugh, 2009; W. Lee et al., 2007; Schones et al., 2008; G.-C. Yuan et al., 2005). The +1 nucleosome typically sits just downstream of or partially overlapping the TSS (C. Jiang and Pugh, 2009; Schones et al., 2008), and a well-phased nucleosome array extends downstream into the gene body (C. Jiang and Pugh, 2009; Schones et al., 2008). Nucleosome positioning and spacing are at least in part an actively regulated process (Gkikopoulos et al., 2011; Krietenstein et al., 2016; Z. Zhang et al., 2011), with ATP-dependent chromatin remodelers including classes of enzymes able to slide, exchange, and evict nucleosomes (for review see (Clapier et al., 2017)). Chromatin-remodeler catalyzed sliding of the +1 nucleosome can represses transcription through occlusion of the TSS or other promoter elements (Hirschhorn et al., 1992; Moreira and Holmberg, 1999; Parnell et al., 2008; Whitehouse et al., 1999; L. Wu and Winston, 1997), whereas a well-positioned +1 nucleosome interacts with transcription factors, including TFIID, and is thought to aid transcription (Jacobson et al., 2000; Lorch et al., 2000; Rhee et al., 2014; Rhee and Pugh, 2012). This is consistent with chromatin, rather than merely representing a repressive force needing to be alleviated, also at times acting to potentiate transcription (Cirillo and Zaret, 1999; Durrin et al., 1991; Nagai et al., 2017). Nucleosome positioning and phasing also impact RNAPII elongation through nucleosome arrays (Fitz et al., 2016; Kireeva et al., 2005; Ocampo et al., 2016), providing another layer of regulatory control. Thus, nucleosome positioning represents a key part of transcriptional regulation.

1.3 MODIFYING CHROMATIN STRUCTURE: HISTONE VARIANTS AND POST-TRANSLATIONAL MODIFICATIONS

Nucleosome composition can be altered by incorporation of variants of the canonical histone proteins. In mammals multiple variants of histones H2A, H2B and H3 have been described, but thus far none for histone H4 (Kennani et al., 2017). One frequently studied variant, conserved across eukaryotes (Thatcher and Gorovsky, 1994), is H2A.Z. This variant, first described in 1980 (West and W. M. Bonner, 1980), contains ~60% sequence identity to the canonical H2A (Zlatanova and Thakar, 2008). Despite its divergence from canonical H2A, H2A.Z-containing nucleosomes have a structure similar to that of canonical nucleosomes, with some subtle destabilizations at the interface of the H2A.Z/H2B dimer and the H3/H4 tetramer (Suto et al., 2000). The effect of H2A.Z incorporation on nucleosome stability remains contentious, with conflicting results reported *in vitro* (Abbott et al., 2001; Bönisch and Hake, 2012; W. Li et al., 1993; Y.-J. Park et al., 2004; Suto et al., 2000; Thambirajah et al., 2006; H. Zhang et al., 2005). *In vivo* however, H2A.Z facilitates RNAPII progress through nucleosomes (Santisteban et al., 2011; Weber et al., 2014), which results in eviction of H2A.Z/H2B dimers (Tramantano et al., 2016). H2A.Z deposition into nucleosomes is catalyzed by a conserved chromatin remodeler complex called SWR1 in yeast and SRCAP in mammals (Y. Cai et al., 2005; Kobor et al., 2004; Krogan et al., 2003b; Mizuguchi et al., 2004), and in yeast this most often happens at the TSS distal side of the +1 nucleosome. While other histone variants are associated with a wide range of functions (for review see (Weber and Henikoff, 2014),(Biterge and R. Schneider, 2014)), altering nucleosome composition clearly affords a mechanism for regulation of gene expression.

Allowing for dynamic alteration of chromatin structure, the histone proteins undergo extensive post-translational modifications (PTMs). Numerous types of PTMs have been described including acetylation, methylation, phosphorylation, and ubiquitylation (Allfrey et al., 1964; Goldknopf and Busch, 1977; Hunt and Dayhoff, 1977; Ord and Stocken, 1966; Stevely and Stocken, 1966), with increasingly powerful mass spectrometers and analytical approaches, the number of known histone PTMs and residues at which they occur has dramatically expanded in recent years (Yue Chen et al., 2007; He Huang et al., 2014; Q. Q. Li et al., 2017; Nie et al., 2017; Sabari et al., 2017; M. Tan et al., 2011). Two of the longest studied modifications, however, are the methylation and acetylation of lysine residues, which were first identified in the 1960s (Allfrey et al., 1964; Gershey et al., 1968; Murray, 1964; Phillips, 1963). Acetylation and methylation occur on numerous lysine residues of the histone proteins, the majority of which are located in the unstructured amino-terminal tails (Figure 1.1, Table 1.1), giving rise to vast combinatorial complexity of potential states. Such complexity, however, is not seen *in vivo*, where only a small fraction of states are observed ((Barski et al., 2007; C. L. Liu et al., 2005; Z. Wang et al., 2008) and reviewed in (Rando, 2012)), and understanding how histone modifications regulate chromatin structure and gene expression is a major focus of the field.

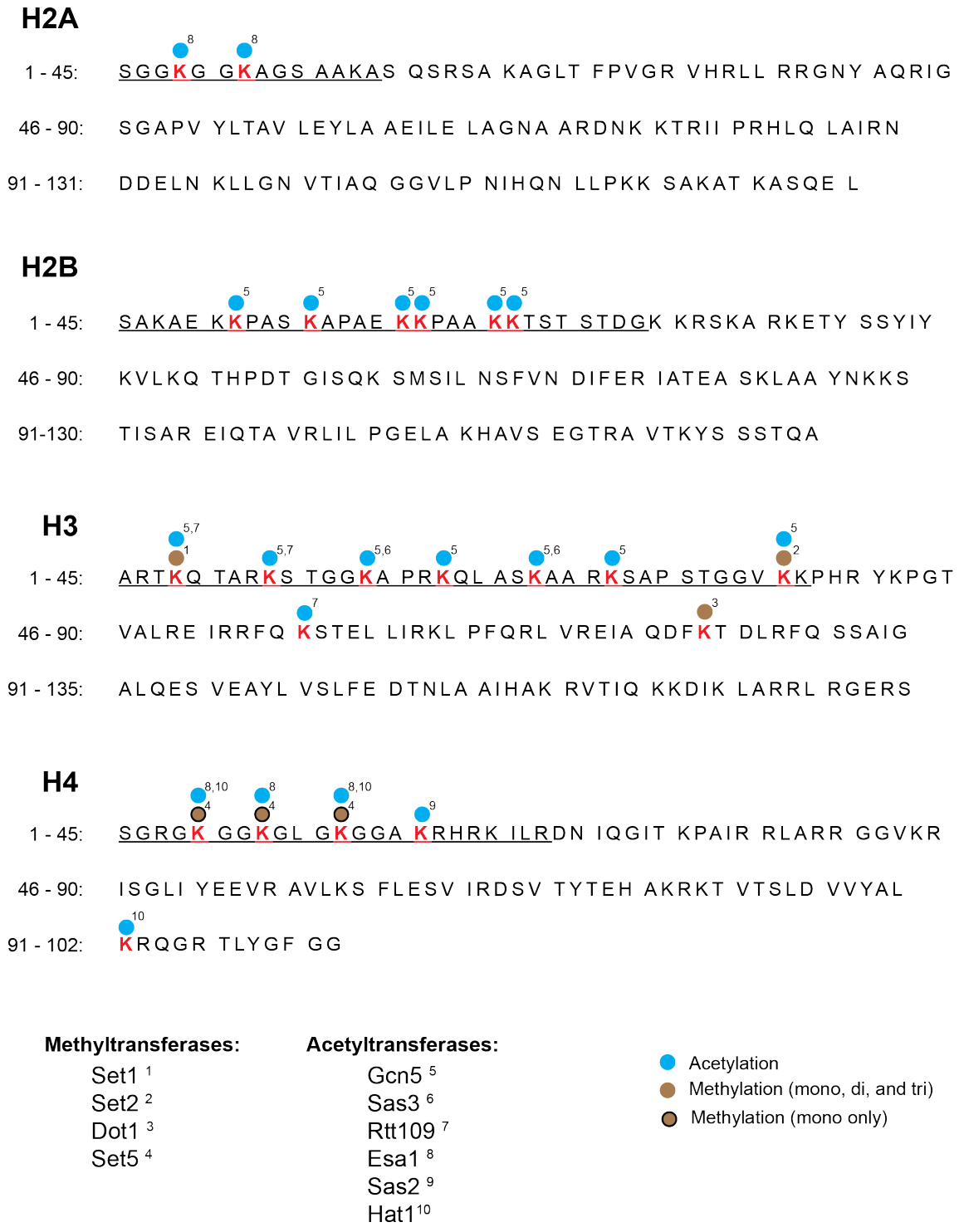

Figure 1.1: Characterized *S. cerevisiae* lysine acetylation and methylation sites on the four core histones. Sites of lysine acetylation and methylation on the four core histones in *S. cerevisiae*. Only sites for which an acetyltransferase or methyltransferase

has been identified are shown, and enzyme specificity is indicated by the superscript numbers. The unstructured N-terminal tails (White et al., 2001) are underlined**.**

Table 1.1: Histone lysine methylation and acetylation sites in *S. cerevisiae.* Sites of lysine acetylation and methylation on the four core histones in *S. cerevisiae*. Only sites with known acetyltransferase or methyltransferase are shown. Ac refers to acetylation. Me refers to methylation, with the numbers in parentheses indicating the methylation states observe *in vivo*.

Histone residue	Modification	Catalyzing Enzyme(s)	Reference
H2AK5	Ac	Esa1	(Clarke et al., 1999)
H2AK7	Ac	Esa1	(Suka et al., 2001) (Clarke et al., 1999)
H2BK6	Ac	Gcn5	(L. Jiang et al., 2007)
H2BK11	Ac	Gcn5	(L. Jiang et al., 2007)
H2BK16	Ac	Gcn5	(L. Jiang et al., 2007)
H2BK17	Ac	Gcn5	(L. Jiang et al., 2007)
H2BK21	Ac	Gcn5	(L. Jiang et al., 2007)
H2BK22	Ac	Gcn5	(L. Jiang et al., 2007)
H3K4	Ac	Gcn5, Rtt109	(Guillemette et al., 2011)
H3K4	Me(1,2,3)	Set1	(Briggs et al., 2001) (Roguev et al., 2001) (Krogan et al., 2002) (P. L. Nagy et al., 2002)
H3K9	Ac	Gcn5, Rtt109	(Grant et al., 1999) (Fillingham et al., 2008) (L. Jiang et al., 2007) (Cieniewicz et al., 2014)
H3K14	Ac	Gcn5, Sas3	(Grant et al., 1999) (Howe et al., 2001) (Cieniewicz et al., 2014) (L. Jiang et al., 2007)
H3K18	Ac	Gcn5	(Grant et al., 1999) (L. Jiang et al., 2007) (Cieniewicz et al., 2014)
H3K23	Ac	Gcn5, Sas3	(Grant et al., 1999)

Histone residue	Modification	Catalyzing Enzyme(s)	Reference
			(Howe et al., 2001) (L. Jiang et al., 2007) (Cieniewicz et al., 2014)
H3K27	Ac	Gcn5	(Cieniewicz et al., 2014)
H3K36	Ac	Gcn5	(Morris et al., 2007) (Cieniewicz et al., 2014)
H3K36	Me(1,2,3)	Set2	(Strahl et al., 2002)
H3K56	Ac	Rtt109	(Rufiange et al., 2007) (J. Han et al., 2007) (Tsubota et al., 2007)
H3K79	Me(1,2,3)	Dot1	(Ng et al., 2002) (Feng et al., 2002) (van Leeuwen et al., 2002) (Lacoste et al., 2002)
H4K5	Ac	Esa1, Hat1	(A. Kimura et al., 2002) (Parthun et al., 1996)
H4K5	Me(1)	Set5	(E. M. Green et al., 2012)
H4K8	Ac	Esa1	(A. Kimura et al., 2002)
H4K8	Me(1)	Set5	(E. M. Green et al., 2012)
H4K12	Ac	Esa1, Hat1	(A. Kimura et al., 2002) (Parthun et al., 1996)
H4K12	Me(1)	Set5	(E. M. Green et al., 2012)
H4K16	Ac	Sas2	(A. Kimura et al., 2002)
H4K91	Ac	Hat1	(Ye et al., 2005)

1.4 HISTONE METHYLATION

Histone methylation is a reversible modification, which involves the addition of up to three methyl groups to lysine residues. The steady-state levels of methylation are the product of competing activities of methyltransferase and demethylase enzymes, which have activity for distinct lysine residues (Rea et al., 2000; Y. Shi et al., 2004). For example the yeast Set1 enzyme of the COMPASS complex specifically catalyzes mono-, di-, and tri- methylation of lysine 4 of histone H3 (H3K4me1, H3K4me2, and H3K4me3) (Briggs et al., 2001; Miller et al., 2001; Roguev et al., 2001), a site that is demethylated

by the Jhd2 demethylase (Liang et al., 2007; Seward et al., 2007). Distinct methylation states of specific residues are associated with either gene activation or repression and many groups have studied the mechanisms by which histone methylation regulates transcription.

The primary mechanism by which histone methylation functions is via mediating protein-protein interactions (Wilkinson and Gozani, 2014). Numerous protein domains interact with methylated lysines and these group into ten main families (Wilkinson and Gozani, 2014), including the Chromodomain (Bannister et al., 2001; Lachner et al., 2001), WD40 repeat (Z. Han et al., 2006; Wysocka et al., 2005), PHD finger (X. Shi et al., 2006; Wysocka et al., 2006), Tudor (Botuyan et al., 2006), Malignant Brain Tumor (MBT) (J. Kim et al., 2006; Klymenko et al., 2006; Trojer et al., 2007), Proline–Tryptophan–Tryptophan–Proline (PWWP) (Y. Wang et al., 2009), Ankyrin repeat (Chang et al., 2011), ATRX–DNMT3A–DNMT3L (ADD) (Dhayalan et al., 2011), zinc-finger CW (He et al., 2010) (Hoppmann et al., 2011), and Bromo Adjacent Homology (BAH) (A. J. Kuo et al., 2012) domains. Methyl-binding domains interact with specific lysine residues with mono-, di-, or tri- methylation. For instance the chromodomain of the heterochromatic protein HP1 binds to H3K9 trimethylation, promoting gene repression (Bannister et al., 2001; Lachner et al., 2001), while a PWWP domain within the Isw1b chromatin remodeling complex binds H3K36me3, helping to maintain chromatin structure over transcribed genes (Maltby et al., 2012b; Smolle et al., 2012), and the PHD finger of human TFIID binds to H3K4me3, promoting its interaction with chromatin and transcription initiation (Vermeulen et al., 2007). Thus, depending on the effector protein

interacting with a given methylation site, histone methylation can have varied functions in the regulation of chromatin structure and gene expression.

1.5 HISTONE ACETYLATION

Two classes of enzymes regulate histone acetylation. Histone acetyltransferases (HATs) catalyze the addition of acetyl groups to lysine residues, while histone deacetylase complexes (HDACs) catalyze their removal (Brownell et al., 1996; Taunton et al., 1996). HATs and HDACs generally exist as a catalytic enzyme in complex with auxiliary factors necessary for activity and targeting (Grant et al., 1997; Lechner et al., 2000; J. Wu et al., 2001a). These complexes often have broad and overlapping specificity. In yeast for instance, Gcn5-containing HAT complexes catalyze acetylation of multiple lysine residues on H2B and H3 (Grant et al., 1997; L. Jiang et al., 2007), and some of the same residues on H3 are acetylated by the Sas3-containing NuA3 HAT complex. Gcn5 and Sas3 together are necessary for acetylation at shared sites (Howe et al., 2001), and these acetyl groups are removed by the Rpd3 and Hda1 deacetylases (Henriksen et al., 2012; Rundlett et al., 1996; J. Wu et al., 2001b). Thus, HATs and HDACs reversibly modify chromatin through histone acetylation, and how this covalent mark affects chromatin structure and DNA-borne processes such as transcription has been the subject of decades of research.

Histone acetylation neutralizes the positive charge of lysine residues, weakening the electrostatic interactions between histones and DNA. Acetylated nucleosomes, while not undergoing gross structural changes, exhibit modestly decreased thermal and salt stability

(Ausio and van Holde, 1986; Bode et al., 1980; Gansen et al., 2009; W. Li et al., 1993; Siino et al., 2003; Wakamori et al., 2015; Yau et al., 1982) and exhibit increased unwrapping of the outer-turn of nucleosomal DNA (Brower-Toland et al., 2005; Norton et al., 1990; X. Wang and Hayes, 2008). In nucleosome arrays, hyperacetylation of histones causes an unfolding of higher-order chromatin structure, with the largest effects for acetylation of histones H2B and H4 (Allahverdi et al., 2011; Garcia-Ramirez et al., 1995; Robinson et al., 2008; Shogren-Knaak et al., 2006; Tse et al., 1998; Wakamori et al., 2015; X. Wang and Hayes, 2008). Histone acetylation can thus directly relax the structure of individual nucleosomes and higher-order chromatin, albeit subtly, thereby creating a template more permissible to transcription (Bintu et al., 2012; Tse et al., 1998).

Histone acetylation can also modulate chromatin structure indirectly by mediating protein-protein interactions. Acetylated lysine residues are bound by several families of protein domains, namely bromodomains (Dhalluin et al., 1999; Haynes et al., 1992; Tamkun et al., 1992), YEATS (Ynl107, ENL, AF9, Taf14 and Sas5) (Le Masson et al., 2003; Y. Li et al., 2014), and double PHD (Zeng et al., 2010) domains. The first characterized acetyl-lysine binding domain was the bromodomain of the PCAF acetyltransferase (Dhalluin et al., 1999). Bromodomains have since been found in several other HATs and are often linked to their catalytic activity (Owen et al., 2000), potentially as a positive feedback loop (Carlson and Glass, 2014; Cieniewicz et al., 2014; Hassan et al., 2002; S. Li and Shogren-Knaak, 2009). Other bromodomain containing proteins such as Brd2 and Brd3 associate with highly acetylated gene bodies to promote transcription elongation (Leroy et al., 2008). Additionally, human TFIID (Jacobson et al., 2000) and

yeast Bdf1 (Matangkasombut et al., 2000) have double bromodomains which stabilize PIC formation near acetylated histones and aid in gene expression. Also chromatin remodelers, exemplified by RSC and SWI/SNF in yeast, contain numerous bromodomains and have increased sliding and eviction activities for acetylated substrates (Chatterjee et al., 2011). Acetylated nucleosomes can also block the action of chromatin proteins such as ACF (Shogren-Knaak et al., 2006), histone H1 (Lawrence et al., 2017; Ridsdale et al., 1990), and histone demethylases (Maltby et al., 2012a). Histone acetylation, thus, indirectly regulates both chromatin structure and transcription by interacting with a wide range of chromatin proteins.

Histone acetylation has long been implicated in regulation of gene expression, and this was first recognized by Vincent Allfrey in 1964 (Allfrey et al., 1964). Histone acetylation has since been subject to decades of intensive research, and one of the central questions has been that of specificity, namely, how is histone acetylation targeted to transcribed regions of chromatin? Answering this question has been a central focus of histone acetylation research for over 50 years.

1.6 TARGETING OF HISTONE ACETYLATION TO TRANSCRIBED CHROMATIN – AN HISTORICAL PERSPECTIVE

At the time of Vincent Allfrey's work, the histone proteins had been shown to repress transcription *in vitro* (Allfrey et al., 1963; Hindley, 1963; Huang and J. Bonner, 1962; Stedman, 1950), which while lacking a mechanism for specificity was still an exciting new development for proteins that had previously been viewed as little more than

structural components of chromatin (reviewed in supplemental discussion: (Campos and Reinberg, 2009) and (Georgiev, 1969)). Then in 1963, a paper was published by David Phillips (Phillips, 1963), which while not focusing on gene regulation itself, would set the stage for Vincent Allfrey's subsequent work. In this study, Phillips described the presence of acetyl groups in histone proteins, but whether these occurred at the time of synthesis or post-translationally was unknown. The following year Vincent Allfrey, Robert Faulkner, and Alfred Mirsky demonstrated post-translational addition of acetyl and methyl groups to histone proteins, and also tested the effect of histone acetylation on an *in vitro* transcription assay (Allfrey et al., 1964). They found that acetylating histones alleviated their suppression of *in vitro* transcription without affecting their affinity for DNA. Based on these results they proposed that histone acetylation could act as a switch for transcriptional activity, quickly relieving histone-mediated repression and permitting gene activation.

Following Vincent Allfrey's proposed link between histone acetylation and gene expression, researchers began to study temporal and spatial correlations between the two *in vivo*. Early experiments involved monitoring changes in global RNA synthesis and histone acetylation through cellular processes such as lymphocyte activation (Pogo et al., 1966) or liver regeneration (Pogo et al., 1968), and these experiments demonstrated the temporal correlation between histone acetylation and transcription. While there were some exceptions to this trend (Gallwitz and Sekeris, 1969), the tight relationship between histone acetylation and transcription was observed across a wide range of systems, pointing to a general phenomenon (Allfrey et al., 1968; Davie et al., 1981; Jiakuntorn and

Mathias, 1981; Pogo et al., 1968; 1966; Ruiz-Carrillo et al., 1974; Supakar and Kanungo, 1981; Wangh et al., 1972). Then as techniques to fractionate nuclear material developed, histone acetylation was found to occur primarily in chromatin fractions undergoing active transcription (Davie and Candido, 1980; 1978; Gorovsky et al., 1973; Levy-Wilson et al., 1979; Nelson et al., 1980; Vavra et al., 1982). These early studies demonstrated tight, if not absolute, temporal and spatial correlations between histone acetylation and transcribed chromatin.

Now after these early successes demonstrating the correlation between histone acetylation and transcription *in vivo*, the big question concerned specificity, specifically, how is histone acetylation targeted to transcribed regions? The issue, articulated by Pavel Georgiev in 1969 (Georgiev, 1969), was to determine how histone acetylation and even chromatin more generally functioned in activation and repression of specific genes. Without a mechanism for targeting it was difficult for the field to progress, and this became a major unanswered question in the field.

Central to the targeting of histone acetylation is the nature of the correlation between histone acetylation and transcription. Namely does one of these lead to the occurrence of the other? To uncover causality between the two, researchers inhibited transcription and looked for loss of histone acetylation, with mixed results (Jiakuntorn and Mathias, 1981; Krause and Stein, 1976; Moore et al., 1979). These were early days in the field, and a number of factors confounded a facile interpretation of the experiments. For instance, many of the experiments used actinomycin D at concentrations that would primarily

inhibit rDNA synthesis (Bensaude, 2014; Krause and Stein, 1976; Moore et al., 1979), which while reducing the radiolabeled RNA fraction would have minimal effects on the bulk of RNAPII transcribed chromatin. In contrast, one study treating rat liver slices with concentrations of actinomycin D necessary to inhibit RNAPII (Bensaude, 2014) observed a rapid decrease in labeling of histone acetylation (Jiakuntorn and Mathias, 1981). These early studies were also hampered by imprecise techniques, assessing RNA and histone labeling in bulk, and the use of a variety of cell types and species deterred direct comparison of findings. With these mixed results the question of causality was left unresolved and was largely put aside.

To address the question of how histone acetylation is targeted, researchers needed to study the enzymes, but HATs are not highly abundant proteins and purifying them to homogeneity would not be achieved for decades. Instead scientists were limited to observing enzymatic acetylation of histone in cellular extracts (Bondy et al., 1970; Gallwitz, 1968; Nohara et al., 1966) and in partially purified preparations (Cano and Pestaña, 1979; Wiegand and Brutlag, 1981). These experiments permitted basic enzymatic characterizations, but revealed little of their mechanisms for targeting. Researchers also characterized the deacetylases (Inoue and Fujimoto, 1969; Libby, 1970) (Inoue and Fujimoto, 1970) (Cousens et al., 1979; Inoue and Fujimoto, 1972), enzymes that actively remove histone acetylation. Similar to the HATs, purifying deacetylases to homogeneity eluded scientists at the time. Without purification and cloning of the genes for the enzymes regulating histone acetylation, major discoveries were limited, but some

notable steps forward in understanding targeting of histone acetylation were still achieved.

As steady-state levels of histone acetylation are the product of competing acetylating and deacetylating enzymes, either one of these activities could drive the correlations between histone acetylation and transcription. To differentiate between these possibilities researchers utilized a newly discovered deacetylase inhibitor called butyrate (Boffa et al., 1978; Riggs et al., 1977). In butyrate-treated cells acetylation primarily increased on a subset of histones, and these were the histones in the fractions containing template-active chromatin (Nelson et al., 1980). These results were important as they demonstrated that the correlation between histone acetylation and transcription was due to the targeting of HAT activity.

The slow progress in acetyltransferase research rapidly changed in 1996, when James Brownell and David Allis finally purified a HAT to homogeneity from *Tetrahymena* (Brownell et al., 1996). The HAT turned out to be the homologue of a previously identified yeast co-activator protein, Gcn5 (Georgakopoulos and Thireos, 1992), thus providing a mechanistic link between histone acetylation and transcription. These experiments suggested that HATs were co-activator proteins recruited during transcription initiation, and the acetyltransferase activity of Gcn5 was soon shown to play this role *in vivo* (M. H. Kuo et al., 1998). Three other known co-activators (p300, CBP, and Tip60) (Arany et al., 1994; Chrivia et al., 1993; Eckner et al., 1994; Kamine et al., 1996) were subsequently found to be HATs (Bannister and Kouzarides, 1996; A. Kimura

and Horikoshi, 1998; Ogryzko et al., 1996; Yamamoto and Horikoshi, 1997), establishing activator-recruitment as a general model for HAT targeting. These results provided an answer to the decades-old question regarding HAT targeting, showing that HATs were recruited during transcription initiation by sequence-specific activators.

In the same year that Gcn5 was identified as a HAT, the first deacetylase was also purified (Taunton et al., 1996). This previously identified transcriptional regulator, Rpd3 (Vidal and Gaber, 1991) was soon shown to be recruited by sequence-specific factors for gene repression (Kadosh and Struhl, 1997; W. M. Yang et al., 1996), with repression depending on its deacetylase activity (Kadosh and Struhl, 1998). These results established targeted recruitment of HATs and HDACs by sequence-specific activators and repressors as key mechanisms for gene regulation. This mechanistic handle for understanding the role of histone acetylation in transcriptional regulation electrified the field and coincided with a rapid increase in research into histone acetylation and the field of chromatin as a whole (Figure 1.2).

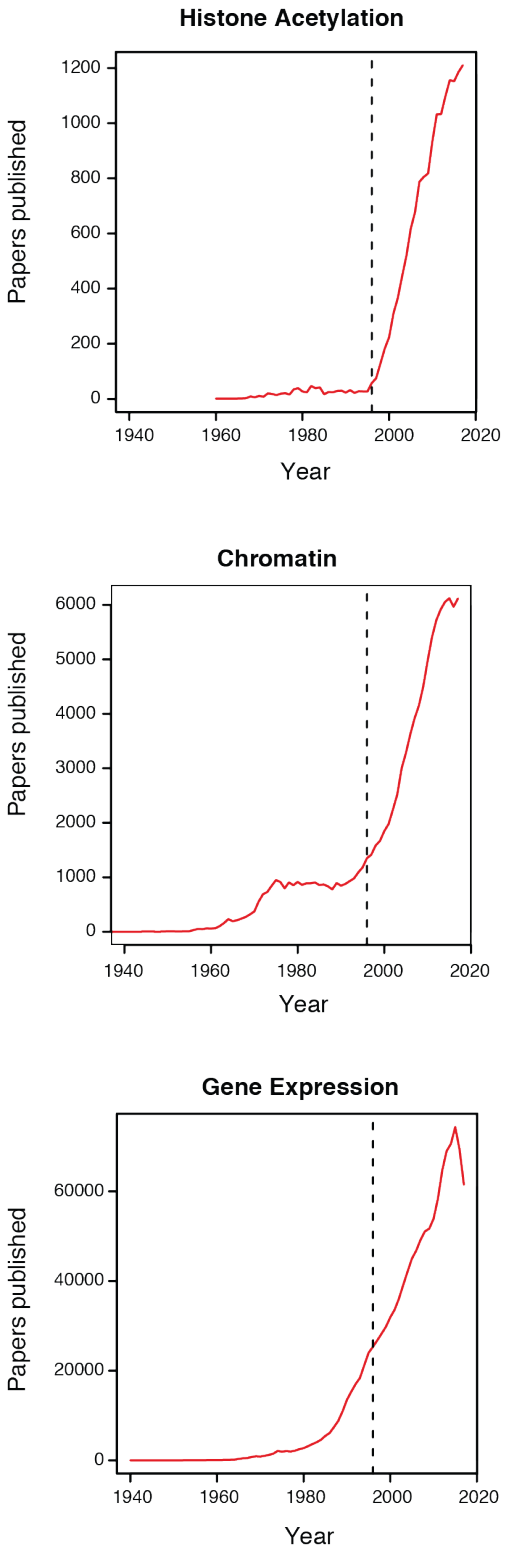

Figure 1.2: Papers published per year on histone acetylation, chromatin, and gene expression. The number of Pubmed search hits by year for histone acetylation (A),

chromatin (B) and gene expression (C). The dashed line indicates 1996, the year that Gcn5 and Rpd3 were identified as a histone acetyltransferase and deacetylase respectively.

As the HATs were identified, one peculiarity of their activity invited further study. Most acetyltransferases, while able to acetylate free histones, had little activity on nucleosome substrates (Grant et al., 1997). The hypothesis was that the enzymes required additional proteins to efficiently acetylate nucleosomes, and, in 1997 the first HAT complexes were purified from yeast. Aided by a fortuitous discovery that almost all of yeast nucleosomal HAT activity bound to nickel agarose columns, the yeast HAT complexes were quickly characterized (Grant et al., 1997). Four HATs were observed eluting from the nickel agarose columns, leading to initial purification of the Gcn5-containing SAGA and ADA complexes (Grant et al., 1997). SAGA is a massive 1.8 megadalton complex, containing the Tra1 protein (Grant et al., 1998; Saleh et al., 1998), a number of the TAFs, Spt proteins, and submodules containing activity for histone deubiquitylation and histone acetylation (Daniel et al., 2004; Grant et al., 1997; K. K. Lee et al., 2011). ADA consists of the HAT submodule from SAGA with an additional two unique subunits, Ahc1 and Ahc2 (Eberharter et al., 1999; Grant et al., 1997; K. K. Lee et al., 2011). The nickel agarose approach (Eberharter et al., 1998; Grant et al., 1997) also enabled purification of the Esa1-containing NuA4 HAT complex (Allard et al., 1999), specific for H4 and H2A acetylation. NuA4 is another large complex and shares Tra1 with SAGA. These discoveries paved the way for further elucidation of mechanisms targeting histone acetylation.

Tra1 turned out to be a key factor for recruitment by activators, making direct contact with the activation domains of multiple sequence-specific activators (C. E. Brown et al., 2001; Utley et al., 1998; Wallberg et al., 1999). Homologous HAT complexes in mammalian cells employ a similar mode of recruitment with the Tra1-related proteins PAF400 in PCAF and TRRAP in STAGA, TFTC, and Tip60 mediating HAT recruitment during transcription initiation (Ikura et al., 2000; McMahon et al., 1998; 2000; Vassilev et al., 1998). These studies, along with similar findings for the CBP and p300 HATs (Dai et al., 1996; Oelgeschläger et al., 1996; Sartorelli et al., 1997; W. Yuan et al., 1996), provided a mechanistic basis for understanding activator targeting of HATs to promoter regions, creating the paradigm of HAT recruitment by activators during transcription initiation. This model of HAT targeting also appeared to provide an answer to the question of causality in the long observed correlation between histone acetylation and transcription, suggesting that histone acetylation occurred prior to and as a cause of transcription. However, as noted by Michael Hampsey at the time (Hampsey, 1998), while being suggestive of an answer, these experiments did not directly test the question of causality.

Indeed, a number of HAT complexes were also discovered that did not appear to be promoter targeted. In yeast these included the Gcn5-containing ADA and HAT-A2 complexes, the Sas3-containing NuA3 complex (John et al., 2000), and the Esa1-containing piccolo NuA4 complex (Boudreault et al., 2003). These HATs were deemed "untargeted" due to their lack of sequence-specific targeting (Vogelauer et al., 2000).

However genome-wide acetylation patterns, once determined, revealed that histone acetylation is highly correlated with transcription, suggesting that most histone acetylation is targeted in one form or another (C. L. Liu et al., 2005; Pokholok et al., 2005; Z. Wang et al., 2008). In fact, it was soon discovered that multiple mechanisms recruit both "untargeted" and "targeted" HAT complexes to chromatin as a consequence of transcription. Importantly these new mechanisms occurred coincident with or following RNAPII transcription, suggesting that histone acetylation could also occur as a consequence of the transcription process.

One such mechanism for histone acetylation occurring downstream of transcription is mediated through methylation of histone proteins. In the early 2000s, methylation of histone H3 at lysines 4 and 36 was discovered to occur co-transcriptionally. First, the Set1 methyltransferase was discovered to methylate H3K4 (Briggs et al., 2001; Krogan et al., 2002; P. L. Nagy et al., 2002; Roguev et al., 2001) and to be targeted to 5' gene regions through RNAPII (Krogan et al., 2003a; J.-S. Lee et al., 2007; Ng et al., 2003; Wood et al., 2003). Then H3K36 methylation was found to be catalyzed by Set2 (Strahl et al., 2002), which was targeted to elongating RNAPII via an interaction with serine 2 phosphorylation of the RNAPII CTD (Krogan et al., 2003c; B. Li et al., 2003; J. Li et al., 2002; Schaft et al., 2003; Xiao et al., 2003). Shortly thereafter numerous HATs were discovered to bind these cotranscriptional histone methylation marks. For H3K4me3, the yeast NuA3 HAT complex binds via the PHD finger of its Yng1 subunit (D. G. E. Martin et al., 2006; X. Shi et al., 2006; 2007; Taverna et al., 2006). The yeast Esa1-containing HAT complexes bind H3K4 methylation through the PHD finger of Yng2 (X. Shi et al.,

2007; 2006; Steunou et al., 2016). Mammalian and yeast Gcn5-containing HAT complexes bind H3K4me3 through the tudor domain of Sgf29 (Bian et al., 2011; Vermeulen et al., 2010). Mammalian HATs MOZ, MORF, and HBO1 bind H3K4 methylation through their ING protein subunits (Doyon et al., 2006; Hung et al., 2009; Lalonde et al., 2013; Saksouk et al., 2009; X. Shi et al., 2006). Mammalian TIP60 is reported to bind H4K3me3 through its chromodomain (C.-H. Kim et al., 2015). HAT binding via H3K36 methylation is not as well established, but binding of several HATs has been described. The NuA4 subunit Eaf3 binds to H3K36me2/3 through its chromodomain (B. Sun et al., 2008; Xu et al., 2008), recruiting NuA4 to mid and 3' gene regions (Ginsburg et al., 2014; Rossetto et al., 2014; Sathianathan et al., 2016). Also the NuA3 HAT can bind to H3K36me3 through the PWWP domain of Pdp3 (Gilbert et al., 2014), and the MOZ/MORF subunit BRPF1 subunit binds H3K36me3 through its PWWP domain (Vezzoli et al., 2010). These interactions of HATs with H3K4 and H3K36 methylation provide a mechanism to target histone acetylation to transcribed chromatin.

Another mechanism for targeting HATs is mediated through RNAPII itself. First an acetyltransferase complex, called Elongator, was found to directly interact with RNAPII in yeast (Otero et al., 1999; Wittschieben et al., 1999). However Elongator was subsequently shown to be primarily located in the cytoplasm (Huh et al., 2003; Pokholok et al., 2002; Rahl et al., 2005) functioning in tRNA modification (Bo Huang et al., 2005). The initial findings implicating Elongator in histone acetylation (Winkler et al., 2002; Wittschieben et al., 2000) were shown to be indirect effects of a translation defect (Bo

Huang et al., 2005), and Elongator is no longer thought to acetylate histones *in vivo.* Despite this early setback several other bonafide HATs were found to interact with RNAPII. Both NuA4 and SAGA in yeast and PCAF and Tip60 in mammals interact with phosphorylated RNAPII during elongation (Ginsburg et al., 2009; Govind et al., 2007; Obrdlik et al., 2008; Z. Wang et al., 2009). More recently, the RNAPII-interacting elongation factor BRD4 (Kanno et al., 2014) was discovered to be a histone acetyltransferase (Devaiah et al., 2016). Thus, numerous HATs interact directly with RNAPII thereby targeting histone acetylation to transcribed chromatin.

Histones are exchanged from nucleosomes outside of replication in an RNAPII-dependent manner (Jackson, 1990). The incorporated histones are at least in part composed of newly synthesized histones H2A, H2B, H3, and H4 (Jackson, 1990), promoting incorporation of histones with marks representative of newly synthesized histones. Newly synthesized histones are acetylated (Allis et al., 1985; Jackson et al., 1976; Ruiz-Carrillo et al., 1975) in the cytoplasm by the Hat1 acetyltransferase (Kleff et al., 1995; Parthun et al., 1996) at lysines 5 and 12 of histone H4 (Chicoine et al., 1986; Sobel et al., 1995). Histone H4 is also reported to be acetylated at lysine 91 during histone deposition (Ye et al., 2005). In yeast, histone H3 is also acetylated by Rtt109 at lysine 56 as part of the Asf1 histone deposition pathway (Driscoll et al., 2007; J. Han et al., 2007; Masumoto et al., 2005; J. Schneider et al., 2006; Tsubota et al., 2007). Mutants increasing histone exchange cause an Asf1/Rtt109-dependent increase in histone acetylation (Venkatesh et al., 2012), demonstrating how this pathway can target histone acetylation to transcribed chromatin.

Recently RNA transcripts have also been implicated in regulating histone acetylation. RNA can mediate recruitment of CBP and TIP60 to chromatin (Poshen B Chen et al., 2015; Pnueli et al., 2015; Postepska-Igielska et al., 2015), with TIP60 binding directed towards RNA-DNA hybrids involving the nascent transcript. Furthermore CBP activity is stimulated by enhancer RNAs both *in vitro* and *in vivo* (Bose et al., 2017). In yeast, Esa1 contains a tudor/chromo barrel domain that is reported to bind RNA (Shimojo et al., 2008) and DNA (Jiehuan Huang and S. Tan, 2013) *in vitro,* but its *in vivo* binding target is still unclear. Thus RNA interaction with HATs presents an emerging mechanism of regulation.

Despite the elucidation of numerous pathways that target histone acetylation to transcribed chromatin, the causal nature of histone acetylation and transcription remains unclear. While activator targeting suggests histone acetylation is instructive for transcription, numerous pathways targeting histone acetylation to or following RNAPII support its occurrence as a consequence of transcription. However the conclusive experiments to directly test causality remain to be performed.

This issue of causality underlying correlations with histone modifications is not unique to histone acetylation (Henikoff and Shilatifard, 2011), and a few recent studies suggest that it is a question worth revisiting. Experiments on SV40 chromosomes found p300 associated with RNAPII-bound acetylated chromatin (Balakrishnan and Milavetz, 2007a). Importantly this association was lost upon treatment with the transcription

inhibitor alpha-amanitin (Balakrishnan and Milavetz, 2007b), consistent with, at least in this system, histone acetylation occurring in an RNAPII-dependent manner. Another study in mouse embryonic stem cells (mESCs) revealed that Tip60 recruitment to gene bodies genome-wide is lost upon transcription inhibition (Poshen B Chen et al., 2015). While this study did not assess the effect of transcription inhibition on histone acetylation itself, the genome-wide RNAPII dependence of Tip60 recruitment suggests that the bulk of Tip60-mediated histone acetylation may also be RNAPII-dependent. However, while these studies are suggestive, whether histone acetylation by Tip60 or by other HATs is primarily occurring in an RNAPII-dependent manner remains to be determined.

1.7 CHAPTER SUMMARIES

The overarching focus of this thesis is the question of specificity in histone acetylation, and, in particular, how is histone acetylation targeted to regions of chromatin undergoing active transcription?

In chapter 2 of this thesis, I examined how the acetyltransferase NuA3 is recruited to chromatin loci in *S. cerevisiae.* Previous work from our lab and others has described binding of NuA3 subunits Yng1 and Pdp3 to methylated H3K4 and H3K36 through a PHD finger and a PWWP domain respectively. While the binding of these domains to methylated peptides has been well characterized *in vitro*, the relative *in vivo* contributions of these histone PTMs in targeting NuA3 was unknown. I interrogated the individual and combined roles of these domains in targeting NuA3 to methylated chromatin. First, I

measured NuA3 binding to nucleosomes genome-wide, finding that NuA3 binds to H3K4 mono-, di-, and tri- methylation (H3K4me1/2/3) and H3K36me3 modified nucleosomes. Then through mutational interrogation, I found that the PHD finger of Yng1 and the PWWP domain of Pdp3 independently target NuA3 to H3K4 and H3K36 methylated chromatin respectively. Collectively these results suggest that these modifications can work independently to recruit NuA3 to chromatin. Finally, I found that NuA3 binding to nucleosomes was not sufficient for histone acetylation, and this was not due to HDAC activity, indicating that targeting of NuA3 to chromatin is not the only mechanism regulating NuA3 acetyltransferase activity.

Next, as presented in chapter 3, I turned to the regulation of histone acetylation itself, specifically addressing the question of causality in the correlation between histone acetylation and transcription. I found that in *S. cerevisiae* as well as mammalian cells, histone acetylation is tightly linked with RNAPII occupancy. I went on to show that genetically and chemically altering RNAPII occupancy results in corresponding changes in histone acetylation. These results reveal that the majority of histone acetylation is targeted to histones through RNAPII as a consequence of transcription. Similar to my results in chapter 2, I found that a simple model of HAT targeting couldn't explain targeting of histone acetylation by RNAPII. First, Gcn5 and Epl1 HAT binding is a poor predictor of genome-wide histone acetylation, and this cannot be explained by HDAC activity. Second, I found that recruitment of NuA4 to upstream activation sequences does not result in increased histone acetylation in the absence of transcription. These findings

suggest that regulation of HAT activity post-recruitment is a crucial step in histone acetylation and that this regulation is RNAPII-dependent.

CHAPTER 2 – HISTONE H3K4 AND H3K36 METHYLATION INDEPENDENTLY RECRUIT THE NUA3 HISTONE ACETYLTRANSFERASE IN *SACCHAROMYCES CEREVISIAE*

The results presented in this chapter have been published: Martin, B. J. E., McBurney, K. L., Maltby, V. E., Jensen, K. N., Brind'Amour, J., & Howe, L. J. (2017). **Histone H3K4 and H3K36 Methylation Independently Recruit the NuA3 Histone Acetyltransferase in Saccharomyces cerevisiae**. *Genetics*, *205*(3), 1113–1123.

2.1 INTRODUCTION

Eukaryotic DNA is packaged into a nucleoprotein structure known as chromatin, which consists of DNA, histones, and non-histone proteins. Histones are extensively post-translationally modified, with specific modifications reflecting activities occurring on the underlying DNA. For example, genes transcribed by RNA polymerase II (RNAPII) have acetylated, crotonylated, and H3K4 tri-methylated histones (H3K4me3) at their 5' ends and H3K36 tri-methylated histones (H3K36me3) over the gene body (C. L. Liu et al., 2005; Pokholok et al., 2005; Sabari et al., 2015). While histone acetylation and methylation have long been studied, lysine crotonylation is a recently discovered histone PTM (M. Tan et al., 2011). This acyl-histone modification is regulated by intracellular crotonyl-CoA levels and occurs at similar genomic regions to histone acetylation (Sabari et al., 2015). The various histone modifications are often thought to promote the biological processes to which they are associated.

Although some histone post-translational modifications (PTMs) can directly alter chromatin structure, most function as recognition sites for histone PTM binding domains (Yun et al., 2011). Histone PTM binding domains are found in complexes that facilitate transcription or alter chromatin structure, such as basal transcription factors, chromatin-remodeling complexes and even enzymes that post-translationally modify histones. The majority of chromatin-modifying complexes have multiple histone PTM binding domains, the purpose of which has been the subject of much speculation. The generally weak affinity of these domains for their requisite histone PTMs has led to the hypothesis that multiple histone-binding interactions are required to stabilize the recruitment of complexes to chromatin (Yun et al., 2011). Indeed, it is suggested that multiple histone-binding domains function synergistically to translate "a code" of histone PTMs into a single biological outcome (Strahl and Allis, 2000). Alternatively, multiple histone binding domains could act independently to target a chromatin-binding complex to a range of genomic loci.

One complex containing multiple histone PTM binding domains is the NuA3 histone acetyltransferase (HAT) complex in *S. cerevisiae*, which acetylates H3K14 and H3K23 (Howe et al., 2001). NuA3 contains six subunits: the catalytic subunit Sas3, Nto1, Eaf6 and three histone PTM-binding proteins: Yng1, Pdp3, and Taf14 (Howe et al., 2002; John et al., 2000; Taverna et al., 2006). Yng1 contains a PHD finger which binds to H3K4 mono-, di- and trimethylation, with binding affinity increasing with the number of methyl groups (D. G. E. Martin et al., 2006; X. Shi et al., 2007; Taverna et al., 2006). Pdp3 contains a PWWP domain, which recognizes H3K36me3 (Gilbert et al., 2014). Taf14,

through its YEATS domain, binds to acetylated (H3K9ac) and crotonylated (H3K9cr) histone H3K9 (Andrews et al., 2016; Shanle et al., 2015). While the *in vitro* binding of these proteins to histone PTMs has been well characterized (Table 2.3), the relative contributions these histone PTMs make to NuA3 targeting *in vivo* remains unknown.

In mammalian cells, two HAT complexes appear analogous to NuA3: the MOZ/MORF complex and the HBO1–BRPF1 complex. Both complexes contain BRPF1 (bromodomain PHD finger protein 1) or one of its paralogs, BRPF2 or 3 (Doyon et al., 2006; Lalonde et al., 2013). BRPF1/2/3 share sequence similarity with yNto1, but additionally contain carboxy-terminal, H3K36me3-specific PWWP domains (Vezzoli et al., 2010), and thus may serve the role of both yNto1 and yPdp3 in mammalian complexes. The MOZ/MORF complex also has an H3K4me2/3-specific PHD finger in its subunit, ING5 (inhibitor of growth 5), while the HBO1–BRPF1 uses ING4 or ING5 to bind to H3K4me2/3 (Doyon et al., 2006; Lalonde et al., 2013). Finally, although the MOZ/MORF and HBO1-BRPF1 complexes lack a Taf14 equivalent, a bromodomain within BRPF1/2/3 and a double PHD finger in MOZ/MORF show specificity for acetylated histones (Ali et al., 2012; Laue et al., 2008; L. Liu et al., 2012; Y. Qiu et al., 2012). Thus, the histone PTM binding domains in NuA3 are conserved in analogous complexes in other organisms, although the relative contribution that these domains make in targeting NuA3 has yet to be determined.

In this study we show that NuA3 is primarily targeted to mid-gene regions via interactions with H3K36me3 and H3K4me1/2/3, while H3K9ac and H3K9cr are unlikely

to play a role in recruitment. Simultaneous disruption of H3K4 and H3K36 methylation abolishes NuA3 recruitment to actively transcribed genes. In contrast, disruption of H3K4 or H3K36 methylation singularly results in partial loss of NuA3 recruitment, suggesting that these PTMs recruit NuA3 independently and arguing against a synergistic effect. Finally, we show that NuA3 occupancy does not dictate histone acetylation indicating that controlled targeting is not the only mechanism for regulation of NuA3 function.

2.2 MATERIALS AND METHODS

2.2.1 Yeast strains and plasmids

All strains used in this study were isogenic to S288C, and are listed in Table 2.1. All strains are available upon request. Yeast culture and genetic manipulations were performed using standard protocols. Genomic deletions were verified by PCR analysis and whole cell extracts were generated as previously described (Kushnirov, 2000). The previously described *kanMX-GAL1pr-flo8-HIS3* strains (Cheung et al., 2008) were generous gifts of Fred Winston.

Table 2.1: Yeast strains used in this study

Strain	Parent	Mating type	Genotype	Source
YLH101	FY602	Mat a	*his3D200 leu2D1 lys2-128d ura3-52 trp1D63*	
YVM138	YLH101	Mat a	*his3D200 leu2D1 lys2-128d ura3-52 trp1D63 SAS3-6HA::TRP*	
YVM142	YLR008 x YLH354	Mat a	*his3D200 leu2D1 lys2-128d ura3-52 trp1D63 SAS3-6HA::HIS set1D::KANMX6 set2D::TRP*	
YVM147	YVM144	Mat a	*his3D200 leu2D1 lys2-128d ura3-52 trp1D63 SAS3-6HA::TRP yng1DPHD::KANMX6*	
YVM157	YVM146	Mat a	*his3D200 leu2D1 lys2-128d ura3-52 trp1D63 SAS3-6HA::TRP set1D::HISMX6*	
YVM158	YVM146	Mat a	*his3D200 leu2D1 lys2-128d ura3-52 trp1D63 SAS3-6HA::TRP set2D::HISMX6*	
YVM207	YVM146	Mat a	*his3D200 leu2D1 lys2-128d ura3-52 trp1D63 SAS3-6HA::TRP ylr455w::HIS*	
YLH696	YVM147	Mat a	*his3D200 leu2D1 lys2-128d ura3-52 trp1D63 SAS3-6HA::TRP yng1DPHD::KANMX6 ylr455w::HISMX6*	
YLH787	YLH101	Mat a	*his3D200 leu2D1 lys2-128d ura3-52 trp1D63 bar1::KAN*	
FY2173		*MAT*a	*his3D200 leu2D1 lys2-128D trp1D63 ura3-52 kanMX-GAL1pr-FLO8-HIS3*	(Cheung et al., 2008)
L1106		Mat a	*his3D200 ura3D0 kanMX-GAL1pr-FLO8-HIS3 rco1D0::kanMX*	(Cheung et al., 2008)
YLH510	L1106	Mat a	*his3D200 ura3D0 kanMX-GAL1pr-FLO8-HIS3 rco1D0::kanMX sas3::URA3*	

2.2.2 Drug treatments

For H3K23ac ChIP-seq, *bar1*Δ cells were arrested in G1 by 2.5 hour treatment with 5 μM α-factor. Culture synchrony in G1 was confirmed by the appearance of "shmooing" cells, as seen under the microscope. TSA was added for 15 minutes at 25 μM, from 5 mM DMSO stock.

2.2.3 Chromatin immunoprecipitation with sequencing (ChIP-seq)

The ChIP-seq protocol was based on that outlined in (Maltby et al., 2012a). Cell pellets were resuspended in lysis buffer (50mM HEPES pH 7.5, 140mM NaCl, 1mM EDTA, 2% Triton X-100, 0.2% Na-deoxycholate, 1X Roche protease inhibitor cocktail, 1mM PMSF) and lysed by bead beating. Cell lysates were spun down at 15,000g for 30 minutes. The chromatin pellets were re-suspended in NP-S buffer (0.5 mM spermidine, 1 mM β-ME, 0.075% NP-40, 50 mM NaCl, 10 mM Tris pH 7.4, 5 mM MgCl2, 1 mM $CaCl_2$) and digested with micrococcal nuclease at 37°C for 10 minutes to obtain predominantly mono-nucleosomal DNA. Reactions were stopped with the addition of EDTA to 10 mM and digested lysates were clarified by centrifugation at 9000g for 10 minutes. To extract insoluble chromatin, pellets were re-suspended in 300 μl of lysis buffer with 0.2% SDS and sonicated in a Diagenode Bioruptor at high output for four cycles of 30 seconds. Extracts were then re-clarified by centrifugation at 9000g for 10 minutes, and the supernatant pooled with the pre-existing extract. The buffer composition of the lysate was adjusted to that of the original lysate, and 10% was set aside as input. The supernatant was pre-cleared by incubation with magnetic protein-G Dynabeads (Life Technologies) for 1 hour at 4°C. Pre-cleared lysates were incubated with αHA (Roche, cat no.

12013819001), αH3K4me3 (Abcam, cat no. ab1012), αH3K23ac (Active Motif, cat no. 39131), or αIgG (Millipore, cat no. PP64) antibodies at 4°C overnight. Immune complexes were precipitated by incubation with magnetic protein-G Dynabeads for one hour at 4°C. Beads were washed twice with lysis buffer, high salt wash buffer (50mM HEPES pH 7.5, 640mM NaCl, 1mM EDTA, 2% Triton X-100, 0.2% Na-deoxycholate), LiCl wash buffer (10mM Tris-HCL pH 8.0, 250mM LiCl, 0.6% NP-40, 0.5% Na-deoxycholate, 1mM EDTA), and once with TE. The immunoprecipitated DNA was subjected to Illumina HiSeq paired-end sequencing. Reads were aligned to the *S. cerevisiae* genome (Saccer3 genome assembly) using BWA (H. Li and Durbin, 2010). Average gene profiles were generated using the sitepro tool in the CEAS genome package (Shin et al., 2009) and plotted using R. The H3K23ac signal represents the average of two independent replicates. For average plots showing the IP divided by input, a coverage value of one was added to both the IP and the input to avoid division by zero. Values past the polyadenylation site (D. Park et al., 2014) were excluded from the average calculation, and the fraction of genes included in the average calculation at any given distance from the TSS shown.

2.2.4 Data availability

The ChIP-seq data generated for this study have been deposited in the Gene Expression Omnibus (GEO) database, GEO accession: GSE93059.

2.2.5 Published datasets

The datasets for the co-occurring nucleosomes and for H3K4me3 in the H3K36R mutant (Sadeh et al., 2016) were downloaded from the SRA study SRP078243. Histone methylation and acetylation datasets from (Weiner et al., 2015) were downloaded from SRA study SRP048526. H3K9ac datasets from (Bonnet et al., 2014) were downloaded from SRA study SRP033513. The H3K4me3 dataset from (Maltby et al., 2012a) was from our previous study. The fastq files were mapped to saccer3 using BWA (H. Li and Durbin, 2010). The methylation data from (Schulze et al., 2011) was downloaded from *Saccharomyces* Genome Database (Cherry et al., 2012) as mapped MAT scores. The Yng1 data from (Taverna et al., 2006) was kindly provided by the authors as mapped intensity scores for IPs and inputs. The NET-seq data from (Churchman and Weissman, 2011) was downloaded from SRA study SRP004431 and mapped to saccer3 using bowtie (Langmead et al., 2009). The processed data for Gcn5 from (Xue-Franzén et al., 2013) was downloaded from the GEO depository, series GSE36600. For average gene profiles, the +1 nucleosome was called using BEDTools (Quinlan and Hall, 2010) as the closest consensus nucleosome position (Brogaard et al., 2012) to the TSS (Brogaard et al., 2012). Cell cycle regulated genes (Eser et al., 2014) were excluded from analysis comparing G1-arrested and asynchronous datasets.

2.2.6 Nucleosome enrichments

For each dataset the average coverage over genome wide nucleosome positions (Weiner et al., 2015) was calculated. When available the IPs were normalized to input files.

Spearman correlation matrix was calculated in R, considering all pairwise complete observations.

2.2.7 Gene peak enrichment

For each gene, 100 bp windows were constructed in 5 bp steps, from the upstream edge of +1 NCP to the polyadenylation site to a maximum of 3000 bp. The average signal (IP coverage for data from (Sadeh et al., 2016) and IP/input for all others) was calculated for each bin, and centre of the most enriched bin was defined as the peak enrichment.

2.2.8 Boxplots

Methylation enrichment defined as having an IP/input of greater than 1.5 and depletion corresponded to an IP/input of less than 0.75. Boxplots extend from the 1st to 3rd quartiles, with whiskers extending to 1.5 times the interquartile range or to the extreme of the data. Notches extend +/- 1/58 IQR /sqrt(n) and give an approximation of the 95% confidence interval for the difference in 2 medians.

2.2.9 Chromatin immunoprecipitation with quantitative PCR (ChIP-qPCR) of Sas3

Cells were grown in 50 ml YPD to an OD600 of 0.8 and cross-linked with 1% formaldehyde for 30 minutes at room temperature. The reaction was stopped by the addition of 125 mM glycine and incubated at room temperature for a further 15 minutes. Pellets were washed twice with cold PBS, resuspended in 600 µl of lysis buffer (50 mM HEPES pH 7.5, 140 mM NaCl, 0.5 mM EDTA, 1% Triton X-100, 0.1% sodium

deoxycholate), and lysed mechanically by vortexing with glass beads for 25 minutes at 4°C. The lysates were spun down by centrifugation at 15,000g for 30 minutes, the supernatant was discarded and the pellet was washed and resuspended in 500 µL lysis buffer. The resuspended pellets were sonicated at high output for 30 seconds on, with 30 seconds break, for 30 cycles to obtain an average fragment length of 250 bp. A further 200 µl of lysis buffer was added to each sample, and the lysates were clarified by centrifugation at 9,000g for 10 minutes. Ten percent of the lysate was reserved for input. Lysates were incubated with 1 µg anti-HA antibody (Roche, cat no. 12CA5) at 4°C overnight, followed by precipitation of immune complexes with 25 µl protein G Dynabeads at 4°C for 1 hour. Beads were washed twice with lysis buffer, high salt wash buffer (50mM HEPES pH 7.5, 640mM NaCl, 1mM EDTA, 2% Triton X-100, 0.2% Na-deoxycholate), LiCl wash buffer (10mM Tris-HCL pH 8.0, 250mM LiCl, 0.6% NP-40, 0.5% Na-deoxycholate, 1mM EDTA), and once with TE. The DNA was eluted and processed as described previously (Maltby et al., 2012a) and qPCR was performed in technical triplicate using the primers listed in Table 2.2.

Table 2.2: ChIP-qPCR primers used in this study

qPCR primer	Sequence (5' to 3')
NUP145 s+3214	GTATCTTCTGCTGCCTTGTCATC
NUP145 a+3335	CGAAGGAAACTAGCGATGAGG
NUP145 a+1611	CATTGGTTTGGTGGCTTCGTC
NUP145 s+1488	CAACATGATGTGGATCTCACAGC
NUP145 a+281	GTAGCGCCAAATAAGCCACC
NUP145 s+148	CTTCAACACCTAGCCCATCTGG
SEC15 a+2230	GACCCATGAATTGTCTCGTCAAGG
SEC15 s+2082	GTAAGGCAAGACCCGGATATCTC
SEC15 a+1312	GTGACAACCTGTCCATGAGTC
SEC15 s+1092	GGTACAGGTACTACTCCTGGATC
SEC15 a+370	GCACCATACCTTGGATGTTTGC
SEC15 s+230	GGACCCCGTAATTGATGAATTGG
LOS1 a+1395	CAGACTTGGGTCAATTACCACG
LOS1 a+2940	GTCGTCATTATCCAAGCAGGTCC
LOS1 s+2831	CTATACGCCGCAAGAGATCCAG
LOS1 s+1301	GGTCACACAGGATGATTTTGAGG
LOS1 a+230	CCATTTGGATTAGCGTTCACGC
LOS1 s+69	CAAGCCATCGAGCTGCTAAATG
PUT4 a+714	CACGCATAGAAAGATCGTGATCC
PUT4 s+546	CTGGTCACTAGGTACGTTGAC
RPS28A s + 15	CCAGTCACTTTAGCCAAGGTC
RPS28A a +191	CGAGCTTCACGTTCAGATTCC

2.3 RESULTS

2.3.1 NuA3 is primarily bound to mid-gene regions of actively transcribed genes

The NuA3 histone acetyltransferase complex contains three histone PTM binding domains: the Yng1 PHD finger, the Pdp3 PWWP domain, and the Taf14 YEATS domain, which show specificity for H3K4me1/2/3, H3K36me3 and H3K9ac/H3K9cr respectively (Andrews et al., 2016; Gilbert et al., 2014; Shanle et al., 2015; Taverna et al., 2006) (Table 2.3). To determine the relative contribution of each histone PTM in targeting the NuA3 complex, we reasoned that histone PTMs that promote the interaction of NuA3 with chromatin would co-localize with Sas3. To this end, we mapped NuA3-bound nucleosomes at high resolution *in vivo* using an MNase-based ChIP-seq approach, which has previously been used to map chromatin remodelers (Floer et al., 2010; Koerber et al., 2009; Ramachandran et al., 2015; Yen et al., 2012). We immunoprecipitated HA-tagged Sas3, in parallel with an untagged control, from crosslinked MNase-digested chromatin and performed paired-end sequencing. We could not detect any DNA in the untagged control mock IP, but nonetheless constructed a library and included the sample in the pool for sequencing. While sequencing of the Sas3 IP and inputs produced over 8 million DNA fragments, only 84,973 DNA fragments were recovered from the untagged control IP, confirming the specificity of our Sas3 ChIP-seq experiment.

We mapped the sequenced DNA fragments to the *S. cerevisiae* genome, aligned genes by the +1 nucleosome, and calculated the average profile for each sample (Figure 2.1 A). Relative to the input Sas3 was enriched in the gene body, but not at the +1 nucleosome, and this enrichment was specific to the Sas3 IP and was not observed for the untagged

control. We next compared Sas3 occupancy to a previously reported sonication-based mapping of Yng1 (Taverna et al., 2006). Unsurprisingly, Yng1 and Sas3 levels correlated positively genome-wide with a Spearman correlation coefficient of 0.48 (Figure 2.1 B, C). Additionally both of the Yng1 and Sas3 input-normalized distributions peaked in enrichment 600 bp to 800 bp downstream of the +1 nucleosome (Figure 2.1 D). Thus our mapping of Sas3 agreed well with the previous mapping of Yng1, but the MNase-based approach increased the resolution of the assay, and we found that NuA3 was primarily recruited to 'mid-gene' regions containing the +5 to +7 NCPs (Figure 2.1 D). We also observed that Sas3 was enriched on long genes and modestly enriched on genes transcribed by RNAPII (Figure 2.2 A-C), consistent with Sas3 recruitment to mid-gene regions of actively transcribed genes.

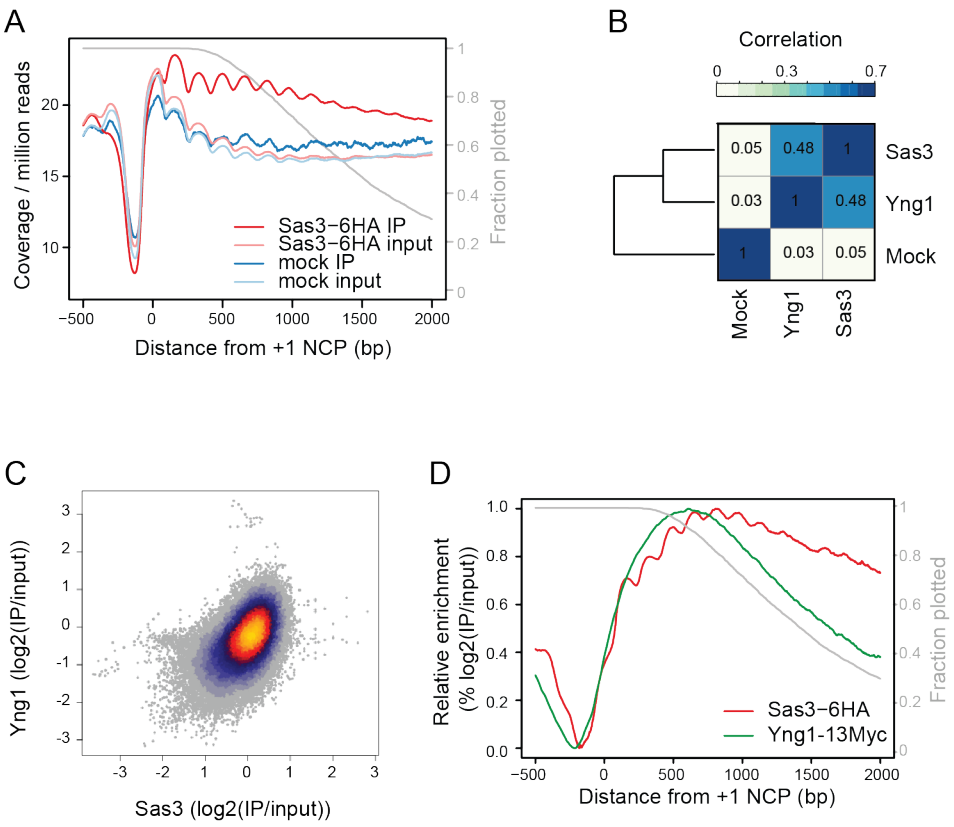

Figure 2.1: Nua3 is primarily bound to mid-gene regions. A. The average sequence coverage relative to 4701 +1 nucleosomes. **B.** Genome-wide spearman correlations (500 bp windows, 100bp steps) for input-normalized Sas3 and Yng1 (Taverna et al., 2006). **C.** Scatter plot of Yng1 (Taverna et al., 2006) and Sas3 genome-wide enrichments. **D.** Average enrichment for Yng1 and Sas3 relative to the +1 nucleosome. Signal represents the $\log_2$(IP/input) and plotted as the relative signal within each sample. Average plots only include data until the polyadenylation site (PAS), and the grey line represents the fraction of genes still being plotted.

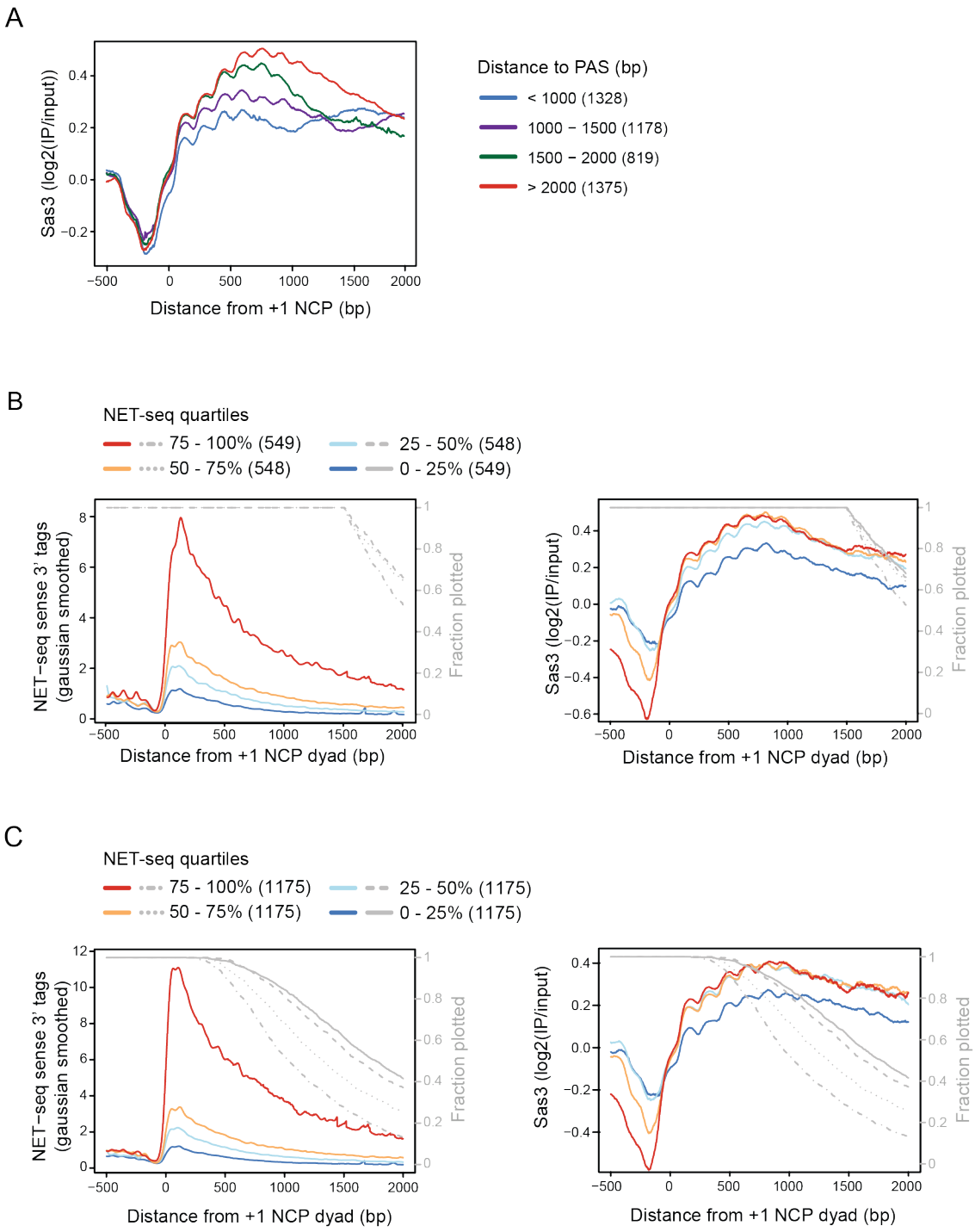

Figure 2.2: NuA3 is primarily bound to mid-gene regions of actively transcribed genes. A. Sas3 enrichment by gene length, with gene length defined as the distance from the +1 nucleosome to the polyadenylation site (PAS)**. B.** Sas3 enrichment by quartiles of sense NET-seq (Churchman and Weissman, 2011) signal for genes longer than 1500 bp.

Only genes longer than 1500 bp were plotted to avoid gene length effects but results are similar when all genes analyzed (**C**). Except for gene length plot, all average plots only include data until the PAS, and the grey line represents the fraction of genes still being plotted.

2.3.2 NuA3 is associated with H3K4me3, H3K4me2, H3K4me1, and H3K36me3 nucleosomes genome wide

As domains within NuA3 have been reported to bind to H3K4me3, H3K4me2, H3K4me1, H3K36me3, H3K9ac, and H3K9cr *in vitro* (Table 2.3), we hypothesized that if these modifications recruit NuA3 to nucleosomes *in vivo* they will correlate positively with Sas3. To conduct this meta-analysis, we made use of published genome-wide studies of these histone PTMs to calculate nucleosome-based Spearman correlations with Sas3 and Yng1 (Figure 2.3 A). Since crotonylation has not been mapped in *S. cerevisiae* but colocalizes with acetylation in mammalian cells (Sabari et al., 2015), we used H3K9ac as a proxy for H3K9cr. To our surprise, H3K9ac did not correlate with Sas3 or Yng1, which suggests that despite Taf14 binding *in vitro,* it does not function in NuA3 recruitment *in vivo.* Conversely, H3K36me3, H3K4me3, H3K4me2 and H3K4me1 all correlated positively with Sas3 and Yng1, supporting their role in NuA3-nucleosome binding *in vivo.* Furthermore co-occurring H3K4me3 and H3K36me3 nucleosomes, identified through sequential IPs (Sadeh et al., 2016), strongly correlated with Sas3 with Spearman correlation coefficients above 0.5 (Figure 2.3 A). The dual H3K4me3 and H3K36me3 methylated nucleosomes also specifically grouped with Sas3 and Yng1 following

Hierarchical clustering, consistent with NuA3 binding to nucleosomes through the combined effects of H3K36me3 and H3K4 methylation.

Table 2.3: Published *in vitro* dissociation constants for NuA3 and MOZ/MORF histone-PTM binding domains.

Domain	Peptide	K_D (μM)	Reference
Yng1 PHD finger	H3K4me3	2.3 +/- 0.9, 9.1 +/- 1.6	(X. Shi et al., 2007), (Taverna et al., 2006)
	H3K4me2	21.4 +/- 3.0	(Taverna et al., 2006)
	H3K4me1	50.7 +/- 7.6	(Taverna et al., 2006)
	H3K4me0	>400	(Taverna et al., 2006)
Pdp3 PWWP	H3K36me3	69.5 +/- 3.7	(Gilbert et al., 2014)
	H3K36me2	414 +/- 23	(Gilbert et al., 2014)
	H3K36me1	>1000	(Gilbert et al., 2014)
	H3K36me0	>1000	(Gilbert et al., 2014)
	H3K79me3	434 +/- 49	(Gilbert et al., 2014)
	H4K20me3	> 1000	(Gilbert et al., 2014)
Taf14 YEATS	H3K9ac	150.6 +/- 14.5	(Shanle et al., 2015)
	H3K9,14,18ac	49.9 +/- 2	(Shanle et al., 2015)
	H3K9cr	9.5 +/- 0.5	(Andrews et al., 2016)
ING5 PHD finger	H3K4me3	2.4 +/- 1.0	(Champagne et al., 2008)
	H3K4me2	16 +/- 1.2	(Champagne et al., 2008)
	H3K4me1	222 +/- 17	(Champagne et al., 2008)
	H3K4me0	261 +/- 34	(Champagne et al., 2008)
BRPF1 PWWP	H3K36me3	2700 +/- 200, 2900 - 4000	(Vezzoli et al., 2010), (H. Wu et al., 2011)
	H3K36me2	very weak	(H. Wu et al., 2011)
	H3K36me0	NB	(H. Wu et al., 2011)
	H3K4me3	NB	(H. Wu et al., 2011)
	H3K79me3	very weak	(H. Wu et al., 2011)
	H3K9me3	NB	(H. Wu et al., 2011)

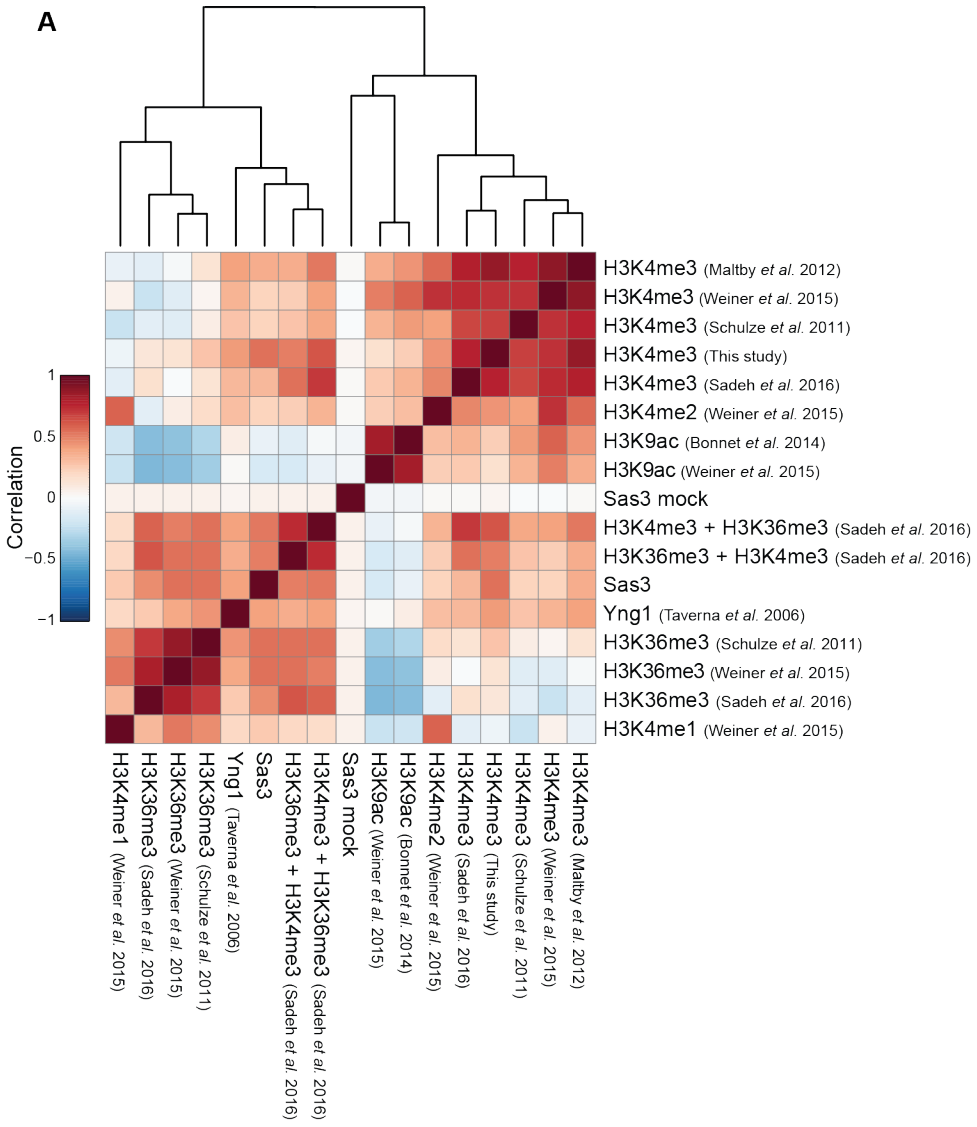

Figure 2.3: NuA3 correlates with H3K4me3, H3K4me2, H3K4me1, and H3K36me3 nucleosomes genome wide. A. Spearman correlation matrix for Sas3, Yng1 and histone PTM enrichments at 66360 genome-wide nucleosome positions. The rows and columns were sorted by hierarchical clustering, and the clustering is represented by the dendrogram.

Next, we compared the locations of peak enrichment for Sas3, Yng1, H3K36me3, and H3K4 methylation (Figure 2.4 A). Sas3 and Yng1 had median peak enrichments at 750 bp and 657 bp downstream of the +1 dyad respectively, which was in between the peak enrichments for H3K4me3 and H3K36me3. Notably Yng1 and Sas3 peaked in enrichment slightly downstream of co-occurring H3K4me3 and H3K36me3, suggesting that H3K4me2 and H3K4me1 are also important for NuA3 targeting. Altogether the peak enrichments of Sas3 and Yng1 were consistent with NuA3 being primarily recruited to mid-gene regions through the combined effects of H3K36me3 and H3K4 mono, di, and trimethylation.

We next assessed Sas3 enrichment on nucleosomes containing H3K4me1/2/3 or H3K36me3 singularly or in combination (Figure 2.4 B). In the absence of H3K36me3 or H3K4 methylation Sas3 was depleted from nucleosomes. Likewise nucleosomes solely enriched in H3K4me1 were also depleted in Sas3, albeit with the caveat that we only identified 90 such nucleosomes and these may represent noise within one of the datasets or be atypical cases in the genome. H3K4me2 enriched nucleosomes are in all but a handful of nucleosomes also enriched for H3K4me1 or H3K4me3, and we were unable to interrogate this modification in isolation. Nucleosomes enriched singularly with H3K36me3 or H3K4me3 were enriched for Sas3 to a similar extent, suggesting that each of these modifications recruit Sas3 to nucleosomes independently. Nucleosomes enriched with both H3K4me1 and H3K36me3 were enriched for Sas3 to a greater extent than H3K36me3 alone, suggesting that H3K4me1 does indeed function in Sas3 recruitment.

Nucleosomes enriched for both H3K4me3 and H3K36me3 were enriched further still in Sas3 binding, consistent with NuA3 preferentially binding H3K4me3 over H3K4me1. Altogether this analysis supports H3K36me3 and H3K4me1/2/3 functioning to recruit NuA3 to chromatin *in vivo*.

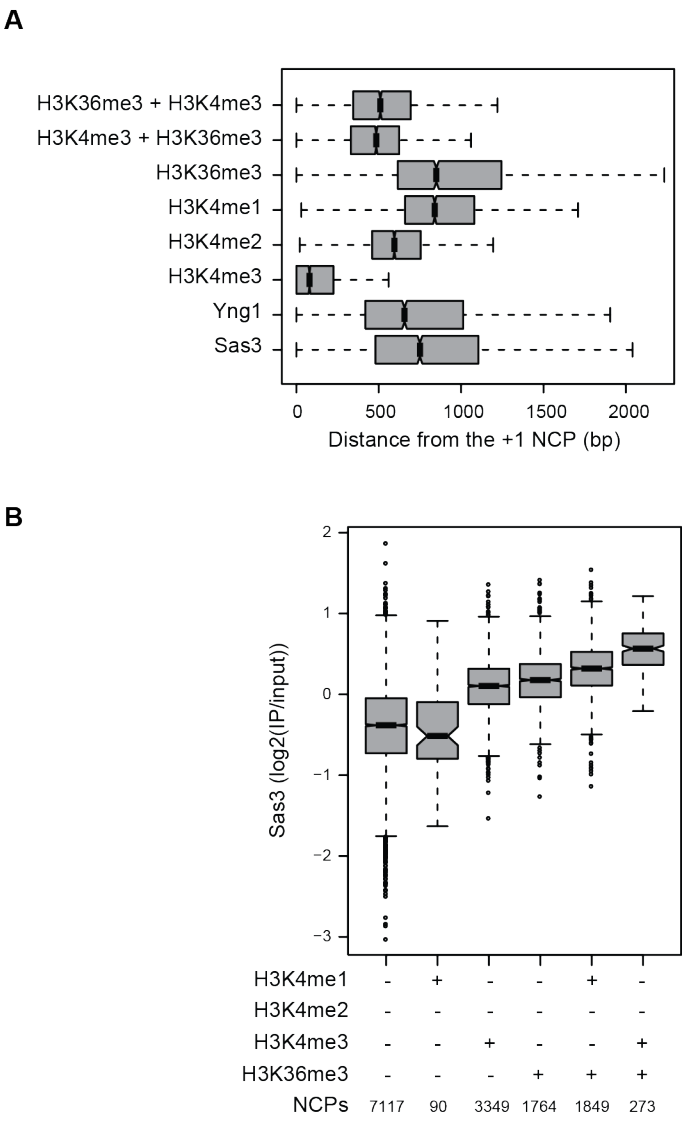

Figure 2.4: NuA3 is associated with H3K4me3, H3K4me2, H3K4me1, and H3K36me3 genome wide. A. Gene peak enrichments relative to 4701 +1 nucleosome dyads for co-occurring H3K4me3 and H3K36me3 (Sadeh et al., 2016), H3K4me1/2/3 (Weiner et al., 2015), H3K36me3 (Weiner et al., 2015), Yng1 (Taverna et al., 2006), and Sas3**. B.** Sas3 enrichment at nucleosome positioned enriched or depleted for H3K4me1/2/3 and H3K36me3 (Weiner et al., 2015).

2.3.3 H3K4 and H3K36 methylation are necessary for Sas3 binding to active genes through Pdp3 and Yng1 respectively

The genome-wide analysis suggested that H3K4 and H3K36 methylation are the major mechanisms for recruiting NuA3 to chromatin, and we next sought to test this directly. H3K4 and H3K36 methylation are entirely dependent on the histone methyltransferases Set1 and Set2 respectively, so we performed ChIP-qPCR for Sas3 in strains lacking the methyltransferases singularly and in combination. Mutation of either *SET1* or *SET2* individually resulted in a partial loss of Sas3 at *LOS1, SEC15, NUP145,* and *RPS28A* (Figure 2.5 A). However Sas3 remained enriched over background at these four genes, and was also enriched relative to a repressed gene, *PUT4.* In contrast to the modest loss in the single mutants, the *set1Δ set2Δ* double mutant reduced Sas3 recruitment to background levels, demonstrating that Set1 and Set2 are necessary for Sas3 recruitment to chromatin. Furthermore, the Set1-dependence of Sas3 binding to the mid and 3' regions of *LOS1, SEC15,* and *NUP145* occurred in regions depleted for H3K4me3 (Figure 2.5 B) but enriched for H3K4me2 and H3K4me1 (Figure 2.6), which supports these modifications recruiting Sas3 *in vivo.* Set2-dependent binding of Sas3 occurred at regions containing H3K36me3 (Figure 2.5 C), consistent with this PTM recruiting Sas3 *in vivo.* Additionally, comparing the single to double mutants, Sas3 displayed a stepwise reduction in binding, consistent with H3K36me3 and H3K4me1/2/3 recruiting Sas3 to chromatin in an independent and additive manner.

To test if Sas3 recruitment to chromatin was dependent on the NuA3 domains reported to bind histone methylation we performed ChIP-qPCR for Sas3 in *yng1ΔPHD*, *pdp3Δ*, and

yng1ΔPHD pdp3Δ strains (Figure 2.5 D). The *pdp3Δ* mutant had a similar reduction in Sas3 binding as the *set2Δ* mutant at all but *RPS28A*. However, disrupting H3K36 methylation at this locus caused a reduction in H3K4me3 (Figure 2.7), so the greater loss of Sas3 binding in the *set2Δ* compared to the *pdp3Δ* mutant was likely an indirect effect. Thus we demonstrate for the first time that Pdp3 is necessary for NuA3 recruitment to chromatin *in vivo.* The *yng1ΔPHD* mutation caused a reduction in Sas3 recruitment at 5', mid, and 3' regions, consistent with Yng1 targeting NuA3 to H3K4me3, H3K4me2, and H3K4me1. The *yng1ΔPHD pdp3Δ* double mutant resulted in Sas3 recruitment comparable to the untagged control at all loci tested. Altogether our ChIP-qPCR results support the hypothesis that Sas3 binds to actively transcribed chromatin due to binding of H3K4me1/2/3 and H3K36me3 by the Yng1 PHD finger and the Pdp3 PWWP domain respectively.

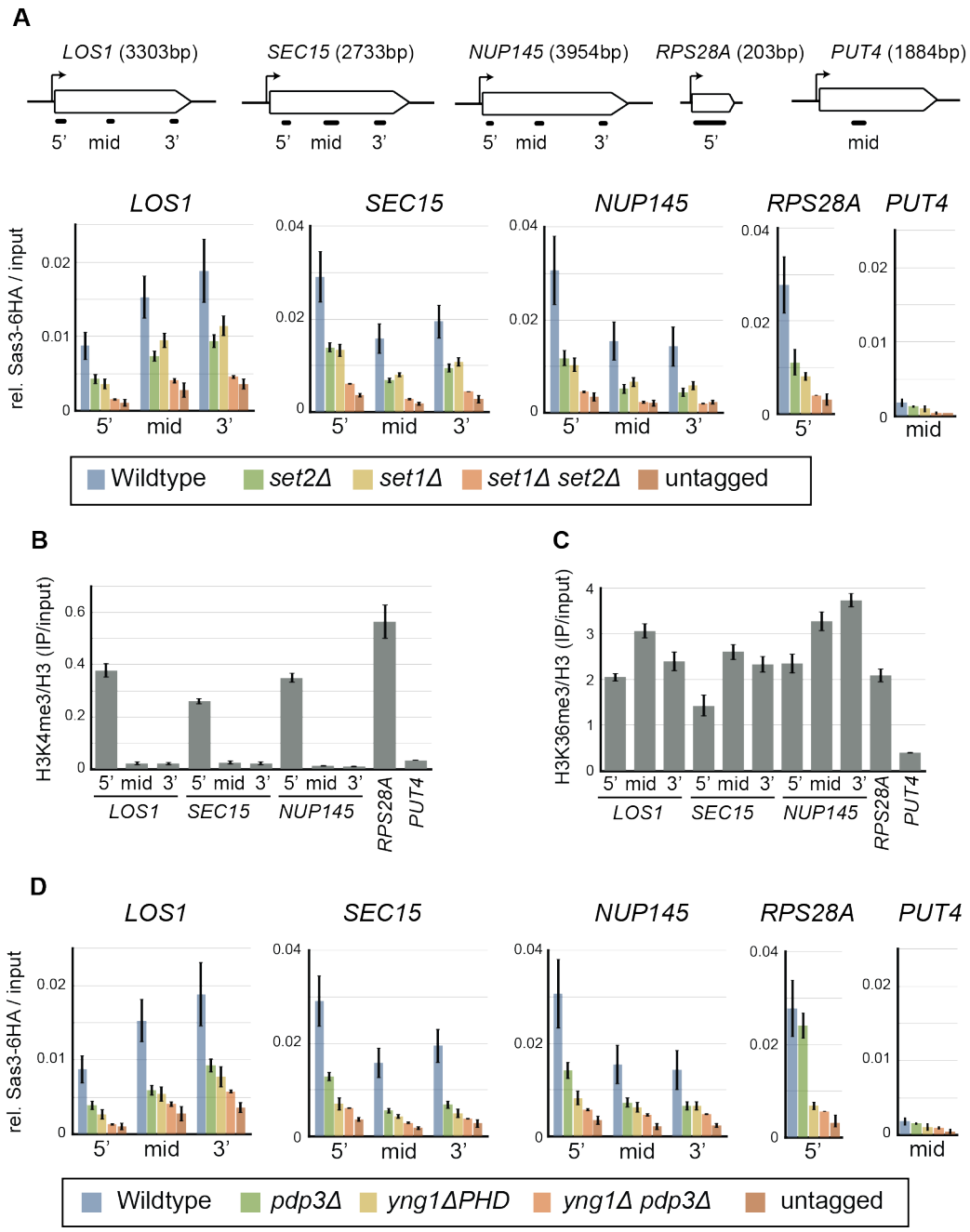

Figure 2.5: H3K4 and H3K36 methylation are necessary for Sas3 binding to active genes through Pdp3 and Yng1 respectively. A, C. Sas3 ChIP-qPCR in the indicated strains at *LOS1, SEC15, NUP145, RPS28A,* and *PUT4*. Primer positions on genes are indicated in the schematic**. B.** H3K4me3 and H3K36me3 ChIP-qPCR in wild type cells.

Values represent the mean of at least three independent replicates. Error bars represent the standard error of the mean.

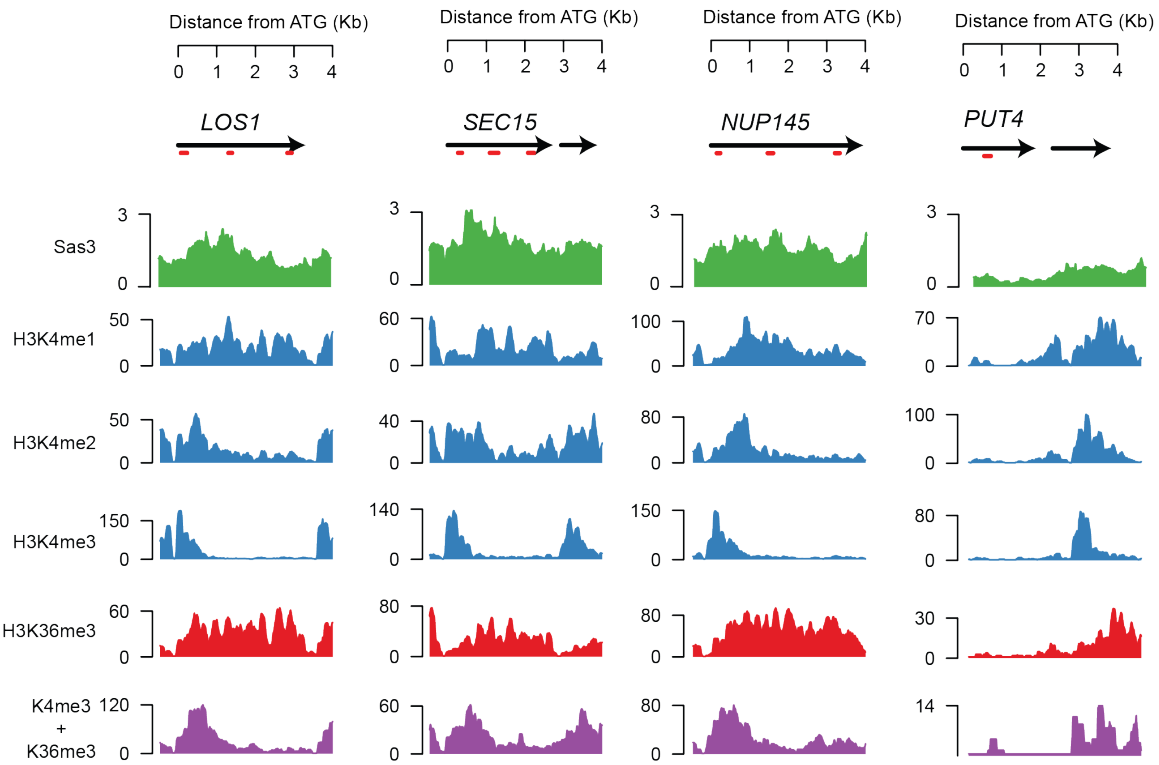

Figure 2.6: Histone methylation and Sas3 at candidate genes. Input-normalized Sas3 and histone methylation ChIP-seq coverage at *LOS1, SEC15, NUP145,* and *PUT4* genes. ChIP-qPCR amplicons are indicated by red bars on the schematic. ChIP-seq data for histone methylation is from (Weiner et al., 2015) and (Sadeh et al., 2016).

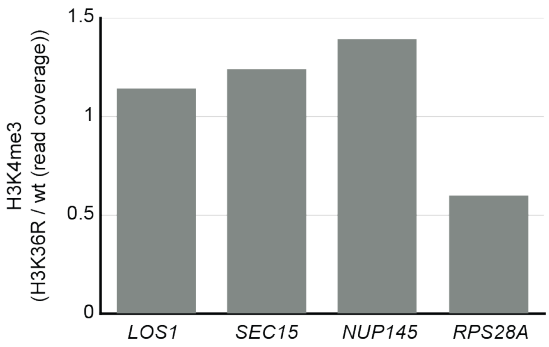

Figure 2.7: H3K4me3 decreases at *RPS28A* when H3K36 methylation is disrupted. H3K4me3 from wild type and H3K36R strains was quantitatively compared by competitive immunoprecipitation (data from Sadeh *et al.* 2016). The amount of H3K4me3 in wild type and H3K36R at 5' qPCR loci (+100 bp on either side to account for the change in resolution) was determined, and the change in methylation is plotted.

2.3.4 Sas3 occupancy does not dictate histone H3K23 acetylation

Histone H3K14 and H3K23 acetylation localize to the 5' ends of genes (Weiner et al., 2015), which is inconsistent with our demonstrated occupancy of Sas3. One explanation for this discrepancy is the presence of the histone deacetylase complex (HDAC), Rpd3S, which deacetylates nucleosomes in the body of transcribed genes (Carrozza et al., 2005; Joshi and Struhl, 2005; Keogh et al., 2005). To test whether HDAC inhibition could reveal acetylation in the bodies of genes, we performed ChIP-seq analysis for H3K23ac in cells treated with the HDAC inhibitor, trichostatin A (TSA) (Figure 2.8 A). Following TSA treatment, H3K23ac spread further downstream of the transcription start site (TSS), but this PTM was still largely restricted to the 5' ends of genes contrary to NuA3 occupancy, which was found across the bodies of genes. Further, deletion of *SAS3* failed

to suppress cryptic transcription initiation of a reporter construct in a strain lacking the TSA-sensitive HDAC, RPD3S (Figure 2.8 B) (Cheung et al., 2008), again suggesting that Sas3 was not responsible for acetylation at downstream targets.

A disconnect between Sas3 occupancy and H3K23ac levels is surprising as it is generally thought that histone acetylation is regulated through control of HAT targeting. To further confirm these observations, we assessed the relationship between Sas3 and H3K23ac at the +1 to +10 nucleosomes, and while we did observe a modest association between Sas3 occupancy and H3K23ac, the predominant determinant of H3K23ac was the nucleosome position relative to the TSS (Figure 2.8 C). H3K23ac decreased into the gene body, and this was largely independent of Sas3 occupancy and was seen with or without TSA treatment. The H3 HAT, Gcn5, with Sas3, is necessary for global H3 acetylation (Howe et al., 2001), and so we asked if Gcn5 occupancy (Xue-Franzén et al., 2013) could explain the disparity between Sas3 occupancy and H3K23ac. Similar to Sas3, Gcn5 displayed a subtle association with H3K23ac, but again this was a modest effect compared to gene position (Figure 2.8 D). We observed similar effects when selecting for nucleosomes enriched for one or both of Sas3 and Gcn5 (Figure 2.9). Thus the lack of association of Sas3 with H3K23ac cannot be explained by Gcn5 occupancy, and the similar lack of association of Gcn5 with H3K23ac suggests that regulating HAT activity post-recruitment may be a general phenomenon. Collectively these results indicate that while histone methylation promotes the association of Sas3 with chromatin in gene bodies, this does not necessarily result in histone acetylation.

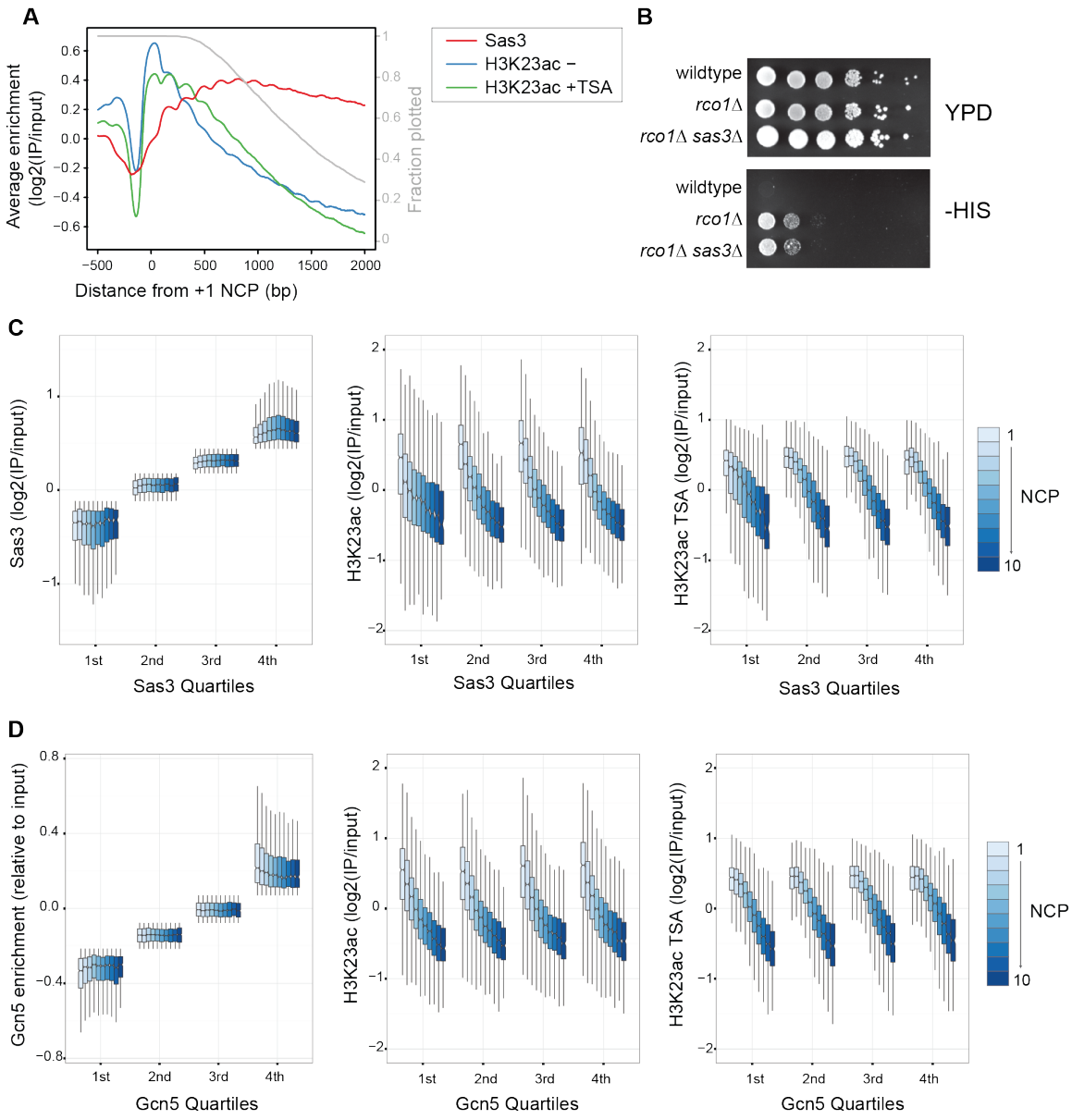

Figure 2.8: Sas3 occupancy does not dictate histone H3K23 acetylation. A. The average enrichment relative to 4264 +1 nucleosomes for Sas3 and H3K23ac before and after 15 minute incubation with 25μM TSA. Cell cycle regulated genes were excluded from this plot. Each gene is only included in the average calculation until its polyadenylation site. The fractions of genes still contributing to the average profile are represented by the gray line. **B.** Ten-fold serial dilutions of the indicated strains containing the *kanMX-GAL1pr-flo8-HIS3* reporter were plated on rich media (YPD) and

complete synthetic media lacking histidine and incubated at 30°C for four days. **C,D.** HAT and H3K23ac before and after TSA enrichments by nucleosome position and by Sas3 (C) or Gcn5 (Xue-Franzén et al., 2013) (D) quartiles, represented as boxplots. Nucleosomes from cell-cycle regulated genes were excluded, leaving 33942 nucleosomes from +1 to +10 positions relative to the TSS. Outliers were not plotted.

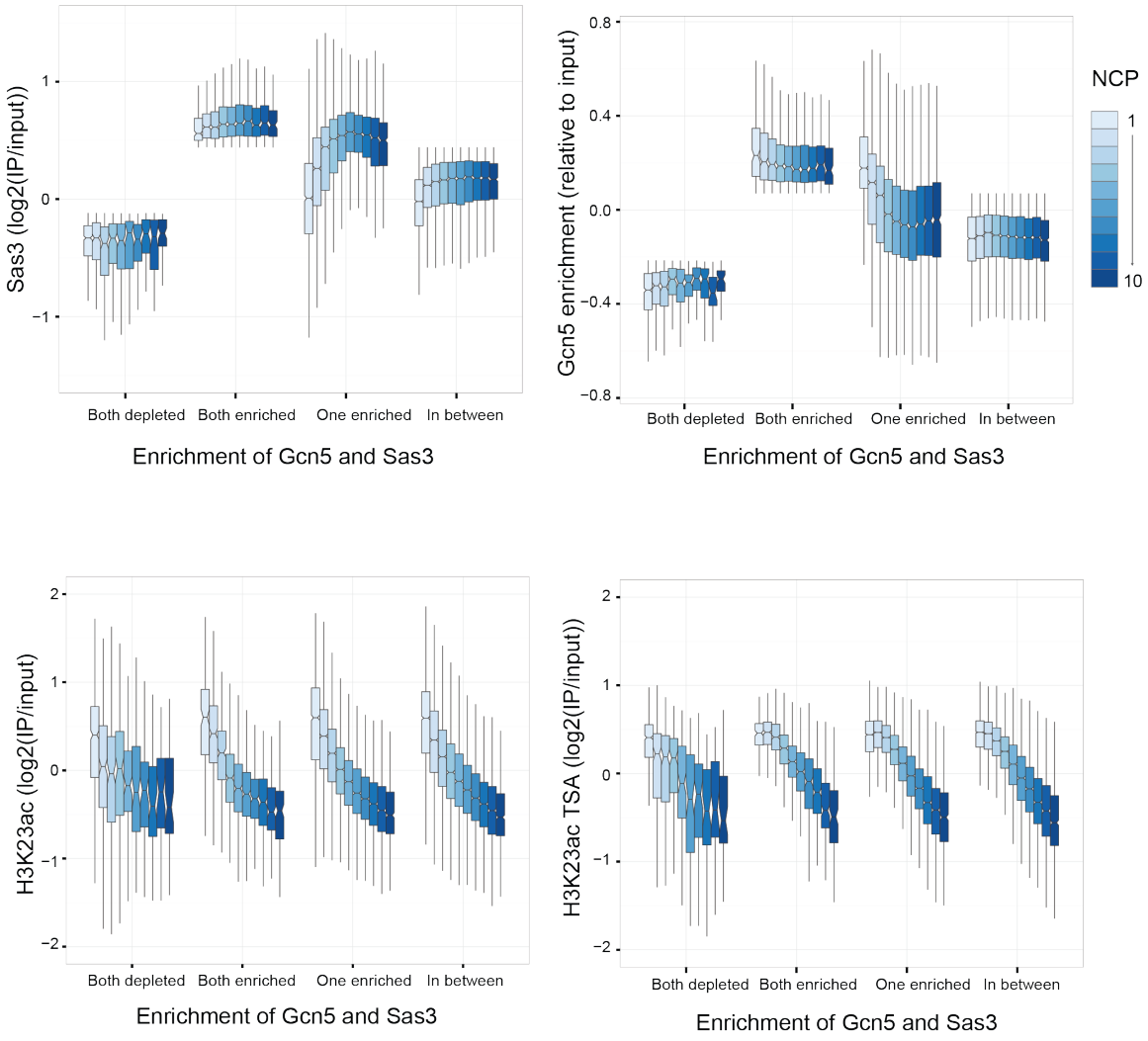

Figure 2.9: Gcn5 and Sas3 enrichment together does not dictate H3K23ac.

Nucleosomes were classified as being enriched or depleted based on being the top or bottom quartile of HAT occupancy respectively. Nucleosomes were grouped as being depleted or enriched for both of Gcn5 or Sas3, enriched for one but not the other, and for not being in one of the above categories. Sas3, Gcn5, and H3K23ac before and after TSA treatment enrichments for each category were visualized by boxplot. Outliers were not plotted. Gcn5 data is from (Xue-Franzén et al., 2013).

2.4 DISCUSSION AND CONCLUSIONS

In this study we investigated the relative contributions of histone PTMs in targeting NuA3 to chromatin. Using both genome-wide and locus-specific approaches we showed that H3K36me3 and H3K4me1/2/3 both independently and additively promoted the association of Sas3 with chromatin. We provide the first *in vivo* evidence for Pdp3 recruiting NuA3 to H3K36 trimethylated chromatin and for Yng1 recruiting NuA3 to H3K4me2 and H3K4me1. The additive effects of H3K36me3 and H3K4me1/2/3 resulted in NuA3 being primarily recruited to the +5 to +7 nucleosomes, approximately 700 bp into the gene. This is close to but slightly further into the gene body than where the mammalian homologue MOZ/MORF is predominantly found, approximately 400 bp downstream of the TSS (Lalonde et al., 2013). This 5' shift in MOZ/MORF localization could be due to the mammalian complex's reduced affinity for H3K4me1 (Champagne et al., 2008) (Table S1) and H3K36me3 (Vezzoli et al., 2010; H. Wu et al., 2011) (Table 2.3), resulting in a much greater dependence on H3K4me2/3 for recruitment to chromatin. The differing methyl-histone binding properties of NuA3 and MOZ/MORF coincide with differing genome-wide localization of H3K4me1 and H3K36me3. With longer mammalian genes H3K36me3 can stretch more than 20 kb from the TSS, while H3K4me1 is associated with enhancers (Barski et al., 2007). Thus the reduction in binding affinity for H3K36me3 and H3K4me1 has maintained MOZ/MORF targeting close to but downstream of the TSS, which suggests a conserved function in this genomic region.

Despite H3K4me3 being enriched at +1 NCP, we found that this nucleosome was relatively depleted of Sas3. As Sas3 is enriched genome-wide at nucleosomes with H3K4me3 in the absence of H3K36me3, it seems unlikely that this depletion is solely due to low H3K36me3. The +1 NCP, however, is a key nucleosome for regulation of transcription and is bound by many protein complexes (Koerber et al., 2009; Mayer et al., 2010; Ramachandran et al., 2015; Rhee and Pugh, 2012; Yen et al., 2013). It is possible that NuA3 is occluded from binding as a result of other factors binding to the H3K4me3 moiety.

Unlike for histone methylation, we found no evidence to support a role for histone acetylation or crotonylation in NuA3 recruitment. While we did not test the effect of loss of acetylation or Taf14 on NuA3 binding, the complete loss of Sas3 recruitment in the absence of H3K4 and H3K36 methylation demonstrated that the YEATS domain was not sufficient for NuA3 recruitment. While it is possible that this domain has no function in NuA3, the retention of acetyl-binding domains in mammalian MOZ/MORF argues for a functional role. It is possible that binding to acetyl or crotonyl lysines of the histone tail may regulate NuA3's activity, similar to the role of histone methylation in stimulating the activity of the Rpd3S deacetylase complex (Govind et al., 2010). Alternatively, regulation could occur through binding to non-histone substrates. Indeed proteomic studies show that Nto1 and Taf14 both contain acetylated lysines (Henriksen et al., 2012), and so it is possible that the YEATS domain is binding to a modified lysine in the NuA3 complex. Such a role is seen for the Rsc4 bromodomain, which binds to an acetylated lysine in the complex to regulate its function (Choi et al., 2008; VanDemark et al., 2007).

Our results showed that Sas3 was localized across the body of transcribed genes, which is inconsistent with the predominantly TSS-proximal patterns of H3K14ac and H3K23ac (Weiner et al., 2015). This is unsurprising however as other studies have shown that HAT occupancy is a poor predictor of histone acetylation (Rossetto et al., 2014; Xue-Franzén et al., 2010). Instead, these results suggest that there is a level of regulation of histone acetylation that is independent of HAT recruitment. Molecular simulation studies predict histone tails to be tightly intertwined with nucleosomal DNA (Z. Li and Kono, 2016; Shaytan et al., 2016), and thus disruption of these interactions may be required for acetylation by available HATs. Interestingly, although RNAPII is also found across gene bodies, NETseq and PAR-CLIP experiments show that RNAPII struggles to transcribe through the 5' ends of genes (Churchman and Weissman, 2011; Schaughency et al., 2014), where the majority of histone acetylation is found. Thus an attractive hypothesis is that histones are acetylated by available HATs in response to DNA unwrapping during slow RNAPII passage. Although other molecular mechanisms could explain our observations, our data underscore the fact that the presence of a histone PTM-binding domain within a chromatin-modifying complex does not ensure that the associated enzymatic activity will function on all nucleosomes with the requisite PTM.

The lack of histone tail acetylation associated with NuA3 or Gcn5 binding in mid and 3' gene regions does not exclude the possibility that these HATs function in elongation in a histone-tail-independent manner. Histone acetyltransferases have been shown to acetylate many non-histone substrates, and recruitment to gene bodies may in fact regulate

transcription through acetylation of other proteins. In support of this hypothesis the *S. pombe* homologue of Sas3, Mst2, was recently shown to acetylate an H2B ubiquitin ligase (Flury et al., 2017). This acetylation promotes the ligase activity and positively regulates transcription elongation. Interestingly, H2B ubiquitin is important for di and trimethylation of H3K4 (Briggs et al., 2002; Dover et al., 2002; Z.-W. Sun and Allis, 2002) (J.-S. Lee et al., 2007), and so H3K4 di and trimethylation may function with Sas3 and H2B ubiquitin in a positive feedback loop. Acetylation of the H2B ubiquitin ligase is but one example of a non-histone acetyltransferase role in transcription elongation.

CHAPTER 3 – THE MAJORITY OF HISTONE ACETYLATION IS DEPENDENT ON RNAPII

3.1 INTRODUCTION

Lysine acetylation of histone amino terminal tails has long been linked with gene expression. *In vitro* transcription first suggested a relationship in 1964 (Allfrey et al., 1964), and in the following decades time course and fractionation experiments demonstrated the *in vivo* spatial and temporal enrichments of acetylated histones in transcribed chromatin (Davie and Candido, 1978; Pogo et al., 1968; 1966). More recently, genome-wide localization studies across eukaryotes, including yeast and mammals, revealed that histone tail acetylation primarily occurs at the promoters and 5' ends of transcribed genes (Pokholok et al., 2005; Z. Wang et al., 2008). Although terms such as "global" and "non- targeted" have been used to refer to some forms of acetylation (Friis and Schultz, 2009; Vogelauer et al., 2000), genome-wide occupancy studies show that histone acetylation levels correlate strongly with transcription, implicating a causal relationship between the two.

Histone tail acetylation is catalyzed by conserved histone acetyltransferases (HATs), generally consisting of a catalytic subunit complexed with auxiliary subunits required for enzymatic activity and targeting (reviewed in (K. K. Lee and Workman, 2007) and (L. Wang et al., 2008)). Most HAT complexes preferentially modify multiple lysine residues within either H3 or H4. Consistent with this relatively low substrate specificity, histone

acetylation sites within H3 and H4 generally show similar distributions genome wide (Rando, 2012; Z. Wang et al., 2008; Weiner et al., 2015), and mutations of histone lysine residues, with the exception of H4K16, result in comparable changes in gene expression (Dion et al., 2005; A. M. Martin et al., 2004). Nuclear HATs, defined by their catalytic subunits, fall into three main categories. The GCN5-Related N-acetyltransferases (GNAT) HATs include Gcn5 in yeast and Gcn5 and PCAF in humans. The MYST family of HATs includes Esa1, Sas2, and Sas3 in yeast, and MOZ, MOF, HBO1, and Tip60 in humans. The p300/CBP family includes paralogues p300 and CBP in mammalian cells, which do not have yeast homologues, and Rtt109 in yeast. Histone acetylation is a dynamic mark with a relatively short half-life (Waterborg, 2002; Zheng et al., 2013) due to the activity of histone deacetylase complexes (HDACs). Similar to HATs, HDACs generally exist as multi-protein complexes with a catalytic subunit that can deacetylate multiple lysines on one or more histones (X.-J. Yang and Seto, 2008).

In *S. cerevisiae*, the most well characterized HAT complexes are SAGA and NuA4, which are major HATs for H3 and H4 respectively. These HATs are directed to gene promoters via an interaction between a shared subunit, Tra1, and DNA-bound transcriptional activators (C. E. Brown et al., 2001; Grant et al., 1998), which is thought to target acetylation of nucleosomes flanking promoters. This, together with the observation that these HATs are required for pre-initiation complex formation at multiple genes (Bhaumik and M. R. Green, 2002; H. Qiu et al., 2004; Reid et al., 2000), has led to the widely accepted hypothesis that histone acetylation acts “upstream” of transcription. It should be noted however that, in addition to canonical histones, SAGA and NuA4 have

been shown to acetylate many non-histone proteins involved in transcription initiation (Choi et al., 2008; Downey et al., 2015; 2013; J.-H. Kim et al., 2010; Mitchell et al., 2013; VanDemark et al., 2007). As such, whether SAGA and NuA4 activate transcription primarily through acetylation of the core histones remains uncertain.

While the current model is widely accepted, there are numerous examples of histone acetylation being deposited as a consequence of transcription. Numerous HATs interact with H3K4me3 (Bian et al., 2011; D. G. E. Martin et al., 2006; X. Shi et al., 2007), which occurs cotranscriptionally (Krogan et al., 2003a; J.-S. Lee et al., 2007; Ng et al., 2003; Wood et al., 2003), providing one mechanism for histone acetylation to occur as a consequence of transcription. Furthermore, both the SAGA and NuA4 HATs in yeast and the PCAF and Tip60 HATs in mammals bind the phosphorylated RNAPII CTD (Ginsburg et al., 2009; Govind et al., 2007; Obrdlik et al., 2008; Z. Wang et al., 2009), and cotranscriptional histone exchange mediates incorporation of acetylated histones into nucleosomes within transcribed regions (Venkatesh et al., 2012). Recent work has also shown that RNA can promote the activity of CBP at enhancers (Bose et al., 2017). Taken together these observations are consistent with the model that histone acetylation occurs as a consequence, rather than a cause, of the transcription process.

In this study we sought to determine the relative contributions of the “causal” vs “consequential” pathways for targeting histone acetylation to transcribed genes. Surprisingly, we found that in both yeast and mammals, histone acetylation is much more tightly linked to RNAPII occupancy than previously believed. Notably, acetylation

upstream of promoters, which had previously been attributed to activator targeting (Z. Nagy and Tora, 2007), is associated more closely with divergent transcription. Furthermore, using multiple approaches, we show that yeast RNAPII, rather than being uniformly distributed across the transcription unit, as previously described, is actually enriched in 5' regions, in association with histone acetylation. Additionally, inducing RNAPII stalling and backtracking with a dominant negative TFIIS yeast mutant increased histone acetylation in gene bodies. Furthermore in both yeast and mESCs, the majority of histone tail acetylation was lost upon inhibition of transcription, strongly supporting the model that histone acetylation is deposited as a consequence of RNAPII occupancy. Finally we found that HAT recruitment in *S. cerevisiae* is not sufficient for histone acetylation, indicative of post-recruitment regulation of acetyltransferase activity. Specifically, we show that NuA4 recruitment to upstream activation sequences of both Taf1 depleted and enriched promoters occurs in the absence of acetylation, suggesting that NuA4 function in these regions may be independent of histone tail acetylation. Taken together, the results of this study demonstrate that the majority of histone acetylation occurs as a consequence of the association of RNAPII with chromatin during transcription.

3.2 MATERIALS AND METHODS

3.2.1 Yeast strains and plasmids

All strains used in this study were isogenic to S288C, and are listed in Table 3.1. Yeast culture and genetic manipulations were performed using standard protocols. Genomic deletions were verified by PCR analysis and whole cell extracts were generated as

previously described (Kushnirov, 2000). The Rpb1 anchor away strain was generously provided by Craig Peterson, and the TFIIS plasmids were generously provided by Jesper Q. Svejstrup.

Table 3.1: Yeast Strains used in this study

Strain	Parent	Mating type	Genotype	Source
YLH101	FY602	Mat a	*his3D200 leu2D1 lys2-128d ura3-52 trp1D63*	
YLH787	YLH101	Mat a	*his3D200 leu2D1 lys2-128d ura3-52 trp1D63 bar1::KAN*	
YLH404	YLH101	Mat a	*his3D200 leu2D1 lys2-128d ura3-52 trp1D63 rpd3::TRP*	
YLH828	YLH101	Mat a	*his3D200 leu2D1 lys2-128d ura3-52 trp1D63 EPL1-6HA*	
YLH602	YLH101	Mat a	*his3D200 leu2D1 lys2-128d ura3-52 trp1D63 kin28as*	
YLH601	YLH101	Mat a	*his3D200 leu2D1 lys2-128d ura3-52 trp1D63 KIN28*	
YLH220	YLH101	Mat a	*his3D200 leu2D1 lys2-128d ura3-52 trp1D63 set1::HISMX6*	
YLH644	YLH101	Mat a	*his3D200 leu2D1 lys2-128d ura3-52 trp1D63 asf1::HIS*	
YLH882	YLH101	Mat a	*his3D200 leu2D1 lys2-128d ura3-52 trp1D63 def1::KAN*	
Y40353		Mat @	*tor1-1 fpr1::NAT RPL13A-2xFKBP12::TRP1 RPO21-FRB::kanMX6*	Euroscarf
YLH559	YLH101	Mat a	*his3D200 leu2D1 lys2-128d ura3-52 trp1D63 hos2::KAN*	
YLH556	YLH101	Mat a	*his3D200 leu2D1 lys2-128d ura3-52 trp1D63 set3::KAN*	
YAC41	YLH101	Mat a	*his3D200 leu2D1 lys2-128d ura3-52 trp1D63 hda1::KAN*	
YLH562	YLH101	Mat a	*his3D200 leu2D1 lys2-128d ura3-52 trp1D63 hst1::KAN*	
YLH561	YLH101	Mat a	*his3D200 leu2D1 lys2-128d ura3-52 trp1D63 sir2::KAN*	
YLH975	YLH101	Mat a	*his3D200 leu2D1 lys2-128d ura3-52 trp1D63 SPT16-HA6::HIS3*	

Table 3.2: Plasmids used in this study

Plasmids	Parent	Description	Source
pYC2/CT		Invitrogen Gal expression vector (URA3 marker)	(Sigurdsson et al., 2010)
A7-28	pYC2/CT	pGAL TFIIS wt	(Sigurdsson et al., 2010)
A7-29	pYC2/CT	pGAL TFISmut	(Sigurdsson et al., 2010)

3.2.2 Cell lines and cell culture

FUCCI reporter mESCs (a kind gift from M. Lorincz) (Carol C L Chen et al., 2017) were grown in standard feeder-free conditions in complete mESC media: Dulbecco Modified Eagle's Medium (DMEM) high glucose, 15% fetal bovine serum (HyClone Laboratories), 20 mM HEPES, 1 mM L-glutamine, 100 U/ml penicillin-streptomycin,1 mM nonessential amino acids, ~10-50 ng/ml of recombinant LIF, 1 mM sodium pyruvate and 0.1 mM β-mercaptoethanol on 0.2% type A gelatinized tissue culture plates.

3.2.3 Drug treatments

Yeast drug treatments were performed in YPD media at the following concentrations: 1,10 phenanthroline monohydrate (400 μg/mL in ethanol), thiolutin (10 μg/mL in DMSO), 1-Naphthyl PP1 (5 μM in DMSO), trichostatin A (25 μM in DMSO), α factor (10 μM, in 100 mM sodium acetate, pH=5.2). mESCs were treated with Actinomycin D at 25 μg/mL (in DMSO).

3.2.4 Immunoblot analysis

Whole cell lysates or cellular fractions were analyzed by SDS-PAGE using the antibodies listed in table 3.3. Blots were scanned and fluorescent signal quantified using the Licor Odyssey scanner.

3.2.5 Sonicated ChIP-seq

Yeast cells, grown to mid-log in YPD, were arrested in G1 by three-hour treatment with 10 μM alpha factor. Cell synchronization was verified by cell "shmooing," as seen under the microscope. For transcription inhibition, cells were treated with 400 μg/mL 1,10 phenanthroline monohydrate for 15 minutes. Cells were crosslinked in 1% formaldehyde for 15 minutes and quenched with 125 mM liquid glycine for a further 15 minutes.
For sonicated ChIP-seq, cells were lysed by bead beating, and cell lysate was spun down at 15,000g for 30 minutes. The pellet was resuspended in lysis buffer (50 mM HEPES, pH 7.5, 140 mM NaCl, 0.5 mM EDTA, 1% Triton X-100, 0.1% sodium deoxycholate) and sonicated (Biorupter, Diagenode) to produce an average fragment size of 250 bp. The lysate was spun down at 9,000g for 10 minutes, and the supernatant was precleared by rotating with Protein G Dynabeads for 1 hour at 4 °C. 20% of the lysate was reserved for input, and the remaining was split into two and incubated with α-HA or α-Rpb3 antibodies overnight at 4 °C. Magnetic Protein G Dynabeads were added for 1 hour, and 5 minute washes were performed twice with lysis buffer, twice with high salt buffer (50mM HEPES pH 7.5, 640mM NaCl, 1mM EDTA, 2% Triton X-100, 0.2% Na-deoxycholate), twice with LiCl wash buffer (10mM Tris-HCL pH 8.0, 250mM LiCl, 0.6% NP-40, 0.5% Na-deoxycholate, 1mM EDTA), and once with TE. Synthetic spike-in

DNA was added to eluates. Following proteinase K digestion, DNA was purified by PCI and RNase A treated. Libraries for paired-end sequencing were constructed as described previously (Maltby et al., 2012), and 100nt paired-end sequencing was performed on a HiSeq 2500.

3.2.6 MNase ChIP-seq

Yeast cells, grown to mid-log in YPD, were arrested in G1 by three hour treatment with 10 μM alpha factor. Cell synchronization was verified by cell "shmooing," as seen under the microscope. For transcription inhibition, cells were treated with 400 μg/mL 1,10 phenanthroline monohydrate for 15 minutes. Cells were crosslinked in 1% formaldehyde for 15 minutes and quenched with 125 mM liquid glycine for a further 15 minutes.
For MNase ChIP-seq, cells were lysed by bead beating, and cell lysate was spun down at 15,000g for 30 minutes. The pellet was washed and resuspended in MNase digestion buffer (0.5 mM spermidine, 1 mM β-ME, 0.075% NP-40, 50 mM NaCl, 10 mM Tris pH 7.4, 5 mM MgCl2, 1 mM $CaCl_2$). Samples were incubated with 100 units of MNase for 10 minutes at 37 °C. Lysates were clarified by centrifugation at 9000g for 10 minutes. To extract insoluble chromatin, pellets were re-suspended in 200 μL of lysis buffer with 0.2% SDS, and sonicated in a Diagenode Bioruptor at medium output for 30 seconds on and 30 seconds off for four cycles, before centrifugation at 9000g for 10 minutes. The second supernatant was pooled with the first, and the buffer composition of the lysate was adjusted to that of the original lysis buffer (50mM HEPES pH 7.5, 140mM NaCl, 1mM EDTA, 2% Triton X-100, 0.2% Na-deoxycholate, 1X Roche protease inhibitor cocktail, 1mM PMSF). Ten percent of the lysate was reserved for input, and immunoprecipitations

were performed using α-HA, α-H3K23ac, α-H4K12ac, α-H4K8ac, or α-H3K9ac antibodies. DNA purification and libraries were prepared as per the sonicated ChIP-seq experiments.

3.2.7 Analysis of ChIP-seq data

Adapter sequences were removed from paired-end fastq files using cutadapt (M. Martin, 2011), before aligning to the saccer3 genome using BWA (H. Li and Durbin, 2010). Aligned reads were filtered for mapped and paired reads passing a quality filter of 10 using samtools (H. Li et al., 2009). Fragment coverage across the genome was calculated using BEDtools (Quinlan and Hall, 2010), and wig files generated using the java genomics toolkit (Palpant, 2011). For IP over input tracks, a value of 1 coverage per million fragments was added to both to avoid division by 0, and the resultant track was smoothed with a 10bp moving average window and log2 transformed. Replicates were pooled for subsequent analysis.

Similar to other groups (Petrenko et al., 2017; 2016; Steunou et al., 2016), ChIP-seq datasets comparing across RNAPII perturbations were normalized to silent regions. The genome was divided into 250 bp bins, bins outside the interquartile range for coverage in the input were discarded, the 100 regions with the lowest Rpb3 signal were defined as silent regions, and these silent regions were used to normalized ChIP-seq datasets for cross-condition comparisons. We also added synthetic DNA spike-ins to our ChIP eluates and inputs, but this approach to normalization did not work well for all samples, possibly due to low coverage of the spike-ins in some samples.

For transcribed nucleosomes classified by Rpb3 change upon 1,10-pt treatment (Figure 5G and S5E), genome-wide nucleosome positions (Weiner et al., 2015) with Rpb3 signal greater than the median were classified as transcribed. Nucleosomes where Rpb3 changed by less than 10 % were classified as "Rpb3 stable", while those decreasing by at least 3x were classified as "Rpb3 lost". Boxplots represent the 1st to 3rd quartiles, with whiskers extending to 1.5 times the interquartile range or to the extreme of the data. Notches are equal to +/- 1/58 IQR /sqrt(n), giving an approximation of the 95% confidence interval for the difference in 2 medians.

3.2.8 Accessing of publically available datasets mammalian datasets

For H1-hESCs, processed ChIP-seq data for histone acetylation and methylation were downloaded from the IHEC data portal (Bujold et al., 2016) and replicates were pooled using the UCSC BigWigMerge tool. Processed MNase-seq (Yazdi et al., 2015) GRO-seq (Yupeng Chen et al., 2014) data were downloaded from GEO accession GSM1194220 and GSM1503828 respectively. For IMR90 cells, processed ChIP-seq data for histone acetylation and methylation were downloaded from the IHEC data portal (Bujold et al., 2016) and replicates were pooled using the UCSC BigWigMerge tool. Processed GRO-seq data (Danko et al., 2015) were downloaded from GEO accession GSE66031. MNase-seq (Gaidatzis et al., 2014) fastq files were downloaded from SRP019045, aligned to hg19 genome using bowtie2 (Langmead and Salzberg, 2012), and quality filtered using samtools (H. Li et al., 2009). Replicates were pooled, aligned sequences extended to 150bp and converted to bedgraph using bedtools (Quinlan and Hall, 2010). For K562 cells, processed ChIP-seq data for histone acetylation and methylation were downloaded

from the IHEC data portal (Bujold et al., 2016) and replicates were pooled using the UCSC BigWigMerge tool. Processed non heat shock H4ac ChIP-seq and PRO-seq data (Vihervaara et al., 2017) was downloaded from GEO accession GSE89382 and GSE89230 respectively. For HeLaS3 cells, aligned BAM files for histone acetylation and methylation downloaded from ENCODE. BAM files were converted to BED, reads were extended to 250bp, and converted to bedgraph using BEDTools. Processed NET-seq bedgraph files (Mayer et al., 2015) were downloaded from GEO accession GSM1505438. For mESCs, processed ChIP-seq data for histone acetylation and methylation were downloaded from the IHEC data portal (Bujold et al., 2016) and replicates were pooled using the UCSC BigWigMerge tool. Processed GRO-seq data (Jonkers et al., 2014) was downloaded from GEO accession GSE48895. Processed H4ac data from (Gonzales-Cope et al., 2016) was downloaded from GEO accession GSE76760 and replicated were pooled. For MEFs, processed bigWig files for H3K27ac, H3K4me1, and H3K4me3 were downloaded from ENCODE. Aligned BED file for H3K9ac (Kraushaar et al., 2013) was downloaded from GEO accession GSE51505. H4ac ChIP-seq fastq files (Conerly et al., 2016) were downloaded from SRA study SRP066628. Reads were aligned to mm9 genome using bowtie2 (Langmead and Salzberg, 2012) and quality filtered using samtools (H. Li et al., 2009). Replicated were pooled, aligned sequences extended to 250bp and converted to bedgraph using bedtools (Quinlan and Hall, 2010).

3.2.9 Accessing of publically available datasets yeast datasets

Histone modification ChIP-seq data (tp0) from (Weiner et al., 2015) was downloaded as fastq files from SRA study SRP048526 and mapped to saccer3 using BWA (H. Li and

Durbin, 2010). Aligned reads were extended to 147bp using BEDTools (Quinlan and Hall, 2010) and converted to wig coverage tracks using java-genomics-toolkit (Palpant, 2011). A coverage score of 1 per million reads was added to both the IP and input to avoid dividing by zero, before diving the IPs by the matching input files. IP over input tracks were smoothed using a 10bp moving average window and log2 transformed using Java genomics toolkit (Palpant, 2011). For H3K18ac ChIP-seq in wildtype and H3K4R strains (Sadeh et al., 2016), fastq files were downloaded from SRA study SRP078243. Reads were aligned to saccer3 using BWA, and aligned reads were extended to 147bp using bedtools. Coverage over genome-wide nucleosome positions was normalized for MNase coverage calculated from (Weiner et al., 2015). For Rpb2 PAR-clip experiments (Schaughency et al., 2014), fastq files were downloaded from the SRA study SRP040778. Reads were aligned to saccer3 using BWA, and reads mapping to tRNA regions were removed using BEDtools. Remaining reads were converted to stranded wig coverage tracks using AWK and the Java genomics toolkit (Palpant, 2011). For Rpb3 ChIP-exo experiments (Van Oss et al., 2016) fastq files were downloaded from SRA study SRP076548. Reads were aligned to saccer3 using the BWA mem algorithm (H. Li and Durbin, 2010). The crosslinking point was taken as the first nucleotide sequenced from the 1st read of the read pair. The Java genomics toolkit (Palpant, 2011) was used to generate wig coverage tracks of crosslinking points, pool replicates, and apply a Gaussian smoothing curve using a standard deviation of 3 bp. For other sequencing datasets, the fastq files for Set1 ChIP-seq (S. Li et al., 2015), RNAPII ChIP-seq (Wong et al., 2014), sonicated H3K9ac ChIP-seq (Bonnet et al., 2014), H4K8ac ChIP-seq in wildtype and *yng2W254A* strains (Steunou et al., 2016), and RNAPII ChIPseq and 4tU-seq (Schulz et

al., 2013) were downloaded from SRA studies SRP063896, SRP036647, SRP033513, and SRP070154 and from Array Express accession E-MTAB-1766 respectively. Fastq files were quality filtered and adapter sequences removed using cutadapt (M. Martin, 2011), before aligning to the saccer3 genome using BWA (H. Li and Durbin, 2010). For single end sequencing experiment, the aligned reads were extended to reported fragment length using BEDtools. Fragment coverage was calculated and files converted to wig coverage tracks using the Java genomics toolkit (Palpant, 2011). Processed data for Mediator ChIP-seq (Petrenko et al., 2016), NET-seq (Harlen et al., 2016), chromatin RNA-seq (Harlen et al., 2016), and RNA-seq (Harlen et al., 2016), Gcn5 ChIP-chip (Xue-Franzén et al., 2013), PRO-seq (Booth et al., 2016), RNAPII CRAC-seq (Milligan et al., 2016) and H2A.Z ChIP-seq experiments were downloaded from GEO series GSE82082, GSE68484, GSE68484, GSE68484, GSE36600, GSE76142, and GSE69676 and from Dryad under the Digital Object Identifier: doi:10.5061/dryad.dj782 respectively. The predicted probability of nucleosome occupancy data (N. Kaplan et al., 2009) was downloaded as a normalized wig file from *Saccharomyces* Genome Database (Cherry et al., 2012).

3.2.10 Accessing published genome annotation datasets

For genome annotations, genome-wide nucleosome positions were downloaded from the supplemental files of (Weiner et al., 2015). For +2, +3, and +4 nucleosome positions, called nucleosome positions from chemical mapping of dyads (Brogaard et al., 2012) were assigned a nucleosome position relative to the TSS (D. Park et al., 2014). The +1 NCP was called as the nucleosome positions (Brogaard et al., 2012) closest to the TSS

(D. Park et al., 2014). Transcript start sites and polyadenylation sites were downloaded from supplementary data of (D. Park et al., 2014). TATA and TATA-like element locations, as well as Taf1 enrichment, were downloaded from supplementary data of (Rhee and Pugh, 2012).

3.2.11 Statistical analysis of histone acetylation flanking promoters

We quantified the average enrichment for ChIP-seq IPs and inputs and strand-specific RNAPII data (GRO-seq, PRO-seq, or NET-seq) in 500 bp windows spanning from 0 to 500 bp or -100 to -600 bp relative to the TSS (having collapsed overlapping TSSs into one entry in the TSS dataset). We then removed genes with very low or high coverage in the input to remove cases with poor recovery, copy number variations, or sequencing biases, before selecting for genes in the 70 – 95 % range of downstream RNAPII reads (transcribed genes). We classified transcribed genes as having promoters with high or low divergent transcription as being those in the bottom or top quartile for upstream divergent RNAPII reads. For a histone PTM at a promoter, the ratio of upstream to downstream signal is defined as the bidirectional profile. The average ratio for promoters with high or low divergent transcription was calculated and compared to 10,000 random samplings of transcribed genes. The mean and standard deviation of the random set was used to generate a Z-score of enrichment and p-value for the significance (similar to (Gossett and Lieb, 2012)). The p-value was adjusted for multiple testing using the p.adjust function in R to calculate the FDR.

3.2.12 Smoothed scatter plots

Smoothed scatter plots were plotted in R using a custom script using the smoothScatterCalcDensity function. The plot area is split into 500 bins and smoothed by transforming the data by the square root.

3.2.13 Antibodies

Antibodies in ChIP and immunoblot experiments are listed in Table 3.3.

Table 3.3: Antibodies used in this study

Antibody (epitope recognized)	Company	Product and Lot numbers	Notes
H3K4me3	Abcam	ab1012, lot #1276040	Mouse monoclonal
H3K9ac	(H. Kimura et al., 2008)	CMA305	Mouse monoclonal
H3K14ac	GeneScript	Affinity-purified rabbit polyclonal antibody	Raised against acetylated H3K14 peptide
H3K18ac	Abcam	ab1191	Rabbit polyclonal
H3K23ac	Active Motif	39131, lot # 1008001	Rabbit polyclonal
H4K5ac	Millipore	07-327, lot # 2524676	Rabbit polyclonal
H4K8ac	Abcam	ab45166, clone # EP1002Y	Rabbit monoclonal
H4K12ac	Active Motif	39165, lot # 1008001	Rabbit polyclonal
H4K16ac	Millipore	07-329, lot # 2506422	Rabbit polyclonal
H3	GeneScript	Affinity-purified rabbit polyclonal antibody	Raised against scH3 peptide (CKDILARRLRGERS)
H4 (C-terminal region)	Abcam	ab31830, myeloma: Sp2/0-Ag14	Mouse monoclonal
IgG	Millipore	PP64, lot # LV1602263	Purified rabbit IgG
HA	Roche	12CA5, lot # 11849700	Mouse monoclonal
Rpb3	Biolegend	665004, clone number: EP1002Y	Mouse monoclonal
3e8 (ser5p)	Millipore	04-1572, lot # 2585825	Rat IgG2ak monoclonal

3.3 RESULTS

3.3.1 Histone acetylation in mammals is tightly linked with RNAPII occupancy

Nucleosomes flanking transcriptionally active promoters are highly acetylated. This lack of "directionality" is more consistent with activator targeting, as opposed to acetylation targeting as a consequence of transcription. Pervasive divergent transcription, however, confounds a simple attribution of upstream acetylation to activator targeting, and upon accounting for divergent transcription recent studies in mammalian cells have shown that H3K27ac is depleted upstream of unidirectional active promoters (Lacadie et al., 2016; Scruggs et al., 2015). To see if this depletion is a general feature of histone acetylation in mammals, we analyzed published data from human and mouse cells. Using strand-specific high-resolution mapping of RNAPII, we identified transcribed genes with high or low levels of divergent transcription and assessed the profile of histone acetylation flanking the TSS. In human IMR90, H1-hESC, HeLa, and K562 cells (Figure 3.1, 3.2, Table 3.4) we found that acetylation on histones H3 and H4 upstream of promoters occurs almost exclusively with divergent transcription and is depleted in genes showing unidirectional transcription. Notably, acetylation of different residues on H3 and H4 behaved similarly, suggesting a common mode of regulation. Furthermore the enrichment with divergent transcription for histone acetylation was comparable to the co-transcriptional modification H3K4me3. Similar results were seen in mouse cells (Figure 3.3, Table 3.4), demonstrating that in mice and humans histone acetylation is tightly linked with RNAPII occupancy flanking promoters.

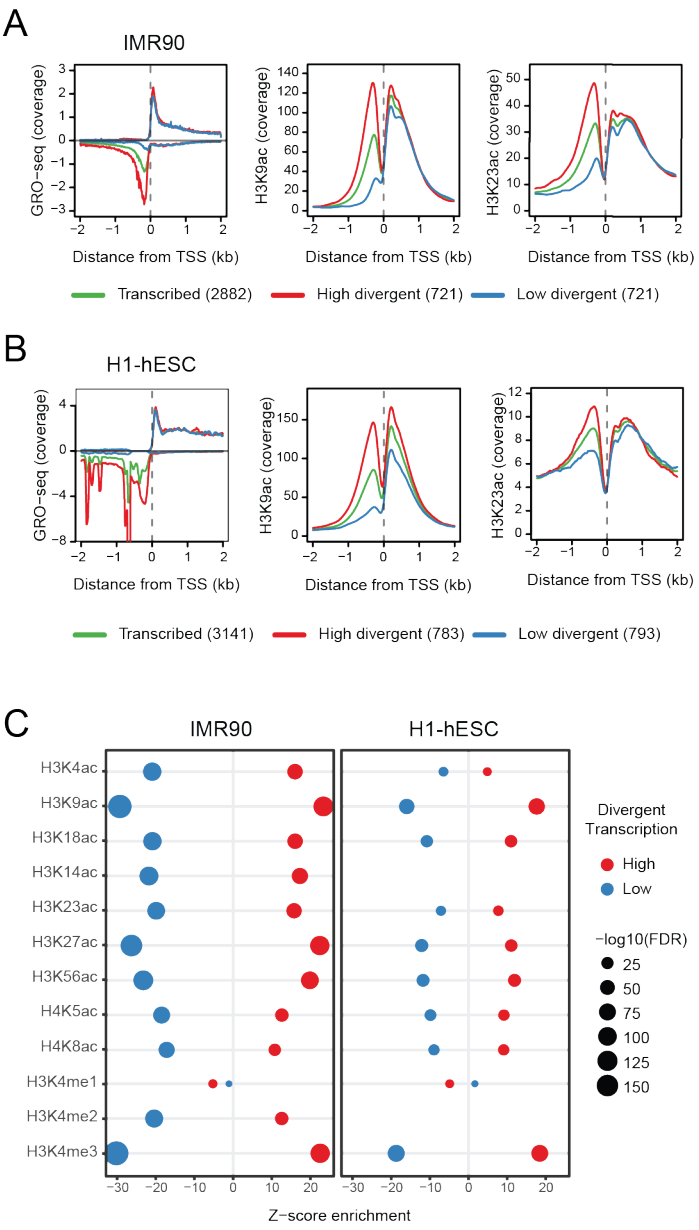

Figure 3.1: Histone acetylation flanking promoters in human IMR90 and H1 ES human cells is tightly linked with RNAPII occupancy. A, B. The average sequence coverage relative to the transcription start sites for GRO-seq (Yupeng Chen et al., 2014), H3K9ac, and H3K23ac (Hawkins et al., 2010; Leung et al., 2015) in IMR90 (A) and H1 ES (B) cells at transcribed genes with high and low divergent transcription. **C.** IMR90 and H1-hESC bidirectional enrichment of histone PTMs for genes with high and low

divergent transcription relative to transcribed gene groups from A and B. Z-scores and FDR values are listed in table 3.4.

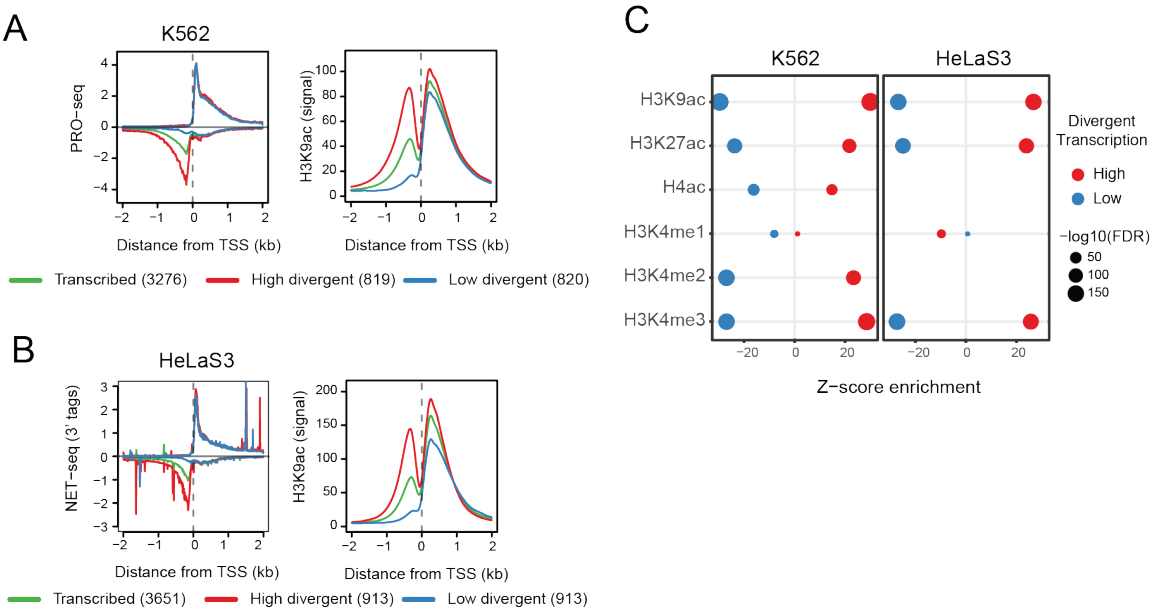

Figure 3.2: Histone acetylation flanking promoters in human cancer cell lines is tightly linked with RNAPII occupancy. A, B. The average sequence coverage relative to the transcription start sites for PRO-seq (A) (Vihervaara et al., 2017), NET-seq (B) (Mayer et al., 2015), and H3K9ac (Hawkins et al., 2010; Leung et al., 2015) in K562 (A) and HeLaS3 (B) cells at transcribed genes with high and low divergent transcription**. B**. K562 and HeLaS3 bidirectional enrichment of histone PTMs for genes with high and low divergent transcription relative to transcribed gene groups from A and B. Z-scores and FDR values are listed in table 3.4.

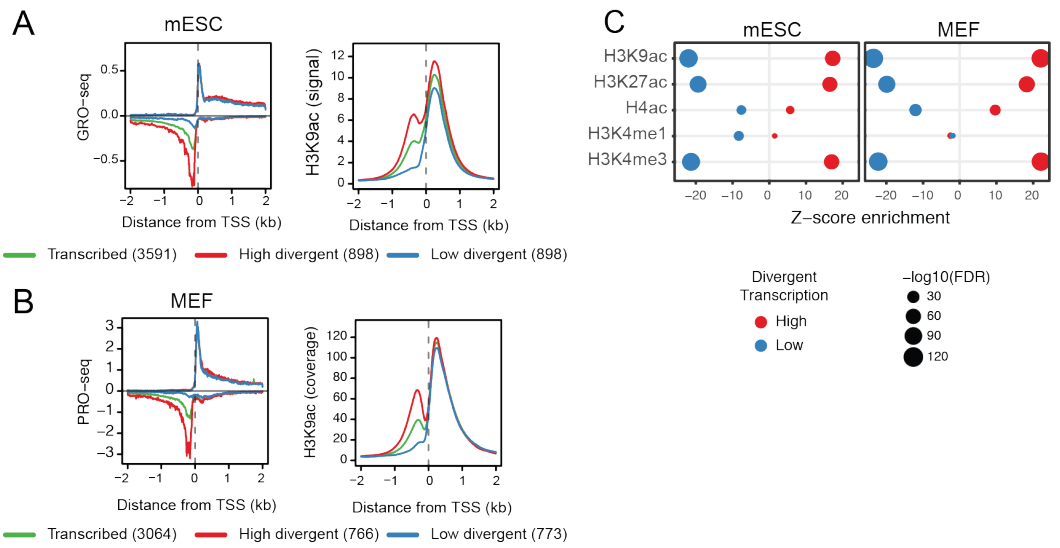

Figure 3.3: Histone acetylation flanking promoters in mouse cells is tightly linked with RNAPII occupancy. A, B. The average sequence coverage relative to the transcription start sites for GRO-seq (A) [ref], PRO-seq [ref] (B), and H3K9ac (Hawkins et al., 2010; Leung et al., 2015) in mESC (A) and MEF (B) cells at transcribed genes with high and low divergent transcription. **B.** mESC and MEF bidirectional enrichment of histone PTMs for genes with high and low divergent transcription relative to transcribed gene groups from A. Z-scores and FDR values are listed in table 3.4.

3.3.2 Histone acetylation in S. cerevisiae is tightly linked with RNAPII occupancy

We next asked if histone acetylation was similarly depleted upstream of unidirectional promoters in the highly versatile model system *S. cerevisiae*. We assessed histone acetylation profiles flanking active promoters classified as having high or low levels of divergent RNAPII. Acetylation of histones H3 and H4 upstream of promoters was

strongly linked with divergent transcription (Figure 3.4 A, B, Table 3.4), similar to mammalian cells. Importantly, the link with divergent transcription was clearly evident for H3K14ac, H3K18ac, H3K23ac, H4K5ac, H4K8ac, and H4K12ac, which are sites catalyzed by the major H3 and H4 HATs, Gcn5 and Esa1 respectively (Howe et al., 2001; A. Kimura et al., 2002). Notably the link between these acetylation sites and divergent transcription was comparable to that of H3K4me3. H4K16ac was only modestly linked with divergent transcription, reflecting its deposition by Sas2, which is not tightly linked to promoter-containing regions in yeast (Heise et al., 2012; A. Kimura et al., 2002; Sutton et al., 2003). H3K56ac is catalyzed by Rtt109 and was also only modestly enriched with divergent transcription, consistent with its role at both silent and active promoters (Rufiange et al., 2007), while H3K4ac and H3K9ac show enrichments consistent with overlapping activities of Gcn5 and Rtt109 (Fillingham et al., 2008; Guillemette et al., 2011). The depletion of acetylation upstream of unidirectional active genes could be due to HDAC activity. However, acetylation upstream of promoters for two representative sites, H3K23 and H4K12, was more tightly linked with divergent RNAPII following HDAC inhibition (Figure 3.4 C, D, Table 3.4), confirming that the low level of acetylation upstream of unidirectional promoters is due to low HAT activity. Thus histone acetylation upstream of promoters occurs primarily with divergent transcripts, reflecting a tight link between RNAPII occupancy and histone acetylation flanking both classes of promoters.

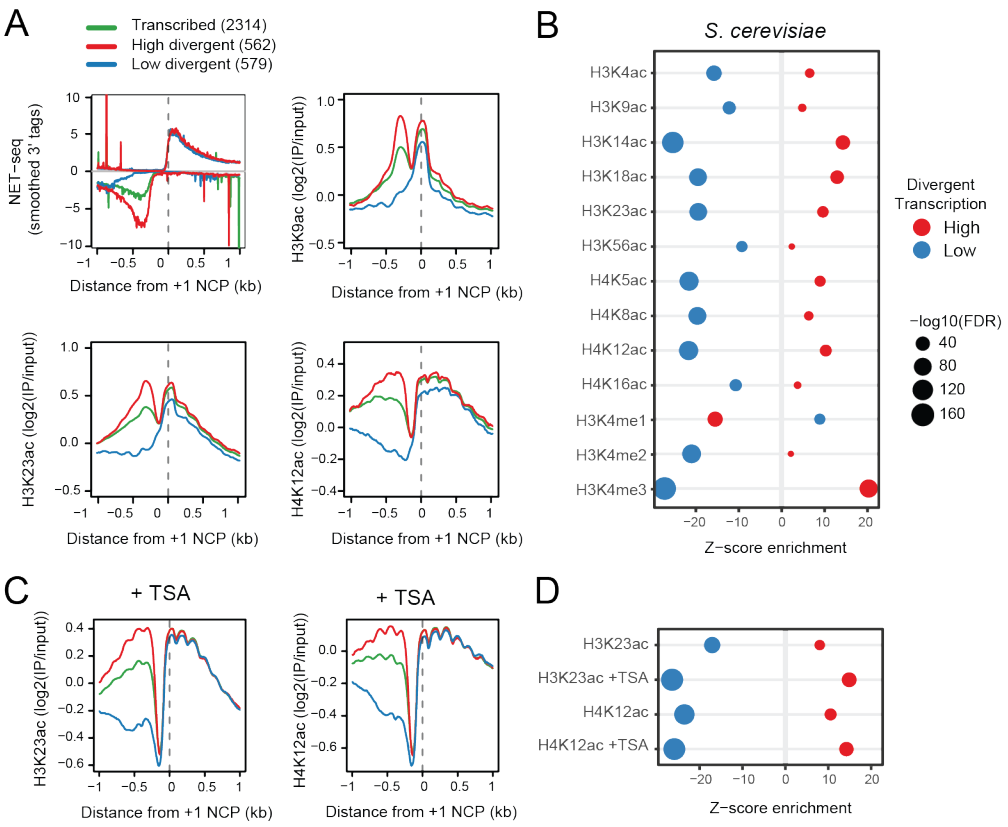

Figure 3.4: Histone acetylation flanking promoters in yeast cells is tightly linked with RNAPII occupancy. A. The average signal relative to the +1 NCP for NET-seq (Harlen et al., 2016) and histone acetylation data (Weiner et al., 2015). **B.** Bidirectional enrichment of histone PTMs (Weiner et al., 2015) for 562 genes with high and 579 genes with low divergent transcription relative to 2314 transcribed genes. **C.** The average signal relative to the +1 NCP for NET-seq (Harlen et al., 2016) and H3K23ac (B. J. E. Martin et al., 2017) and H4K12ac following 15 minute TSA treatment at gene groups from A. **D.** Bidirectional enrichment of H3K23ac (B. J. E. Martin et al., 2017) and H4K12ac before and after 15 minutes TSA treatment for gene groups from A. Z-scores and FDR values are listed in table 3.4.

Table 3 4: Bidirectional histone PTM enrichments for promoters with high or low divergent transcription relative to transcribed promoters.

Cell Type	PTM	Z-score: high divergent	$-\log_{10}$(FDR): high divergent	Z-score: low divergent	$-\log_{10}$(FDR): low divergent
IMR90	H3K18ac	16.06	56.83	-20.87	95.55
IMR90	H3K23ac	15.80	55.08	-19.89	87.00
IMR90	H3K27ac	22.45	110.02	-26.30	150.84
IMR90	H3K4ac	16.04	56.72	-20.91	95.94
IMR90	H3K4me1	-5.22	6.72	-1.07	0.53
IMR90	H3K4me2	12.60	35.43	-20.41	91.48
IMR90	H3K4me3	22.55	110.87	-30.19	198.32
IMR90	H3K56ac	19.89	86.59	-23.24	118.11
IMR90	H3K9ac	23.38	118.95	-29.30	186.92
IMR90	H3K14ac	17.30	65.76	-21.77	103.89
IMR90	H4K5ac	12.63	35.58	-18.48	75.25
IMR90	H4K8ac	10.81	26.35	-17.18	65.16
IMR90	H4K91ac	14.54	46.86	-20.04	88.22
H1-hESC	H3K18ac	11.01	26.89	-10.78	25.79
H1-hESC	H3K23ac	7.72	13.61	-7.13	11.66
H1-hESC	H3K27ac	11.07	27.11	-12.12	32.32
H1-hESC	H3K4ac	4.88	5.81	-6.48	9.80
H1-hESC	H3K4me1	-4.87	5.81	1.66	0.99
H1-hESC	H3K4me3	18.45	73.92	-18.70	75.99
H1-hESC	H3K56ac	11.92	31.28	-11.76	30.54
H1-hESC	H3K9ac	17.66	68.02	-15.98	55.71
H1-hESC	H4K5ac	9.17	18.82	-9.84	21.61
H1-hESC	H4K8ac	9.11	18.65	-8.92	17.91
H1-hESC	H4K91ac	6.84	10.86	-6.56	10.01
K562	H4ac	14.79	48.65	-16.19	58.08
K562	H3K27ac	21.68	103.28	-23.73	123.56
K562	H3K4me1	1.18	0.56	-8.04	15.05
K562	H3K4me2	23.32	119.25	-26.96	158.97
K562	H3K4me3	28.51	177.43	-26.92	158.62
K562	H3K9ac	29.97	195.69	-29.64	191.43
HeLa	H3K4me1	-9.70	21.46	0.71	0.32
HeLa	H3K4me3	25.69	144.51	-27.28	162.66
HeLa	H3K9ac	26.72	156.07	-26.74	156.52

Cell Type	PTM	Z-score: high divergent	$-\log_{10}$(FDR): high divergent	Z-score: low divergent	$-\log_{10}$(FDR): low divergent
HeLa	H3K27ac	23.95	125.86	-24.90	135.95
mESC	H3K4me1	1.48	0.78	-8.30	15.78
mESC	H3K9ac	17.28	65.60	-22.00	105.86
mESC	H3K4me3	16.98	63.43	-21.30	99.47
mESC	H3K27ac	16.50	60.04	-19.38	82.52
mESC	H4ac	5.68	7.67	-7.61	13.37
mESC	H2AZ	2.77	2.11	-8.93	18.12
MEF	H3K27ac	18.27	73.60	-19.87	86.79
MEF	H3K4me1	-2.50	1.83	-1.93	1.25
MEF	H3K4me3	22.13	107.23	-22.19	107.91
MEF	H3K9ac	22.08	106.83	-23.50	120.62
MEF	H2AZ	10.66	25.59	-13.19	38.76
MEF	H4ac	9.68	21.26	-12.04	32.52
S. cerevisiae	H3K4ac	6.54	9.94	-15.78	54.99
S. cerevisiae	H3K9ac	4.80	5.63	-12.22	33.37
S. cerevisiae	H3K14ac	14.28	44.71	-25.37	140.29
S. cerevisiae	H3K18ac	12.94	36.90	-19.50	83.53
S. cerevisiae	H3K23ac	9.63	20.71	-19.44	83.08
S. cerevisiae	H3K56ac	2.37	1.66	-9.27	19.55
S. cerevisiae	H4K5ac	8.96	18.04	-21.58	101.99
S. cerevisiae	H4K8ac	6.32	9.34	-19.65	84.73
S. cerevisiae	H4K12ac	10.29	23.58	-21.69	102.97
S. cerevisiae	H4K16ac	3.71	3.54	-10.70	25.81
S. cerevisiae	H3K4me1	-15.50	52.34	8.90	18.07
S. cerevisiae	H3K4me2	2.15	1.42	-21.00	96.64
S. cerevisiae	H3K4me3	20.29	89.20	-27.28	161.56
S. cerevisiae	H3K23ac - TSA	7.99	14.51	-17.07	64.25
S. cerevisiae	H3K23ac +TSA	14.86	48.26	-26.43	151.90
S. cerevisiae	H4K12ac - TSA	10.53	24.61	-23.56	121.17
S. cerevisiae	H4K12ac +TSA	14.22	44.41	-25.91	146.14

Consistent with the tight association between RNAPII occupancy and histone acetylation, in metazoans RNAPII occupancy across gene bodies is highest in 5' regions, where acetylation is predominant. In *S. cerevisiae*, however, this relationship is more tenuous. Yeast lack the metazoan pausing factor NELF (Adelman and Lis, 2012) and exhibit largely unvarying RNAPII ChIP occupancy across transcribed units, which has led to the belief that RNAPII is uniformly enriched across genes. However, RNAPII mapping approaches targeting the nascent transcript, such as NET-seq or CRAC-seq, reveal a clear 5' bias in RNAPII enrichment (Churchman and Weissman, 2011; Milligan et al., 2016). To reconcile this discrepancy, we directly compared the relative distributions of ChIP and transcript based mapping of RNAPII across genes ordered by transcript length. For ChIP-seq data (Wong et al., 2014), we observed higher RNAPII enrichment at the 5' and 3' ends of longer transcribed genes, with depletion in the centre (Figure 3.5 A). At shorter genes, these peaks merge but are clearly distinct in the higher-resolution ChIP-exo mapping of RNAPII (Van Oss et al., 2016). As the majority of yeast genes are relatively short (Figure 3.5 B) the 5' and 3' enrichments combined with the low resolution of ChIP-seq give rise to seemingly uniform metagene profiles of RNAPII. Indeed, sequencing of RNAPII-associated nascent transcripts via NET-seq (Harlen et al., 2016) or CRAC-seq (Milligan et al., 2016) preferentially recovers the 5' peak of RNAPII. The lower recovery of the 3' peak may indicate that this occurs following cleavage at the polyadenylation site and Rat1 exonuclease attack (Fong et al., 2015). The 5' peak of RNAPII occurs prior to CTD serine 2 phosphorylation and loading of elongation factors (Mayer et al., 2010), which is consistent with Cdk9 activity positively regulating RNAPII elongation rate (Booth et al., 2017), and suggests that RNAPII progresses slowly in early elongation.

Thus both transcript-based and ChIP-based methods of RNAPII mapping reveal a 5' enrichment of RNAPII, which is consistent with a tight link between RNAPII occupancy and histone acetylation.

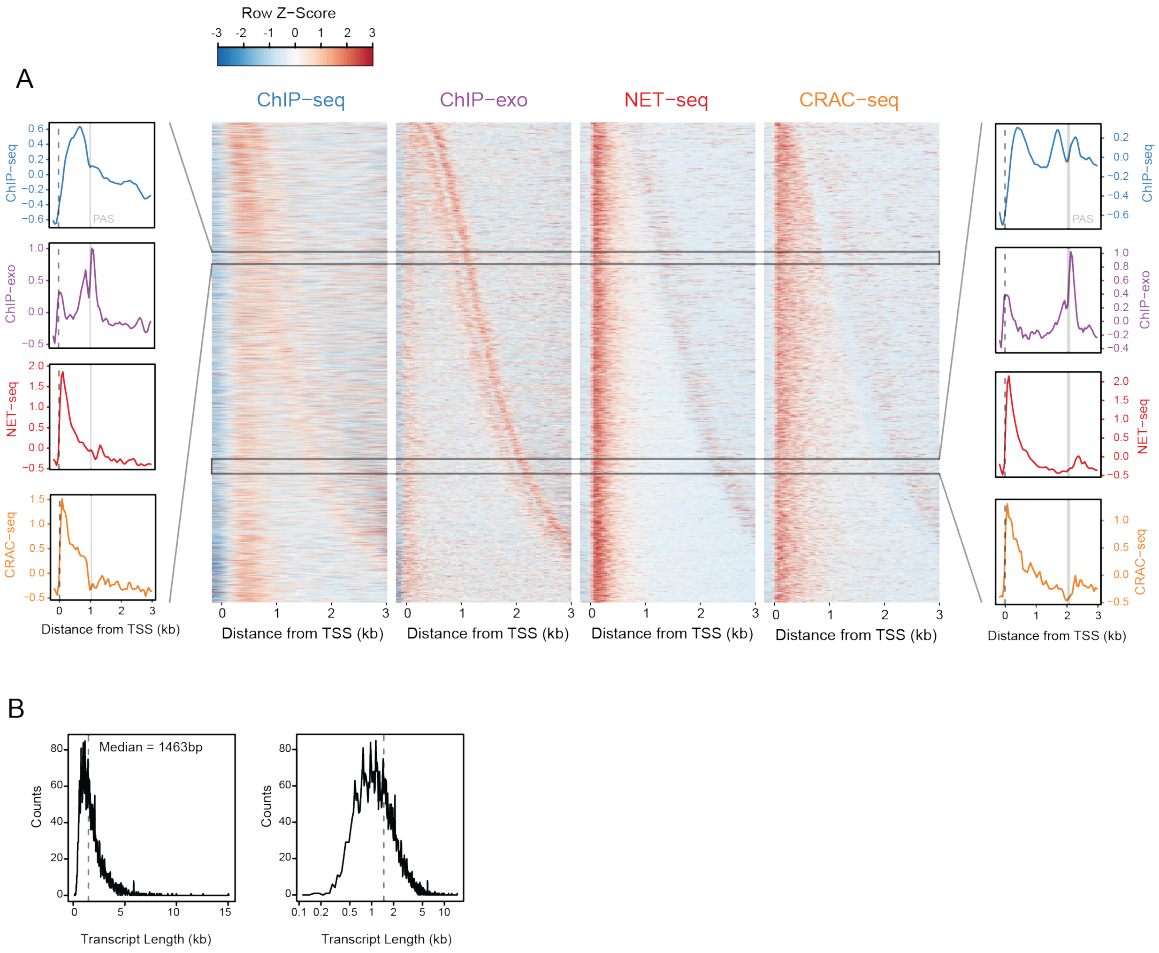

Figure 3.5: RNAPII accumulates at 5' and 3' gene regions in *S. cerevisiae*. A. ChIP-seq (Wong et al., 2014), ChIP-exo (Van Oss et al., 2016), NET-seq (Harlen et al., 2016), and CRAC-seq (Milligan et al., 2016) RNAPII datasets were aligned by the TSS, sorted by distance to the polyadenylation site and represented as a heatmap (4973 genes in total). To highlight intragenic distributions of RNAPII, the data was row-scaled, whereby the data is expressed in standard deviations from the mean for each gene. The average

profile for each dataset is shown for transcripts 1000 to 1050 and 2000 to 2100 bp in length. B. Average gene lengths, defined as the distance from the annotated TSS to PAS (D. Park et al., 2014), shown by histogram for 4973 genes.

3.3.3 Histone acetylation is linked with RNAPII occupancy rather than transcription *per se*

To investigate which features of transcription are linked with histone acetylation, we compared correlations of histone acetylation with different measurements of transcription (Figure 3.6). We focused our analysis on H4K12ac and H3K23ac from TSA treated cells, to avoid confounding effects of HDAC activity. We found that histone acetylation was strongly correlated and clustered with engaged RNAPII, as measured by sequencing of nascent transcripts through NET-seq (Harlen et al., 2016), CRAC-seq (Milligan et al., 2016), or PAR-clip (Schaughency et al., 2014). In contrast, histone acetylation levels were poorly correlated with PRO-seq, which measures elongation competent RNAPII (Booth et al., 2016), perhaps indicative of histone acetylation being linked to inefficient RNAPII elongation. Furthermore, histone acetylation was more modestly correlated with RNAPII measured by ChIP-seq (Schulz et al., 2013) or ChIP-exo (Van Oss et al., 2016), and poorly correlated with transcript levels measured by RNA-seq (Harlen et al., 2016) or transcript synthesis by 4tU-seq (Schulz et al., 2013) (Figure 3.6). Discrepancies between transcript synthesis and RNAPII occupancy can be indicative of local enrichment of RNAPII signal at regions of relatively slow elongation or low processivity (Ehrensberger et al., 2013). Notably, we observed similar results for a broad range of histone acetylation

sites (Figure 3.7), indicating that this is a general feature of histone acetylation. These results support a tight link between histone acetylation and engaged RNAPII occupancy specifically rather than transcription *per se*.

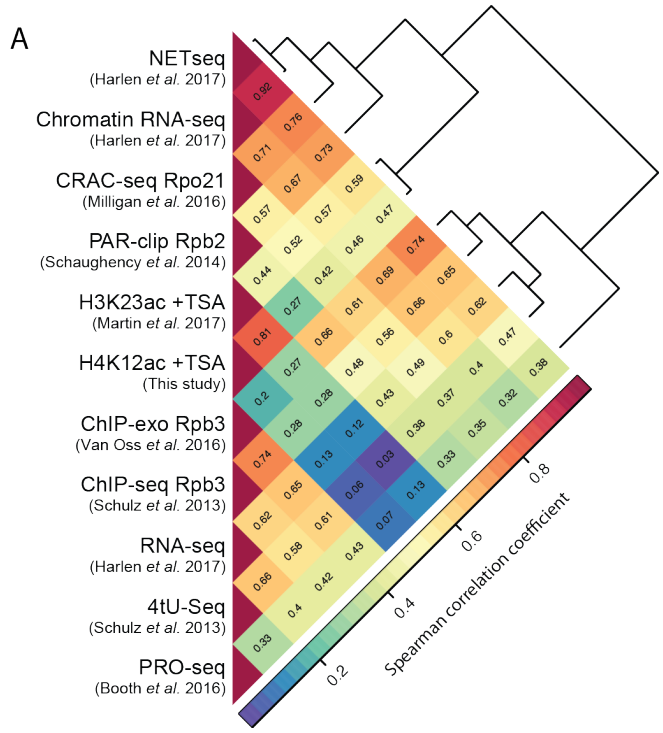

Figure 3 6: H3K23ac and H4K12ac are strongly linked with RNAPII occupancy. A. Spearman correlation matrix for enrichments of H3K23ac and H4K12ac following 15 minutes TSA treatment and various measures of transcription across 60620 genome wide nucleosome positions. The rows and columns were sorted by hierarchical clustering, and the clustering is represented by the dendrogram.

A

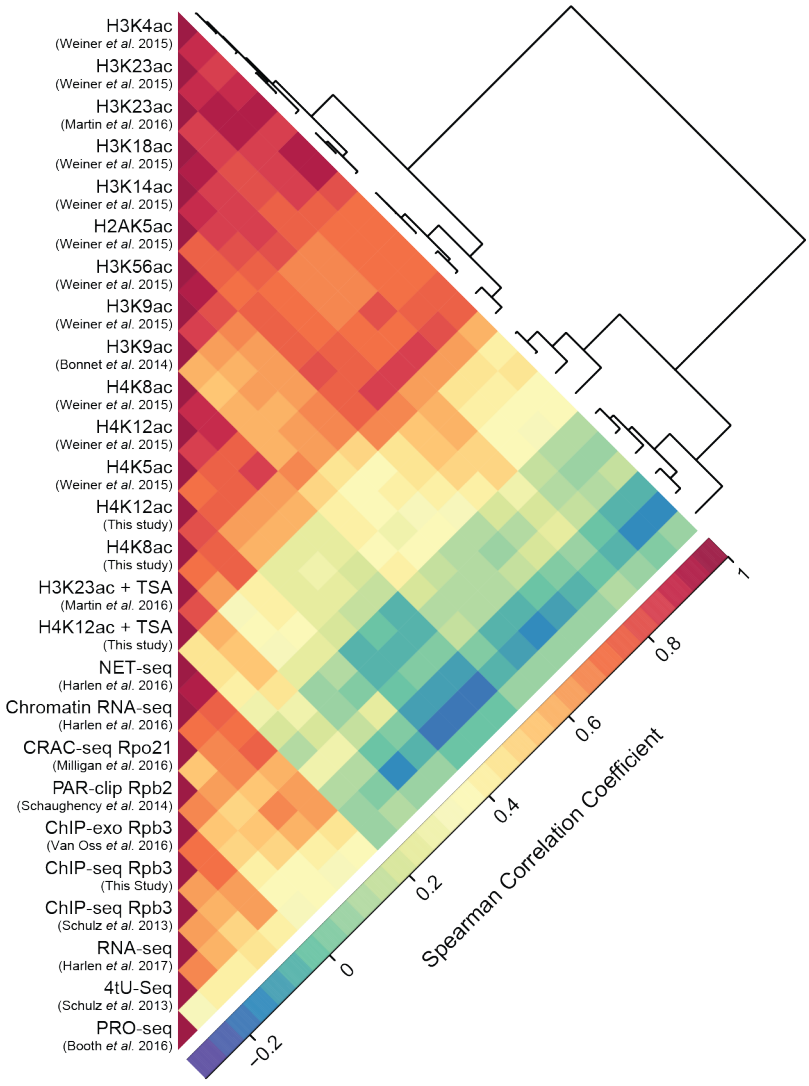

Figure 3.7: Histone acetylation is strongly linked with RNAPII occupancy. A. Spearman correlation matrix for enrichments of H3K23ac and H4K12ac following 15 minutes TSA treatment and various measures of transcription across 60620 genome wide nucleosome positions. The rows and columns were sorted by hierarchical clustering, and the clustering is represented by the dendrogram.

To further test the link between RNAPII occupancy and histone acetylation, we addressed whether variations in intragenic distributions of RNAPII could predict intragenic histone acetylation. We used NET-seq data to classify genes displaying either a pronounced 5' peak or a bias towards RNAPII enrichment downstream (Figure 3.8 A). Confirming that these classifications were consistent across techniques, CRAC-seq mirrored NET-seq RNAPII profiles (Figure 3.8 A). Strikingly, genes with a pronounced 5' enrichment of RNAPII were predominantly acetylated at H3K23 and H4K12 of the +1 and +2 NCPs, while H3K23ac and H4K12ac were shifted downstream at genes with a more even distribution of RNAPII (Figure 3.8 A). These data demonstrate that intragenic variation in RNAPII dwell time coincides with alterations in histone acetylation.

As strongly positioned nucleosomes *in vitro* pose a major impediment to RNAPII progress, we next asked if DNA sequences predicted to form stable nucleosomes exhibit increased RNAPII stalling and histone acetylation *in vivo*. We scored the +2, +3, and +4 NCPs, controlling for MNase-seq signal, and identified nucleosome with sequences predicted to strongly or weakly form nucleosomes (N. Kaplan et al., 2009) (Figure 3.8 B). Consistent with *in vitro* data suggesting that DNA sequence can determine the strength of the nucleosomal impediment to RNAPII passage (Bondarenko et al., 2006), nucleosome favouring sequences had increased RNAPII signal (Figure 3.8 B), indicative of slowed elongation. Importantly, these nucleosomes were also enriched for H3K23ac and H4K12ac (Figure 3.8 B, C). Of note, predicted nucleosome strength, RNAPII, and histone acetylation appeared to be largely independent of adjacent nucleosomes,

suggesting that they vary on a nucleosomal rather than gene-by-gene resolution. These data further demonstrate the tight link between RNAPII and histone acetylation and show that strongly positioned nucleosomes can regulate both RNAPII elongation and histone acetylation *in vivo*.

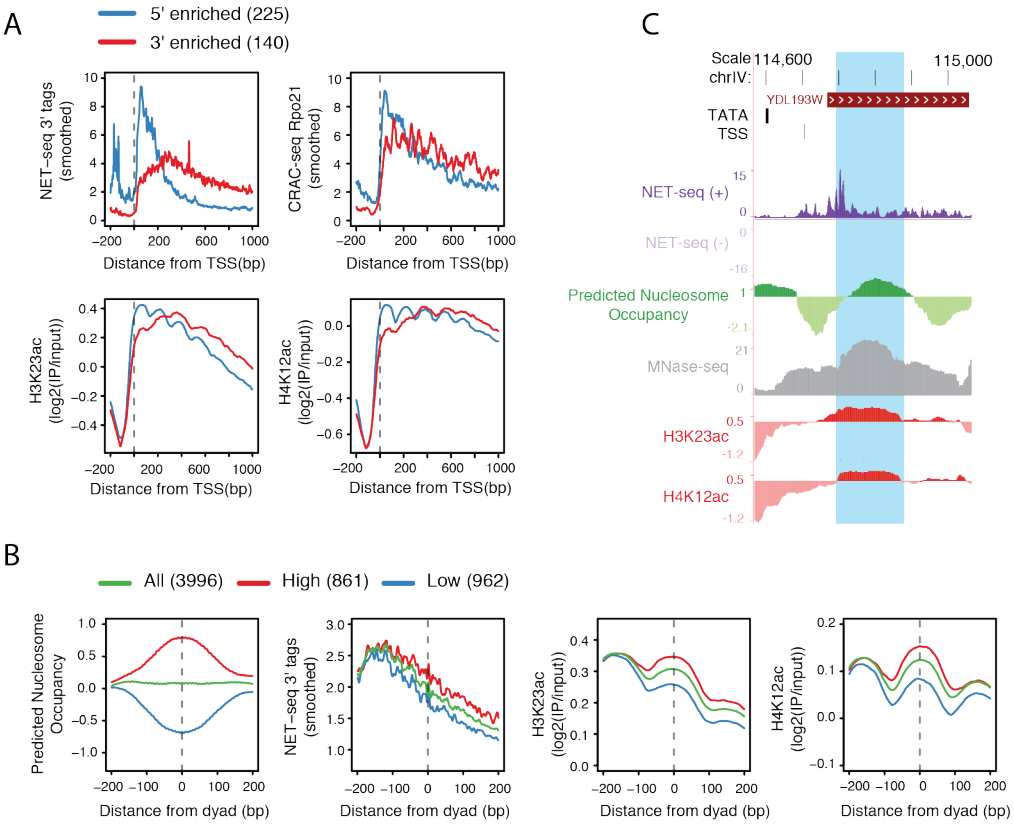

Figure 3.8: Histone acetylation is strongly linked with RNAPII localization. A. The average enrichment relative to the TSS for H3K23ac and H4K12ac following TSA treatment, NET-seq (Harlen et al., 2016), and Rpb1 CRAC-seq (Milligan et al., 2016) for genes with 5' or 3' NET-seq profiles. Note that only genes longer than 1000 bp were included in this analysis. **B.** The average enrichment relative to +2, +3, and +4 NCP dyad positions for H3K23ac (B. J. E. Martin et al., 2017) and H4K12ac following TSA

treatment, NET-seq (Harlen et al., 2016), and predicted nucleosome occupancy (N. Kaplan et al., 2009). C. H3K23ac (B. J. E. Martin et al., 2017), H4K12ac, and MNase-seq (B. J. E. Martin et al., 2017) following TSA treatment, NET-seq (Harlen et al., 2016), and predicted nucleosome (N. Kaplan et al., 2009). **C**. H3K23ac (B. J. E. Martin et al., 2017), H4K12ac, and MNase-seq (B. J. E. Martin et al., 2017) following TSA treatment, NET-seq (Harlen et al., 2016), and predicted nucleosome occupancy (N. Kaplan et al., 2009) at the 5' region of *YDL193W*.

3.3.4 Inducing stalling and backtracking of RNAPII promotes enhanced histone acetylation in gene bodies

Thus far we have observed a tight link between RNAPII occupancy and histone acetylation, but much of this data is correlative in nature. To determine whether RNAPII occupancy is causative for histone acetylation we overexpressed a dominant-negative TFIIS mutant, *dst1 D290A/E291A* ($TFIIS_{MUT}$), which causes stalling, backtracking, and arrest of RNAPII (Imashimizu et al., 2013; Sigurdsson et al., 2010). This analysis was performed in a strain lacking Rpd3, a major histone deacetylase, to prevent histone deacetylation of potentially transiently acetylated intermediates. As stable overexpression of $TFIIS_{MUT}$ is lethal, we induced expression of $TFIIS_{MUT}$ or a vector control for just 90 minutes and performed ChIP-seq for Rpb3, H3K9ac, H3K23ac, H4K8ac, and H4K12ac. Consistent with previous studies (Petrenko et al., 2016; Steunou et al., 2016), we used non-transcribed regions to account for global changes in ChIP-seq experiments (see methods). Also, consistent with a recent report (Warfield et al., 2017) RNAPII peaked at

the +1 NCP in minimal media. However Rpb3 occupancy increased in gene bodies upon overexpression of $TFIIS_{MUT}$, especially in 5' regions, consistent with stalling, backtracking, and arrest of RNAPII. Crucially, $TFIIS_{MUT}$ overexpression also caused increased H3K9ac, H3K23ac, H4K8ac, and H4K12ac in gene bodies (Figure 3.9 A) and at sites of stalled polymerase (Figure 3.9 B). The increase in histone acetylation was more pronounced further into the gene body relative to RNAPII, perhaps due to preferential polyubiquitylation and degradation of RNAPII lacking serine 5 phosphorylation (Somesh et al., 2005), leading to an underrepresentation of RNAPII stalling in mid and 3' regions. Supporting this interpretation, disruption of RNAPII ubiquitylation in a *def1Δ* mutant (Woudstra et al., 2002) partially rescues the lethality of $TFIIS_{MUT}$ overexpression (Figure 3.9 C), suggesting that the lethality is a consequence of widespread RNAPII degradation. Collectively these results reveal that increasing gene body RNAPII residence time targets histone acetylation to gene bodies, thus providing a causal link between RNAPII occupancy and histone acetylation.

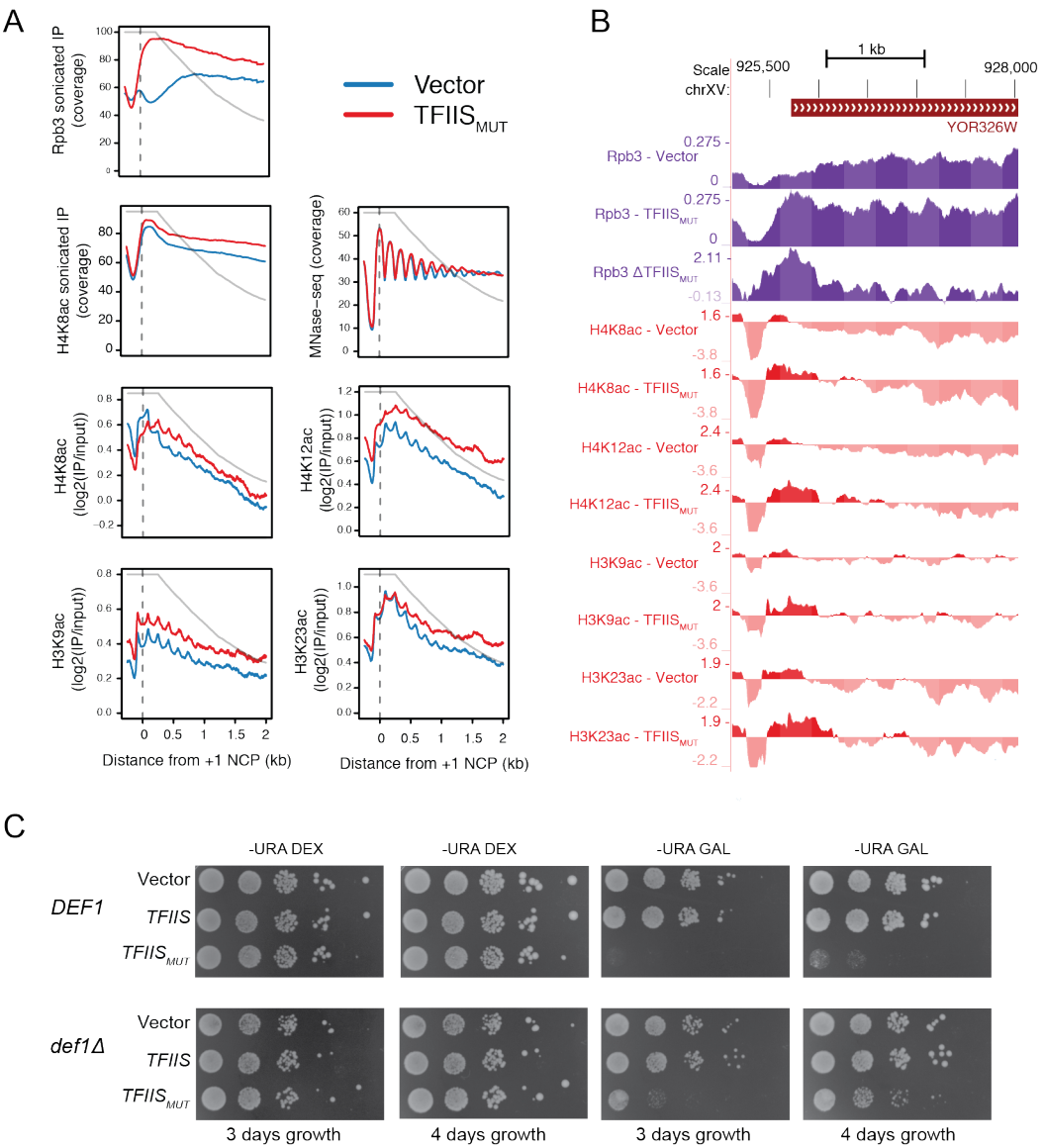

Figure 3.9: Inducing stalling and backtracking of RNAPII promotes enhanced histone acetylation in gene bodies. A. The average enrichments relative to the +1 NCP for Rpb3, MNase-seq, and Histone acetylation ChIP-seq from cells bearing a vector control or overexpressing TFIIS$_{MUT}$. **B.** Rpb3 and Histone acetylation ChIP-seq from cells bearing a vector control or overexpressing TFIIS$_{MUT}$ at *YOR326*. **C.** Widltype and *def1Δ* cells with indicated plasmids were serially diluted onto –URA synthetic drop-out

plates containing either 2% dextrose or galactose. Images were taken after 3 and 4 days growth at 30 °C.

3.3.5 The majority of histone acetylation is dependent on RNAPII

To further test the role of RNAPII occupancy in targeting of histone tail acetylation, we next assessed the dependence of histone acetylation on RNAPII by inhibiting transcription. Previous studies have used the *rpb1-1* temperature sensitive mutant to inhibit transcription (Durant and Pugh, 2006). However recent experiments have suggested that this mutant does not directly inhibit RNAPII, as shifting the mutant to the restrictive temperature has minimal effects on transcript synthesis itself (M. Sun et al., 2013) and does not lead to rapid dissociation of RNAPII from gene bodies (Felipe-Abrio et al., 2015; T. S. Kim et al., 2010). In order to achieve effective inhibition of RNAPII we first attempted to use the Rpb1 anchor-away system (Haruki et al., 2008), but rapamycin treatment failed to efficiently deplete phosphorylated RNAPII from chromatin in our hands (Figure 3.10). As an alternative we treated cells with 1,10 phenanthroline (1,10-pt), a metal chelator (Adams and Gross, 1991; Drew, 1984; Grigull et al., 2004), which rapidly inhibits transcript synthesis (M. Sun et al., 2013). Within 15 minutes of transcription inhibition, we observed global loss of a broad suite of H3 and H4 acetylation marks (Figure 3.11 A, B). Notably this loss of acetylation was dependent on the histone deacetylase Rpd3 and could also be blocked by treatment with HDAC inhibitor TSA (Figure 3.12 A-E), confirming active deacetylation upon transcription inhibition. Histone acetylation loss was due to disruption of HAT activity, rather than increased HDAC activity, as treatment with TSA following 1,10-pt failed to restore

histone acetylation (Figure 3.12 F, G). Additionally, treatment with thiolutin, an unrelated inhibitor of yeast RNA polymerases (Jimenez et al., 1973; Tipper, 1973), caused a similar global loss of histone tail acetylation (Figure 3.11 A, B). We then tested if histone acetylation dependence on transcription was conserved in mammalian cells. Indeed, we found that inhibition of transcription by actinomycin D in mESCs resulted in a global loss of H3K9ac and H3K27ac (Figure 3.13). Thus, in yeast and in mouse cells, we find that the majority of histone acetylation is dependent on transcription.

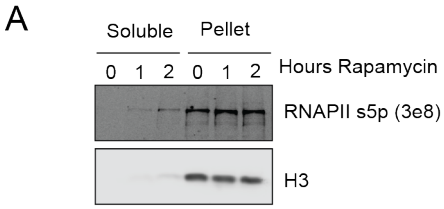

Figure 3.10: Characterization of transcription inhibition by Rpb1 anchor-away. A. The Rpb1 anchor away strain was treated with rapamycin and crude fractionation was performed to assess depletion of Rpb1 from chromatin fraction. Crosslinked cells were lysed and chromatin components were pelleted by centrifugation. Soluble and pellet fractions were analyzed by immunoblotting with antibodies recognizing histone H3 and serine 5 phosphorylation of the RNAPII CTD (3e8).

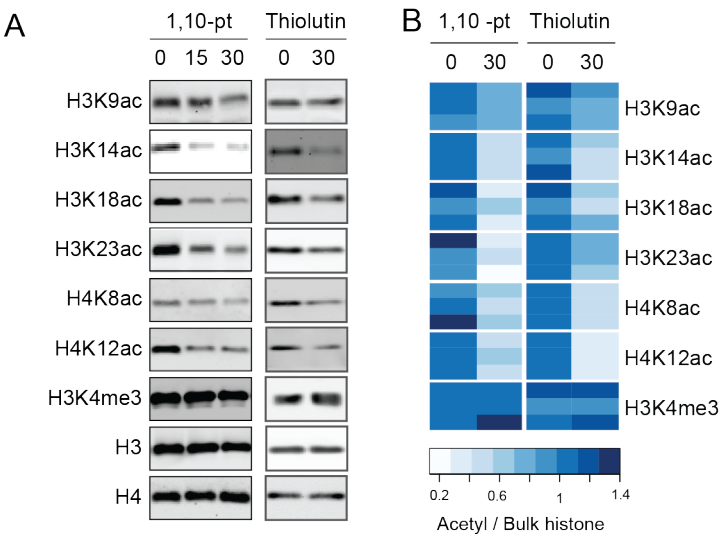

Figure 3.11: Histone acetylation is dependent on RNAPII. A, B. Immunoblot analysis of whole cell extracts from wild type cells treated with thiolutin or 1,10-pt for the indicated acetylation marks. Signals were normalized to total histone levels and individual biological replicates presented as a heat map.

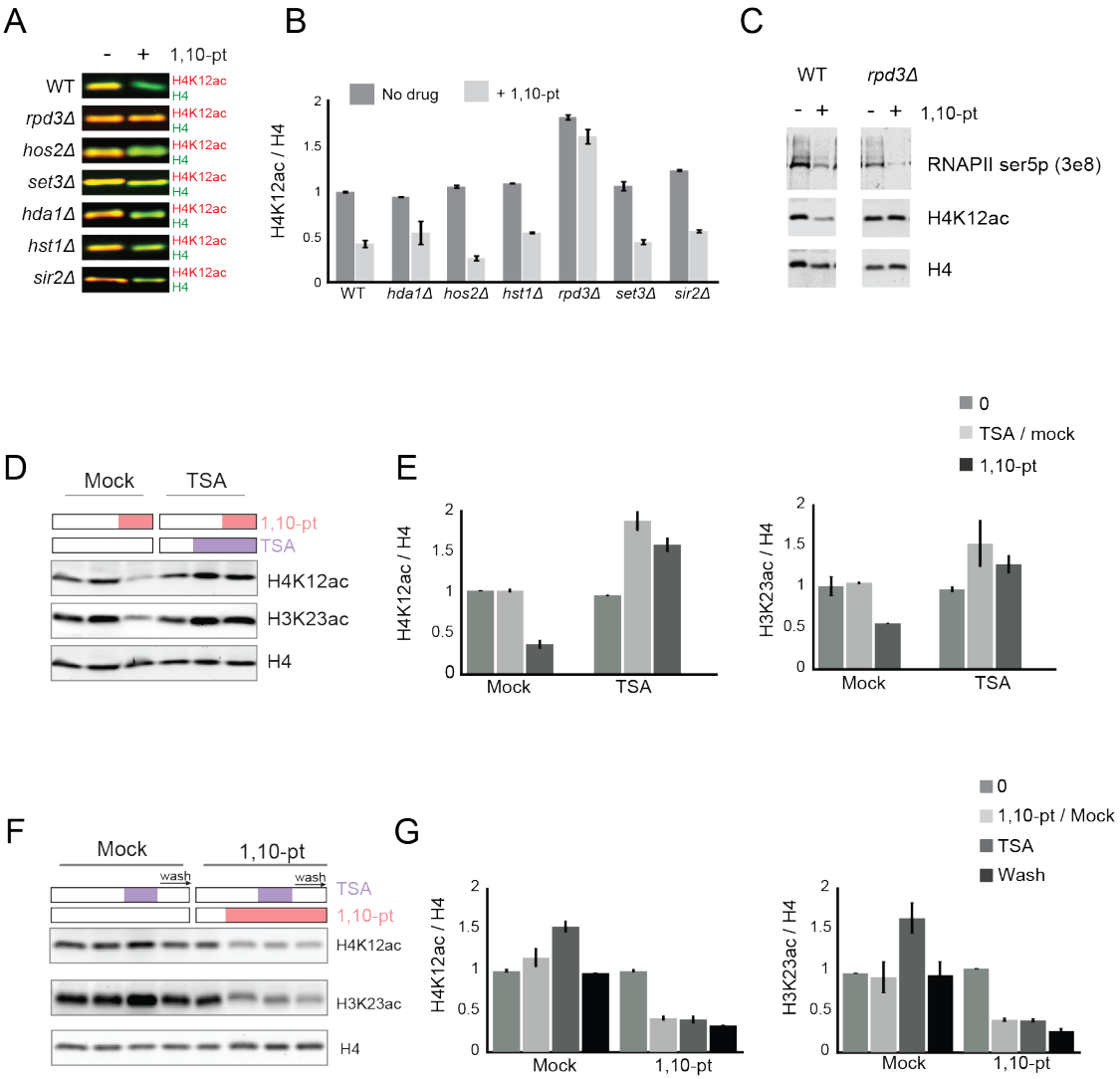

Figure 3.12: Effects of genetic and chemical perturbations on bulk histone acetylation levels in *S. cerevisiae.* A, B. Wildtype and deacetylase mutant strains were treated with 1,10-pt for 30 minutes and bulk H4K12ac was assessed by immunoblotting. A representative blot is shown (A) as well as quantification of at least three replicates (B). **C.** *rpd3Δ* mutants have no effect on loss of serine 5 phosphorylation of RNAPII CTD upon treatment with 1,10-pt. Wildtype and *rpd3Δ* strains were treated with 1,10-pt for 30 minutes and bulk serine 5 phosphorylation and H4K12ac was assessed by immunoblotting. **D, E.** Cells were pretreated with the HDAC inhibitor trichostatin A

(TSA) or DMSO for 15 minutes before a 30 minute treatment with 1,10-phenanthroline monohydrate (1,10-pt). Whole cell extracts were subjected to immunoblot analysis and a representative blot (D) and quantification of two replicates (E) are shown**. F, G.** Cells were pretreated with 1,10-phenanthroline monohydrate (1,10-pt) or ethanol for 15 minutes, followed by a 15 minute treatment with trichostatin A (TSA), and washed into fresh media containing 1,10-pt or ethanol without TSA for 15 minutes. Whole cell extracts were subjected to immunoblot analysis. Shown are a representative blot (F) and quantification of three replicates (G).

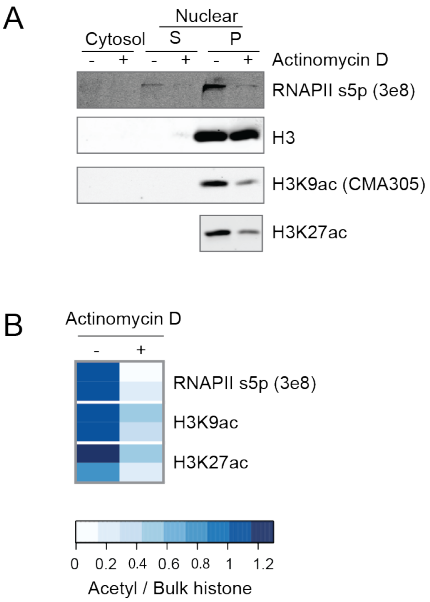

Figure 3.13: Histone acetylation is dependent on RNAPII in mESC. A, B. Immunoblot analysis of RIPA buffer soluble (S) and insoluble (P) nuclear extracts from

mESCs treated with actinomycin D for the indicated antibodies. Acetylation signals were normalized to total histone levels and the individual replicates presented as a heat map.

To further characterize the dependence of histone tail acetylation on transcription, we treated *S. cerevisiae* cells with 1,10-pt for 15 minutes and subsequently performed ChIP-seq for RNAPII, H3K23ac, H4K12ac, and H4K8ac. While the mechanism of action for transcription inhibition by 1,10-pt has not been extensively characterized, we observed loss of Rpb3 across gene bodies, with the strongest effect at 5' regions (Figure 3.14 A, B), consistent with 1,10-pt inhibiting both initiation and elongation of RNAPII. Importantly, H4K12ac, H3K23ac, and H4K8ac mirrored RNAPII loss (Figure 3.14 A, B) and histone deacetylation was limited to nucleosomes that lost Rpb3 upon 1,10-pt treatment (Figure 3.14 C). In contrast regions with more stable RNAPII, including the 3' ends of genes, showed an increase in histone acetylation. While this may result from enhanced HAT targeting by residual RNAPII, we cannot rule out the possibility that our scaling approach does not fully account for global decreases in histone acetylation. Regardless, we find that H3K23ac, H4K12ac, and H4K8ac are deacetylated at regions that lose RNAPII upon transcription inhibition, indicative of a direct effect. Collectively these results demonstrate that the majority of histone tail acetylation is targeted through RNAPII.

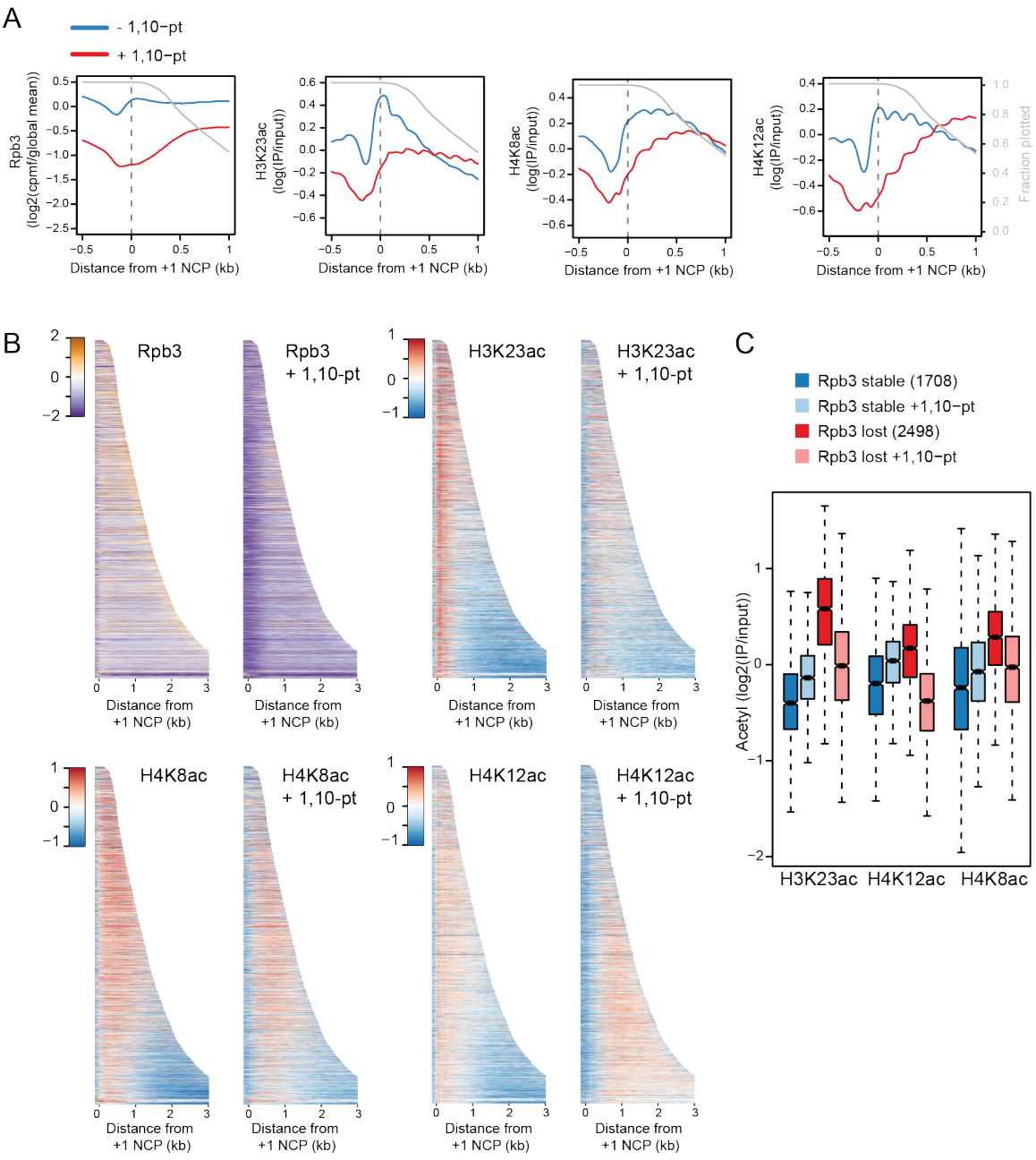

Figure 3.14: Histone acetylation is dependent on RNAPII. A, B. ChIP-seq data for Rpb3 and Histone acetylation from *S. cerevisiae* cells before and after a 15 minute treatment with 1,10-pt at 4029 transcribed +1 NCPs, showing the average enrichments relative to +1 NCP (A) and heatmap visualization of enrichments at genes aligned by the +1 NCP and sorted by the distance to the PAS (B). Only data until the PAS was included, and the grey line (A) represents the fraction of genes still being plotted. **C.** Histone

acetylation enrichments at nucleosomes with stable Rpb3 and those that lost Rpb3 upon treatment with 1,10-pt.

3.3.6 Mechanism of RNAPII-dependent histone acetylation

Three main pathways have been described for RNAPII-dependent histone acetylation in yeast: binding of HATs to the phosphorylated CTD of RNAPII, interaction of HATs with cotranscriptional histone methylation, and replication-independent (RI) histone exchange. We next examined if the established pathways targeting RNAPII-dependent histone acetylation were necessary for bulk histone tail acetylation. First, we found that RNAPII CTD phosphorylation by Kin28 is not necessary for reestablishment of bulk H4K12 or H3K23ac following alleviation of transcription inhibition (Figure 3.15 A, B). Second, as H3K4 methylation can also target HDACs (T. Kim and Buratowski, 2009; X. Shi et al., 2007), we assessed the reestablishment of H4K12ac and H3K23ac following transcription inhibition in the presence of the HDAC inhibitor TSA, but we found no difference in acetylation dynamics between wildtype and *set1Δ* cells (Figure 3.15 C, D). Furthermore, disruption of NuA4 binding to H3K4me3, by truncating the PHD finger of Yng2, had negligible effects on bulk H4K5ac or H4K12ac and only reduced H4K8ac by 30% (Figure 3.14 E, F). Additionally, reanalysis of published ChIP-seq mapping of H4K8ac in a Yng2 PHD finger mutant (Steunou et al., 2016) and H3K18ac in a H3K4R mutant (Sadeh et al., 2016) revealed only subtle alterations in genome wide histone acetylation patterns, demonstrating that H3K4me3 plays a relatively minor role in targeting H3 and H4 tail acetylation (Figure 3.14 G). Third, we found that loss of Asf1, a histone

chaperone implicated in RI histone exchange (T. Kaplan et al., 2008; Rufiange et al., 2007; Schwabish and Struhl, 2006), had minimal effects on H4K12ac or H3K23ac (Figure 3.14 H, I), consistent with ChIP-chip studies showing that H4ac is largely unaffected in *asf1Δ* mutants (Venkatesh et al., 2012). Thus, although we cannot rule out the possibility that RI histone exchange, H3K4 methylation, or RNAPII serine 5 phosphorylation functions in regulating histone acetylation at some genes, these pathways do not seem to play a general role in mediating global histone acetylation.

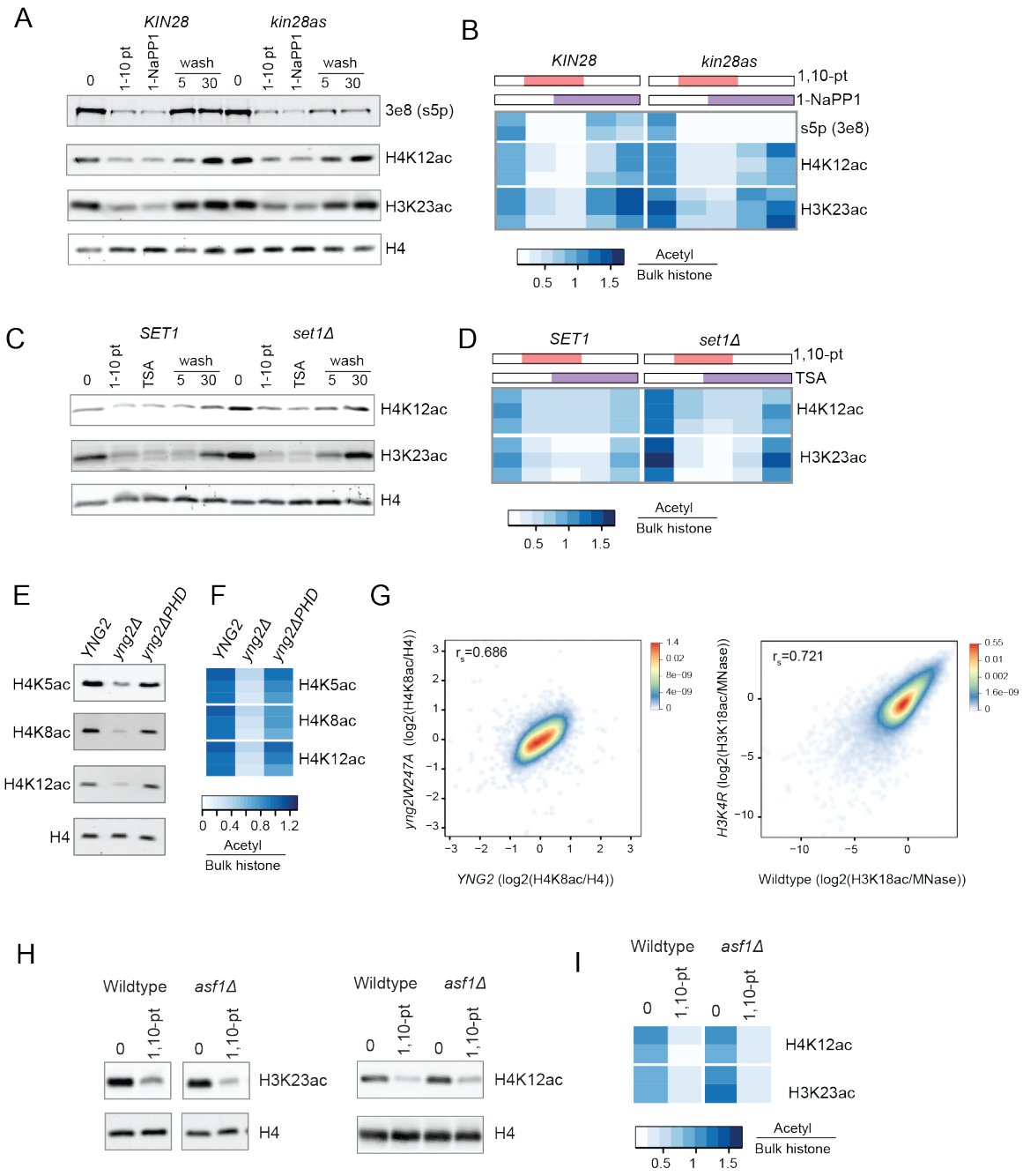

Figure 3.15: Mechanisms for RNAPII-dependent histone acetylation. A, B. An analog sensitive *KIN28* mutant (*kin28as*) and an isogenic wild type strains were treated with 1,10-pt for 30 minutes, followed by 1-NaPP1 for an additional 20 minutes, before being washed into fresh media containing only 1-NaPP1. Samples, including those taken 5 and 30 minutes post-wash were subjected to immunoblot analysis for serine 5 CTD

phosphorylation (3e8), H4K12ac, or H3K23ac. Acetylation signals were normalized to total histone levels and the individual replicates presented as a heat map. **C, D.** Immunoblot analysis of wild type and *set1Δ* cells treated with 1,10-pt for 30 minutes, followed by TSA treatment for an additional 30 minutes, before being washed into fresh media containing TSA. Samples were collected 5 and 30 minutes post-wash. **E, F.** Immunoblot analysis of wild type, *yng2Δ,* and *yng2ΔPHD* cells. **G.** Smoothed scatter plots across genome wide nucleosome positions for H4K8ac (Steunou et al., 2016) and H3K18ac (Sadeh et al., 2016) showing wildtype versus *yng2W247A* and H3K4R strains respectively. The Spearman correlation coefficient between the plotted samples is indicated by r_s. **H, I.** Immunoblot analysis of wild type and *asf1Δ* cells treated with 1,10-pt for 30 minutes.

To further investigate the mechanism targeting RNAPII-dependent histone acetylation, we determined whether histone acetylation is regulated at the level of HAT recruitment. We mapped the NuA4 component Epl1 by ChIP-seq and compared H4 acetylation across genome wide nucleosome positions. Surprisingly, Epl1 correlated poorly with H4K12ac following TSA treatment (Figure 3.16 A), suggesting that NuA4 binding to chromatin often does not result in histone tail acetylation. Confirming that this wasn't a product of our mapping approach, we observed similar effects for Epl1 immunoprecipitated from MNase-digested lysates (Figure 3.16 A). As H4K12ac is primarily regulated by the TSA-sensitive HDAC Rpd3 (Figure 3.12 A-C, (Bernstein et al., 2000)), hypoacetylation at Epl1 bound nucleosomes is unlikely due to HDAC activity, but rather reflects low

activity of NuA4. We also observed a poor correlation for Gcn5 with H3K23ac (Figure 3.16 A), and previous studies have reported discordance between HAT occupancy and histone acetylation (B. J. E. Martin et al., 2017; Steunou et al., 2016). We note however that this observation should not be generalized to other chromatin modifying enzymes, as the H3K4 methyltransferase Set1 positively correlated with H3K4me3 (Figure 3.16 B), so specifically for HATs we find that enzyme occupancy is a poor predictor of histone acetylation. These data show that HAT occupancy is not sufficient for histone acetylation and highlight the importance of post-recruitment regulation of activity.

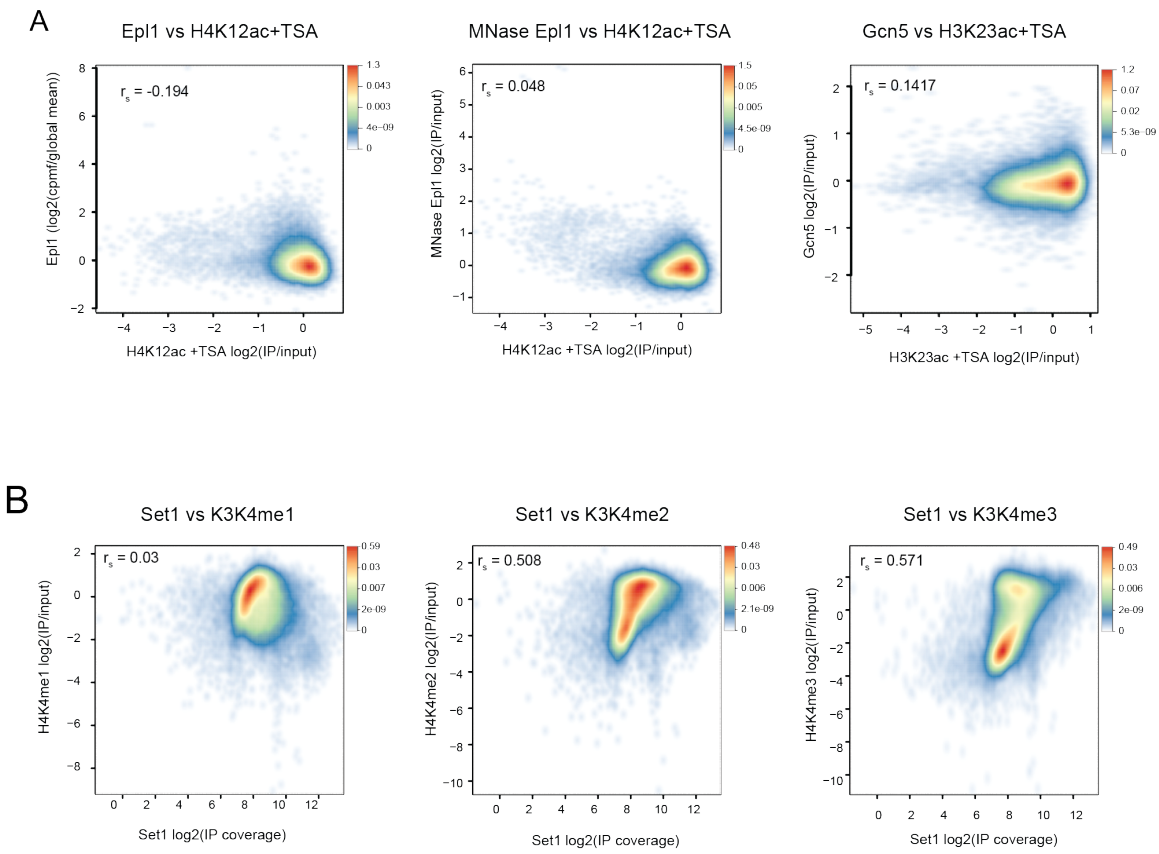

Figure 3.16: Genome wide scatter plots of chromatin modifying enzymes versus histone PTMs. A. Smoothed scatter plots across genome wide nucleosome positions for Epl1 from sonicated or MNase digested lysates and Gcn5 (Xue-Franzén et al., 2013) versus H4K12ac and H3K23ac (B. J. E. Martin et al., 2017) following TSA treatment. The Spearman correlation coefficient between the plotted samples is indicated by r_s. **B.** Smoothed scatter plots across genome wide nucleosome positions for the fragment coverage of Set1 (S. Li et al., 2015) and H3K4 methylations (Weiner et al., 2015). The Spearman correlation coefficient between the plotted samples is indicated by r_s.

Although RNAPII-mediated targeting of HATs does not fully explain histone acetylation patterns, this does not rule out the possibility that HATs are targeted predominantly via RNAPII recruitment. To test if HAT occupancy depends on RNAPII, we mapped Epl1 following transcription inhibition (Figure 3.17 A, B), and found that Epl1 occupancy decreased in 5' regions, indicating RNAPII-dependent association of NuA4 with gene bodies. RNAPII-dependent targeting of NuA4 has been proposed to occur through serine 5 phosphorylated RNAPII CTD (Ginsburg et al., 2009) and H3K4 methylation (X. Shi et al., 2007), but as these pathways are not required for bulk histone acetylation they are unlikely to be mediating the RNAPII-dependent recruitment of Epl1 to gene bodies. Rather, Epl1 recruitment to gene bodies may be through a novel mechanism. In any case our results suggest that RNAPII targets histone acetylation, at least in part, through promoting the interaction of HATs with chromatin.

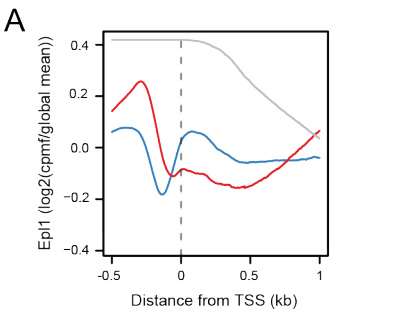

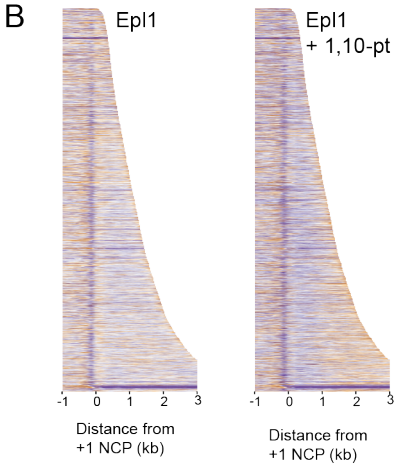

Figure 3 17: Epl1 is lost from gene bodies upon transcription inhibition. A, B. ChIP-seq data for Epl1 before and after a 15 minute treatment with 1,10-pt at 4029 transcribed +1 NCPs, showing the average enrichments relative to +1 NCP (A) and heatmap visualization of enrichments at genes aligned by the +1 NCP and sorted by the distance to the PAS (B). Only data until the PAS was included, and the grey line (A) represents the fraction of genes still being plotted.

3.3.7 NuA4 is recruited to both TAF1 enriched and depleted promoters

With transcription inhibition, we noticed that Epl1 occupancy increased upstream of the +1 nucleosome suggestive of activator-dependent recruitment to upstream activation sequences (UASs). To assess this directly, we analyzed Epl1 enrichment flanking TATA and TATA-like sequences (Rhee and Pugh, 2012), restricting our analysis to genes with low upstream Rpb3 signal so as to avoid confounding effects of divergent transcripts. We found increased binding of Epl1 ~200 bp upstream of the TATA element, coincident with mediator binding (Figure 3.18 A-C) and consistent with activator recruitment to UASs. This increase in Epl1 occupancy did not result in increased H4 acetylation, indicating that activator recruitment of NuA4 is not sufficient for nucleosomal HAT activity.

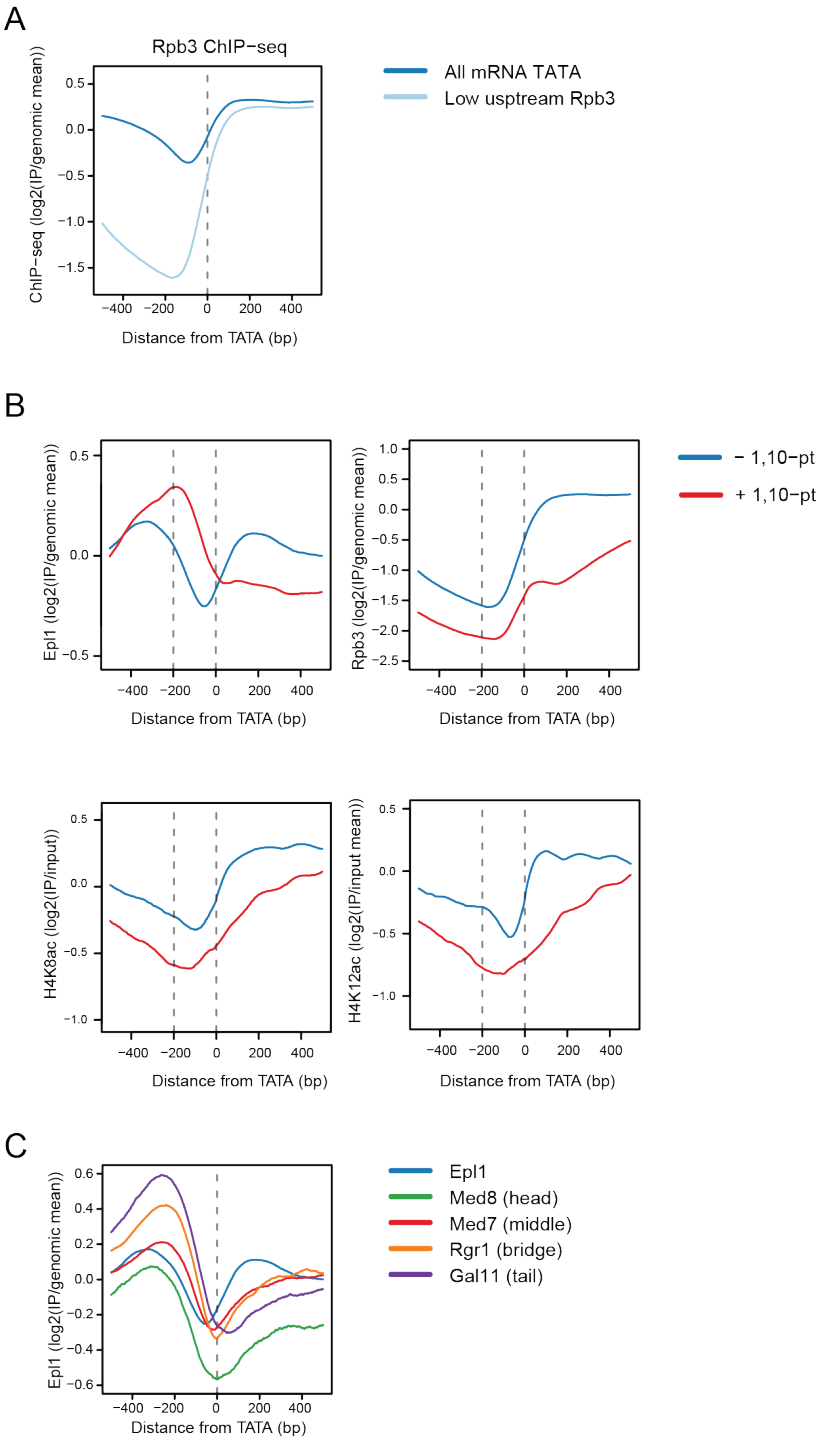

Figure 3.18: Epl1 increases at UASs following transcription inhibition. A. The average enrichment of Rpb3 ChIP-seq flanking 4231 mRNA-linked TATA and TATA-like elements (Rhee and Pugh, 2012) and for 1416 classified as having low upstream

Rpb3. **B.** The average enrichments relative to 1416 mRNA-linked TATA and TATA-like elements (Rhee and Pugh, 2012) with low upstream RNAPII for Rpb3, Epl1, H4K8ac, and H4K12ac before and after 1,10-pt treatment. **C.** The average enrichment of Mediator subunits (Petrenko et al., 2016) and Epl1 flanking 1416 mRNA-linked TATA and TATA-like elements (Rhee and Pugh, 2012) with low upstream RNAPII.

As NuA4 was previously linked with TFIID occupancy (Durant and Pugh, 2007), we next split promoters by Taf1 (TFIID) enrichment (Rhee and Pugh, 2012). While the underlying basis for these promoter classes has been a matter of debate, that they reflect underlying biological differences is widely agreed upon (Joo et al., 2017; Warfield et al., 2017), and as such are useful classifications to compare our results to previous work. As Taf1-depleted genes are on average more highly transcribed we limited our analysis to highly transcribed genes, but similar results were observed at all genes (Figure 3.19 A-B). Consistent with previous work (Durant and Pugh, 2007), Epl1 binding was enriched at UASs of Taf1-enriched promoters, and this binding was largely unaffected by transcription inhibition. In contrast, at Taf1-depleted promoters, while Epl1 was initially depleted, binding at UASs increased dramatically following transcription inhibition. The increase in Epl1 binding coincided with increased RNAPII occupancy between the TATA and TSS elements, as exemplified by the *ACT1* gene (Figure 3.19 C), and suggests that PIC formation still occurs but initiation is inhibited, consistent with *in vitro* experiments (Lattke and Weser, 1977). The increase in Epl1 suggests that NuA4 recruitment to activators is stabilized through interactions with the PIC at Taf1-depleted

genes, and thus only occurs transiently during transcription initiation. This transient binding explains why NuA4 recruitment to Taf1-depleted promoters has not previously been observed and points to a general function for NuA4 in transcription initiation. However, the lack of histone acetylation upstream of promoters suggests that HAT function in transcription initiation involves an activity other than histone tail acetylation.

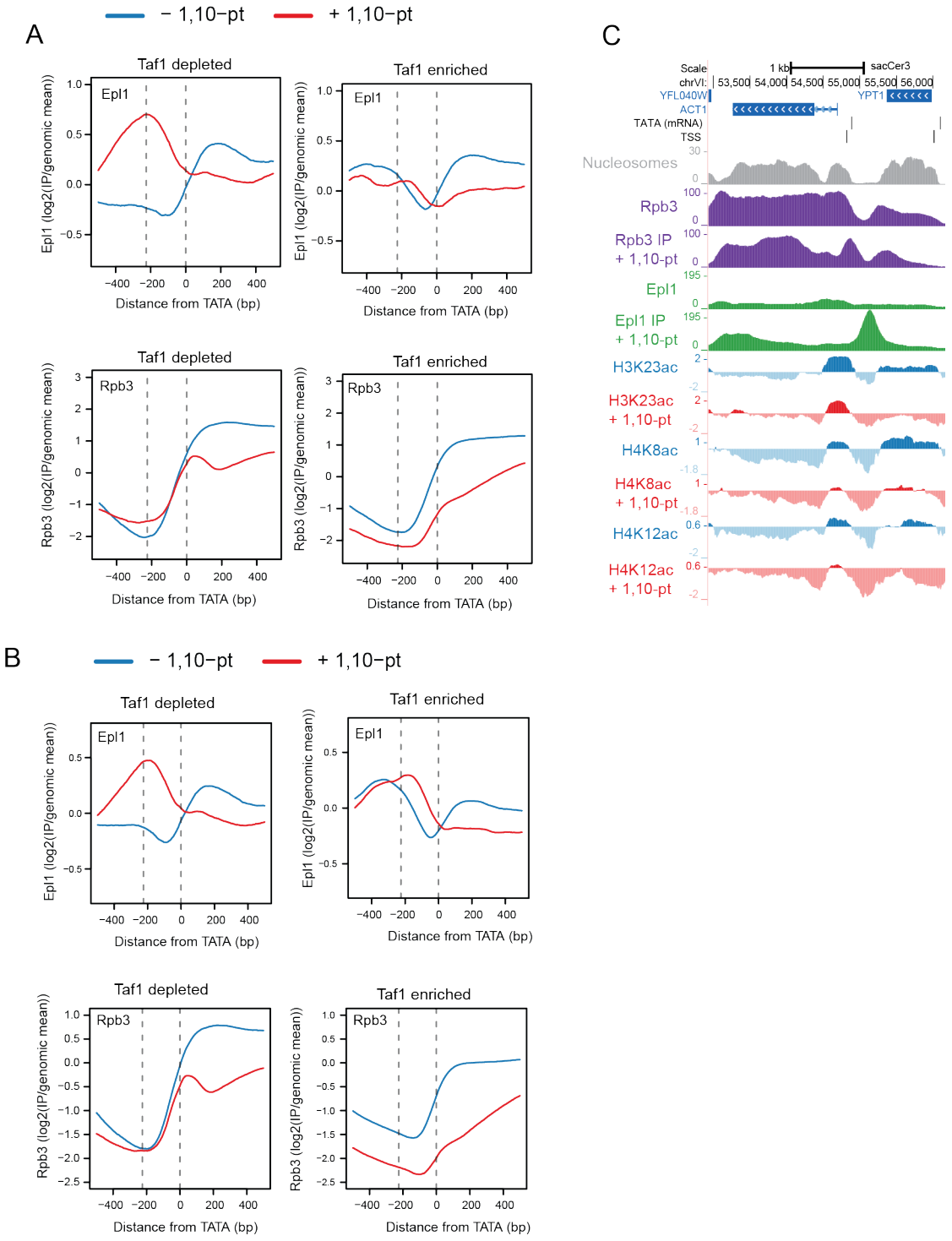

Figure 3.19: Epl1 dynamics at UAS of Taf1 enriched and depleted promoters. A. The average enrichments relative to highly transcribed mRNA-linked TATA and TATA-like elements (Rhee and Pugh, 2012) with low upstream RNAPII classified as enriched

(234 genes) or depleted (164 genes) for Taf1 (Rhee and Pugh, 2012). **B.** Same as in A but for without selecting for highly transcribed genes, giving 364 promoters enriched and 1052 promoters depleted for Taf1**. C.** Rpb3, Epl1, and Histone acetylation ChIP-seq from cells before and after treatment with 1,10-pt at a region surrounding *ACT1*.

3.4 DISCUSSION AND CONCLUSIONS

In this study, we found that the majority of histone acetylation is dependent on RNAPII and is targeted to nucleosomes at sites of RNAPII accumulation, consistent with an intriguing model where histone acetylation functions to rescue the stalled RNAPII molecule. Histone acetylation could aid resumption of RNAPII elongation by directly modulating histone-DNA contacts or by targeting chromatin remodelers to disrupt the offending nucleosomes (Carey et al., 2006). Supporting a function in elongation, H3 tail mutants mimicking unacetylatable lysine sensitize yeast to the transcription elongation inhibitor 6-azauracil (Hailiang Huang et al., 2009), and disruption of histone acetylation impedes early elongation of RNAPII (Church et al., 2017; Church and Fleming, 2017). As well as aiding the current RNAPII-molecule, RNAPII-targeted histone acetylation may also influence subsequent rounds of transcription. Although the rapid deacetylation we observed following loss of RNAPII leaves only a short temporal window, histone acetylation could influence subsequent rounds of transcription in the case of transcriptional bursting. Additionally, if RNAPII arrests due to DNA damage (Gerasimova et al., 2016), then targeting histone acetylation to stalled RNAPII could facilitate transcription-coupled repair (S. Li, 2012).

While we observed RNAPII-dependent HAT binding to chromatin, the mechanism of targeting histone acetylation to RNAPII bound nucleosomes is not clear. Epl1 binding to 5' gene regions was lost upon transcription inhibition, and this is similar to what has been seen for Tip60 in mammalian cells (Poshen B Chen et al., 2015). Tip60 recruitment is proposed to occur via R-loops, which has not been reported before for NuA4. However as Esa1, and most HATs in yeast, contains a nucleic acid binding domain (Shimojo et al., 2008), this may be a conserved mechanism of HAT recruitment to transcribed regions. However while it may be necessary, HAT recruitment is not sufficient for histone acetylation. In fact genome-wide we found that HAT binding to nucleosomes cannot predict histone acetylation, indicative of additional levels of regulation.

One possibility is that RNAPII elongation and stalling could also alter the nucleosome structure, making it a better substrate for acetylation. The histone tails impede RNAPII progression through the nucleosome and must be displaced from DNA during elongation (Chirinos et al., 1998; Ujvári et al., 2008), and this could provide a better substrate for acetylation. In support of this mechanism the H3 tail becomes 10 fold less accessible when assembled into nucleosomes *in vitro* (Gatchalian et al., 2017) and HAT activity is enhanced by disrupting interactions between DNA and the H3 tail (Stützer et al., 2016). Additionally, intranucleosomal stalling of RNAPII leads to unwrapping of DNA from the histone core (Crickard et al., 2017), exposing histone surfaces normally bound to DNA, and potentially enhancing interactions with acetyltransferases.

Another possibility is that RNAPII, or an associated factor, regulates histone acetyltransferase activity of HAT complexes. This may be an allosteric regulator, as has been observed for enhancer RNAs and CBP (Bose et al., 2017), but altered subunit composition is another promising mechanism of regulation. Esa1 exhibits reduced nucleosome HAT activity when incorporated into NuA4 as oppose to the HAT submodule known as Piccolo (Boudreault et al., 2003). Similarly, Gcn5 nucleosomal HAT activity is lower when incorporated into SAGA than when present in the smaller ADA or HAT-A2 complexes (Burgess et al., 2010). It is unclear how assembly of Piccolo and ADA/HATA2 is specifically regulated, but only the full NuA4 and SAGA complexes target Esa1 and Gcn5 to activators. Additionally only the full NuA4 complex is targeted to H3K36me3 (Sathianathan et al., 2016). Both nucleosomes upstream of promoters and modified by H3K36me3 are hypoacetylated, which is consistent with the full NuA4 and SAGA complexes being only weakly active for nucleosome acetylation. The relative targeting of the various subcomplexes to RNAPII and their *in vivo* stoichiometries are largely unknown, and represent promising avenues for future research to understand acetylation of nucleosomes *in vivo*.

Recruitment of HATs to promoters by transcriptional activators underlies the model that histone acetylation primarily occurs during transcription initiation, but whether this recruitment aids transcription initiation through histone tail acetylation or through some other function has largely been unexplored. We found that NuA4 recruitment to UASs did not lead to histone tail acetylation, and generally observed that HAT association with chromatin, in the absence of RNAPII stalling, rarely led to efficient histone tail

acetylation. This suggests that HAT recruitment by sequence-specific activators is not efficient for histone tail acetylation. However, decades of research point to an important role for NuA4, and other HATs, in transcription initiation, so if not tail acetylation what is the function of HATs in transcription initiation?

While activator targeting does not lead to histone tail acetylation, acetylation of other targets may be important for transcription initiation. In addition to the histone tails, HATs acetylate lysine residues in histone globular domains, on the lateral surface of the nucleosome (Di Cerbo et al., 2014; Pradeepa et al., 2016; Tropberger et al., 2013). Also subunits of the RSC and SWI/SNF chromatin remodeling complexes are known to be acetylated (Choi et al., 2008; J.-H. Kim et al., 2010), as are some of the general transcription factors (Imhof et al., 1997), and these represent potential targets for non-histone acetylation. Supporting a non-histone tail acetyltransferase function for HATs in transcription initiation, *in vitro* transcription of chromatin templates is stimulated by recruitment of p300 even when chromatin is assembled using tail-less histones (Georges et al., 2003). The transcription stimulation depends on acetyltransferase activity, and radiolabeled acetate incorporation show acetylation of both non-histone proteins and at least one of the tail-less histones. Compared to the tails the role of non-histone-tail acetylation is a relatively unexplored avenue of research, and our results highlight its potential importance in transcription initiation.

Activator targeting could also serve to increase the local concentration of HAT complexes at transcribed genes, facilitating RNAPII-HAT interactions in 5' genic

regions. This model could explain the increase in NuA4 binding to UAS regions following transcription inhibition. NuA4 interaction with activators could function to increase its local concentration and enable efficient recruitment into the gene body in an RNAPII-dependent manner. Thus, activator recruitment of HATs may facilitate RNAPII-dependent targeting to gene 5' regions.

CHAPTER 4 – CONCLUSIONS AND PERSPECTIVES

4.1 CHAPTER SUMMARY

The enrichment of histone acetylation within transcribed chromatin was first observed in the 1960s, and how specific histones are acetylated has been a central question of chromatin biology ever since. This question has been the overarching focus of this thesis, with experiments addressing how histone acetyltransferases are recruited to transcribed regions of chromatin as well as investigating how histone acetylation itself is deposited. The experiments are largely conducted in the versatile model system of *S. cerevisiae,* but results in mammalian cells suggest that the mechanisms described are conserved across eukaryotic cells. The experiments in this thesis utilize multiple approaches to further our understanding of how histone acetylation targeting is mediated in eukaryotic cells.

In chapter 2, we focused on the NuA3 HAT complex in *S. cerevisiae*, which was known to bind to H3K4 and H3K36 methylation through the PHD finger of Yng1 and the PWWP domain of Pdp3 respectively. Previous work, however, largely considered these

domains in isolation without elucidating the relative contributions of each domain to NuA3 recruitment. We investigated the contributions of both domains first through genome wide analysis of NuA3-bound nucleosomes, and then by interrogating the dependence of NuA3 recruitment on each of the domains and histone methylation. Through these experiments we found that Yng1 binding to H3K4me1/2/3 and Pdp3 binding to H3K36me3 are necessary for full recruitment, but just one of these interactions can still mediate some binding of NuA3, which is consistent with these domains functioning independently. H3K4 and H3K36 methylation occur co-transcriptionally, and so mediates NuA3 recruitment to the bodies of transcribed genes.

Chapter 3 focuses on the causality of the relationship between histone acetylation and RNAPII transcription. In yeast we found that the majority of histone acetylation is dependent on RNAPII, and demonstrated this result through multiple approaches. We observed enrichment of histone acetylation specifically where RNAPII resides, and alterations of RNAPII residence time at different genes and at strongly positioned nucleosomes were reflected in corresponding changes in histone acetylation. Furthermore, and importantly, genetically inducing RNAPII stalling led to increased histone acetylation in gene bodies and inhibiting transcription by the use of two independent transcription inhibitors resulted in a global loss of histone acetylation. ChIP-seq analysis revealed that histone acetylation loss was specific to regions that lost RNAPII upon transcription inhibition. Thus, we comprehensively showed that histone acetylation in yeast is dependent on RNAPII. We also provided evidence that in mammalian cells histone acetylation is also dependent on RNAPII. We found that in

human and mouse cells histone acetylation across a broad range of sites was tightly linked to RNAPII occupancy, and transcription inhibition of transcription in mESCs with actinomycin D resulted in a global loss of histone acetylation. Thus, we provide an answer to an important question concerning histone acetylation biology, finding the bulk of histone acetylation across eukaryotic systems occurs as a consequence of RNAPII occupancy.

In both chapters 2 and 3, we also find that HAT association with chromatin does not always coincide with histone acetylation. This observation could not be explained by histone deacetylase action masking acetyltransferase activity, and instead suggests that regulation of HAT activity post-recruitment to chromatin is a major regulatory step in histone acetylation. This is not to say that HAT recruitment does not play a part but does show that HAT recruitment cannot explain observed histone acetylation patterns. Thus, to understand how histone acetylation is targeted to specific regions of chromatin both mechanisms regulating HAT recruitment and HAT activity must be considered.

4.2 GENERAL DISCUSSION and FUTURE DIRECTIONS

One surprising aspect of NuA3 recruitment is the ability of weak interactions to mediate its association with chromatin (Table 2.1). NuA3 binding to H3K4me1 and H3K36me3, especially, occurs with dissociation constants over 50 μM. These are not strong interactions, and it is puzzling how they enable targeting of NuA3. It's possible that other, still weaker interactions facilitate cooperative multivalent binding, but we see no evidence for this. Another possibility is that the nuclear environment may facilitate weak

interactions by increasing effective concentrations through molecular crowding (E. J. Cho and J. S. Kim, 2012; Matsuda et al., 2014; Richter et al., 2008). In any case our results demonstrate that despite their weak interactions, histone binding by the PHD finger of Yng1 and the PWWP domain of Pdp3 mediate recruitment of NuA3 to chromatin, and can do so independent of one another. These results highlight how even weak interactions can still be functionally relevant in chromatin biology.

We also found histone acetylation tightly linked to transcription from divergent promoters, much of which results in short non-coding transcripts (Core et al., 2008). The functional relevance of non-coding transcription is not always clear, but our results suggest a function at least in chromatin regulation. Our results show that short non-coding transcription will target histone acetylation, thereby altering chromatin structure. The relevance of this is currently unknown, but may have implications for chromatin accessibility at upstream promoter regions and higher order chromatin structure (Kieffer-Kwon et al., 2017). Active enhancers are also linked with divergent promoters (Core et al., 2014; Jin et al., 2017), and eRNAs may also function to increase acetylation, consistent with a reported role for eRNAs in activating CBP acetyltransferase activity (Bose et al., 2017). Thus transcription-coupled histone acetylation provides a mechanism for short non-coding transcripts to target histone acetylation and alter chromatin structure.

Histone acetylation was also enriched in regions of increased RNAPII occupancy, and this was linked with intrinsically stable nucleosomes. One explanation for this result, discussed in chapter 3, is that RNAPII progression through or stalling within the

nucleosome causes an altered nucleosome structure. This altered nucleosome could be a better substrate for acetylation, perhaps through greater accessibility of the histone tails, leading to increased histone acetylation. While it is an intriguing model, future experiments are needed to determine if this is in fact what is happening. Due to the complexity within the cell, *in vitro* experiments may be best suited to uncover how HAT activity is affected by RNAPII stalling within the nucleosome.

We also found a general disconnect between HAT recruitment and histone acetylation. First for NuA3 and then for Gcn5 and Esa1 as well, we observed HAT binding to chromatin was often not associated with histone acetylation, suggesting that histone acetyltransferase activity is regulated at a step following chromatin interaction. This type of regulation is similar to what is seen for other chromatin enzymes, where allosteric modulation of activity is a key regulatory step. For instance the histone deacetylase complex Rpd3S was found to be regulated both on the level of recruitment and allosteric regulation of activity (Drouin et al., 2010). Also the chromodomain of the Chd1 chromatin remodeler regulates access to its ATPase motor activity (Hauk et al., 2010; Morettini et al., 2011). We expect that for most chromatin enzymes, function will be regulated both on the level of recruitment and allosteric regulation of activity. However which of these are the determining steps may vary for different enzymes. In fact we observed that the Set1 methyltransferase positively correlated with H3K4me3, suggesting that recruitment is a major determinant of Set1-directed H3K4 methylation. The balance between recruitment and allosteric regulation of a given enzyme may also vary with

environmental or metabolic conditions, with many avenues of research still to be explored.

There is growing evidence for a strong link between enzymatic activity of chromatin enzymes, and HATs specifically, and metabolism. For HATs, they consume acetyl-CoA, a key metabolite, in order to acetylate lysine residues, and the metabolic state of the cell, and acetyl-CoA specifically, dictates HAT activity (L. Cai et al., 2011; Friis et al., 2009; Galdieri and Vancura, 2012; Takahashi et al., 2006; Wellen et al., 2009). Interestingly, recent papers have also observed an association of acetyl-CoA synthetases with HAT complexes leading to local generation of acetyl-CoA for histone acetylation (X. Li et al., 2017; Mews et al., 2017; Sivanand et al., 2017). These experiments suggest that under some conditions, presumably those in which acetyl-CoA is limiting, local generation of acetyl-CoA is critical for HAT activity. How acetyl-CoA regulates histone acetylation is a fast-growing aspect of histone acetylation research, with many new discoveries every year.

Highlighting the importance of metabolic regulation, HATs were recently discovered to catalyze a variety of histone lysine acylation reactions. Eight non-acetyl short acylations have now been described, which are: propionylation, butyrylation, 2-hydroxyisobutyrylation, succinylation, malonylation, glutarylation, crotonylation and β-hydroxybutyrylation ((Simithy et al., 2017) and reviewed in (Sabari et al., 2017)). While the bulkier acyl groups are not as readily catalyzed by HATs, the choice for which modification the enzyme will catalyze is largely a function of the concentrations of

various acyl-CoA molecules (Sabari et al., 2015; Simithy et al., 2017). Increasing cellular crotonyl-CoA levels shifts the balance from histone acetylation to histone crotonylation (Sabari et al., 2015), and similar effects are seen for other acyl-CoA molecules (Simithy et al., 2017). As with acetylation the various acylations neutralize the positive charge of the modified lysine and so have comparable electrostatic effects on chromatin structure. However due to their unique shape, histone acylations have been found to have unique binding partners and consequentially have distinct chromatin functions (Y. Li et al., 2016; Xiong et al., 2016). Thus, metabolism can have diverse effects on histone acetyltransferases and chromatin enzymes more generally and is an emerging field in chromatin biology.

While we focused on histone acetylation in this thesis, the results also highlighted the importance of non-histone acetylation. We found that HATs often interact with chromatin in the absence of histone acetylation, with implications for histone acetylation, which we discussed above. However, the lack of histone acetylation does not preclude the acetyltransferases from still being active to acetylate non-histone proteins. In fact, the *gcn5Δ sas3Δ* synthetic lethality, which is due to loss of acetylation of H3 and of Rsc4, is not recapitulated in an *ada2Δ sas3Δ* mutant (Choi et al., 2008). In an *ada2Δ* mutant Gcn5, while unable to acetylate nucleosomes, can still acetylate Rsc4 (Choi et al., 2008), explaining the viability of the mutant. A number of studies have reported examples of non-histone protein acetylation functioning in transcription (Downey et al., 2013; Flury et al., 2017; J.-H. Kim et al., 2010), and proteomic and genetic approaches have observed acetylation of many more proteins involved in transcription (Downey et al., 2015;

Henriksen et al., 2012; Kaluarachchi Duffy et al., 2012; Mitchell et al., 2013). Thus, we think it likely that HATs widely function in transcription and chromatin regulation through the acetylation of non-histone proteins.

References:

Abbott, D.W., Ivanova, V.S., Wang, X., Bonner, W.M., Ausio, J., 2001. Characterization of the stability and folding of H2A.Z chromatin particles: implications for transcriptional activation. J. Biol. Chem. 276, 41945–41949. doi:10.1074/jbc.M108217200

Adams, C.C., Gross, D.S., 1991. The yeast heat shock response is induced by conversion of cells to spheroplasts and by potent transcriptional inhibitors. J. Bacteriol. 173, 7429–7435.

Adelman, K., Lis, J.T., 2012. Promoter-proximal pausing of RNA polymerase II: emerging roles in metazoans. Nat. Rev. Genet. 13, 720–731. doi:10.1038/nrg3293

Ahn, S.H., Kim, M., Buratowski, S., 2004. Phosphorylation of serine 2 within the RNA polymerase II C-terminal domain couples transcription and 3' end processing. Molecular Cell 13, 67–76.

Ali, M., Yan, K., Lalonde, M.-E., Degerny, C., Rothbart, S.B., Strahl, B.D., Côté, J., Yang, X.-J., Kutateladze, T.G., 2012. Tandem PHD Fingers of MORF/MOZ Acetyltransferases Display Selectivity for Acetylated Histone H3 and Are Required for the Association with Chromatin. Journal of Molecular Biology 424, 328–338. doi:10.1016/j.jmb.2012.10.004

Allahverdi, A., Yang, R., Korolev, N., Fan, Y., Davey, C.A., Liu, C.-F., Nordenskiöld, L., 2011. The effects of histone H4 tail acetylations on cation-induced chromatin folding and self-association. Nucleic Acids Res. 39, 1680–1691. doi:10.1093/nar/gkq900

Allard, S., Utley, R.T., Savard, J., Clarke, A., Grant, P., Brandl, C.J., Pillus, L., Workman, J.L., Cote, J., 1999. NuA4, an essential transcription adaptor/histone H4 acetyltransferase complex containing Esa1p and the ATM-related cofactor Tra1p. EMBO J. 18, 5108–5119. doi:10.1093/emboj/18.18.5108

Allfrey, V.G., Faulkner, R., Mirsky, A.E., 1964. Acetylation and methylation of histones and their possible role in the regulation of RNA synthesis. Proc. Natl. Acad. Sci. U.S.A. 51, 786–794.

Allfrey, V.G., Littau, V.C., Mirsky, A.E., 1963. On the role of of histones in regulation ribonucleic acid synthesis in the cell nucleus. Proc. Natl. Acad. Sci. U.S.A. 49, 414–421.

Allfrey, V.G., Pogo, B.G., Littau, V.C., Gershey, E.L., MIRSKY, A.E., 1968. Histone acetylation in insect chromosomes. Science 159, 314–316.

Allis, C.D., Chicoine, L.G., Richman, R., Schulman, I.G., 1985. Deposition-related

histone acetylation in micronuclei of conjugating Tetrahymena. Proc. Natl. Acad. Sci. U.S.A. 82, 8048–8052.

Allison, L.A., Wong, J.K., Fitzpatrick, V.D., Moyle, M., Ingles, C.J., 1988. The C-terminal domain of the largest subunit of RNA polymerase II of Saccharomyces cerevisiae, Drosophila melanogaster, and mammals: a conserved structure with an essential function. Mol. Cell. Biol. 8, 321–329.

Andrews, F.H., Shinsky, S.A., Shanle, E.K., Bridgers, J.B., Gest, A., Tsun, I.K., Krajewski, K., Shi, X., Strahl, B.D., Kutateladze, T.G., 2016. The Taf14 YEATS domain is a reader of histone crotonylation. Nature Chemical Biology 12, 396–398. doi:10.1038/nchembio.2065

Ansari, A., Hampsey, M., 2005. A role for the CPF 3'-end processing machinery in RNAP II-dependent gene looping. Genes & Development 19, 2969–2978. doi:10.1101/gad.1362305

Arany, Z., Sellers, W.R., Livingston, D.M., Eckner, R., 1994. E1A-associated p300 and CREB-associated CBP belong to a conserved family of coactivators. Cell 77, 799–800.

Archer, T.K., Cordingley, M.G., Wolford, R.G., Hager, G.L., 1991. Transcription factor access is mediated by accurately positioned nucleosomes on the mouse mammary tumor virus promoter. Mol. Cell. Biol. 11, 688–698.

Armache, K.-J., Kettenberger, H., Cramer, P., 2003. Architecture of initiation-competent 12-subunit RNA polymerase II. Proc. Natl. Acad. Sci. U.S.A. 100, 6964–6968. doi:10.1073/pnas.1030608100

Aso, T., Conaway, J.W., Conaway, R.C., 1994. Role of core promoter structure in assembly of the RNA polymerase II preinitiation complex. A common pathway for formation of preinitiation intermediates at many TATA and TATA-less promoters. J. Biol. Chem. 269, 26575–26583.

Ausio, J., van Holde, K.E., 1986. Histone hyperacetylation: its effects on nucleosome conformation and stability. Biochemistry 25, 1421–1428. doi:10.1021/bi00354a035

Balakrishnan, L., Milavetz, B., 2007a. Histone Hyperacetylation in the Coding Region of Chromatin Undergoing Transcription in SV40 Minichromosomes Is a Dynamic Process Regulated Directly by the Presence of RNA Polymerase II. Journal of Molecular Biology 365, 18–30. doi:10.1016/j.jmb.2006.09.044

Balakrishnan, L., Milavetz, B., 2007b. Histone Hyperacetylation during SV40 Transcription Is Regulated by p300 and RNA Polymerase II Translocation. Journal of Molecular Biology 371, 1022–1037. doi:10.1016/j.jmb.2007.06.080

Banerji, J., Rusconi, S., Schaffner, W., 1981. Expression of a beta-globin gene is enhanced by remote SV40 DNA sequences. Cell 27, 299–308.

Bannister, A.J., Kouzarides, T., 1996. The CBP co-activator is a histone acetyltransferase. Nature 384, 641–643. doi:10.1038/384641a0

Bannister, A.J., Zegerman, P., Partridge, J.F., Miska, E.A., Thomas, J.O., Allshire, R.C., Kouzarides, T., 2001. Selective recognition of methylated lysine 9 on histone H3 by the HP1 chromo domain. Nature 410, 120–124. doi:10.1038/35065138

Barski, A., Cuddapah, S., Cui, K., Roh, T.-Y., Schones, D.E., Wang, Z., Wei, G., Chepelev, I., Zhao, K., 2007. High-resolution profiling of histone methylations in the human genome. Cell 129, 823–837. doi:10.1016/j.cell.2007.05.009

Bartkowiak, B., Liu, P., Phatnani, H.P., Fuda, N.J., Cooper, J.J., Price, D.H., Adelman, K., Lis, J.T., Greenleaf, A.L., 2010. CDK12 is a transcription elongation-associated CTD kinase, the metazoan ortholog of yeast Ctk1. Genes Dev. 24, 2303–2316. doi:10.1101/gad.1968210

Baskaran, R., Dahmus, M.E., Wang, J.Y., 1993. Tyrosine phosphorylation of mammalian RNA polymerase II carboxyl-terminal domain. Proc. Natl. Acad. Sci. U.S.A. 90, 11167–11171.

Beck, M., Schmidt, A., Malmstroem, J., Claassen, M., Ori, A., Szymborska, A., Herzog, F., Rinner, O., Ellenberg, J., Aebersold, R., 2011. The quantitative proteome of a human cell line. Mol. Syst. Biol. 7, 549–549. doi:10.1038/msb.2011.82

Bensaude, O., 2014. Inhibiting eukaryotic transcription. Which compound to choose? How to evaluate its activity? Transcription 2, 103–108. doi:10.4161/trns.2.3.16172

Bernstein, B.E., Tong, J.K., Schreiber, S.L., 2000. Genomewide studies of histone deacetylase function in yeast. Proc. Natl. Acad. Sci. U.S.A. 97, 13708–13713. doi:10.1073/pnas.250477697

Bhaumik, S.R., Green, M.R., 2002. Differential requirement of SAGA components for recruitment of TATA-box-binding protein to promoters in vivo. Mol. Cell. Biol. 22, 7365–7371. doi:10.1128/MCB.22.21.7365-7371.2002

Bian, C., Xu, C., Ruan, J., Lee, K.K., Burke, T.L., Tempel, W., Barsyte, D., Li, J., Wu, M., Zhou, B.O., Fleharty, B.E., Paulson, A., Allali-Hassani, A., Zhou, J.-Q., Mer, G., Grant, P.A., Workman, J.L., Zang, J., Min, J., 2011. Sgf29 binds histone H3K4me2/3 and is required for SAGA complex recruitment and histone H3 acetylation. EMBO J. 30, 2829–2842. doi:10.1038/emboj.2011.193

Bintu, L., Ishibashi, T., Dangkulwanich, M., Wu, Y.-Y., Lubkowska, L., Kashlev, M., Bustamante, C., 2012. Nucleosomal Elements that Control the Topography of the Barrier to Transcription. Cell 151, 738–749. doi:10.1016/j.cell.2012.10.009

Biterge, B., Schneider, R., 2014. Histone variants: key players of chromatin. Cell Tissue Res. 356, 457–466. doi:10.1007/s00441-014-1862-4

Bode, J., Henco, K., Wingender, E., 1980. Modulation of the nucleosome structure by histone acetylation. Eur. J. Biochem. 110, 143–152.

Boffa, L.C., Vidali, G., Mann, R.S., Allfrey, V.G., 1978. Suppression of histone deacetylation in vivo and in vitro by sodium butyrate. J. Biol. Chem. 253, 3364–3366.

Bondarenko, V.A., Steele, L.M., Ujvári, A., Gaykalova, D.A., Kulaeva, O.I., Polikanov, Y.S., Luse, D.S., Studitsky, V.M., 2006. Nucleosomes can form a polar barrier to transcript elongation by RNA polymerase II. Molecular Cell 24, 469–479. doi:10.1016/j.molcel.2006.09.009

Bondy, S.C., Roberts, S., Morelos, B.S., 1970. Histone-acetylating enzyme of brain. Biochem. J. 119, 665–672.

Bonnet, J., Wang, C.-Y., Baptista, T., Vincent, S.D., Hsiao, W.-C., Stierle, M., Kao, C.-F., Tora, L., Devys, D., 2014. The SAGA coactivator complex acts on the whole transcribed genome and is required for RNA polymerase II transcription. Genes Dev. 28, 1999–2012. doi:10.1101/gad.250225.114

Booth, G.T., Parua, P.K., Sanso, M., Fisher, R.P., Lis, J.T., 2017. Cdk9 regulates a promoter-proximal checkpoint to modulate RNA Polymerase II elongation rate. Biorxiv. doi:10.1101/190512

Booth, G.T., Wang, I.X., Cheung, V.G., Lis, J.T., 2016. Divergence of a conserved elongation factor and transcription regulation in budding and fission yeast. Genome Res. 26, 799–811. doi:10.1101/gr.204578.116

Bose, D.A., Donahue, G., Reinberg, D., Shiekhattar, R., Bonasio, R., Berger, S.L., 2017. RNA Binding to CBP Stimulates Histone Acetylation and Transcription. Cell 168, 135–149.e22. doi:10.1016/j.cell.2016.12.020

Botuyan, M.V., Lee, J., Ward, I.M., Kim, J.-E., Thompson, J.R., Chen, J., Mer, G., 2006. Structural basis for the methylation state-specific recognition of histone H4-K20 by 53BP1 and Crb2 in DNA repair. Cell 127, 1361–1373. doi:10.1016/j.cell.2006.10.043

Boudreault, A.A., Cronier, D., Selleck, W., Lacoste, N., Utley, R.T., Allard, S., Savard, J., Lane, W.S., Tan, S., Côté, J., 2003. Yeast enhancer of polycomb defines global Esa1-dependent acetylation of chromatin. Genes Dev. 17, 1415–1428. doi:10.1101/gad.1056603

Bönisch, C., Hake, S.B., 2012. Histone H2A variants in nucleosomes and chromatin: more or less stable? Nucleic Acids Res. 40, 10719–10741. doi:10.1093/nar/gks865

Bram, R.J., Kornberg, R.D., 1985. Specific protein binding to far upstream activating sequences in polymerase II promoters. Proc. Natl. Acad. Sci. U.S.A. 82, 43–47.

Brent, R., Ptashne, M., 1985. A eukaryotic transcriptional activator bearing the DNA specificity of a prokaryotic repressor. Cell 43, 729–736.

Briggs, S.D., Bryk, M., Strahl, B.D., Cheung, W.L., Davie, J.K., Dent, S.Y., Winston, F., Allis, C.D., 2001. Histone H3 lysine 4 methylation is mediated by Set1 and required for cell growth and rDNA silencing in Saccharomyces cerevisiae. Genes & Development 15, 3286–3295. doi:10.1101/gad.940201

Briggs, S.D., Xiao, T., Sun, Z.-W., Caldwell, J.A., Shabanowitz, J., Hunt, D.F., Allis, C.D., Strahl, B.D., 2002. Gene silencing: trans-histone regulatory pathway in chromatin. Nature 418, 498. doi:10.1038/nature00970

Brogaard, K., Xi, L., Wang, J.-P., Widom, J., 2012. A map of nucleosome positions in yeast at base-pair resolution. Nature 486, 496–501. doi:10.1038/nature11142

Brower-Toland, B., Wacker, D.A., Fulbright, R.M., Lis, J.T., Kraus, W.L., Wang, M.D., 2005. Specific Contributions of Histone Tails and their Acetylation to the Mechanical Stability of Nucleosomes. Journal of Molecular Biology 346, 135–146. doi:10.1016/j.jmb.2004.11.056

Brown, C.E., Howe, L., Sousa, K., Alley, S.C., Carrozza, M.J., Tan, S., Workman, J.L., 2001. Recruitment of HAT complexes by direct activator interactions with the ATM-related Tra1 subunit. Science 292, 2333–2337. doi:10.1126/science.1060214

Brown, I.R., Sutcliffe, J.G., 1987. Atypical nucleosome spacing of rat neuronal identifier elements in non-neuronal chromatin. Nucleic Acids Res. 15, 3563–3571. doi:10.1111/ijlh.12329

Brownell, J.E., Zhou, J., Ranalli, T., Kobayashi, R., Edmondson, D.G., Roth, S.Y., Allis, C.D., 1996. Tetrahymena histone acetyltransferase A: a homolog to yeast Gcn5p linking histone acetylation to gene activation. Cell 84, 843–851.

Bujold, D., Morais, D.A. de L., Gauthier, C., Côté, C., Caron, M., Kwan, T., Chen, K.C., Laperle, J., Markovits, A.N., Pastinen, T., Caron, B., Veilleux, A., Jacques, P.-É., Bourque, G., 2016. The International Human Epigenome Consortium Data Portal. Cell Syst 3, 496–499.e2. doi:10.1016/j.cels.2016.10.019

Buratowski, S., 2003. The CTD code. Nat. Struct. Biol. 10, 679–680. doi:10.1038/nsb0903-679

Burgess, R.J., Zhou, H., Han, J., Zhang, Z., 2010. A role for Gcn5 in replication-coupled nucleosome assembly. Molecular Cell 37, 469–480. doi:10.1016/j.molcel.2010.01.020

Burke, T.W., Kadonaga, J.T., 1996. Drosophila TFIID binds to a conserved downstream basal promoter element that is present in many TATA-box-deficient promoters. Genes & Development 10, 711–724.

Bushnell, D.A., Kornberg, R.D., 2003. Complete, 12-subunit RNA polymerase II at 4.1-A resolution: implications for the initiation of transcription. Proc. Natl. Acad. Sci. U.S.A. 100, 6969–6973. doi:10.1073/pnas.1130601100

Cai, L., Sutter, B.M., Li, B., Tu, B.P., 2011. Acetyl-CoA Induces Cell Growth and Proliferation by Promoting the Acetylation of Histones at Growth Genes. Molecular Cell 42, 426–437. doi:10.1016/j.molcel.2011.05.004

Cai, Y., Jin, J., Florens, L., Swanson, S.K., Kusch, T., Li, B., Workman, J.L., Washburn, M.P., Conaway, R.C., Conaway, J.W., 2005. The mammalian YL1 protein is a shared subunit of the TRRAP/TIP60 histone acetyltransferase and SRCAP complexes. J. Biol. Chem. 280, 13665–13670. doi:10.1074/jbc.M500001200

Campos, E.I., Reinberg, D., 2009. Histones: Annotating Chromatin. Annu. Rev. Genet. 43, 559–599. doi:10.1146/annurev.genet.032608.103928

Cano, A., Pestaña, A., 1979. Purification and properties of a histone acetyltransferase from Artemia salina, highly efficient with H1 histone. Eur. J. Biochem. 97, 65–72.

Carey, M., Li, B., Workman, J.L., 2006. RSC exploits histone acetylation to abrogate the nucleosomal block to RNA polymerase II elongation. Molecular Cell 24, 481–487. doi:10.1016/j.molcel.2006.09.012

Carlson, S., Glass, K.C., 2014. The MOZ histone acetyltransferase in epigenetic signaling and disease. J. Cell. Physiol. 229, 1571–1574. doi:10.1002/jcp.24617

Carrozza, M.J., Li, B., Florens, L., Suganuma, T., Swanson, S.K., Lee, K.K., Shia, W.-J., Anderson, S., Yates, J., Washburn, M.P., Workman, J.L., 2005. Histone H3 methylation by Set2 directs deacetylation of coding regions by Rpd3S to suppress spurious intragenic transcription. Cell 123, 581–592. doi:10.1016/j.cell.2005.10.023

Champagne, K.S., Saksouk, N., Peña, P.V., Johnson, K., Ullah, M., Yang, X.-J., Côté, J., Kutateladze, T.G., 2008. The crystal structure of the ING5 PHD finger in complex with an H3K4me3 histone peptide. Proteins 72, 1371–1376. doi:10.1002/prot.22140

Chang, Y., Levy, D., Horton, J.R., Peng, J., Zhang, X., Gozani, O., Cheng, X., 2011. Structural basis of SETD6-mediated regulation of the NF-kB network via methyl-lysine signaling. Nucleic Acids Res. 39, 6380–6389. doi:10.1093/nar/gkr256

Chatterjee, N., Sinha, D., Lemma-Dechassa, M., Tan, S., Shogren-Knaak, M.A., Bartholomew, B., 2011. Histone H3 tail acetylation modulates ATP-dependent remodeling through multiple mechanisms. Nucleic Acids Res. 39, 8378–8391. doi:10.1093/nar/gkr535

Chen, Carol C L, Goyal, P., Karimi, M.M., Abildgaard, M.H., Kimura, H., Lorincz, M.C., 2017. H3S10ph broadly marks early-replicating domains in interphase ESCs and shows reciprocal antagonism with H3K9me2. Genome Res. 1–16. doi:10.1101/gr.224717.117

Chen, Poshen B, Chen, H.V., Acharya, D., Rando, O.J., Fazzio, T.G., 2015. R loops regulate promoter-proximal chromatin architecture and cellular differentiation. Nat. Struct. Mol. Biol. 22, 999–1007. doi:10.1038/nsmb.3122

Chen, Yue, Sprung, R., Tang, Y., Ball, H., Sangras, B., Kim, S.C., Falck, J.R., Peng, J., Gu, W., Zhao, Y., 2007. Lysine propionylation and butyrylation are novel post-translational modifications in histones. Molecular & Cellular Proteomics 6, 812–819. doi:10.1074/mcp.M700021-MCP200

Chen, Yupeng, Zhang, L., Estarás, C., Choi, S.H., Moreno, L., Karn, J., Moresco, J.J., Yates, J.R., Jones, K.A., 2014. A gene-specific role for the Ssu72 RNAPII CTD phosphatase in HIV-1 Tat transactivation. Genes Dev. 28, 2261–2275. doi:10.1101/gad.250449.114

Chereji, R.V., Morozov, A.V., 2014. Ubiquitous nucleosome crowding in the yeast genome. Proc Natl Acad Sci USA 111, 5236–5241. doi:10.1073/pnas.1321001111

Cherry, J.M., Hong, E.L., Amundsen, C., Balakrishnan, R., Binkley, G., Chan, E.T., Christie, K.R., Costanzo, M.C., Dwight, S.S., Engel, S.R., Fisk, D.G., Hirschman, J.E., Hitz, B.C., Karra, K., Krieger, C.J., Miyasato, S.R., Nash, R.S., Park, J., Skrzypek, M.S., Simison, M., Weng, S., Wong, E.D., 2012. Saccharomyces Genome Database: the genomics resource of budding yeast. Nucleic Acids Res. 40, D700–5. doi:10.1093/nar/gkr1029

Chesnut, J.D., Stephens, J.H., Dahmus, M.E., 1992. The interaction of RNA polymerase II with the adenovirus-2 major late promoter is precluded by phosphorylation of the C-terminal domain of subunit IIa. J. Biol. Chem. 267, 10500–10506.

Cheung, V., Chua, G., Batada, N.N., Landry, C.R., Michnick, S.W., Hughes, T.R., Winston, F., 2008. Chromatin- and transcription-related factors repress transcription from within coding regions throughout the Saccharomyces cerevisiae genome. PLoS Biol 6, e277. doi:10.1371/journal.pbio.0060277

Chicoine, L.G., Schulman, I.G., Richman, R., Cook, R.G., Allis, C.D., 1986. Nonrandom utilization of acetylation sites in histones isolated from Tetrahymena. Evidence for functionally distinct H4 acetylation sites. J. Biol. Chem. 261, 1071–1076.

Chirinos, M., Hernández, F., Palacián, E., 1998. Repressive effect on oligonucleosome transcription of the core histone tail domains. Biochemistry 37, 7251–7259. doi:10.1021/bi9729817

Cho, E.J., Kim, J.S., 2012. Crowding effects on the formation and maintenance of nuclear bodies: insights from molecular-dynamics simulations of simple spherical model particles. Biophys. J. 103, 424–433. doi:10.1016/j.bpj.2012.07.007

Cho, E.J., Takagi, T., Moore, C.R., Buratowski, S., 1997. mRNA capping enzyme is recruited to the transcription complex by phosphorylation of the RNA polymerase II carboxy-terminal domain. Genes & Development 11, 3319–3326.

Cho, H., Kim, T.K., Mancebo, H., Lane, W.S., Flores, O., Reinberg, D., 1999. A protein phosphatase functions to recycle RNA polymerase II. Genes & Development 13, 1540–1552.

Choi, J.K., Grimes, D.E., Rowe, K.M., Howe, L.J., 2008. Acetylation of Rsc4p by Gcn5p is essential in the absence of histone H3 acetylation. Mol. Cell. Biol. 28, 6967–6972. doi:10.1128/MCB.00570-08

Chrivia, J.C., Kwok, R.P., Lamb, N., Hagiwara, M., Montminy, M.R., Goodman, R.H., 1993. Phosphorylated CREB binds specifically to the nuclear protein CBP. Nature 365, 855–859. doi:10.1038/365855a0

Church, M., Smith, K.C., Alhussain, M.M., Pennings, S., Fleming, A.B., 2017. Sas3 and Ada2(Gcn5)-dependent histone H3 acetylation is required for transcription elongation at the de-repressed FLO1 gene. Nucleic Acids Res. 45, 4413–4430. doi:10.1093/nar/gkx028

Church, M.C., Fleming, A.B., 2017. A role for histone acetylation in regulating transcription elongation. Transcription 45, 1–8. doi:10.1080/21541264.2017.1394423

Churchman, L.S., Weissman, J.S., 2011. Nascent transcript sequencing visualizes transcription at nucleotide resolution. Nature 469, 368–373. doi:10.1038/nature09652

Cieniewicz, A.M., Moreland, L., Ringel, A.E., Mackintosh, S.G., Raman, A., Gilbert, T.M., Wolberger, C., Tackett, A.J., Taverna, S.D., 2014. The bromodomain of Gcn5 regulates site specificity of lysine acetylation on histone H3. Mol. Cell Proteomics 13, 2896–2910. doi:10.1074/mcp.M114.038174

Cirillo, L.A., Zaret, K.S., 1999. An early developmental transcription factor complex that is more stable on nucleosome core particles than on free DNA. Molecular Cell 4, 961–969.

Clapier, C.R., Iwasa, J., Cairns, B.R., Peterson, C.L., 2017. Mechanisms of action and regulation of ATP-dependent chromatin-remodelling complexes. Nature Publishing Group 29, 2563. doi:10.1038/nrm.2017.26

Clarke, A.S., Lowell, J.E., Jacobson, S.J., Pillus, L., 1999. Esa1p is an essential histone acetyltransferase required for cell cycle progression. Mol. Cell. Biol. 19, 2515–2526.

Conerly, M.L., Yao, Z., Zhong, J.W., Groudine, M., Tapscott, S.J., 2016. Distinct Activities of Myf5 and MyoD Indicate Separate Roles in Skeletal Muscle Lineage Specification and Differentiation. Dev. Cell 36, 375–385. doi:10.1016/j.devcel.2016.01.021

Connelly, S., Manley, J.L., 1988. A functional mRNA polyadenylation signal is required for transcription termination by RNA polymerase II. Genes & Development 2, 440–452.

Core, L.J., Martins, A.L., Danko, C.G., Waters, C.T., Siepel, A., Lis, J.T., 2014. Analysis of nascent RNA identifies a unified architecture of initiation regions at mammalian promoters and enhancers. Nature Publishing Group 46, 1311–1320. doi:10.1038/ng.3142

Core, L.J., Waterfall, J.J., Lis, J.T., 2008. Nascent RNA sequencing reveals widespread pausing and divergent initiation at human promoters. Science 322, 1845–1848. doi:10.1126/science.1162228

Cormack, B.P., Struhl, K., 1992. The TATA-binding protein is required for transcription by all three nuclear RNA polymerases in yeast cells. Cell 69, 685–696.

Cote, J., Quinn, J., Workman, J.L., Peterson, C.L., 1994. Stimulation of GAL4 derivative binding to nucleosomal DNA by the yeast SWI/SNF complex. Science 265, 53–60.

Cousens, L.S., Gallwitz, D., Alberts, B.M., 1979. Different accessibilities in chromatin to histone acetylase. J. Biol. Chem. 254, 1716–1723.

Cramer, P., Bushnell, D.A., Kornberg, R.D., 2001. Structural basis of transcription: RNA polymerase II at 2.8 angstrom resolution. Science 292, 1863–1876. doi:10.1126/science.1059493

Crickard, J.B., Lee, J., Lee, T.-H., Reese, J.C., 2017. The elongation factor Spt4/5 regulates RNA polymerase II transcription through the nucleosome. Nucleic Acids Res. doi:10.1093/nar/gkx220

D'Anna, J.A., Isenberg, I., 1974a. Interactions of histone LAK (f2a2) with histones KAS (f2b) and GRK (f2a1). Biochemistry 13, 2098–2104. doi:10.1021/bi00707a016

D'Anna, J.A., Isenberg, I., 1974b. A histone cross-complexing pattern. Biochemistry 13, 4992–4997. doi:10.1021/bi00721a019

Dai, P., Akimaru, H., Tanaka, Y., Hou, D.X., Yasukawa, T., Kanei-Ishii, C., Takahashi, T., Ishii, S., 1996. CBP as a transcriptional coactivator of c-Myb. Genes & Development 10, 528–540.

Daniel, J.A., Torok, M.S., Sun, Z.-W., Schieltz, D., Allis, C.D., Yates, J.R., Grant, P.A., 2004. Deubiquitination of histone H2B by a yeast acetyltransferase complex regulates transcription. J. Biol. Chem. 279, 1867–1871. doi:10.1074/jbc.C300494200

Danko, C.G., Hyland, S.L., Core, L.J., Martins, A.L., Waters, C.T., Lee, H.W., Cheung, V.G., Kraus, W.L., Lis, J.T., Siepel, A., 2015. Identification of active transcriptional regulatory elements from GRO-seq data. Nat. Methods 12, 433–438. doi:10.1038/nmeth.3329

Davey, C.A., Sargent, D.F., Luger, K., Maeder, A.W., Richmond, T.J., 2002. Solvent mediated interactions in the structure of the nucleosome core particle at 1.9 a resolution. Journal of Molecular Biology 319, 1097–1113. doi:10.1016/S0022-

2836(02)00386-8

Davie, J.R., Candido, E.P., 1980. DNase I sensitive chromatin is enriched in the acetylated species of histone H4. FEBS Lett. 110, 164–168.

Davie, J.R., Candido, E.P., 1978. Acetylated histone H4 is preferentially associated with template-active chromatin. Proc. Natl. Acad. Sci. U.S.A. 75, 3574–3577.

Davie, J.R., Saunders, C.A., Walsh, J.M., Weber, S.C., 1981. Histone modifications in the yeast S. Cerevisiae. Nucleic Acids Res. 9, 3205–3216.

de Villiers, J., Schaffner, W., 1981. A small segment of polyoma virus DNA enhances the expression of a cloned beta-globin gene over a distance of 1400 base pairs. Nucleic Acids Res. 9, 6251–6264.

Dedrick, R.L., Kane, C.M., Chamberlin, M.J., 1987. Purified RNA polymerase II recognizes specific termination sites during transcription in vitro. J. Biol. Chem. 262, 9098–9108.

Devaiah, B.N., Case-Borden, C., Gegonne, A., Hsu, C.H., Chen, Q., Meerzaman, D., Dey, A., Ozato, K., Singer, D.S., 2016. BRD4 is a histone acetyltransferase that evicts nucleosomes from chromatin. Nat. Struct. Mol. Biol. doi:10.1038/nsmb.3228

Dhalluin, C., Carlson, J.E., Zeng, L., He, C., Aggarwal, A.K., Zhou, M.M., 1999. Structure and ligand of a histone acetyltransferase bromodomain. Nature 399, 491–496. doi:10.1038/20974

Dhayalan, A., Tamas, R., Bock, I., Tattermusch, A., Dimitrova, E., Kudithipudi, S., Ragozin, S., Jeltsch, A., 2011. The ATRX-ADD domain binds to H3 tail peptides and reads the combined methylation state of K4 and K9. Human Molecular Genetics 20, 2195–2203. doi:10.1093/hmg/ddr107

Di Cerbo, V., Mohn, F., Ryan, D.P., Montellier, E., Kacem, S., Tropberger, P., Kallis, E., Holzner, M., Hoerner, L., Feldmann, A., Richter, F.M., Bannister, A.J., Mittler, G., Michaelis, J., Khochbin, S., Feil, R., Schuebeler, D., Owen-Hughes, T., Daujat, S., Schneider, R., 2014. Acetylation of histone H3 at lysine 64 regulates nucleosome dynamics and facilitates transcription. Elife 3, e01632. doi:10.7554/eLife.01632

Dion, M.F., Altschuler, S.J., Wu, L.F., Rando, O.J., 2005. Genomic characterization reveals a simple histone H4 acetylation code. Proc. Natl. Acad. Sci. U.S.A. 102, 5501–5506. doi:10.1073/pnas.0500136102

Dover, J., Schneider, J., Tawiah-Boateng, M.A., Wood, A., Dean, K., Johnston, M., Shilatifard, A., 2002. Methylation of histone H3 by COMPASS requires ubiquitination of histone H2B by Rad6. J. Biol. Chem. 277, 28368–28371. doi:10.1074/jbc.C200348200

Downey, M., Johnson, J.R., Davey, N.E., Newton, B.W., Johnson, T.L., Galaang, S.,

Seller, C.A., Krogan, N., Toczyski, D.P., 2015. Acetylome profiling reveals overlap in the regulation of diverse processes by sirtuins, gcn5, and esa1. Mol. Cell Proteomics 14, 162–176. doi:10.1074/mcp.M114.043141

Downey, M., Knight, B., Vashisht, A.A., Seller, C.A., Wohlschlegel, J.A., Shore, D., Toczyski, D.P., 2013. Gcn5 and sirtuins regulate acetylation of the ribosomal protein transcription factor Ifh1. Curr. Biol. 23, 1638–1648. doi:10.1016/j.cub.2013.06.050

Doyon, Y., Cayrou, C., Ullah, M., Landry, A.-J., COtE, V., Selleck, W., Lane, W.S., Tan, S., Yang, X.-J., Côté, J., 2006. ING tumor suppressor proteins are critical regulators of chromatin acetylation required for genome expression and perpetuation. Molecular Cell 21, 51–64. doi:10.1016/j.molcel.2005.12.007

Drew, H.R., 1984. Structural specificities of five commonly used DNA nucleases. Journal of Molecular Biology 176, 535–557.

Driscoll, R., Hudson, A., Jackson, S.P., 2007. Yeast Rtt109 promotes genome stability by acetylating histone H3 on lysine 56. Science 315, 649–652. doi:10.1126/science.1135862

Drouin, S., Laramée, L., Jacques, P.-É., Forest, A., Bergeron, M., Robert, F., 2010. DSIF and RNA polymerase II CTD phosphorylation coordinate the recruitment of Rpd3S to actively transcribed genes. PLoS Genet 6, e1001173. doi:10.1371/journal.pgen.1001173

Durant, M., Pugh, B.F., 2007. NuA4-directed chromatin transactions throughout the Saccharomyces cerevisiae genome. Mol. Cell. Biol. 27, 5327–5335. doi:10.1128/MCB.00468-07

Durant, M., Pugh, B.F., 2006. Genome-wide relationships between TAF1 and histone acetyltransferases in Saccharomyces cerevisiae. Mol. Cell. Biol. 26, 2791–2802. doi:10.1128/MCB.26.7.2791-2802.2006

Durrin, L.K., Mann, R.K., Kayne, P.S., Grunstein, M., 1991. Yeast histone H4 N-terminal sequence is required for promoter activation in vivo. Cell 65, 1023–1031.

Eberharter, A., John, S., Grant, P.A., Utley, R.T., Workman, J.L., 1998. Identification and analysis of yeast nucleosomal histone acetyltransferase complexes. Methods 15, 315–321. doi:10.1006/meth.1998.0635

Eberharter, A., Sterner, D.E., Schieltz, D., Hassan, A., Yates, J.R., Berger, S.L., Workman, J.L., 1999. The ADA complex is a distinct histone acetyltransferase complex in Saccharomyces cerevisiae. Mol. Cell. Biol. 19, 6621–6631.

Eckner, R., Ewen, M.E., Newsome, D., Gerdes, M., DeCaprio, J.A., Lawrence, J.B., Livingston, D.M., 1994. Molecular cloning and functional analysis of the adenovirus E1A-associated 300-kD protein (p300) reveals a protein with properties of a transcriptional adaptor. Genes & Development 8, 869–884.

Ehrensberger, A.H., Kelly, G.P., Svejstrup, J.Q., 2013. Mechanistic Interpretation of Promoter-Proximal Peaks and RNAPII Density Maps. Cell 154, 713–715. doi:10.1016/j.cell.2013.07.032

ENCODE Project Consortium, 2004. The ENCODE (ENCyclopedia Of DNA Elements) Project. Science 306, 636–640. doi:10.1126/science.1105136

Eser, P., Demel, C., Maier, K.C., Schwalb, B., Pirkl, N., Martin, D.E., Cramer, P., Tresch, A., 2014. Periodic mRNA synthesis and degradation co-operate during cell cycle gene expression. Mol. Syst. Biol. 10, 717. doi:10.1002/msb.134886

Feaver, W.J., Gileadi, O., Li, Y., Kornberg, R.D., 1991. CTD kinase associated with yeast RNA polymerase II initiation factor b. Cell 67, 1223–1230.

Feaver, W.J., Svejstrup, J.Q., Henry, N.L., Kornberg, R.D., 1994. Relationship of CDK-activating kinase and RNA polymerase II CTD kinase TFIIH/TFIIK. Cell 79, 1103–1109.

Felipe-Abrio, I., Lafuente-Barquero, J., García-Rubio, M.L., Aguilera, A., 2015. RNA polymerase II contributes to preventing transcription-mediated replication fork stalls. EMBO J. 34, 236–250. doi:10.15252/embj.201488544

Feng, Q., Wang, H., Ng, H.H., Erdjument-Bromage, H., Tempst, P., Struhl, K., Zhang, Y., 2002. Methylation of H3-lysine 79 is mediated by a new family of HMTases without a SET domain. Current Biology 12, 1052–1058.

Fillingham, J., Recht, J., Silva, A.C., Suter, B., Emili, A., Stagljar, I., Krogan, N.J., Allis, C.D., Keogh, M.-C., Greenblatt, J.F., 2008. Chaperone control of the activity and specificity of the histone H3 acetyltransferase Rtt109. Mol. Cell. Biol. 28, 4342–4353. doi:10.1128/MCB.00182-08

Fitz, V., Shin, J., Ehrlich, C., Farnung, L., Cramer, P., Zaburdaev, V., Grill, S.W., 2016. Nucleosomal arrangement affects single-molecule transcription dynamics. Proc Natl Acad Sci USA. doi:10.1073/pnas.1602764113

Flanagan, P.M., Kelleher, R.J., Sayre, M.H., Tschochner, H., Kornberg, R.D., 1991. A mediator required for activation of RNA polymerase II transcription in vitro. Nature 350, 436–438. doi:10.1038/350436a0

Floer, M., Wang, X., Prabhu, V., Berrozpe, G., Narayan, S., Spagna, D., Alvarez, D., Kendall, J., Krasnitz, A., Stepansky, A., Hicks, J., Bryant, G.O., Ptashne, M., 2010. A RSC/nucleosome complex determines chromatin architecture and facilitates activator binding. Cell 141, 407–418. doi:10.1016/j.cell.2010.03.048

Flury, V., Georgescu, P.R., Iesmantavicius, V., Shimada, Y., Kuzdere, T., Braun, S., Bühler, M., 2017. The Histone Acetyltransferase Mst2 Protects Active Chromatin from Epigenetic Silencing by Acetylating the Ubiquitin Ligase Brl1. Molecular Cell 67, 294–307.e9. doi:10.1016/j.molcel.2017.05.026

Fong, N., Brannan, K., Erickson, B., Kim, H., Cortazar, M.A., Sheridan, R.M., Nguyen, T., Karp, S., Bentley, D.L., 2015. Effects of Transcription Elongation Rate and Xrn2 Exonuclease Activity on RNA Polymerase II Termination Suggest Widespread Kinetic Competition. Molecular Cell 60, 256–267. doi:10.1016/j.molcel.2015.09.026

Friis, R.M.N., Schultz, M.C., 2009. Untargeted tail acetylation of histones in chromatin: lessons from yeast. Biochem. Cell Biol. 87, 107–116. doi:10.1139/O08-097

Friis, R.M.N., Wu, B.P., Reinke, S.N., Hockman, D.J., Sykes, B.D., Schultz, M.C., 2009. A glycolytic burst drives glucose induction of global histone acetylation by picNuA4 and SAGA. Nucleic Acids Res. 37, 3969–3980. doi:10.1093/nar/gkp270

Fuda, N.J., Ardehali, M.B., Lis, J.T., 2009. Defining mechanisms that regulate RNA polymerase II transcription in vivo. Nature 461, 186–192. doi:10.1038/nature08449

Gaidatzis, D., Burger, L., Murr, R., Lerch, A., Dessus-Babus, S., Schübeler, D., Stadler, M.B., 2014. DNA sequence explains seemingly disordered methylation levels in partially methylated domains of Mammalian genomes. PLoS Genet 10, e1004143. doi:10.1371/journal.pgen.1004143

Galdieri, L., Vancura, A., 2012. Acetyl-CoA carboxylase regulates global histone acetylation. Journal of Biological Chemistry 287, 23865–23876. doi:10.1074/jbc.M112.380519

Gallwitz, D., 1968. Acetylation of histones by a kinase from rat liver nucle. Biochem. Biophys. Res. Commun. 32, 117–121.

Gallwitz, D., Sekeris, C.E., 1969. Stimulation of RNA polymerase activity of rat liver nuclei by cortisol in vitro independent of effects on the acetylation and methylation of histones. FEBS Lett. 3, 99–102.

Ganem, C., Devaux, F., Torchet, C., Jacq, C., Quevillon-Cheruel, S., Labesse, G., Facca, C., Faye, G., 2003. Ssu72 is a phosphatase essential for transcription termination of snoRNAs and specific mRNAs in yeast. EMBO J. 22, 1588–1598. doi:10.1093/emboj/cdg141

Gansen, A., Tóth, K., Schwarz, N., Langowski, J., 2009. Structural variability of nucleosomes detected by single-pair Förster resonance energy transfer: histone acetylation, sequence variation, and salt effects. J Phys Chem B 113, 2604–2613. doi:10.1021/jp7114737

Garcia-Ramirez, M., Rocchini, C., Ausio, J., 1995. Modulation of chromatin folding by histone acetylation. J. Biol. Chem. 270, 17923–17928.

Gatchalian, J., Wang, X., Ikebe, J., Cox, K.L., Tencer, A.H., Zhang, Y., Burge, N.L., Di, L., Gibson, M.D., Musselman, C.A., Poirier, M.G., Kono, H., Hayes, J.J., Kutateladze, T.G., 2017. Accessibility of the histone H3 tail in the nucleosome for binding of paired readers. Nat Commun 1–10. doi:10.1038/s41467-017-01598-x

Geiger, T., Wehner, A., Schaab, C., Cox, J., Mann, M., 2012. Comparative proteomic analysis of eleven common cell lines reveals ubiquitous but varying expression of most proteins. Mol. Cell Proteomics 11, M111.014050. doi:10.1074/mcp.M111.014050

Georgakopoulos, T., Thireos, G., 1992. Two distinct yeast transcriptional activators require the function of the GCN5 protein to promote normal levels of transcription. EMBO J. 11, 4145–4152.

Georges, S.A., Giebler, H.A., Cole, P.A., Luger, K., Laybourn, P.J., Nyborg, J.K., 2003. Tax recruitment of CBP/p300, via the KIX domain, reveals a potent requirement for acetyltransferase activity that is chromatin dependent and histone tail independent. Mol. Cell. Biol. 23, 3392–3404. doi:10.1128/MCB.23.10.3392-3404.2003

Georgiev, P.G., 1969. Histones and the control of gene action. Annu. Rev. Genet. 3, 155–180.

Gerasimova, N.S., Pestov, N.A., Kulaeva, O.I., Clark, D.J., Studitsky, V.M., 2016. Transcription-induced DNA supercoiling: New roles of intranucleosomal DNA loops in DNA repair and transcription. Transcription 7, 91–95. doi:10.1080/21541264.2016.1182240

Gershey, E.L., Vidali, G., Allfrey, V.G., 1968. Chemical studies of histone acetylation. The occurrence of epsilon-N-acetyllysine in the f2a1 histone. J. Biol. Chem. 243, 5018–5022.

Gilbert, T.M., McDaniel, S.L., Byrum, S.D., Cades, J.A., Dancy, B.C.R., Wade, H., Tackett, A.J., Strahl, B.D., Taverna, S.D., 2014. A PWWP domain-containing protein targets the NuA3 acetyltransferase complex via histone H3 lysine 36 trimethylation to coordinate transcriptional elongation at coding regions. Mol. Cell Proteomics 13, 2883–2895. doi:10.1074/mcp.M114.038224

Gilmour, D.S., Lis, J.T., 1986. RNA polymerase II interacts with the promoter region of the noninduced hsp70 gene in Drosophila melanogaster cells. Mol. Cell. Biol. 6, 3984–3989.

Ginsburg, D.S., Anlembom, T.E., Wang, J., Patel, S.R., Li, B., Hinnebusch, A.G., 2014. NuA4 links methylation of histone H3 lysines 4 and 36 to acetylation of histones H4 and H3. Journal of Biological Chemistry 289, 32656–32670. doi:10.1074/jbc.M114.585588

Ginsburg, D.S., Govind, C.K., Hinnebusch, A.G., 2009. NuA4 lysine acetyltransferase Esa1 is targeted to coding regions and stimulates transcription elongation with Gcn5. Mol. Cell. Biol. 29, 6473–6487. doi:10.1128/MCB.01033-09

Gkikopoulos, T., Schofield, P., Singh, V., Pinskaya, M., Mellor, J., Smolle, M., Workman, J.L., Barton, G.J., Owen-Hughes, T., 2011. A role for Snf2-related nucleosome-spacing enzymes in genome-wide nucleosome organization. Science

333, 1758–1760. doi:10.1126/science.1206097

Goldknopf, I.L., Busch, H., 1977. Isopeptide linkage between nonhistone and histone 2A polypeptides of chromosomal conjugate-protein A24. Proc. Natl. Acad. Sci. U.S.A. 74, 864–868.

Gonzales-Cope, M., Sidoli, S., Bhanu, N.V., Won, K.-J., Garcia, B.A., 2016. Histone H4 acetylation and the epigenetic reader Brd4 are critical regulators of pluripotency in embryonic stem cells. BMC Genomics 17, 95. doi:10.1186/s12864-016-2414-y

Gorovsky, M.A., Pleger, G.L., Keevert, J.B., Johmann, C.A., 1973. Studies on histone fraction F2A1 in macro- and micronuclei of Tetrahymena pyriformis. The Journal of Cell Biology 57, 773–781.

Gossett, A.J., Lieb, J.D., 2012. In vivo effects of histone H3 depletion on nucleosome occupancy and position in Saccharomyces cerevisiae. PLoS Genet 8, e1002771. doi:10.1371/journal.pgen.1002771

Govind, C.K., Qiu, H., Ginsburg, D.S., Ruan, C., Hofmeyer, K., Hu, C., Swaminathan, V., Workman, J.L., Li, B., Hinnebusch, A.G., 2010. Phosphorylated Pol II CTD recruits multiple HDACs, including Rpd3C(S), for methylation-dependent deacetylation of ORF nucleosomes. Molecular Cell 39, 234–246. doi:10.1016/j.molcel.2010.07.003

Govind, C.K., Zhang, F., Qiu, H., Hofmeyer, K., Hinnebusch, A.G., 2007. Gcn5 promotes acetylation, eviction, and methylation of nucleosomes in transcribed coding regions. Molecular Cell 25, 31–42. doi:10.1016/j.molcel.2006.11.020

Grant, P.A., Duggan, L., Cote, J., Roberts, S.M., Brownell, J.E., Candau, R., Ohba, R., Owen-Hughes, T., Allis, C.D., Winston, F., Berger, S.L., Workman, J.L., 1997. Yeast Gcn5 functions in two multisubunit complexes to acetylate nucleosomal histones: characterization of an Ada complex and the SAGA (Spt/Ada) complex. Genes & Development 11, 1640–1650.

Grant, P.A., Eberharter, A., John, S., Cook, R.G., Turner, B.M., Workman, J.L., 1999. Expanded lysine acetylation specificity of Gcn5 in native complexes. J. Biol. Chem. 274, 5895–5900.

Grant, P.A., Schieltz, D., Pray-Grant, M.G., Yates, J.R., Workman, J.L., 1998. The ATM-related cofactor Tra1 is a component of the purified SAGA complex. Molecular Cell 2, 863–867.

Green, E.M., Mas, G., Young, N.L., Garcia, B.A., Gozani, O., 2012. Methylation of H4 lysines 5, 8 and 12 by yeast Set5 calibrates chromatin stress responses. Nature Structural & Molecular Biology 19, 361–363. doi:10.1038/nsmb.2252

Grigull, J., Mnaimneh, S., Pootoolal, J., Robinson, M.D., Hughes, T.R., 2004. Genome-wide analysis of mRNA stability using transcription inhibitors and microarrays

reveals posttranscriptional control of ribosome biogenesis factors. Mol. Cell. Biol. 24, 5534–5547. doi:10.1128/MCB.24.12.5534-5547.2004

Guillemette, B., Drogaris, P., Lin, H.-H.S., Armstrong, H., Hiragami-Hamada, K., Imhof, A., Bonneil, É., Thibault, P., Verreault, A., Festenstein, R.J., 2011. H3 lysine 4 is acetylated at active gene promoters and is regulated by H3 lysine 4 methylation. PLoS Genet 7, e1001354. doi:10.1371/journal.pgen.1001354

Hahn, S., Buratowski, S., Sharp, P.A., Guarente, L., 1989. Yeast TATA-binding protein TFIID binds to TATA elements with both consensus and nonconsensus DNA sequences. Proc. Natl. Acad. Sci. U.S.A. 86, 5718–5722.

Hamada, H., 1986. Random isolation of gene activator elements from the human genome. Mol. Cell. Biol. 6, 4185–4194.

Hampsey, M., 1998. Molecular genetics of the RNA polymerase II general transcriptional machinery. Microbiol. Mol. Biol. Rev. 62, 465–503.

Han, J., Zhou, H., Horazdovsky, B., Zhang, K., Xu, R.-M., Zhang, Z., 2007. Rtt109 acetylates histone H3 lysine 56 and functions in DNA replication. Science 315, 653–655. doi:10.1126/science.1133234

Han, Z., Guo, L., Wang, H., Shen, Y., Deng, X.W., Chai, J., 2006. Structural basis for the specific recognition of methylated histone H3 lysine 4 by the WD-40 protein WDR5. Molecular Cell 22, 137–144. doi:10.1016/j.molcel.2006.03.018

Harlen, K.M., Trotta, K.L., Smith, E.E., Mosaheb, M.M., Fuchs, S.M., Churchman, L.S., 2016. Comprehensive RNA Polymerase II Interactomes Reveal Distinct and Varied Roles for Each Phospho-CTD Residue. Cell Rep 15, 2147–2158. doi:10.1016/j.celrep.2016.05.010

Haruki, H., Nishikawa, J., Laemmli, U.K., 2008. The anchor-away technique: rapid, conditional establishment of yeast mutant phenotypes. Molecular Cell 31, 925–932. doi:10.1016/j.molcel.2008.07.020

Hassan, A.H., Prochasson, P., Neely, K.E., Galasinski, S.C., Chandy, M., Carrozza, M.J., Workman, J.L., 2002. Function and selectivity of bromodomains in anchoring chromatin-modifying complexes to promoter nucleosomes. Cell 111, 369–379.

Hauk, G., McKnight, J.N., Nodelman, I.M., Bowman, G.D., 2010. The chromodomains of the Chd1 chromatin remodeler regulate DNA access to the ATPase motor. Molecular Cell 39, 711–723. doi:10.1016/j.molcel.2010.08.012

Hawkins, R.D., Hon, G.C., Lee, L.K., Ngo, Q., Lister, R., Pelizzola, M., Edsall, L.E., Kuan, S., Luu, Y., Klugman, S., Antosiewicz-Bourget, J., Ye, Z., Espinoza, C., Agarwahl, S., Shen, L., Ruotti, V., Wang, W., Stewart, R., Thomson, J.A., Ecker, J.R., Ren, B., 2010. Distinct epigenomic landscapes of pluripotent and lineage-committed human cells. Cell Stem Cell 6, 479–491. doi:10.1016/j.stem.2010.03.018

Haynes, S.R., Dollard, C., Winston, F., Beck, S., Trowsdale, J., Dawid, I.B., 1992. The bromodomain: a conserved sequence found in human, Drosophila and yeast proteins. Nucleic Acids Res. 20, 2603.

He, F., Umehara, T., Saito, K., Harada, T., Watanabe, S., Yabuki, T., Kigawa, T., Takahashi, M., Kuwasako, K., Tsuda, K., Matsuda, T., Aoki, M., Seki, E., Kobayashi, N., Güntert, P., Yokoyama, S., Muto, Y., 2010. Structural insight into the zinc finger CW domain as a histone modification reader. Structure 18, 1127–1139. doi:10.1016/j.str.2010.06.012

Heise, F., Chung, H.-R., Weber, J.M., Xu, Z., Klein-Hitpass, L., Steinmetz, L.M., Vingron, M., Ehrenhofer-Murray, A.E., 2012. Genome-wide H4 K16 acetylation by SAS-I is deposited independently of transcription and histone exchange. Nucleic Acids Res. 40, 65–74. doi:10.1093/nar/gkr649

Henikoff, S., Shilatifard, A., 2011. Histone modification: cause or cog? Trends Genet. 27, 389–396. doi:10.1016/j.tig.2011.06.006

Henriksen, P., Wagner, S.A., Weinert, B.T., Sharma, S., Bacinskaja, G., Rehman, M., Juffer, A.H., Walther, T.C., Lisby, M., Choudhary, C., 2012. Proteome-wide analysis of lysine acetylation suggests its broad regulatory scope in Saccharomyces cerevisiae. Mol. Cell Proteomics 11, 1510–1522. doi:10.1074/mcp.M112.017251

Hewish, D.R., Burgoyne, L.A., 1973. Chromatin sub-structure. The digestion of chromatin DNA at regularly spaced sites by a nuclear deoxyribonuclease. Biochem. Biophys. Res. Commun. 52, 504–510.

Hindley, J., 1963. The relative ability of reconstituted nucleohistones to allow DNA-dependent RNA synthesis. Biochem. Biophys. Res. Commun. 12, 175–179.

Hirschhorn, J.N., Brown, S.A., Clark, C.D., Winston, F., 1992. Evidence that SNF2/SWI2 and SNF5 activate transcription in yeast by altering chromatin structure. Genes & Development 6, 2288–2298.

Hoppmann, V., Thorstensen, T., Kristiansen, P.E., Veiseth, S.V., Rahman, M.A., Finne, K., Aalen, R.B., Aasland, R., 2011. The CW domain, a new histone recognition module in chromatin proteins. EMBO J. 30, 1939–1952. doi:10.1038/emboj.2011.108

Howe, L., Auston, D., Grant, P., John, S., Cook, R.G., Workman, J.L., Pillus, L., 2001. Histone H3 specific acetyltransferases are essential for cell cycle progression. Genes & Development 15, 3144–3154. doi:10.1101/gad.931401

Howe, L., Kusch, T., Muster, N., Chaterji, R., Yates, J.R., Workman, J.L., 2002. Yng1p modulates the activity of Sas3p as a component of the yeast NuA3 Hhistone acetyltransferase complex. Mol. Cell. Biol. 22, 5047–5053. doi:10.1128/MCB.22.14.5047-5053.2002

Huang, Bo, Johansson, M.J.O., Byström, A.S., 2005. An early step in wobble uridine tRNA modification requires the Elongator complex. RNA 11, 424–436. doi:10.1261/rna.7247705

Huang, Hailiang, Maertens, A.M., Hyland, E.M., Dai, J., Norris, A., Boeke, J.D., Bader, J.S., 2009. HistoneHits: a database for histone mutations and their phenotypes. Genome Res. 19, 674–681. doi:10.1101/gr.083402.108

Huang, He, Sabari, B.R., Garcia, B.A., Allis, C.D., Zhao, Y., 2014. SnapShot: histone modifications. Cell 159, 458–458.e1. doi:10.1016/j.cell.2014.09.037

Huang, Jiehuan, Tan, S., 2013. Piccolo NuA4-catalyzed acetylation of nucleosomal histones: critical roles of an Esa1 Tudor/chromo barrel loop and an Epl1 enhancer of polycomb A (EPcA) basic region. Mol. Cell. Biol. 33, 159–169. doi:10.1128/MCB.01131-12

Huang, R.C., Bonner, J., 1962. Histone, a suppressor of chromosomal RNA synthesis. Proc. Natl. Acad. Sci. U.S.A. 48, 1216–1222.

Huh, W.-K., Falvo, J.V., Gerke, L.C., Carroll, A.S., Howson, R.W., Weissman, J.S., O'Shea, E.K., 2003. Global analysis of protein localization in budding yeast. Nature 425, 686–691. doi:10.1038/nature02026

Hung, T., Binda, O., Champagne, K.S., Kuo, A.J., Johnson, K., Chang, H.Y., Simon, M.D., Kutateladze, T.G., Gozani, O., 2009. ING4 mediates crosstalk between histone H3 K4 trimethylation and H3 acetylation to attenuate cellular transformation. Molecular Cell 33, 248–256. doi:10.1016/j.molcel.2008.12.016

Hunt, L.T., Dayhoff, M.O., 1977. Amino-terminal sequence identity of ubiquitin and the nonhistone component of nuclear protein A24. Biochem. Biophys. Res. Commun. 74, 650–655.

Ikura, T., Ogryzko, V.V., Grigoriev, M., Groisman, R., Wang, J., Horikoshi, M., Scully, R., Qin, J., Nakatani, Y., 2000. Involvement of the TIP60 histone acetylase complex in DNA repair and apoptosis. Cell 102, 463–473. doi:10.1038/35036020

Imashimizu, M., Kireeva, M.L., Lubkowska, L., Gotte, D., Parks, A.R., Strathern, J.N., Kashlev, M., 2013. Intrinsic translocation barrier as an initial step in pausing by RNA polymerase II. Journal of Molecular Biology 425, 697–712. doi:10.1016/j.jmb.2012.12.002

Imbalzano, A.N., Kwon, H., Green, M.R., Kingston, R.E., 1994. Facilitated binding of TATA-binding protein to nucleosomal DNA. Nature 370, 481–485. doi:10.1038/370481a0

Imhof, A., Yang, X.J., Ogryzko, V.V., Nakatani, Y., Wolffe, A.P., Ge, H., 1997. Acetylation of general transcription factors by histone acetyltransferases. Current Biology 7, 689–692.

Inoue, A., Fujimoto, D., 1972. Substrate specificity of histone deacetylase from calf thymus. J. Biochem. 72, 427–431.

Inoue, A., Fujimoto, D., 1970. Histone deacetylase from calf thymus. Biochim. Biophys. Acta 220, 307–316.

Inoue, A., Fujimoto, D., 1969. Enzymatic deacetylation of histone. Biochem. Biophys. Res. Commun. 36, 146–150.

Jackson, V., 1990. In vivo studies on the dynamics of histone-DNA interaction: evidence for nucleosome dissolution during replication and transcription and a low level of dissolution independent of both. Biochemistry 29, 719–731. doi:10.1021/bi00455a019

Jackson, V., Shires, A., Tanphaichitr, N., Chalkley, R., 1976. Modifications to histones immediately after synthesis. Journal of Molecular Biology 104, 471–483.

Jacobson, R.H., Ladurner, A.G., King, D.S., Tjian, R., 2000. Structure and function of a human TAFII250 double bromodomain module. Science 288, 1422–1425.

Jeronimo, C., Robert, F., 2014. Kin28 regulates the transient association of Mediator with core promoters. Nature Structural & Molecular Biology 21, 449–455. doi:10.1038/nsmb.2810

Jiakuntorn, Y., Mathias, A.P., 1981. Effects of gene modulators on the acetylation of chromosomal proteins of rat liver slices. Biochem. Biophys. Res. Commun. 102, 811–817.

Jiang, C., Pugh, B.F., 2009. A compiled and systematic reference map of nucleosome positions across the Saccharomyces cerevisiae genome. Genome Biol. 10, R109. doi:10.1186/gb-2009-10-10-r109

Jiang, L., Smith, J.N., Anderson, S.L., Ma, P., Mizzen, C.A., Kelleher, N.L., 2007. Global assessment of combinatorial post-translational modification of core histones in yeast using contemporary mass spectrometry. LYS4 trimethylation correlates with degree of acetylation on the same H3 tail. J. Biol. Chem. 282, 27923–27934. doi:10.1074/jbc.M704194200

Jimenez, A., Tipper, D.J., Davies, J., 1973. Mode of action of thiolutin, an inhibitor of macromolecular synthesis in Saccharomyces cerevisiae. Antimicrob. Agents Chemother. 3, 729–738.

Jin, Y., Eser, U., Struhl, K., Churchman, L.S., 2017. The Ground State and Evolution of Promoter Region Directionality. Cell 170, 889–898.e10. doi:10.1016/j.cell.2017.07.006

John, S., Howe, L., Tafrov, S.T., Grant, P.A., Sternglanz, R., Workman, J.L., 2000. The something about silencing protein, Sas3, is the catalytic subunit of NuA3, a

yTAF(II)30-containing HAT complex that interacts with the Spt16 subunit of the yeast CP (Cdc68/Pob3)-FACT complex. Genes Dev. 14, 1196–1208.

Jonkers, I., Kwak, H., Lis, J.T., 2014. Genome-wide dynamics of Pol II elongation and its interplay with promoter proximal pausing, chromatin, and exons. Elife 3, e02407. doi:10.7554/eLife.02407.025

Joo, Y.J., Ficarro, S.B., Soares, L.M., Chun, Y., Marto, J.A., Buratowski, S., 2017. Downstream promoter interactions of TFIID TAFs facilitate transcription reinitiation. Genes Dev. doi:10.1101/gad.306324.117

Joshi, A.A., Struhl, K., 2005. Eaf3 chromodomain interaction with methylated H3-K36 links histone deacetylation to Pol II elongation. Molecular Cell 20, 971–978. doi:10.1016/j.molcel.2005.11.021

Kadosh, D., Struhl, K., 1998. Histone deacetylase activity of Rpd3 is important for transcriptional repression in vivo. Genes & Development 12, 797–805.

Kadosh, D., Struhl, K., 1997. Repression by Ume6 involves recruitment of a complex containing Sin3 corepressor and Rpd3 histone deacetylase to target promoters. Cell 89, 365–371.

Kaluarachchi Duffy, S., Friesen, H., Baryshnikova, A., Lambert, J.-P., Chong, Y.T., Figeys, D., Andrews, B., 2012. Exploring the yeast acetylome using functional genomics. Cell 149, 936–948. doi:10.1016/j.cell.2012.02.064

Kamine, J., Elangovan, B., Subramanian, T., Coleman, D., Chinnadurai, G., 1996. Identification of a cellular protein that specifically interacts with the essential cysteine region of the HIV-1 Tat transactivator. Virology 216, 357–366. doi:10.1006/viro.1996.0071

Kanno, T., Kanno, Y., Leroy, G., Campos, E., Sun, H.-W., Brooks, S.R., Vahedi, G., Heightman, T.D., Garcia, B.A., Reinberg, D., Siebenlist, U., O'Shea, J.J., Ozato, K., 2014. BRD4 assists elongation of both coding and enhancer RNAs by interacting with acetylated histones. Nature Structural & Molecular Biology 21, 1047–1057. doi:10.1038/nsmb.2912

Kaplan, C.D., Laprade, L., Winston, F., 2003. Transcription elongation factors repress transcription initiation from cryptic sites. Science 301, 1096–1099. doi:10.1126/science.1087374

Kaplan, N., Moore, I.K., Fondufe-Mittendorf, Y., Gossett, A.J., Tillo, D., Field, Y., LeProust, E.M., Hughes, T.R., Lieb, J.D., Widom, J., Segal, E., 2009. The DNA-encoded nucleosome organization of a eukaryotic genome. Nature 458, 362–366. doi:10.1038/nature07667

Kaplan, T., Liu, C.L., Erkmann, J.A., Holik, J., Grunstein, M., Kaufman, P.D., Friedman, N., Rando, O.J., 2008. Cell cycle- and chaperone-mediated regulation of H3K56ac

incorporation in yeast. PLoS Genet 4, e1000270. doi:10.1371/journal.pgen.1000270

Kelleher, R.J., Flanagan, P.M., Kornberg, R.D., 1990. A novel mediator between activator proteins and the RNA polymerase II transcription apparatus. Cell 61, 1209–1215.

Kennani, El, S., Adrait, A., Shaytan, A.K., Khochbin, S., Bruley, C., Panchenko, A.R., Landsman, D., Pflieger, D., Govin, J., 2017. MS_HistoneDB, a manually curated resource for proteomic analysis of human and mouse histones. Epigenetics Chromatin 10, 2. doi:10.1186/s13072-016-0109-x

Keogh, M.-C., Kurdistani, S.K., Morris, S.A., Ahn, S.H., Podolny, V., Collins, S.R., Schuldiner, M., Chin, K., Punna, T., Thompson, N.J., Boone, C., Emili, A., Weissman, J.S., Hughes, T.R., Strahl, B.D., Grunstein, M., Greenblatt, J.F., Buratowski, S., Krogan, N.J., 2005. Cotranscriptional set2 methylation of histone H3 lysine 36 recruits a repressive Rpd3 complex. Cell 123, 593–605. doi:10.1016/j.cell.2005.10.025

Keogh, M.-C., Podolny, V., Buratowski, S., 2003. Bur1 kinase is required for efficient transcription elongation by RNA polymerase II. Mol. Cell. Biol. 23, 7005–7018. doi:10.1128/MCB.23.19.7005-7018.2003

Kieffer-Kwon, K.-R., Nimura, K., Rao, S.S.P., Xu, J., Jung, S., Pekowska, A., Dose, M., Stevens, E., Mathe, E., Dong, P., Huang, S.-C., Ricci, M.A., Baranello, L., Zheng, Y., Ardori, F.T., Resch, W., Stavreva, D., Nelson, S., McAndrew, M., Casellas, A., Finn, E., Gregory, C., Hilaire, B.G.S., Johnson, S.M., Dubois, W., Cosma, M.P., Batchelor, E., Levens, D., Phair, R.D., Misteli, T., Tessarollo, L., Hager, G., Lakadamyali, M., Liu, Z., Floer, M., Shroff, H., Aiden, E.L., Casellas, R., 2017. Myc Regulates Chromatin Decompaction and Nuclear Architecture during B Cell Activation. Molecular Cell 67, 566–578.e10. doi:10.1016/j.molcel.2017.07.013

Kim, C.-H., Kim, J.-W., Jang, S.-M., An, J.-H., Seo, S.-B., Choi, K.-H., 2015. The chromodomain-containing histone acetyltransferase TIP60 acts as a code reader, recognizing the epigenetic codes for initiating transcription. Biosci. Biotechnol. Biochem. 79, 532–538. doi:10.1080/09168451.2014.993914

Kim, J., Daniel, J., Espejo, A., Lake, A., Krishna, M., Xia, L., Zhang, Y., Bedford, M.T., 2006. Tudor, MBT and chromo domains gauge the degree of lysine methylation. EMBO Rep. 7, 397–403. doi:10.1038/sj.embor.7400625

Kim, J.-H., Saraf, A., Florens, L., Washburn, M., Workman, J.L., 2010. Gcn5 regulates the dissociation of SWI/SNF from chromatin by acetylation of Swi2/Snf2. Genes Dev. 24, 2766–2771. doi:10.1101/gad.1979710

Kim, J.L., Nikolov, D.B., Burley, S.K., 1993. Co-crystal structure of TBP recognizing the minor groove of a TATA element. Nature 365, 520–527. doi:10.1038/365520a0

Kim, T., Buratowski, S., 2009. Dimethylation of H3K4 by Set1 recruits the Set3 histone

deacetylase complex to 5' transcribed regions. Cell 137, 259–272. doi:10.1016/j.cell.2009.02.045

Kim, T.S., Liu, C.L., Yassour, M., Holik, J., Friedman, N., Buratowski, S., Rando, O.J., 2010. RNA polymerase mapping during stress responses reveals widespread nonproductive transcription in yeast. Genome Biol. 11, R75. doi:10.1186/gb-2010-11-7-r75

Kim, Y.J., Björklund, S., Li, Y., Sayre, M.H., Kornberg, R.D., 1994. A multiprotein mediator of transcriptional activation and its interaction with the C-terminal repeat domain of RNA polymerase II. Cell 77, 599–608.

Kimura, A., Horikoshi, M., 1998. Tip60 acetylates six lysines of a specific class in core histones in vitro. Genes Cells 3, 789–800.

Kimura, A., Umehara, T., Horikoshi, M., 2002. Chromosomal gradient of histone acetylation established by Sas2p and Sir2p functions as a shield against gene silencing. Nature Genetics 32, 370–377. doi:10.1038/ng993

Kimura, H., Hayashi-Takanaka, Y., Goto, Y., Takizawa, N., Nozaki, N., 2008. The organization of histone H3 modifications as revealed by a panel of specific monoclonal antibodies. Cell Struct. Funct. 33, 61–73.

Kireeva, M.L., Hancock, B., Cremona, G.H., Walter, W., Studitsky, V.M., Kashlev, M., 2005. Nature of the nucleosomal barrier to RNA polymerase II. Molecular Cell 18, 97–108. doi:10.1016/j.molcel.2005.02.027

Kladde, M.P., Simpson, R.T., 1994. Positioned nucleosomes inhibit Dam methylation in vivo. Proc. Natl. Acad. Sci. U.S.A. 91, 1361–1365.

Kleff, S., Andrulis, E.D., Anderson, C.W., Sternglanz, R., 1995. Identification of a gene encoding a yeast histone H4 acetyltransferase. J. Biol. Chem. 270, 24674–24677.

Klymenko, T., Papp, B., Fischle, W., Köcher, T., Schelder, M., Fritsch, C., Wild, B., Wilm, M., Müller, J., 2006. A Polycomb group protein complex with sequence-specific DNA-binding and selective methyl-lysine-binding activities. Genes & Development 20, 1110–1122. doi:10.1101/gad.377406

Kobor, M.S., Archambault, J., Lester, W., Holstege, F.C., Gileadi, O., Jansma, D.B., Jennings, E.G., Kouyoumdjian, F., Davidson, A.R., Young, R.A., Greenblatt, J., 1999. An unusual eukaryotic protein phosphatase required for transcription by RNA polymerase II and CTD dephosphorylation in S. cerevisiae. Molecular Cell 4, 55–62.

Kobor, M.S., Venkatasubrahmanyam, S., Meneghini, M.D., Gin, J.W., Jennings, J.L., Link, A.J., Madhani, H.D., Rine, J., 2004. A protein complex containing the conserved Swi2/Snf2-related ATPase Swr1p deposits histone variant H2A.Z into euchromatin. PLoS Biol 2, E131. doi:10.1371/journal.pbio.0020131

Koerber, R.T., Rhee, H.S., Jiang, C., Pugh, B.F., 2009. Interaction of transcriptional regulators with specific nucleosomes across the Saccharomyces genome. Molecular Cell 35, 889–902. doi:10.1016/j.molcel.2009.09.011

Komarnitsky, P., Cho, E.J., Buratowski, S., 2000. Different phosphorylated forms of RNA polymerase II and associated mRNA processing factors during transcription. Genes & Development 14, 2452–2460. doi:10.1101/gad.824700

Kornberg, R.D., 1974. Chromatin structure: a repeating unit of histones and DNA. Science 184, 868–871.

Kornberg, R.D., Thomas, J.O., 1974. Chromatin structure; oligomers of the histones. Science 184, 865–868.

Krause, M.O., Stein, G.S., 1976. Arginine-rich histone synthesis and acetylation in WI38 cells stimulated to proliferate. Exp. Cell Res. 100, 63–70.

Kraushaar, D.C., Jin, W., Maunakea, A., Abraham, B., Ha, M., Zhao, K., 2013. Genome-wide incorporation dynamics reveal distinct categories of turnover for the histone variant H3.3. Genome Biol. 14, R121. doi:10.1186/gb-2013-14-10-r121

Krietenstein, N., Wal, M., Watanabe, S., Park, B., Peterson, C.L., Pugh, B.F., Korber, P., 2016. Genomic Nucleosome Organization Reconstituted with Pure Proteins. Cell 167, 709–716.e12. doi:10.1016/j.cell.2016.09.045

Krogan, N.J., Dover, J., Khorrami, S., Greenblatt, J.F., Schneider, J., Johnston, M., Shilatifard, A., 2002. COMPASS, a histone H3 (Lysine 4) methyltransferase required for telomeric silencing of gene expression. J. Biol. Chem. 277, 10753–10755. doi:10.1074/jbc.C200023200

Krogan, N.J., Dover, J., Wood, A., Schneider, J., Heidt, J., Boateng, M.A., Dean, K., Ryan, O.W., Golshani, A., Johnston, M., Greenblatt, J.F., Shilatifard, A., 2003a. The Paf1 complex is required for histone H3 methylation by COMPASS and Dot1p: linking transcriptional elongation to histone methylation. Molecular Cell 11, 721–729. doi:10.1016/S1097-2765(03)00091-1

Krogan, N.J., Keogh, M.-C., Datta, N., Sawa, C., Ryan, O.W., Ding, H., Haw, R.A., Pootoolal, J., Tong, A., Canadien, V., Richards, D.P., Wu, X., Emili, A., Hughes, T.R., Buratowski, S., Greenblatt, J.F., 2003b. A Snf2 family ATPase complex required for recruitment of the histone H2A variant Htz1. Molecular Cell 12, 1565–1576.

Krogan, N.J., Kim, M., Tong, A., Golshani, A., Cagney, G., Canadien, V., Richards, D.P., Beattie, B.K., Emili, A., Boone, C., Shilatifard, A., Buratowski, S., Greenblatt, J., 2003c. Methylation of histone H3 by Set2 in Saccharomyces cerevisiae is linked to transcriptional elongation by RNA polymerase II. Mol. Cell. Biol. 23, 4207–4218. doi:10.1128/MCB.23.12.4207-4218.2003

Kuo, A.J., Song, J., Cheung, P., Ishibe-Murakami, S., Yamazoe, S., Chen, J.K., Patel, D.J., Gozani, O., 2012. The BAH domain of ORC1 links H4K20me2 to DNA replication licensing and Meier-Gorlin syndrome. Nature 484, 115–119. doi:10.1038/nature10956

Kuo, M.H., Zhou, J., Jambeck, P., Churchill, M.E., Allis, C.D., 1998. Histone acetyltransferase activity of yeast Gcn5p is required for the activation of target genes in vivo. Genes & Development 12, 627–639.

Kushnirov, V.V., 2000. Rapid and reliable protein extraction from yeast. Yeast 16, 857–860. doi:10.1002/1097-0061(20000630)16:9<857::AID-YEA561>3.0.CO;2-B

Kwak, H., Fuda, N.J., Core, L.J., Lis, J.T., 2013. Precise maps of RNA polymerase reveal how promoters direct initiation and pausing. Science 339, 950–953. doi:10.1126/science.1229386

Lacadie, S.A., Ibrahim, M.M., Gokhale, S.A., Ohler, U., 2016. Divergent transcription and epigenetic directionality of human promoters. FEBS J. 283, 4214–4222. doi:10.1111/febs.13747

Lachner, M., O'Carroll, D., Rea, S., Mechtler, K., Jenuwein, T., 2001. Methylation of histone H3 lysine 9 creates a binding site for HP1 proteins. Nature 410, 116–120. doi:10.1038/35065132

Lacoste, N., Utley, R.T., Hunter, J.M., Poirier, G.G., Côté, J., 2002. Disruptor of telomeric silencing-1 is a chromatin-specific histone H3 methyltransferase. J. Biol. Chem. 277, 30421–30424. doi:10.1074/jbc.C200366200

Lai, W.K.M., Pugh, B.F., 2017. Understanding nucleosome dynamics and their links to gene expression and DNA replication. Nature Publishing Group 18, 548–562. doi:10.1038/nrm.2017.47

Lalonde, M.-E., Avvakumov, N., Glass, K.C., Joncas, F.-H., Saksouk, N., Holliday, M., Paquet, E., Yan, K., Tong, Q., Klein, B.J., Tan, S., Yang, X.-J., Kutateladze, T.G., Côté, J., 2013. Exchange of associated factors directs a switch in HBO1 acetyltransferase histone tail specificity. Genes Dev. 27, 2009–2024. doi:10.1101/gad.223396.113

Langmead, B., Salzberg, S.L., 2012. Fast gapped-read alignment with Bowtie 2. Nat. Methods 9, 357–359. doi:10.1038/nmeth.1923

Langmead, B., Trapnell, C., Pop, M., Salzberg, S.L., 2009. Ultrafast and memory-efficient alignment of short DNA sequences to the human genome. Genome Biol. 10, R25. doi:10.1186/gb-2009-10-3-r25

Lattke, H., Weser, U., 1977. Functional aspects of zinc in yeast RNA-polymerase B. FEBS Lett. 83, 297–300.

Laue, K., Daujat, S., Crump, J.G., Plaster, N., Roehl, H.H., Tubingen 2000 Screen Consortium, Kimmel, C.B., Schneider, R., Hammerschmidt, M., 2008. The multidomain protein Brpf1 binds histones and is required for Hox gene expression and segmental identity. Development 135, 1935–1946. doi:10.1242/dev.017160

Lawrence, M.B.D., Coutin, N., Choi, J.K., Martin, B.J.E., Irwin, N.A.T., Young, B., Loewen, C., Howe, L.J., 2017. Histone Acetylation, Not Stoichiometry, Regulates Linker Histone Binding in Saccharomyces cerevisiae. Genetics 207, 347–355. doi:10.1534/genetics.117.1132

Le Masson, I., Yu, D.Y., Jensen, K., Chevalier, A., Courbeyrette, R., Boulard, Y., Smith, M.M., Mann, C., 2003. Yaf9, a novel NuA4 histone acetyltransferase subunit, is required for the cellular response to spindle stress in yeast. Mol. Cell. Biol. 23, 6086–6102. doi:10.1128/MCB.23.17.6086-6102.2003

Lechner, T., Carrozza, M.J., Yu, Y., Grant, P.A., Eberharter, A., Vannier, D., Brosch, G., Stillman, D.J., Shore, D., Workman, J.L., 2000. Sds3 (suppressor of defective silencing 3) is an integral component of the yeast Sin3[middle dot]Rpd3 histone deacetylase complex and is required for histone deacetylase activity. J. Biol. Chem. 275, 40961–40966. doi:10.1074/jbc.M005730200

Lee, J.-S., Shukla, A., Schneider, J., Swanson, S.K., Washburn, M.P., Florens, L., Bhaumik, S.R., Shilatifard, A., 2007. Histone crosstalk between H2B monoubiquitination and H3 methylation mediated by COMPASS. Cell 131, 1084–1096. doi:10.1016/j.cell.2007.09.046

Lee, J.M., Greenleaf, A.L., 1991. CTD kinase large subunit is encoded by CTK1, a gene required for normal growth of Saccharomyces cerevisiae. Gene Expr. 1, 149–167.

Lee, J.M., Greenleaf, A.L., 1989. A protein kinase that phosphorylates the C-terminal repeat domain of the largest subunit of RNA polymerase II. Proc. Natl. Acad. Sci. U.S.A. 86, 3624–3628.

Lee, K.K., Sardiu, M.E., Swanson, S.K., Gilmore, J.M., Torok, M., Grant, P.A., Florens, L., Workman, J.L., Washburn, M.P., 2011. Combinatorial depletion analysis to assemble the network architecture of the SAGA and ADA chromatin remodeling complexes. Mol. Syst. Biol. 7, 503. doi:10.1038/msb.2011.40

Lee, K.K., Workman, J.L., 2007. Histone acetyltransferase complexes: one size doesn't fit all. Nat. Rev. Mol. Cell Biol. 8, 284–295. doi:10.1038/nrm2145

Lee, T.I., Young, R.A., 2013. Transcriptional Regulation and Its Misregulation in Disease. Cell 152, 1237–1251. doi:10.1016/j.cell.2013.02.014

Lee, W., Tillo, D., Bray, N., Morse, R.H., Davis, R.W., Hughes, T.R., Nislow, C., 2007. A high-resolution atlas of nucleosome occupancy in yeast. Nature Genetics 39, 1235–1244. doi:10.1038/ng2117

Lee, Y.C., Min, S., Gim, B.S., Kim, Y.J., 1997. A transcriptional mediator protein that is required for activation of many RNA polymerase II promoters and is conserved from yeast to humans. Mol. Cell. Biol. 17, 4622–4632.

Leroy, G., Rickards, B., Flint, S.J., 2008. The double bromodomain proteins Brd2 and Brd3 couple histone acetylation to transcription. Molecular Cell 30, 51–60. doi:10.1016/j.molcel.2008.01.018

Leung, D., Jung, I., Rajagopal, N., Schmitt, A., Selvaraj, S., Lee, A.Y., Yen, C.-A., Lin, S., Lin, Y., Qiu, Y., Xie, W., Yue, F., Hariharan, M., Ray, P., Kuan, S., Edsall, L., Yang, H., Chi, N.C., Zhang, M.Q., Ecker, J.R., Ren, B., 2015. Integrative analysis of haplotype-resolved epigenomes across human tissues. Nature 518, 350–354. doi:10.1038/nature14217

Levine, M., Tjian, R., 2003. Transcription regulation and animal diversity. Nature 424, 147–151. doi:10.1038/nature01763

Levy-Wilson, B., Watson, D.C., Dixon, G.H., 1979. Multiacetylated forms of H4 are found in a putative transcriptionally competent chromatin fraction from trout testis. Nucleic Acids Res. 6, 259–274.

Li, B., Howe, L., Anderson, S., Yates, J.R., Workman, J.L., 2003. The Set2 histone methyltransferase functions through the phosphorylated carboxyl-terminal domain of RNA polymerase II. J. Biol. Chem. 278, 8897–8903. doi:10.1074/jbc.M212134200

Li, H., Durbin, R., 2010. Fast and accurate long-read alignment with Burrows-Wheeler transform. Bioinformatics 26, 589–595. doi:10.1093/bioinformatics/btp698

Li, H., Handsaker, B., Wysoker, A., Fennell, T., Ruan, J., Homer, N., Marth, G., Abecasis, G., Durbin, R., 1000 Genome Project Data Processing Subgroup, 2009. The Sequence Alignment/Map format and SAMtools. Bioinformatics 25, 2078–2079. doi:10.1093/bioinformatics/btp352

Li, J., Moazed, D., Gygi, S.P., 2002. Association of the histone methyltransferase Set2 with RNA polymerase II plays a role in transcription elongation. J. Biol. Chem. 277, 49383–49388. doi:10.1074/jbc.M209294200

Li, Q.Q., Hao, J.-J., Zhang, Z., Krane, L.S., Hammerich, K.H., Sanford, T., Trepel, J.B., Neckers, L., Agarwal, P.K., 2017. Proteomic analysis of proteome and histone post-translational modifications in heat shock protein 90 inhibition-mediated bladder cancer therapeutics. Sci Rep 7, 201. doi:10.1038/s41598-017-00143-6

Li, S., 2012. Implication of posttranslational histone modifications in nucleotide excision repair. IJMS 13, 12461–12486. doi:10.3390/ijms131012461

Li, S., Shogren-Knaak, M.A., 2009. The Gcn5 bromodomain of the SAGA complex facilitates cooperative and cross-tail acetylation of nucleosomes. J. Biol. Chem. 284, 9411–9417. doi:10.1074/jbc.M809617200

Li, S., Swanson, S.K., Gogol, M., Florens, L., Washburn, M.P., Workman, J.L., Suganuma, T., 2015. Serine and SAM Responsive Complex SESAME Regulates Histone Modification Crosstalk by Sensing Cellular Metabolism. Molecular Cell 60, 408–421. doi:10.1016/j.molcel.2015.09.024

Li, W., Nagaraja, S., Delcuve, G.P., Hendzel, M.J., Davie, J.R., 1993. Effects of histone acetylation, ubiquitination and variants on nucleosome stability. Biochem. J. 296 (Pt 3), 737–744.

Li, X., Yu, W., Qian, X., Xia, Y., Zheng, Y., Lee, J.-H., Li, W., Lyu, J., Rao, G., Zhang, X., Qian, C.-N., Rozen, S.G., Jiang, T., Lu, Z., 2017. Nucleus-Translocated ACSS2 Promotes Gene Transcription for Lysosomal Biogenesis and Autophagy. Molecular Cell 66, 684–697.e9. doi:10.1016/j.molcel.2017.04.026

Li, Y., Sabari, B.R., Panchenko, T., Wen, H., Zhao, D., Guan, H., Wan, L., Huang, H., Tang, Z., Zhao, Y., Roeder, R.G., Shi, X., Allis, C.D., Li, H., 2016. Molecular Coupling of Histone Crotonylation and Active Transcription by AF9 YEATS Domain. Molecular Cell 62, 181–193. doi:10.1016/j.molcel.2016.03.028

Li, Y., Wen, H., Xi, Y., Tanaka, K., Wang, H., Peng, D., Ren, Y., Jin, Q., Dent, S.Y.R., Li, W., Li, H., Shi, X., 2014. AF9 YEATS domain links histone acetylation to DOT1L-mediated H3K79 methylation. Cell 159, 558–571. doi:10.1016/j.cell.2014.09.049

Li, Z., Kono, H., 2016. Distinct Roles of Histone H3 and H2A Tails in Nucleosome Stability. Sci Rep 6, 31437. doi:10.1038/srep31437

Liang, G., Klose, R.J., Gardner, K.E., Zhang, Y., 2007. Yeast Jhd2p is a histone H3 Lys4 trimethyl demethylase. Nat. Struct. Mol. Biol. 14, 243–245. doi:10.1038/nsmb1204

Libby, P.R., 1970. Activity of histone deacetylase in rat liver and Novikoff hepatoma. Biochim. Biophys. Acta 213, 234–236.

Licatalosi, D.D., Geiger, G., Minet, M., Schroeder, S., Cilli, K., McNeil, J.B., Bentley, D.L., 2002. Functional interaction of yeast pre-mRNA 3' end processing factors with RNA polymerase II. Molecular Cell 9, 1101–1111.

Liu, C.L., Kaplan, T., Kim, M., Buratowski, S., Schreiber, S.L., Friedman, N., Rando, O.J., 2005. Single-nucleosome mapping of histone modifications in S. cerevisiae. PLoS Biol 3, e328. doi:10.1371/journal.pbio.0030328

Liu, L., Qin, S., Zhang, J., Ji, P., Shi, Y., Wu, J., 2012. Solution structure of an atypical PHD finger in BRPF2 and its interaction with DNA. J. Struct. Biol. 180, 165–173. doi:10.1016/j.jsb.2012.06.014

Liu, Y., Warfield, L., Zhang, C., Luo, J., Allen, J., Lang, W.H., Ranish, J., Shokat, K.M., Hahn, S., 2009. Phosphorylation of the transcription elongation factor Spt5 by yeast Bur1 kinase stimulates recruitment of the PAF complex. Mol. Cell. Biol. 29, 4852–

4863. doi:10.1128/MCB.00609-09

Logan, J., Falck-Pedersen, E., Darnell, J.E., Shenk, T., 1987. A poly(A) addition site and a downstream termination region are required for efficient cessation of transcription by RNA polymerase II in the mouse beta maj-globin gene. Proc. Natl. Acad. Sci. U.S.A. 84, 8306–8310.

Lohr, D., Corden, J., Tatchell, K., Kovacic, R.T., van Holde, K.E., 1977. Comparative subunit structure of HeLa, yeast, and chicken erythrocyte chromatin. Proc. Natl. Acad. Sci. U.S.A. 74, 79–83.

Lorch, Y., Beve, J., Gustafsson, C.M., Myers, L.C., Kornberg, R.D., 2000. Mediator-nucleosome interaction. Molecular Cell 6, 197–201.

Lorch, Y., Maier-Davis, B., Kornberg, R.D., 2014. Role of DNA sequence in chromatin remodeling and the formation of nucleosome-free regions. Genes Dev. 28, 2492–2497. doi:10.1101/gad.250704.114

Lu, H., Flores, O., Weinmann, R., Reinberg, D., 1991. The nonphosphorylated form of RNA polymerase II preferentially associates with the preinitiation complex. Proc. Natl. Acad. Sci. U.S.A. 88, 10004–10008.

Luger, K., Mäder, A.W., Richmond, R.K., Sargent, D.F., Richmond, T.J., 1997. Crystal structure of the nucleosome core particle at 2.8 A resolution. Nature 389, 251–260. doi:10.1038/38444

Ma, J., Ptashne, M., 1987. A new class of yeast transcriptional activators. Cell 51, 113–119.

Maltby, V.E., Martin, B.J.E., Brind'Amour, J., Chruscicki, A.T., McBurney, K.L., Schulze, J.M., Johnson, I.J., Hills, M., Hentrich, T., Kobor, M.S., Lorincz, M.C., Howe, L.J., 2012a. Histone H3K4 demethylation is negatively regulated by histone H3 acetylation in Saccharomyces cerevisiae. Proc. Natl. Acad. Sci. U.S.A. 109, 18505–18510. doi:10.1073/pnas.1202070109

Maltby, V.E., Martin, B.J.E., Schulze, J.M., Johnson, I., Hentrich, T., Sharma, A., Kobor, M.S., Howe, L., 2012b. Histone H3 lysine 36 methylation targets the Isw1b remodeling complex to chromatin. Mol. Cell. Biol. 32, 3479–3485. doi:10.1128/MCB.00389-12

Mapendano, C.K., Lykke-Andersen, S., Kjems, J., Bertrand, E., Jensen, T.H., 2010. Crosstalk between mRNA 3' end processing and transcription initiation. Molecular Cell 40, 410–422. doi:10.1016/j.molcel.2010.10.012

Marshall, N.F., Price, D.H., 1992. Control of formation of two distinct classes of RNA polymerase II elongation complexes. Mol. Cell. Biol. 12, 2078–2090.

Martin, A.M., Pouchnik, D.J., Walker, J.L., Wyrick, J.J., 2004. Redundant roles for

histone H3 N-terminal lysine residues in subtelomeric gene repression in Saccharomyces cerevisiae. Genetics 167, 1123–1132. doi:10.1534/genetics.104.026674

Martin, B.J.E., McBurney, K.L., Maltby, V.E., Jensen, K.N., Brind'Amour, J., Howe, L.J., 2017. Histone H3K4 and H3K36 Methylation Independently Recruit the NuA3 Histone Acetyltransferase in Saccharomyces cerevisiae. Genetics 205, 1113–1123. doi:10.1534/genetics.116.199422

Martin, D.G.E., Baetz, K., Shi, X., Walter, K.L., MacDonald, V.E., Wlodarski, M.J., Gozani, O., Hieter, P., Howe, L., 2006. The Yng1p plant homeodomain finger is a methyl-histone binding module that recognizes lysine 4-methylated histone H3. Mol. Cell. Biol. 26, 7871–7879. doi:10.1128/MCB.00573-06

Martin, M., 2011. Cutadapt removes adapter sequences from high-throughput sequencing reads. EMBnet.journal 17, pp. 10–12. doi:10.14806/ej.17.1.200

Masumoto, H., Hawke, D., Kobayashi, R., Verreault, A., 2005. A role for cell-cycle-regulated histone H3 lysine 56 acetylation in the DNA damage response. Nature 436, 294–298. doi:10.1038/nature03714

Matangkasombut, O., Buratowski, R.M., Swilling, N.W., Buratowski, S., 2000. Bromodomain factor 1 corresponds to a missing piece of yeast TFIID. Genes & Development 14, 951–962.

Matsuda, H., Putzel, G.G., Backman, V., Szleifer, I., 2014. Macromolecular crowding as a regulator of gene transcription. Biophys. J. 106, 1801–1810. doi:10.1016/j.bpj.2014.02.019

Matsui, T., Segall, J., Weil, P.A., Roeder, R.G., 1980. Multiple factors required for accurate initiation of transcription by purified RNA polymerase II. J. Biol. Chem. 255, 11992–11996.

Mayer, A., di Iulio, J., Maleri, S., Eser, U., Vierstra, J., Reynolds, A., Sandstrom, R., Stamatoyannopoulos, J.A., Churchman, L.S., 2015. Native elongating transcript sequencing reveals human transcriptional activity at nucleotide resolution. Cell 161, 541–554. doi:10.1016/j.cell.2015.03.010

Mayer, A., Heidemann, M., Lidschreiber, M., Schreieck, A., Sun, M., Hintermair, C., Kremmer, E., Eick, D., Cramer, P., 2012. CTD tyrosine phosphorylation impairs termination factor recruitment to RNA polymerase II. Science 336, 1723–1725. doi:10.1126/science.1219651

Mayer, A., Lidschreiber, M., Siebert, M., Leike, K., Söding, J., Cramer, P., 2010. Uniform transitions of the general RNA polymerase II transcription complex. Nat. Struct. Mol. Biol. 17, 1272–1278. doi:10.1038/nsmb.1903

McCracken, S., Fong, N., Yankulov, K., Ballantyne, S., Pan, G., Greenblatt, J., Patterson,

S.D., Wickens, M., Bentley, D.L., 1997. The C-terminal domain of RNA polymerase II couples mRNA processing to transcription. Nature 385, 357–361. doi:10.1038/385357a0

McDonagh, K.T., Lin, H.J., Lowrey, C.H., Bodine, D.M., Nienhuis, A.W., 1991. The upstream region of the human gamma-globin gene promoter. Identification and functional analysis of nuclear protein binding sites. J. Biol. Chem. 266, 11965–11974.

McMahon, S.B., Van Buskirk, H.A., Dugan, K.A., Copeland, T.D., Cole, M.D., 1998. The novel ATM-related protein TRRAP is an essential cofactor for the c-Myc and E2F oncoproteins. Cell 94, 363–374.

McMahon, S.B., Wood, M.A., Cole, M.D., 2000. The essential cofactor TRRAP recruits the histone acetyltransferase hGCN5 to c-Myc. Mol. Cell. Biol. 20, 556–562.

Mews, P., Donahue, G., Drake, A.M., Luczak, V., Abel, T., Berger, S.L., 2017. Acetyl-CoA synthetase regulates histone acetylation and hippocampal memory. Nature Publishing Group 546, 381–386. doi:10.1038/nature22405

Miller, T., Krogan, N.J., Dover, J., Erdjument-Bromage, H., Tempst, P., Johnston, M., Greenblatt, J.F., Shilatifard, A., 2001. COMPASS: a complex of proteins associated with a trithorax-related SET domain protein. Proc. Natl. Acad. Sci. U.S.A. 98, 12902–12907. doi:10.1073/pnas.231473398

Milligan, L., Huynh Thu, V.A., Delan Forino, C., Tuck, A., Petfalski, E., Lombraña, R., Sanguinetti, G., Kudla, G., Tollervey, D., 2016. Strand-specific, high-resolution mapping of modified RNA polymerase II. Mol. Syst. Biol. 12, 874. doi:10.15252/msb.20166869

Min, I.M., Waterfall, J.J., Core, L.J., Munroe, R.J., Schimenti, J., Lis, J.T., 2011. Regulating RNA polymerase pausing and transcription elongation in embryonic stem cells. Genes Dev. 25, 742–754. doi:10.1101/gad.2005511

Mitchell, L., Huard, S., Cotrut, M., Pourhanifeh-Lemeri, R., Steunou, A.-L., Hamza, A., Lambert, J.-P., Zhou, H., Ning, Z., Basu, A., Côté, J., Figeys, D.A., Baetz, K., 2013. mChIP-KAT-MS, a method to map protein interactions and acetylation sites for lysine acetyltransferases. Proc Natl Acad Sci USA 110, E1641–50. doi:10.1073/pnas.1218515110

Mizuguchi, G., Shen, X., Landry, J., Wu, W.-H., Sen, S., Wu, C., 2004. ATP-driven exchange of histone H2AZ variant catalyzed by SWR1 chromatin remodeling complex. Science 303, 343–348. doi:10.1126/science.1090701

Moore, M., Jackson, V., Sealy, L., Chalkley, R., 1979. Comparative studies on highly metabolically active histone acetylation. Biochim. Biophys. Acta 561, 248–260.

Moreira, J.M., Holmberg, S., 1999. Transcriptional repression of the yeast CHA1 gene

requires the chromatin-remodeling complex RSC. EMBO J. 18, 2836–2844. doi:10.1093/emboj/18.10.2836

Morettini, S., Tribus, M., Zeilner, A., Sebald, J., Campo-Fernandez, B., Scheran, G., Wörle, H., Podhraski, V., Fyodorov, D.V., Lusser, A., 2011. The chromodomains of CHD1 are critical for enzymatic activity but less important for chromatin localization. Nucleic Acids Res. 39, 3103–3115. doi:10.1093/nar/gkq1298

Morris, S.A., Rao, B., Garcia, B.A., Hake, S.B., Diaz, R.L., Shabanowitz, J., Hunt, D.F., Allis, C.D., Lieb, J.D., Strahl, B.D., 2007. Identification of histone H3 lysine 36 acetylation as a highly conserved histone modification. J. Biol. Chem. 282, 7632–7640. doi:10.1074/jbc.M607909200

Murakami, K., Elmlund, H., Kalisman, N., Bushnell, D.A., Adams, C.M., Azubel, M., Elmlund, D., Levi-Kalisman, Y., Liu, X., Gibbons, B.J., Levitt, M., Kornberg, R.D., 2013. Architecture of an RNA polymerase II transcription pre-initiation complex. Science 342, 1238724. doi:10.1126/science.1238724

Murray, K., 1964. The Occurrence of epsilon-N-methyl lysine in histones. Biochemistry 3, 10–15.

Murray, S., Udupa, R., Yao, S., Hartzog, G., Prelich, G., 2001. Phosphorylation of the RNA polymerase II carboxy-terminal domain by the Bur1 cyclin-dependent kinase. Mol. Cell. Biol. 21, 4089–4096. doi:10.1128/MCB.21.13.4089-4096.2001

Muyldermans, S., Lasters, I., Wyns, L., Hamers, R., 1981. Protection of discrete DNA fragments by the complex H1-octamerhistones or H5-octamerhistones after micrococcal nuclease digestion. Nucleic Acids Res. 9, 3671–3680.

Myers, L.C., Gustafsson, C.M., Hayashibara, K.C., Brown, P.O., Kornberg, R.D., 1999. Mediator protein mutations that selectively abolish activated transcription. Proc. Natl. Acad. Sci. U.S.A. 96, 67–72.

Nagai, S., Davis, R.E., Mattei, P.J., Eagen, K.P., Kornberg, R.D., 2017. Chromatin potentiates transcription. Proc Natl Acad Sci USA 114, 1536–1541. doi:10.1073/pnas.1620312114

Nagy, P.L., Griesenbeck, J., Kornberg, R.D., Cleary, M.L., 2002. A trithorax-group complex purified from Saccharomyces cerevisiae is required for methylation of histone H3. Proc. Natl. Acad. Sci. U.S.A. 99, 90–94. doi:10.1073/pnas.221596698

Nagy, Z., Tora, L., 2007. Distinct GCN5/PCAF-containing complexes function as co-activators and are involved in transcription factor and global histone acetylation. Oncogene 26, 5341–5357. doi:10.1038/sj.onc.1210604

Nelson, D., Covault, J., Chalkley, R., 1980. Segregation of rapidly acetylated histones into a chromatin fraction released from intact nuclei by the action of micrococcal nuclease. Nucleic Acids Res. 8, 1745–1763.

Ng, H.H., Feng, Q., Wang, H., Erdjument-Bromage, H., Tempst, P., Zhang, Y., Struhl, K., 2002. Lysine methylation within the globular domain of histone H3 by Dot1 is important for telomeric silencing and Sir protein association. Genes & Development 16, 1518–1527. doi:10.1101/gad.1001502

Ng, H.H., Robert, F., Young, R.A., Struhl, K., 2003. Targeted recruitment of Set1 histone methylase by elongating Pol II provides a localized mark and memory of recent transcriptional activity. Molecular Cell 11, 709–719. doi:10.1016/S1097-2765(03)00092-3

Nie, L., Shuai, L., Zhu, M., Liu, P., Xie, Z.-F., Jiang, S., Jiang, H.-W., Li, J., Zhao, Y., Li, J.-Y., Tan, M., 2017. The Landscape of Histone Modifications in a High-Fat Diet-Induced Obese (DIO) Mouse Model. Mol. Cell Proteomics 16, 1324–1334. doi:10.1074/mcp.M117.067553

Nohara, H., Takahashi, T., Ogata, K., 1966. Acetylation of histones by pigeon liver enzymes. Biochim. Biophys. Acta 127, 282–284.

Noll, M., 1974. Subunit structure of chromatin. Nature 251, 249–251.

Nonet, M., Sweetser, D., Young, R.A., 1987. Functional redundancy and structural polymorphism in the large subunit of RNA polymerase II. Cell 50, 909–915.

Norton, V.G., Marvin, K.W., Yau, P., Bradbury, E.M., 1990. Nucleosome linking number change controlled by acetylation of histones H3 and H4. J. Biol. Chem. 265, 19848–19852.

O'Sullivan, J.M., Tan-Wong, S.M., Morillon, A., Lee, B., Coles, J., Mellor, J., Proudfoot, N.J., 2004. Gene loops juxtapose promoters and terminators in yeast. Nature Genetics 36, 1014–1018. doi:10.1038/ng1411

Obrdlik, A., Kukalev, A., Louvet, E., Farrants, A.-K.O., Caputo, L., Percipalle, P., 2008. The histone acetyltransferase PCAF associates with actin and hnRNP U for RNA polymerase II transcription. Mol. Cell. Biol. 28, 6342–6357. doi:10.1128/MCB.00766-08

Ocampo, J., Chereji, R.V., Eriksson, P.R., Clark, D.J., 2016. The ISW1 and CHD1 ATP-dependent chromatin remodelers compete to set nucleosome spacing in vivo. Nucleic Acids Res. doi:10.1093/nar/gkw068

Oelgeschläger, M., Janknecht, R., Krieg, J., Schreek, S., Lüscher, B., 1996. Interaction of the co-activator CBP with Myb proteins: effects on Myb-specific transactivation and on the cooperativity with NF-M. EMBO J. 15, 2771–2780.

Ogryzko, V.V., Schiltz, R.L., Russanova, V., Howard, B.H., Nakatani, Y., 1996. The transcriptional coactivators p300 and CBP are histone acetyltransferases. Cell 87, 953–959.

Olesen, J., Hahn, S., Guarente, L., 1987. Yeast HAP2 and HAP3 activators both bind to the CYC1 upstream activation site, UAS2, in an interdependent manner. Cell 51, 953–961.

Olins, A.L., Olins, D.E., 1974. Spheroid chromatin units (v bodies). Science 183, 330–332.

Ord, M.G., Stocken, L.A., 1966. Metabolic properties of histones from rat liver and thymus gland. Biochem. J. 98, 888–897.

Otero, G., Fellows, J., Li, Y., de Bizemont, T., Dirac, A.M., Gustafsson, C.M., Erdjument-Bromage, H., Tempst, P., Svejstrup, J.Q., 1999. Elongator, a multisubunit component of a novel RNA polymerase II holoenzyme for transcriptional elongation. Molecular Cell 3, 109–118.

Owen, D.J., Ornaghi, P., Yang, J.C., Lowe, N., Evans, P.R., Ballario, P., Neuhaus, D., Filetici, P., Travers, A.A., 2000. The structural basis for the recognition of acetylated histone H4 by the bromodomain of histone acetyltransferase gcn5p. EMBO J. 19, 6141–6149. doi:10.1093/emboj/19.22.6141

Ozsolak, F., Song, J.S., Liu, X.S., Fisher, D.E., 2007. High-throughput mapping of the chromatin structure of human promoters. Nat. Biotechnol. 25, 244–248. doi:10.1038/nbt1279

Palpant, T., 2011. Java Genomics Toolkit [WWW Document]. Github. URL https://github.com/timpalpant/java-genomics-toolkit (accessed 3.30.15).

Park, D., Morris, A.R., Battenhouse, A., Iyer, V.R., 2014. Simultaneous mapping of transcript ends at single-nucleotide resolution and identification of widespread promoter-associated non-coding RNA governed by TATA elements. Nucleic Acids Res. 42, 3736–3749. doi:10.1093/nar/gkt1366

Park, Y.-J., Dyer, P.N., Tremethick, D.J., Luger, K., 2004. A new fluorescence resonance energy transfer approach demonstrates that the histone variant H2AZ stabilizes the histone octamer within the nucleosome. J. Biol. Chem. 279, 24274–24282. doi:10.1074/jbc.M313152200

Parker, C.S., Topol, J., 1984. A Drosophila RNA polymerase II transcription factor binds to the regulatory site of an hsp 70 gene. Cell 37, 273–283.

Parnell, T.J., Huff, J.T., Cairns, B.R., 2008. RSC regulates nucleosome positioning at Pol II genes and density at Pol III genes. EMBO J. 27, 100–110. doi:10.1038/sj.emboj.7601946

Parthun, M.R., Widom, J., Gottschling, D.E., 1996. The major cytoplasmic histone acetyltransferase in yeast: links to chromatin replication and histone metabolism. Cell 87, 85–94.

Payne, J.M., Laybourn, P.J., Dahmus, M.E., 1989. The transition of RNA polymerase II from initiation to elongation is associated with phosphorylation of the carboxyl-terminal domain of subunit IIa. J. Biol. Chem. 264, 19621–19629.

Pearson, E.C., Bates, D.L., Prospero, T.D., Thomas, J.O., 1984. Neuronal nuclei and glial nuclei from mammalian cerebral cortex. Nucleosome repeat lengths, DNA contents and H1 contents. Eur. J. Biochem. 144, 353–360.

Pertea, M., Salzberg, S.L., 2010. Between a chicken and a grape: estimating the number of human genes. Genome Biol. 11, 206. doi:10.1186/gb-2010-11-5-206

Petrenko, N., Jin, Y., Wong, K.H., Struhl, K., 2017. Evidence that Mediator is essential for Pol II transcription, but is not a required component of the preinitiation complex in vivo. Elife 6, 155. doi:10.7554/eLife.28447

Petrenko, N., Jin, Y., Wong, K.H., Struhl, K., 2016. Mediator Undergoes a Compositional Change during Transcriptional Activation. Molecular Cell 1–20. doi:10.1016/j.molcel.2016.09.015

Phatnani, H.P., Jones, J.C., Greenleaf, A.L., 2004. Expanding the functional repertoire of CTD kinase I and RNA polymerase II: novel phosphoCTD-associating proteins in the yeast proteome. Biochemistry 43, 15702–15719. doi:10.1021/bi048364h

Phillips, D.M., 1963. The presence of acetyl groups of histones. Biochem. J. 87, 258–263.

Pnueli, L., Rudnizky, S., Yosefzon, Y., Melamed, P., 2015. RNA transcribed from a distal enhancer is required for activating the chromatin at the promoter of the gonadotropin α-subunit gene. Proc Natl Acad Sci USA 112, 4369–4374. doi:10.1073/pnas.1414841112

Pogo, B.G., Allfrey, V.G., Mirsky, A.E., 1966. RNA synthesis and histone acetylation during the course of gene activation in lymphocytes. Proc. Natl. Acad. Sci. U.S.A. 55, 805–812.

Pogo, B.G., Pogo, A.O., Allfrey, V.G., Mirsky, A.E., 1968. Changing patterns of histone acetylation and RNA synthesis in regeneration of the liver. Proc. Natl. Acad. Sci. U.S.A. 59, 1337–1344.

Pokholok, D.K., Hannett, N.M., Young, R.A., 2002. Exchange of RNA polymerase II initiation and elongation factors during gene expression in vivo. Molecular Cell 9, 799–809.

Pokholok, D.K., Harbison, C.T., Levine, S., Cole, M., Hannett, N.M., Lee, T.I., Bell, G.W., Walker, K., Rolfe, P.A., Herbolsheimer, E., Zeitlinger, J., Lewitter, F., Gifford, D.K., Young, R.A., 2005. Genome-wide map of nucleosome acetylation and methylation in yeast. Cell 122, 517–527. doi:10.1016/j.cell.2005.06.026

Postepska-Igielska, A., Giwojna, A., Gasri-Plotnitsky, L., Schmitt, N., Dold, A., Ginsberg, D., Grummt, I., 2015. LncRNA Khps1 Regulates Expression of the Proto-oncogene SPHK1 via Triplex-Mediated Changes in Chromatin Structure. Molecular Cell 60, 626–636. doi:10.1016/j.molcel.2015.10.001

Pradeepa, M.M., Grimes, G.R., Kumar, Y., Olley, G., Taylor, G.C.A., Schneider, R., Bickmore, W.A., 2016. Histone H3 globular domain acetylation identifies a new class of enhancers. Nature Publishing Group 48, 681–686. doi:10.1038/ng.3550

Pruitt, K.D., Tatusova, T., Klimke, W., Maglott, D.R., 2009. NCBI Reference Sequences: current status, policy and new initiatives. Nucleic Acids Res. 37, D32–6. doi:10.1093/nar/gkn721

Puigdomènech, P., José, M., Ruiz-Carrillo, A., Crane-Robinson, C., 1983. Isolation of a 167 basepair chromatosome containing a partially digested histone H5. FEBS Lett. 154, 151–155.

Qiu, H., Hu, C., Hinnebusch, A.G., 2009. Phosphorylation of the Pol II CTD by KIN28 enhances BUR1/BUR2 recruitment and Ser2 CTD phosphorylation near promoters. Molecular Cell 33, 752–762. doi:10.1016/j.molcel.2009.02.018

Qiu, H., Hu, C., Yoon, S., Natarajan, K., Swanson, M.J., Hinnebusch, A.G., 2004. An array of coactivators is required for optimal recruitment of TATA binding protein and RNA polymerase II by promoter-bound Gcn4p. Mol. Cell. Biol. 24, 4104–4117. doi:10.1128/MCB.24.10.4104-4117.2004

Qiu, Y., Liu, L., Zhao, C., Han, C., Li, F., Zhang, J., Wang, Y., Li, G., Mei, Y., Wu, M., Wu, J., Shi, Y., 2012. Combinatorial readout of unmodified H3R2 and acetylated H3K14 by the tandem PHD finger of MOZ reveals a regulatory mechanism for HOXA9 transcription. Genes Dev. 26, 1376–1391. doi:10.1101/gad.188359.112

Quinlan, A.R., Hall, I.M., 2010. BEDTools: a flexible suite of utilities for comparing genomic features. Bioinformatics 26, 841–842. doi:10.1093/bioinformatics/btq033

Rahl, P.B., Chen, C.Z., Collins, R.N., 2005. Elp1p, the yeast homolog of the FD disease syndrome protein, negatively regulates exocytosis independently of transcriptional elongation. Molecular Cell 17, 841–853. doi:10.1016/j.molcel.2005.02.018

Rahl, P.B., Lin, C.Y., Seila, A.C., Flynn, R.A., McCuine, S., Burge, C.B., Sharp, P.A., Young, R.A., 2010. c-Myc regulates transcriptional pause release. Cell 141, 432–445. doi:10.1016/j.cell.2010.03.030

Ramachandran, S., Zentner, G.E., Henikoff, S., 2015. Asymmetric nucleosomes flank promoters in the budding yeast genome. Genome Res. 25, 381–390. doi:10.1101/gr.182618.114

Rando, O.J., 2012. Combinatorial complexity in chromatin structure and function: revisiting the histone code. Current Opinion in Genetics & Development 22, 148–

155. doi:10.1016/j.gde.2012.02.013

Rando, O.J., Winston, F., 2012. Chromatin and transcription in yeast. Genetics 190, 351–387. doi:10.1534/genetics.111.132266

Rea, S., Eisenhaber, F., O'Carroll, D., Strahl, B.D., Sun, Z.W., Schmid, M., Opravil, S., Mechtler, K., Ponting, C.P., Allis, C.D., Jenuwein, T., 2000. Regulation of chromatin structure by site-specific histone H3 methyltransferases. Nature 406, 593–599. doi:10.1038/35020506

Reid, J.L., Iyer, V.R., Brown, P.O., Struhl, K., 2000. Coordinate regulation of yeast ribosomal protein genes is associated with targeted recruitment of Esa1 histone acetylase. Molecular Cell 6, 1297–1307.

Reines, D., Wells, D., Chamberlin, M.J., Kane, C.M., 1987. Identification of intrinsic termination sites in vitro for RNA polymerase II within eukaryotic gene sequences. Journal of Molecular Biology 196, 299–312.

Rhee, H.S., Bataille, A.R., Zhang, L., Pugh, B.F., 2014. Subnucleosomal structures and nucleosome asymmetry across a genome. Cell 159, 1377–1388. doi:10.1016/j.cell.2014.10.054

Rhee, H.S., Pugh, B.F., 2012. Genome-wide structure and organization of eukaryotic pre-initiation complexes. Nature 483, 295–301. doi:10.1038/nature10799

Richter, K., Nessling, M., Lichter, P., 2008. Macromolecular crowding and its potential impact on nuclear function. Biochim. Biophys. Acta 1783, 2100–2107. doi:10.1016/j.bbamcr.2008.07.017

Ridsdale, J.A., Hendzel, M.J., Delcuve, G.P., Davie, J.R., 1990. Histone acetylation alters the capacity of the H1 histones to condense transcriptionally active/competent chromatin. J. Biol. Chem. 265, 5150–5156.

Riggs, M.G., Whittaker, R.G., Neumann, J.R., Ingram, V.M., 1977. n-Butyrate causes histone modification in HeLa and Friend erythroleukaemia cells. Nature 268, 462–464.

Robinson, P.J., Trnka, M.J., Bushnell, D.A., Davis, R.E., Mattei, P.J., Burlingame, A.L., Kornberg, R.D., 2016. Structure of a Complete Mediator-RNA Polymerase II Pre-Initiation Complex. Cell 166, 1411–1422.e16. doi:10.1016/j.cell.2016.08.050

Robinson, P.J.J., An, W., Routh, A., Martino, F., Chapman, L., Roeder, R.G., Rhodes, D., 2008. 30 nm chromatin fibre decompaction requires both H4-K16 acetylation and linker histone eviction. Journal of Molecular Biology 381, 816–825. doi:10.1016/j.jmb.2008.04.050

Rodriguez, C.R., Cho, E.J., Keogh, M.C., Moore, C.L., Greenleaf, A.L., Buratowski, S., 2000. Kin28, the TFIIH-associated carboxy-terminal domain kinase, facilitates the

recruitment of mRNA processing machinery to RNA polymerase II. Mol. Cell. Biol. 20, 104–112.

Roguev, A., Schaft, D., Shevchenko, A., Pijnappel, W.W., Wilm, M., Aasland, R., Stewart, A.F., 2001. The Saccharomyces cerevisiae Set1 complex includes an Ash2 homologue and methylates histone 3 lysine 4. EMBO J. 20, 7137–7148. doi:10.1093/emboj/20.24.7137

Rossetto, D., Cramet, M., Wang, A.Y., Steunou, A.-L., Lacoste, N., Schulze, J.M., COtE, V., Monnet-Saksouk, J., Piquet, S., Nourani, A., Kobor, M.S., Côté, J., 2014. Eaf5/7/3 form a functionally independent NuA4 submodule linked to RNA polymerase II-coupled nucleosome recycling. EMBO J. 33, 1397–1415. doi:10.15252/embj.201386433

Ruden, D.M., Ma, J., Li, Y., Wood, K., Ptashne, M., 1991. Generating yeast transcriptional activators containing no yeast protein sequences. Nature 350, 250–252. doi:10.1038/350250a0

Rufiange, A., Jacques, P.-É., Bhat, W., Robert, F., Nourani, A., 2007. Genome-wide replication-independent histone H3 exchange occurs predominantly at promoters and implicates H3 K56 acetylation and Asf1. Molecular Cell 27, 393–405. doi:10.1016/j.molcel.2007.07.011

Ruiz-Carrillo, A., Wangh, L.J., Allfrey, V.G., 1975. Processing of newly synthesized histone molecules. Science 190, 117–128.

Ruiz-Carrillo, A., Wangh, L.J., Littau, V.C., Allfrey, V.G., 1974. Changes in histone acetyl content and in nuclear non-histone protein composition of avian erythroid cells at different stages of maturation. J. Biol. Chem. 249, 7358–7368.

Rundlett, S.E., Carmen, A.A., Kobayashi, R., Bavykin, S., Turner, B.M., Grunstein, M., 1996. HDA1 and RPD3 are members of distinct yeast histone deacetylase complexes that regulate silencing and transcription. Proc. Natl. Acad. Sci. U.S.A. 93, 14503–14508.

Sabari, B.R., Tang, Z., Huang, H., Yong-Gonzalez, V., Molina, H., Kong, H.E., Dai, L., Shimada, M., Cross, J.R., Zhao, Y., Roeder, R.G., Allis, C.D., 2015. Intracellular crotonyl-CoA stimulates transcription through p300-catalyzed histone crotonylation. Molecular Cell 58, 203–215. doi:10.1016/j.molcel.2015.02.029

Sabari, B.R., Zhang, D., Allis, C.D., Zhao, Y., 2017. Metabolic regulation of gene expression through histone acylations. Nature Publishing Group 18, 90–101. doi:10.1038/nrm.2016.140

Sadeh, R., Launer-Wachs, R., Wandel, H., Rahat, A., Friedman, N., 2016. Elucidating Combinatorial Chromatin States at Single-Nucleosome Resolution. Molecular Cell 1–24. doi:10.1016/j.molcel.2016.07.023

Sahasrabuddhe, C.G., van Holde, K.E., 1974. The effect of trypsin on nuclease-resistant chromatin fragments. J. Biol. Chem. 249, 152–156.

Saksouk, N., Avvakumov, N., Champagne, K.S., Hung, T., Doyon, Y., Cayrou, C., Paquet, E., Ullah, M., Landry, A.-J., COtE, V., Yang, X.-J., Gozani, O., tateladze, T.G.K., Côté, J., 2009. HBO1 HAT Complexes Target Chromatin throughout Gene Coding Regions via Multiple PHD Finger Interactions with Histone H3 Tail. Molecular Cell 33, 257–265. doi:10.1016/j.molcel.2009.01.007

Saleh, A., Schieltz, D., Ting, N., McMahon, S.B., Litchfield, D.W., Yates, J.R., Lees-Miller, S.P., Cole, M.D., Brandl, C.J., 1998. Tra1p is a component of the yeast Ada.Spt transcriptional regulatory complexes. J. Biol. Chem. 273, 26559–26565.

Santisteban, M.S., Hang, M., Smith, M.M., 2011. Histone variant H2A.Z and RNA polymerase II transcription elongation. Mol. Cell. Biol. 31, 1848–1860. doi:10.1128/MCB.01346-10

Sartorelli, V., Huang, J., Hamamori, Y., Kedes, L., 1997. Molecular mechanisms of myogenic coactivation by p300: direct interaction with the activation domain of MyoD and with the MADS box of MEF2C. Mol. Cell. Biol. 17, 1010–1026.

Sathianathan, A., Ravichandran, P., Lippi, J.M., Cohen, L., Messina, A., Shaju, S., Swede, M.J., Ginsburg, D.S., 2016. The Eaf3/5/7 Subcomplex Stimulates NuA4 Interaction with Methylated Histone H3 Lys-36 and RNA Polymerase II. J. Biol. Chem. 291, 21195–21207. doi:10.1074/jbc.M116.718742

Savić, A., Richman, P., Williamson, P., Poccia, D., 1981. Alterations in chromatin structure during early sea urchin embryogenesis. Proc. Natl. Acad. Sci. U.S.A. 78, 3706–3710.

Schaft, D., Roguev, A., Kotovic, K.M., Shevchenko, A., Sarov, M., Shevchenko, A., Neugebauer, K.M., Stewart, A.F., 2003. The histone 3 lysine 36 methyltransferase, SET2, is involved in transcriptional elongation. Nucleic Acids Res. 31, 2475–2482. doi:10.1093/nar/gkg372

Schaughency, P., Merran, J., Corden, J.L., 2014. Genome-wide mapping of yeast RNA polymerase II termination. PLoS Genet 10, e1004632. doi:10.1371/journal.pgen.1004632

Schilbach, S., Hantsche, M., Tegunov, D., Dienemann, C., Wigge, C., Urlaub, H., Cramer, P., 2017. Structures of transcription pre-initiation complex with TFIIH and Mediator. Nature 551, 204–209. doi:10.1038/nature24282

Schneider, J., Bajwa, P., Johnson, F.C., Bhaumik, S.R., Shilatifard, A., 2006. Rtt109 is required for proper H3K56 acetylation: a chromatin mark associated with the elongating RNA polymerase II. J. Biol. Chem. 281, 37270–37274. doi:10.1074/jbc.C600265200

Schones, D.E., Cui, K., Cuddapah, S., Roh, T.-Y., Barski, A., Wang, Z., Wei, G., Zhao, K., 2008. Dynamic regulation of nucleosome positioning in the human genome. Cell 132, 887–898. doi:10.1016/j.cell.2008.02.022

Schulz, D., Schwalb, B., Kiesel, A., Baejen, C., Torkler, P., Gagneur, J., Soeding, J., Cramer, P., 2013. Transcriptome surveillance by selective termination of noncoding RNA synthesis. Cell 155, 1075–1087. doi:10.1016/j.cell.2013.10.024

Schulze, J.M., Hentrich, T., Nakanishi, S., Gupta, A., Emberly, E., Shilatifard, A., Kobor, M.S., 2011. Splitting the task: Ubp8 and Ubp10 deubiquitinate different cellular pools of H2BK123. Genes Dev. 25, 2242–2247. doi:10.1101/gad.177220.111

Schüller, R., Forné, I., Straub, T., Schreieck, A., Texier, Y., Shah, N., Decker, T.-M., Cramer, P., Imhof, A., Eick, D., 2016. Heptad-Specific Phosphorylation of RNA Polymerase II CTD. Molecular Cell 61, 305–314. doi:10.1016/j.molcel.2015.12.003

Schwabish, M.A., Struhl, K., 2006. Asf1 mediates histone eviction and deposition during elongation by RNA polymerase II. Molecular Cell 22, 415–422. doi:10.1016/j.molcel.2006.03.014

Scruggs, B.S., Gilchrist, D.A., Nechaev, S., Muse, G.W., Burkholder, A., Fargo, D.C., Adelman, K., 2015. Bidirectional Transcription Arises from Two Distinct Hubs of Transcription Factor Binding and Active Chromatin. Molecular Cell 58, 1101–1112. doi:10.1016/j.molcel.2015.04.006

Segal, E., Fondufe-Mittendorf, Y., Chen, L., Thåström, A., Field, Y., Moore, I.K., Wang, J.-P.Z., Widom, J., 2006. A genomic code for nucleosome positioning. Nature 442, 772–778. doi:10.1038/nature04979

Seward, D.J., Cubberley, G., Kim, S., Schonewald, M., Zhang, L., Tripet, B., Bentley, D.L., 2007. Demethylation of trimethylated histone H3 Lys4 in vivo by JARID1 JmjC proteins. Nat. Struct. Mol. Biol. 14, 240–242. doi:10.1038/nsmb1200

Shanle, E.K., Andrews, F.H., Meriesh, H., McDaniel, S.L., Dronamraju, R., DiFiore, J.V., Jha, D., Wozniak, G.G., Bridgers, J.B., Kerschner, J.L., Krajewski, K., Martín, G.M., Morrison, A.J., Kutateladze, T.G., Strahl, B.D., 2015. Association of Taf14 with acetylated histone H3 directs gene transcription and the DNA damage response. Genes Dev. 29, 1795–1800. doi:10.1101/gad.269977.115

Shaytan, A.K., Armeev, G.A., Goncearenco, A., Zhurkin, V.B., Landsman, D., Panchenko, A.R., 2016. Coupling between Histone Conformations and DNA Geometry in Nucleosomes on a Microsecond Timescale: Atomistic Insights into Nucleosome Functions. Journal of Molecular Biology 428, 221–237. doi:10.1016/j.jmb.2015.12.004

Shi, X., Hong, T., Walter, K.L., Ewalt, M., Michishita, E., Hung, T., Carney, D., Peña, P., Lan, F., Kaadige, M.R., Lacoste, N., Cayrou, C., Davrazou, F., Saha, A., Cairns, B.R., Ayer, D.E., Kutateladze, T.G., Shi, Y., Côté, J., Chua, K.F., Gozani, O., 2006.

ING2 PHD domain links histone H3 lysine 4 methylation to active gene repression. Nature 442, 96–99. doi:10.1038/nature04835

Shi, X., Kachirskaia, I., Walter, K.L., Kuo, J.-H.A., Lake, A., Davrazou, F., Chan, S.M., Martin, D.G.E., Fingerman, I.M., Briggs, S.D., Howe, L., Utz, P.J., Kutateladze, T.G., Lugovskoy, A.A., Bedford, M.T., Gozani, O., 2007. Proteome-wide analysis in Saccharomyces cerevisiae identifies several PHD fingers as novel direct and selective binding modules of histone H3 methylated at either lysine 4 or lysine 36. J. Biol. Chem. 282, 2450–2455. doi:10.1074/jbc.C600286200

Shi, Y., Lan, F., Matson, C., Mulligan, P., Whetstine, J.R., Cole, P.A., Casero, R.A., Shi, Y., 2004. Histone demethylation mediated by the nuclear amine oxidase homolog LSD1. Cell 119, 941–953. doi:10.1016/j.cell.2004.12.012

Shimojo, H., Sano, N., Moriwaki, Y., Okuda, M., Horikoshi, M., Nishimura, Y., 2008. Novel structural and functional mode of a knot essential for RNA binding activity of the Esa1 presumed chromodomain. Journal of Molecular Biology 378, 987–1001. doi:10.1016/j.jmb.2008.03.021

Shin, H., Liu, T., Manrai, A.K., Liu, X.S., 2009. CEAS: cis-regulatory element annotation system. Bioinformatics 25, 2605–2606. doi:10.1093/bioinformatics/btp479

Shogren-Knaak, M., Ishii, H., Sun, J.-M., Pazin, M.J., Davie, J.R., Peterson, C.L., 2006. Histone H4-K16 acetylation controls chromatin structure and protein interactions. Science 311, 844–847. doi:10.1126/science.1124000

Sigurdsson, S., Dirac-Svejstrup, A.B., Svejstrup, J.Q., 2010. Evidence that transcript cleavage is essential for RNA polymerase II transcription and cell viability. Molecular Cell 38, 202–210. doi:10.1016/j.molcel.2010.02.026

Siino, J.S., Yau, P.M., Imai, B.S., Gatewood, J.M., Bradbury, E.M., 2003. Effect of DNA length and H4 acetylation on the thermal stability of reconstituted nucleosome particles. Biochem. Biophys. Res. Commun. 302, 885–891. doi:10.1016/S0006-291X(03)00277-8

Simithy, J., Sidoli, S., Yuan, Z.-F., Coradin, M., Bhanu, N.V., Marchione, D.M., Klein, B.J., Bazilevsky, G.A., McCullough, C.E., Magin, R.S., Kutateladze, T.G., Snyder, N.W., Marmorstein, R., Garcia, B.A., 2017. Characterization of histone acylations links chromatin modifications with metabolism. Nat Commun 8, 1141. doi:10.1038/s41467-017-01384-9

Simpson, R.T., 1978. Structure of the chromatosome, a chromatin particle containing 160 base pairs of DNA and all the histones. Biochemistry 17, 5524–5531. doi:10.1021/bi00618a030

Sivanand, S., Rhoades, S., Jiang, Q., Lee, J.V., Benci, J., Zhang, J., Yuan, S., Viney, I., Zhao, S., Carrer, A., Bennett, M.J., Minn, A.J., Weljie, A.M., Greenberg, R.A.,

Wellen, K.E., 2017. Nuclear Acetyl-CoA Production by ACLY Promotes Homologous Recombination. Molecular Cell 67, 252–265.e6. doi:10.1016/j.molcel.2017.06.008

Smale, S.T., Baltimore, D., 1989. The “initiator” as a transcription control element. Cell 57, 103–113.

Smolle, M., Venkatesh, S., Gogol, M.M., Li, H., Zhang, Y., Florens, L., Washburn, M.P., Workman, J.L., 2012. Chromatin remodelers Isw1 and Chd1 maintain chromatin structure during transcription by preventing histone exchange. Nature Structural & Molecular Biology 19, 884–892. doi:10.1038/nsmb.2312

Sobel, R.E., Cook, R.G., Perry, C.A., Annunziato, A.T., Allis, C.D., 1995. Conservation of deposition-related acetylation sites in newly synthesized histones H3 and H4. Proc. Natl. Acad. Sci. U.S.A. 92, 1237–1241.

Somesh, B.P., Reid, J., Liu, W.-F., Søgaard, T.M.M., Erdjument-Bromage, H., Tempst, P., Svejstrup, J.Q., 2005. Multiple mechanisms confining RNA polymerase II ubiquitylation to polymerases undergoing transcriptional arrest. Cell 121, 913–923. doi:10.1016/j.cell.2005.04.010

Stedman, E., 1950. Cell specificity of histones. Nature 166, 780–781.

Steunou, A.-L., Cramet, M., Rossetto, D., Aristizabal, M.J., Lacoste, N., Drouin, S., COtE, V., Paquet, E., Utley, R.T., Krogan, N., Robert, F., Kobor, M.S., Côté, J., 2016. Combined Action of Histone Reader Modules Regulates NuA4 Local Acetyltransferase Function but Not Its Recruitment on the Genome. Mol. Cell. Biol. 36, 2768–2781. doi:10.1128/MCB.00112-16

Stevely, W.S., Stocken, L.A., 1966. Phosphorylation of rat-thymus histone. Biochem. J. 100, 20C–1C.

Strahl, B.D., Allis, C.D., 2000. The language of covalent histone modifications. Nature 403, 41–45. doi:10.1038/47412

Strahl, B.D., Grant, P.A., Briggs, S.D., Sun, Z.-W., Bone, J.R., Caldwell, J.A., Mollah, S., Cook, R.G., Shabanowitz, J., Hunt, D.F., Allis, C.D., 2002. Set2 is a nucleosomal histone H3-selective methyltransferase that mediates transcriptional repression. Mol. Cell. Biol. 22, 1298–1306. doi:10.1128/MCB.22.5.1298-1306.2002

Stützer, A., Liokatis, S., Kiesel, A., Schwarzer, D., Sprangers, R., Söding, J., Selenko, P., Fischle, W., 2016. Modulations of DNA Contacts by Linker Histones and Post-translational Modifications Determine the Mobility and Modifiability of Nucleosomal H3 Tails. Molecular Cell 61, 247–259. doi:10.1016/j.molcel.2015.12.015

Suh, H., Ficarro, S.B., Kang, U.-B., Chun, Y., Marto, J.A., Buratowski, S., 2016. Direct Analysis of Phosphorylation Sites on the Rpb1 C-Terminal Domain of RNA

Polymerase II. Molecular Cell 61, 297–304. doi:10.1016/j.molcel.2015.12.021

Suka, N., Suka, Y., Carmen, A.A., Wu, J., Grunstein, M., 2001. Highly specific antibodies determine histone acetylation site usage in yeast heterochromatin and euchromatin., in:. Presented at the Molecular cell, pp. 473–479.

Sun, B., Hong, J., Zhang, P., Dong, X., Shen, X., Lin, D., Ding, J., 2008. Molecular basis of the interaction of Saccharomyces cerevisiae Eaf3 chromo domain with methylated H3K36. J. Biol. Chem. 283, 36504–36512. doi:10.1074/jbc.M806564200

Sun, M., Schwalb, B., Pirkl, N., Maier, K.C., Schenk, A., Failmezger, H., Tresch, A., Cramer, P., 2013. Global analysis of eukaryotic mRNA degradation reveals Xrn1-dependent buffering of transcript levels. Molecular Cell 52, 52–62. doi:10.1016/j.molcel.2013.09.010

Sun, Z.-W., Allis, C.D., 2002. Ubiquitination of histone H2B regulates H3 methylation and gene silencing in yeast. Nature 418, 104–108. doi:10.1038/nature00883

Supakar, P.C., Kanungo, M.S., 1981. Chromatin function in developing brain: acetylation of chromosomal proteins and RNA synthesis. Biochem. Biophys. Res. Commun. 100, 73–78.

Suto, R.K., Clarkson, M.J., Tremethick, D.J., Luger, K., 2000. Crystal structure of a nucleosome core particle containing the variant histone H2A.Z. Nat. Struct. Biol. 7, 1121–1124. doi:10.1038/81971

Sutton, A., Shia, W.-J., Band, D., Kaufman, P.D., Osada, S., Workman, J.L., Sternglanz, R., 2003. Sas4 and Sas5 are required for the histone acetyltransferase activity of Sas2 in the SAS complex. J. Biol. Chem. 278, 16887–16892. doi:10.1074/jbc.M210709200

Svejstrup, J.Q., Feaver, W.J., LaPointe, J., Kornberg, R.D., 1994. RNA polymerase transcription factor IIH holoenzyme from yeast. J. Biol. Chem. 269, 28044–28048.

Takahashi, H., McCaffery, J.M., Irizarry, R.A., Boeke, J.D., 2006. Nucleocytosolic acetyl-coenzyme a synthetase is required for histone acetylation and global transcription. Molecular Cell 23, 207–217. doi:10.1016/j.molcel.2006.05.040

Tamkun, J.W., Deuring, R., Scott, M.P., Kissinger, M., Pattatucci, A.M., Kaufman, T.C., Kennison, J.A., 1992. brahma: a regulator of Drosophila homeotic genes structurally related to the yeast transcriptional activator SNF2/SWI2. Cell 68, 561–572.

Tan, M., Luo, H., Lee, S., Jin, F., Yang, J.S., Montellier, E., Buchou, T., Cheng, Z., Rousseaux, S., Rajagopal, N., Lu, Z., Ye, Z., Zhu, Q., Wysocka, J., Ye, Y., Khochbin, S., Ren, B., Zhao, Y., 2011. Identification of 67 histone marks and histone lysine crotonylation as a new type of histone modification. Cell 146, 1016–1028. doi:10.1016/j.cell.2011.08.008

Taunton, J., Hassig, C.A., Schreiber, S.L., 1996. A mammalian histone deacetylase related to the yeast transcriptional regulator Rpd3p. Science 272, 408–411.

Taverna, S.D., Ilin, S., Rogers, R.S., Tanny, J.C., Lavender, H., Li, H., Baker, L., Boyle, J., Blair, L.P., Chait, B.T., Patel, D.J., Aitchison, J.D., Tackett, A.J., Allis, C.D., 2006. Yng1 PHD finger binding to H3 trimethylated at K4 promotes NuA3 HAT activity at K14 of H3 and transcription at a subset of targeted ORFs. Molecular Cell 24, 785–796. doi:10.1016/j.molcel.2006.10.026

Thambirajah, A.A., Dryhurst, D., Ishibashi, T., Li, A., Maffey, A.H., Ausió, J., 2006. H2A.Z stabilizes chromatin in a way that is dependent on core histone acetylation. J. Biol. Chem. 281, 20036–20044. doi:10.1074/jbc.M601975200

Thatcher, T.H., Gorovsky, M.A., 1994. Phylogenetic analysis of the core histones H2A, H2B, H3, and H4. Nucleic Acids Res. 22, 174–179.

Thomas, J.O., Furber, V., 1976. Yeast chromatin structure. FEBS Lett. 66, 274–280.

Thomas, J.O., Thompson, R.J., 1977. Variation in chromatin structure in two cell types from the same tissue: a short DNA repeat length in cerebral cortex neurons. Cell 10, 633–640.

Thompson, C.M., Koleske, A.J., Chao, D.M., Young, R.A., 1993. A multisubunit complex associated with the RNA polymerase II CTD and TATA-binding protein in yeast. Cell 73, 1361–1375.

Tipper, D.J., 1973. Inhibition of yeast ribonucleic acid polymerases by thiolutin. J. Bacteriol. 116, 245–256.

Topol, J., Ruden, D.M., Parker, C.S., 1985. Sequences required for in vitro transcriptional activation of a Drosophila hsp 70 gene. Cell 42, 527–537.

Tramantano, M., Sun, L., Au, C., Labuz, D., Liu, Z., Chou, M., Shen, C., Luk, E., 2016. Constitutive turnover of histone H2A.Z at yeast promoters requires the preinitiation complex. Elife 5, 6270. doi:10.7554/eLife.14243

Trojer, P., Li, G., Sims, R.J., Vaquero, A., Kalakonda, N., Boccuni, P., Lee, D., Erdjument-Bromage, H., Tempst, P., Nimer, S.D., Wang, Y.-H., Reinberg, D., 2007. L3MBTL1, a histone-methylation-dependent chromatin lock. Cell 129, 915–928. doi:10.1016/j.cell.2007.03.048

Tropberger, P., Pott, S., Keller, C., Kamieniarz-Gdula, K., Caron, M., Richter, F., Li, G., Mittler, G., Liu, E.T., Bühler, M., Margueron, R., Schneider, R., 2013. Regulation of transcription through acetylation of H3K122 on the lateral surface of the histone octamer. Cell 152, 859–872. doi:10.1016/j.cell.2013.01.032

Tse, C., Sera, T., Wolffe, A.P., Hansen, J.C., 1998. Disruption of higher-order folding by core histone acetylation dramatically enhances transcription of nucleosomal arrays by

RNA polymerase III. Mol. Cell. Biol. 18, 4629–4638.

Tsubota, T., Berndsen, C.E., Erkmann, J.A., Smith, C.L., Yang, L., Freitas, M.A., Denu, J.M., Kaufman, P.D., 2007. Histone H3-K56 acetylation is catalyzed by histone chaperone-dependent complexes. Molecular Cell 25, 703–712. doi:10.1016/j.molcel.2007.02.006

Ujvári, A., Hsieh, F.-K., Luse, S.W., Studitsky, V.M., Luse, D.S., 2008. Histone N-terminal tails interfere with nucleosome traversal by RNA polymerase II. J. Biol. Chem. 283, 32236–32243. doi:10.1074/jbc.M806636200

Utley, R.T., Ikeda, K., Grant, P.A., Cote, J., Steger, D.J., Eberharter, A., John, S., Workman, J.L., 1998. Transcriptional activators direct histone acetyltransferase complexes to nucleosomes. Nature 394, 498–502. doi:10.1038/28886

van Bruggen, E.F., Arnberg, A.C., van Holde, K.E., Sahasrabuddhe, C.G., Shaw, B.R., 1974. Electron microscopy of chromatin subunit particles. Biochem. Biophys. Res. Commun. 60, 1365–1370.

van Holde, K.E., Sahasrabuddhe, C.G., Shaw, B.R., 1974. A model for particulate structure in chromatin. Nucleic Acids Res. 1, 1579–1586.

van Leeuwen, F., Gafken, P.R., Gottschling, D.E., 2002. Dot1p modulates silencing in yeast by methylation of the nucleosome core. Cell 109, 745–756.

Van Oss, S.B., Shirra, M.K., Bataille, A.R., Wier, A.D., Yen, K., Vinayachandran, V., Byeon, I.-J.L., Cucinotta, C.E., Heroux, A., Jeon, J., Kim, J., VanDemark, A.P., Pugh, B.F., Arndt, K.M., 2016. The Histone Modification Domain of Paf1 Complex Subunit Rtf1 Directly Stimulates H2B Ubiquitylation through an Interaction with Rad6. Molecular Cell 64, 815–825. doi:10.1016/j.molcel.2016.10.008

VanDemark, A.P., Kasten, M.M., Ferris, E., Heroux, A., Hill, C.P., Cairns, B.R., 2007. Autoregulation of the rsc4 tandem bromodomain by gcn5 acetylation. Molecular Cell 27, 817–828. doi:10.1016/j.molcel.2007.08.018

Vassilev, A., Yamauchi, J., Kotani, T., Prives, C., Avantaggiati, M.L., Qin, J., Nakatani, Y., 1998. The 400 kDa subunit of the PCAF histone acetylase complex belongs to the ATM superfamily. Molecular Cell 2, 869–875.

Vavra, K.J., Allis, C.D., Gorovsky, M.A., 1982. Regulation of histone acetylation in Tetrahymena macro- and micronuclei. J. Biol. Chem. 257, 2591–2598.

Venkatesh, S., Smolle, M., Li, H., Gogol, M.M., Saint, M., Kumar, S., Natarajan, K., Workman, J.L., 2012. Set2 methylation of histone H3 lysine 36 suppresses histone exchange on transcribed genes. Nature 489, 452–455. doi:10.1038/nature11326

Venkatesh, S., Workman, J.L., 2015. Histone exchange, chromatin structure and the regulation of transcription. Nature Publishing Group 16, 178–189.

doi:10.1038/nrm3941

Vermeulen, M., Eberl, H.C., Matarese, F., Marks, H., Denissov, S., Butter, F., Lee, K.K., Olsen, J.V., Hyman, A.A., Stunnenberg, H.G., Mann, M., 2010. Quantitative interaction proteomics and genome-wide profiling of epigenetic histone marks and their readers. Cell 142, 967–980. doi:10.1016/j.cell.2010.08.020

Vermeulen, M., Mulder, K.W., Denissov, S., Pijnappel, W.W.M.P., van Schaik, F.M.A., Varier, R.A., Baltissen, M.P.A., Stunnenberg, H.G., Mann, M., Timmers, H.T.M., 2007. Selective anchoring of TFIID to nucleosomes by trimethylation of histone H3 lysine 4. Cell 131, 58–69. doi:10.1016/j.cell.2007.08.016

Vezzoli, A., Bonadies, N., Allen, M.D., Freund, S.M.V., Santiveri, C.M., Kvinlaug, B.T., Huntly, B.J.P., Göttgens, B., Bycroft, M., 2010. Molecular basis of histone H3K36me3 recognition by the PWWP domain of Brpf1. Nat. Struct. Mol. Biol. 17, 617–619. doi:10.1038/nsmb.1797

Vidal, M., Gaber, R.F., 1991. RPD3 encodes a second factor required to achieve maximum positive and negative transcriptional states in Saccharomyces cerevisiae. Mol. Cell. Biol. 11, 6317–6327.

Vihervaara, A., Mahat, D.B., Guertin, M.J., Chu, T., Danko, C.G., Lis, J.T., Sistonen, L., 2017. Transcriptional response to stress is pre-wired by promoter and enhancer architecture. Nat Commun 8, 255. doi:10.1038/s41467-017-00151-0

Vogelauer, M., Wu, J., Suka, N., Grunstein, M., 2000. Global histone acetylation and deacetylation in yeast. Nature 408, 495–498. doi:10.1038/35044127

Wada, T., Takagi, T., Yamaguchi, Y., Ferdous, A., Imai, T., Hirose, S., Sugimoto, S., Yano, K., Hartzog, G.A., Winston, F., Buratowski, S., Handa, H., 1998a. DSIF, a novel transcription elongation factor that regulates RNA polymerase II processivity, is composed of human Spt4 and Spt5 homologs. Genes & Development 12, 343–356.

Wada, T., Takagi, T., Yamaguchi, Y., Watanabe, D., Handa, H., 1998b. Evidence that P-TEFb alleviates the negative effect of DSIF on RNA polymerase II-dependent transcription in vitro. EMBO J. 17, 7395–7403. doi:10.1093/emboj/17.24.7395

Wakamori, M., Fujii, Y., Suka, N., Shirouzu, M., Sakamoto, K., Umehara, T., Yokoyama, S., 2015. Intra- and inter-nucleosomal interactions of the histone H4 tail revealed with a human nucleosome core particle with genetically-incorporated H4 tetra-acetylation. Nature Publishing Group 5, 17204. doi:10.1038/srep17204

Wallberg, A.E., Neely, K.E., Gustafsson, J.A., Workman, J.L., Wright, A.P., Grant, P.A., 1999. Histone acetyltransferase complexes can mediate transcriptional activation by the major glucocorticoid receptor activation domain. Mol. Cell. Biol. 19, 5952–5959.

Wang, L., Tang, Y., Cole, P.A., Marmorstein, R., 2008. Structure and chemistry of the

p300/CBP and Rtt109 histone acetyltransferases: implications for histone acetyltransferase evolution and function. Curr. Opin. Struct. Biol. 18, 741–747. doi:10.1016/j.sbi.2008.09.004

Wang, X., Hayes, J.J., 2008. Acetylation mimics within individual core histone tail domains indicate distinct roles in regulating the stability of higher-order chromatin structure. Mol. Cell. Biol. 28, 227–236. doi:10.1128/MCB.01245-07

Wang, Y., Reddy, B., Thompson, J., Wang, H., Noma, K.-I., Yates, J.R., Jia, S., 2009. Regulation of Set9-mediated H4K20 methylation by a PWWP domain protein. Molecular Cell 33, 428–437. doi:10.1016/j.molcel.2009.02.002

Wang, Z., Zang, C., Cui, K., Schones, D.E., Barski, A., Peng, W., Zhao, K., 2009. Genome-wide mapping of HATs and HDACs reveals distinct functions in active and inactive genes. Cell 138, 1019–1031. doi:10.1016/j.cell.2009.06.049

Wang, Z., Zang, C., Rosenfeld, J.A., Schones, D.E., Barski, A., Cuddapah, S., Cui, K., Roh, T.-Y., Peng, W., Zhang, M.Q., Zhao, K., 2008. Combinatorial patterns of histone acetylations and methylations in the human genome. Nature Genetics 40, 897–903. doi:10.1038/ng.154

Wangh, L., Ruiz-Carrillo, A., Allfrey, V.G., 1972. Separation and analysis of histone subfractions differing in their degree of acetylation: some correlations with genetic activity in development. Arch. Biochem. Biophys. 150, 44–56.

Warfield, L., Ramachandran, S., Baptista, T., Devys, D., Tora, L., Hahn, S., 2017. Transcription of Nearly All Yeast RNA Polymerase II- Transcribed Genes Is Dependent on Transcription Factor TFIID. Molecular Cell 1–30. doi:10.1016/j.molcel.2017.08.014

Wargo, M.J., Rizzo, P.J., 2001. Exception to eukaryotic rules. Science 294, 2477.

Waterborg, J.H., 2002. Dynamics of histone acetylation in vivo. A function for acetylation turnover? Biochem. Cell Biol. 80, 363–378. doi:10.1139/o02-080

Weber, C.M., Henikoff, S., 2014. Histone variants: dynamic punctuation in transcription. Genes Dev. 28, 672–682. doi:10.1101/gad.238873.114

Weber, C.M., Ramachandran, S., Henikoff, S., 2014. Nucleosomes are context-specific, H2A.Z-modulated barriers to RNA polymerase. Molecular Cell 53, 819–830. doi:10.1016/j.molcel.2014.02.014

Weil, P.A., Luse, D.S., Segall, J., Roeder, R.G., 1979. Selective and accurate initiation of transcription at the Ad2 major late promotor in a soluble system dependent on purified RNA polymerase II and DNA. Cell 18, 469–484.

Weiner, A., Hsieh, T.-H.S., Appleboim, A., Chen, H.V., Rahat, A., Amit, I., Rando, O.J., Friedman, N., 2015. High-resolution chromatin dynamics during a yeast stress

response. Molecular Cell 58, 371–386. doi:10.1016/j.molcel.2015.02.002

Wellen, K.E., Hatzivassiliou, G., Sachdeva, U.M., Bui, T.V., Cross, J.R., Thompson, C.B., 2009. ATP-citrate lyase links cellular metabolism to histone acetylation. Science 324, 1076–1080. doi:10.1126/science.1164097

West, M.H., Bonner, W.M., 1980. Histone 2A, a heteromorphous family of eight protein species. Biochemistry 19, 3238–3245. doi:10.1021/bi00555a022

Whatley, S.A., Hall, C., Lim, L., 1981. Chromatin organization in the rat hypothalamus during early development. Biochem. J. 196, 115–119.

White, C.L., Suto, R.K., Luger, K., 2001. Structure of the yeast nucleosome core particle reveals fundamental changes in internucleosome interactions. EMBO J. 20, 5207–5218. doi:10.1093/emboj/20.18.5207

Whitehouse, I., Flaus, A., Cairns, B.R., White, M.F., Workman, J.L., Owen-Hughes, T., 1999. Nucleosome mobilization catalysed by the yeast SWI/SNF complex. Nature 400, 784–787. doi:10.1038/23506

Wiegand, R.C., Brutlag, D.L., 1981. Histone acetylase from Drosophila melanogaster specific for H4. J. Biol. Chem. 256, 4578–4583.

Wilkinson, A.W., Gozani, O., 2014. Histone-binding domains: strategies for discovery and characterization. Biochim. Biophys. Acta 1839, 669–675. doi:10.1016/j.bbagrm.2014.01.007

Winkler, G.S., Kristjuhan, A., Erdjument-Bromage, H., Tempst, P., Svejstrup, J.Q., 2002. Elongator is a histone H3 and H4 acetyltransferase important for normal histone acetylation levels in vivo. Proc. Natl. Acad. Sci. U.S.A. 99, 3517–3522. doi:10.1073/pnas.022042899

Wittschieben, B.O., Fellows, J., Du, W., Stillman, D.J., Svejstrup, J.Q., 2000. Overlapping roles for the histone acetyltransferase activities of SAGA and elongator in vivo. EMBO J. 19, 3060–3068. doi:10.1093/emboj/19.12.3060

Wittschieben, B.O., Otero, G., de Bizemont, T., Fellows, J., Erdjument-Bromage, H., Ohba, R., Li, Y., Allis, C.D., Tempst, P., Svejstrup, J.Q., 1999. A novel histone acetyltransferase is an integral subunit of elongating RNA polymerase II holoenzyme. Molecular Cell 4, 123–128.

Wong, K.H., Jin, Y., Struhl, K., 2014. TFIIH Phosphorylation of the Pol II CTD Stimulates Mediator Dissociation from the Preinitiation Complex and Promoter Escape. Molecular Cell 54, 601–612. doi:10.1016/j.molcel.2014.03.024

Wood, A., Schneider, J., Dover, J., Johnston, M., Shilatifard, A., 2003. The Paf1 complex is essential for histone monoubiquitination by the Rad6-Bre1 complex, which signals for histone methylation by COMPASS and Dot1p. J. Biol. Chem. 278, 34739–34742.

doi:10.1074/jbc.C300269200

Woudstra, E.C., Gilbert, C., Fellows, J., Jansen, L., Brouwer, J., Erdjument-Bromage, H., Tempst, P., Svejstrup, J.Q., 2002. A Rad26-Def1 complex coordinates repair and RNA pol II proteolysis in response to DNA damage. Nature 415, 929–933. doi:10.1038/415929a

Wu, H., Zeng, H., Lam, R., Tempel, W., Amaya, M.F., Xu, C., Dombrovski, L., Qiu, W., Wang, Y., Min, J., 2011. Structural and histone binding ability characterizations of human PWWP domains. PLoS ONE 6, e18919. doi:10.1371/journal.pone.0018919

Wu, J., Carmen, A.A., Kobayashi, R., Suka, N., Grunstein, M., 2001a. HDA2 and HDA3 are related proteins that interact with and are essential for the activity of the yeast histone deacetylase HDA1. Proc. Natl. Acad. Sci. U.S.A. 98, 4391–4396. doi:10.1073/pnas.081560698

Wu, J., Suka, N., Carlson, M., Grunstein, M., 2001b. TUP1 utilizes histone H3/H2B-specific HDA1 deacetylase to repress gene activity in yeast. Molecular Cell 7, 117–126.

Wu, L., Winston, F., 1997. Evidence that Snf-Swi controls chromatin structure over both the TATA and UAS regions of the SUC2 promoter in Saccharomyces cerevisiae. Nucleic Acids Res. 25, 4230–4234.

Wysocka, J., Swigut, T., Milne, T.A., Dou, Y., Zhang, X., Burlingame, A.L., Roeder, R.G., Brivanlou, A.H., Allis, C.D., 2005. WDR5 associates with histone H3 methylated at K4 and is essential for H3 K4 methylation and vertebrate development. Cell 121, 859–872. doi:10.1016/j.cell.2005.03.036

Wysocka, J., Swigut, T., Xiao, H., Milne, T.A., Kwon, S.Y., Landry, J., Kauer, M., Tackett, A.J., Chait, B.T., Badenhorst, P., Wu, C., Allis, C.D., 2006. A PHD finger of NURF couples histone H3 lysine 4 trimethylation with chromatin remodelling. Nature 442, 86–90. doi:10.1038/nature04815

Xiao, T., Hall, H., Kizer, K.O., Shibata, Y., Hall, M.C., Borchers, C.H., Strahl, B.D., 2003. Phosphorylation of RNA polymerase II CTD regulates H3 methylation in yeast. Genes & Development 17, 654–663. doi:10.1101/gad.1055503

Xiong, X., Panchenko, T., Yang, S., Zhao, S., Yan, P., Zhang, W., Xie, W., Li, Y., Zhao, Y., Allis, C.D., Li, H., 2016. Selective recognition of histone crotonylation by double PHD fingers of MOZ and DPF2. Nature Chemical Biology 12, 1111–1118. doi:10.1038/nchembio.2218

Xu, C., Cui, G., Botuyan, M.V., Mer, G., 2008. Structural basis for the recognition of methylated histone H3K36 by the Eaf3 subunit of histone deacetylase complex Rpd3S. Structure/Folding and Design 16, 1740–1750. doi:10.1016/j.str.2008.08.008

Xue-Franzén, Y., Henriksson, J., Bürglin, T.R., Wright, A.P.H., 2013. Distinct roles of

the Gcn5 histone acetyltransferase revealed during transient stress-induced reprogramming of the genome. BMC Genomics 14, 479. doi:10.1186/1471-2164-14-479

Xue-Franzén, Y., Johnsson, A., Brodin, D., Henriksson, J., Bürglin, T.R., Wright, A.P.H., 2010. Genome-wide characterisation of the Gcn5 histone acetyltransferase in budding yeast during stress adaptation reveals evolutionarily conserved and diverged roles. BMC Genomics 11, 200. doi:10.1186/1471-2164-11-200

Yamaguchi, Y., Takagi, T., Wada, T., Yano, K., Furuya, A., Sugimoto, S., Hasegawa, J., Handa, H., 1999. NELF, a multisubunit complex containing RD, cooperates with DSIF to repress RNA polymerase II elongation. Cell 97, 41–51.

Yamamoto, T., Horikoshi, M., 1997. Novel substrate specificity of the histone acetyltransferase activity of HIV-1-Tat interactive protein Tip60. J. Biol. Chem. 272, 30595–30598.

Yang, W.M., Inouye, C., Zeng, Y., Bearss, D., Seto, E., 1996. Transcriptional repression by YY1 is mediated by interaction with a mammalian homolog of the yeast global regulator RPD3. Proc. Natl. Acad. Sci. U.S.A. 93, 12845–12850.

Yang, X.-J., Seto, E., 2008. Lysine acetylation: codified crosstalk with other posttranslational modifications. Molecular Cell 31, 449–461. doi:10.1016/j.molcel.2008.07.002

Yau, P., Thorne, A.W., Imai, B.S., Matthews, H.R., Bradbury, E.M., 1982. Thermal denaturation studies of acetylated nucleosomes and oligonucleosomes. Eur. J. Biochem. 129, 281–288.

Yazdi, P.G., Pedersen, B.A., Taylor, J.F., Khattab, O.S., Chen, Y.-H., Chen, Y., Jacobsen, S.E., Wang, P.H., 2015. Nucleosome Organization in Human Embryonic Stem Cells. PLoS ONE 10, e0136314. doi:10.1371/journal.pone.0136314

Ye, J., Ai, X., Eugeni, E.E., Zhang, L., Carpenter, L.R., Jelinek, M.A., Freitas, M.A., Parthun, M.R., 2005. Histone H4 lysine 91 acetylation a core domain modification associated with chromatin assembly. Molecular Cell 18, 123–130. doi:10.1016/j.molcel.2005.02.031

Yen, K., Vinayachandran, V., Batta, K., Koerber, R.T., Pugh, B.F., 2012. Genome-wide nucleosome specificity and directionality of chromatin remodelers. Cell 149, 1461–1473. doi:10.1016/j.cell.2012.04.036

Yen, K., Vinayachandran, V., Pugh, B.F., 2013. SWR-C and INO80 chromatin remodelers recognize nucleosome-free regions near +1 nucleosomes. Cell 154, 1246–1256. doi:10.1016/j.cell.2013.08.043

Yuan, G.-C., Liu, Y.-J., Dion, M.F., Slack, M.D., Wu, L.F., Altschuler, S.J., Rando, O.J., 2005. Genome-scale identification of nucleosome positions in S. cerevisiae. Science

309, 626–630. doi:10.1126/science.1112178

Yuan, W., Condorelli, G., Caruso, M., Felsani, A., Giordano, A., 1996. Human p300 protein is a coactivator for the transcription factor MyoD. J. Biol. Chem. 271, 9009–9013.

Yun, M., Wu, J., Workman, J.L., Li, B., 2011. Readers of histone modifications. Nature Publishing Group 21, 564–578. doi:10.1038/cr.2011.42

Zalenskaya, I.A., Pospelov, V.A., Zalensky, A.O., Vorob'ev, V.I., 1981. Nucleosomal structure of sea urchin and starfish sperm chromatin. Histone H2B is possibly involved in determining the length of linker DNA. Nucleic Acids Res. 9, 473–487.

Zeng, L., Zhang, Q., Li, S., Plotnikov, A.N., Walsh, M.J., Zhou, M.-M., 2010. Mechanism and regulation of acetylated histone binding by the tandem PHD finger of DPF3b. Nature 466, 258–262. doi:10.1038/nature09139

Zhang, H., Roberts, D.N., Cairns, B.R., 2005. Genome-wide dynamics of Htz1, a histone H2A variant that poises repressed/basal promoters for activation through histone loss. Cell 123, 219–231. doi:10.1016/j.cell.2005.08.036

Zhang, J., Corden, J.L., 1991. Identification of phosphorylation sites in the repetitive carboxyl-terminal domain of the mouse RNA polymerase II largest subunit. J. Biol. Chem. 266, 2290–2296.

Zhang, Z., Wippo, C.J., Wal, M., Ward, E., Korber, P., Pugh, B.F., 2011. A packing mechanism for nucleosome organization reconstituted across a eukaryotic genome. Science 332, 977–980. doi:10.1126/science.1200508

Zheng, Y., Thomas, P.M., Kelleher, N.L., 2013. Measurement of acetylation turnover at distinct lysines in human histones identifies long-lived acetylation sites. Nat Commun 4, 2203. doi:10.1038/ncomms3203

Zhu, F., Farnung, L., Kaasinen, E., Sahu, B., Yin, Y., Wei, B., Dodonova, S., Cramer, P., Taipale, J., 2017. The interaction landscape between transcription factors and the nucleosome. Biorxiv. doi:10.1101/240598

Zlatanova, J., Thakar, A., 2008. H2A.Z: view from the top. Structure/Folding and Design 16, 166–179. doi:10.1016/j.str.2007.12.008